The development and application of a single cell biosensor for the detection of L-methionine and branched-chain amino acids

A dissertation submitted to the
Mathematisch-Naturwissenschaftliche Fakultät
of the Heinrich-Heine-Universität Düsseldorf

presented by
Nurije Mustafi
born in Tetovo, Macedonia

Düsseldorf, March 2013

The thesis in hand has been performed at the Institute of Bio- and Geosciences, IBG-1: Biotechnology, Research Centre Jülich, from January 2010 until March 2013 under the supervision of Dr. Julia Frunzke.

Printed with acceptance of the Mathematisch-Naturwissenschaftlichen Fakultät of the Heinrich-Heine-Universität Düsseldorf.

Examiner: Dr. Julia Frunzke

Institute of Bio- and Geosciences, IBG-1: Biotechnology

Population heterogeneity and signal transduction group

Research Centre Jülich GmbH

Coexaminer: Prof. Dr. Karl-Erich Jaeger

Institute of Molecular Enzyme Technology

Heinrich-Heine-University Düsseldorf / Research Centre Jülich GmbH

Results described in this dissertation have been published in the following original publications:

Lange, C., **Mustafi, N.**, Frunzke, J., Kennerknecht, N., Wessel M., Bott M., and Wendisch VF. **(2012)** Lrp of *Corynebacterium glutamicum* controls expression of the *brnFE* operon encoding the export system for L-methionine and branched-chain amino acids. ***Journal of Biotechnology*** 158 (4): 231-241.

Mustafi N., Grünberger A., Kohlheyer D., Bott M., and Frunzke J. **(2012)** The development and application of a single-cell biosensor for the detection of L-methionine and branched-chain amino acids. ***Metabolic engineering*** 14 (4): 449-457.

Hentschel E., Will C., **Mustafi N.**, Burkovski A., Rehm N., and Frunzke J. **(2012)** Destabilized eYFP variants for dynamic gene expression studies in *Corynebacterium glutamicum*. ***Microbial Biotechnology*** 6 (2): 196-201.

Mustafi N., Rückert C., Kalinowski J., Bott M., and Frunzke J. **(2013)** L-methionine producing mutants of *Corynebacterium glutamicum* isolated by biosensor-based high throughput screening. ***To be submitted.***

Mustafi N.[*], Grünberger A[*], Mahr R., Helfrich S., Nöh K., Blombach B., Kohlheyer D., and Frunzke J. **(2013)** Application of a genetically-encoded biosensor for the single cell analysis of *Corynebacterium glutamicum* L-valine production strains. ***To be submitted.***

Mustafi N., Bott M., and Frunzke J. **(2013)** Development and application of genetically-encoded biosensors for strain development and single cell analysis of *Corynebacterium glutamicum*. Book Chapter in "*Corynebacterium glutamicum*: Systems Biology, Biotechnological Applications and Control". (Burkovski A., ed.), Caister Academic Press, Norfolk, UK. ***Submitted.***

Patent application:

Eggeling L., Bott M., Binder S., Frunzke J., and **Mustafi N. (2011)** Sensors for the detection of intracellular metabolites. WIPO Patent Application WO/2011/138006.

Results of further projects not discussed in this thesis have been published in:

Baumgart M., **Mustafi N.**, Krug A., and Bott M. **(2011)** Deletion of the aconitase gene in *Corynebacterium glutamicum* causes strong selection pressure for secondary mutations inactivating citrate synthase. ***Journal of Bacteriology*** 193 (24): 6864-6873.

[*]These authors contributed equally to this work.

Content

Abbreviations

ATCC	American Type Culture Collection
ATP	Adenosine-5'-triphosphate
BHI(S)	Brain Heart Infusion (+ Sorbitol)
DNA	deoxyribonucleic acid
et al.	et alii
GFP	green fluorescent protein
FACS	fluorescence-activated cell sorting
IPTG	Isopropyl β-$_D$-1-thiogalactopyranoside
Kan^R	Kanamycin resistance
LB	Luria Bertani
NADPH	Nicotinamide adenine dinucleotide phosphate, reduced form
MNNG	*N*-methyl-*N*′-nitro-*N*-nitrosoguanidine
OD_{600}	optical density at 600 nm
PDHC	pyruvate dehydrogenase complex
RBS	ribosome binding site
uHPLC	ultra high performance liquid chromatography
UV	ultraviolet
v/v	volume per volume
WT	wild type
w/v	weight per volume
eYFP	enhanced yellow fluorescent protein

Further abbreviations not included in this section are according to international standards, as for example listed in the author guidelines of the *FEBS Journal*.

1 Summary

1.1. Summary English

Since the early 20th century, microbes have written a success story as hosts for the production of various small molecules. Traditional approaches for strain development or analysis are, however, typically based on bulk measurements, which do not interface with high-throughput technologies and provide average data for the whole population. Current efforts in the field of biotechnology aim at the development of novel techniques enabling the detection and quantification of metabolites in single microbial cells.

In the present work, a genetically-encoded single cell biosensor was developed, which enables the detection of L-methionine and the branched-chain amino acids in the industrial amino acid producer *Corynebacterium glutamicum*. The principal design of the biosensor is based on the native Lrp-BrnFE module of *C. glutamicum*. In response to cytosolic accumulation of L-methionine and the branched-chain amino acids, the transcriptional regulator Lrp was shown to activate expression of the *brnFE* operon, encoding the transport system for these amino acids. For the construction of the biosensor, a sensor module including *lrp*, the intergenic region of *lrp* and *brnF*, and a transcriptional fusion of *brnF* to the reporter gene *eyfp* was designed. Characterization of the biosensor performance features revealed the highest sensitivity of the Lrp-sensor towards L-methionine followed by L-leucine, L-isoleucine, and L-valine. In the case of L-methionine, the minimal linear range of detection extended from <1 mM up to 25 mM (>78-fold dynamic range) and, thus, covered a range, which is relevant to the development of production strains.

In the following, the biosensor was implemented in FACS-(fluorescence-activated cell sorting) based high-throughput screenings of *C. glutamicum* mutant libraries for the isolation of amino acid producing strains. A secondary uHPLC screen for the measurement of amino acid levels in the supernatant of isolated strains revealed about 20% positive clones producing branched-chain amino acids. Further screening attempts, aiming in particular at the isolation of L-methionine producing mutants, emphasized the strong impact of the strain background, medium composition, and FACS gating strategy on the screening outcome. For example, screening of mutagenized *C. glutamicum* Δ*mcbR*, lacking the master regulator of L-methionine and L-cysteine synthesis, resulted in about 50% positive clones, which exhibited at least a 100% improvement in L-methionine production in comparison to the parental strain (up to 8 mM). Whole genome sequencing of selected mutants revealed mutations in genes contributing to L-methionine biosynthesis as well as in pathways supplying building blocks, precursors (C_1- and sulfur metabolism), redox power (pentose phosphate pathway), and transcriptional regulators involved in the control of sulfur utilization (SsuR and CysR).

In further studies the Lrp-sensor was successfully applied for online monitoring of L-valine production strains based on pyruvate dehydrogenase-deficient *C. glutamicum* strain Δ*aceE* and was shown to provide information with respect to production start and course of metabolite production over time. Furthermore, the sensor was suitable to reveal different levels of productivity in basic as well as in high yield production strains. In order to investigate the phenotypic structure of L-valine production strains, isogenic microcolonies of *C. glutamicum* strains were grown under constant environmental cultivation conditions in microfluidic chip devices. The studies displayed cell-to-cell variation with respect to cell size, doubling time, and metabolite production, which significantly depends on the particular growth conditions. Altogether, the obtained results emphasize suchlike sensor systems as convenient and valuable tool for strain development and single cell analysis and reveal versatile applications for future studies.

1.2. Summary German

Seit Beginn des 20. Jahrhunderts werden Mikroben erfolgreich zur Produktion von verschiedenen Molekülen eingesetzt. Traditionelle Methoden in der Stammentwicklung oder Analyse basieren jedoch auf Messungen, welche nicht mit Hochdurchsatz-Technologien kompatibel sind und lediglich Durchschnittswerte der gesamten Population liefern. Gegenwärtige Bemühungen auf dem Feld der Biotechnologie verfolgen die Entwicklung von neuen Technologien, welche die Detektion und Quantifizierung von Metaboliten auf Einzelzellebene ermöglichen.

In der vorliegenden Arbeit wurde ein genetisch-kodierter Biosensor entwickelt, welcher die Detektion von L-Methionin und den verzweigtkettigen Aminosäuren in dem industriell eingesetzten Aminosäure-Produzenten *Corynebacterium glutamicum* ermöglicht. Das Design des Biosensors beruht auf dem nativen Lrp-BrnFE Modul aus *C. glutamicum.* Bei intrazellulärer Akkumulation von L-Methionin oder den verzweigtkettigen Aminosäuren aktiviert der Transkriptionsregulator Lrp die Expression der *brnFE* Gene, welche für das Transportsystem für die zuvor genannten Aminosäuren kodieren. Zur Konstruktion des Biosensors wurde ein Modul gebaut, welches *lrp*, die intergene Region zwischen *lrp* und *brnFE* sowie eine transkriptionelle Fusion von *brnFE* mit dem Reportergen *eyfp* umfasst. In Charakterisierungsstudien zeigte der Lrp-Biosensor die höchste Affinität gegenüber L-Methionin gefolgt von L-Leucin, L-Isoleucin und L-Valin. Hierbei reichte der minimale Bereich zur linearen Detektion von L-Methionin von <1 mM bis 25 mM (>78-facher dynamischer Messbereich), welcher somit den Messbereich abdeckte, der für die Entwicklung von Produktionsstämmen relevant ist. Im Folgenden wurde der Biosensor in FACS- (fluorescence-activated cell sorting) basierten Hochdurchsatz *Screenings* von *C. glutamicum* Mutanten-Bibliotheken zur Isolation von Aminosäure-produzierenden Stämmen eingesetzt. Ein zweites uHPLC *Screening* zur Messung der Aminosäurekonzentration im Überstand der isolierten Stämme, ergab 20% positive Klone, welche eine Produktion der verzweigtkettigen Aminosäuren zeigten. Weitere *Screening* Versuche, welche insbesondere die Isolation von L-Methionin produzierenden Mutanten verfolgten, stellten heraus wie stark der Ausgangsstamm, die Medienzusammensetzung und die FACS *gating* Strategie das *Screening* Resultat beeinflussen. So resultierte zum Beispiel das *Screening* ausgehend von einer *C. glutamicum* Δ*mcbR* Mutanten-Bibliothek in 50% positiven Mutanten, die mindestens eine um 100% gesteigerte L-Methionin Produktion im Vergleich zum Ausgangsstamm zeigten. Die Sequenzierung des vollständigen Genoms dieser Mutanten offenbarte Mutationen in Genen, welche in der Biosynthese von L-Methionin involviert sind, sowie in Genen der Stoffwechselwege zur Bereitstellung von Ausgangssubstraten und Vorläufermolekülen (C_1- und Schwefelmetabolismus) oder Reduktionsenergie (Pentosephosphatweg). Zudem konnten auch Mutationen in Genen identifiziert werden, die für die Transkriptionsregulatoren des Schwefelstoffwechsels, CysR und SsuR, kodieren. In weiteren Studien wurde der Lrp-Sensor erfolgreich zum *Online Monitoring* in L-Valin Produktionsstämmen eingesetzt, bei welchen er Information über den Produktionsstart sowie über den zeitlichen Verlauf der Produktion lieferte. Desweiteren eignete sich der Sensor dazu verschiedene Produktionslevel in einfachen und leistungsstarken Produktionsstämmen aufzuzeigen. Um die komplexe Populationsstruktur von L-Valin Produktionsstämmen näher zu untersuchen, wurden weitere Versuche in Mikrofluidik-Vorrichtungen durchgeführt, welche konstante Kultvierungsbedingungen bieten. Diese Untersuchungen zeigten Heterogenitäten auf Einzelzellebene in Bezug auf die Zellgröße, Verdopplungszeit sowie die Metabolitproduktion, welche sehr stark von den Kultivierungsbedingungen abhängig waren. Zusammenfassend stellen diese Arbeiten Biosensoren als geeignetes und nützliches Werkzeug zur Einzelzell-Analyse und Stammentwicklung heraus und zeigen deren vielseitige Applikationen für künftige Studien.

2 Introduction

2.1. *Corynebacterium glutamicum* - A versatile microbial factory

In the search for L-glutamate-producing bacteria Udaka and Kinoshita isolated the facultative anaerobic, Gram-positive soil bacterium *Corynebacterium glutamicum* in 1957 (Kinoshita *et al.*, 1957). With this important discovery amino acid fermentation industry and a remarkable success story was born. Today *C. glutamicum* represents one of the most important platform organisms in industrial biotechnology contributing to an annual production of 2.6 million metric tons of L-glutamate and 1.5 million metric tons of L-lysine (Ajinomoto Co., 2012; Ajinomoto Co., 2011). Due to its significant industrial importance, the genome of *C. glutamicum* was sequenced and published to date in three independent projects (Yukawa *et al.*, 2007; Kalinowski *et al.*, 2003; Ikeda & Nakagawa, 2003). This set a milestone in research of this organism since it prepared the ground for the development of new molecular tools such as targeted gene deletion and replacement or the construction of various vectors for cloning and expression. Furthermore, the development of new powerful *omic* techniques, including transcriptomic, proteomic, metabolomic, and fluxomic analysis, allow systems level investigations of this important platform organism and enabled the integration of synthetic biology approaches into metabolic engineering of *C. glutamicum* (Becker & Wittmann, 2012; Vertès *et al.*, 2012). A detailed summary of the current knowledge of physiology and pathway regulation in *C. glutamicum* is provided in two monographs (Eggeling & Bott, 2005; Burkovski, 2008).

Nowadays, *C. glutamicum* strains are available, engineered for production of a broad spectrum of diverse biotechnological relevant chemicals, materials, and fuels, such as ethanol (Inui *et al.*, 2004a), isobutanol (Blombach *et al.*, 2011; Smith *et al.*, 2010; Blombach & Eikmanns, 2011), 1,2 propanediol (Niimi *et al.*, 2011), 1-butanol and 1-propanol formed as byproduct of isobutanol production (Smith *et al.*, 2010), xylitol (Sasaki *et al.*, 2010), diamines, *e.g.* putrescine (Schneider & Wendisch, 2010) and cadaverine (Mimitsuka *et al.*, 2007; Kind *et al.*, 2011), organic acids, *e.g.* pyruvic (Wieschalka *et al.*, 2012), lactic (Okino *et al.*, 2008b; Inui *et al.*, 2004b), 2-ketoisovaleric (Krause *et al.*, 2010), and succinic acid (Litsanov *et al.*, 2012a; Litsanov *et al.*, 2012b; Okino *et al.*, 2008a), pantothenate (Hüser *et al.*, 2005), and polymers, *e.g.* poly-3-hydroxybutyrate (Jo *et al.*, 2006; Matsumoto *et al.*, 2011).

Post-genomic approaches using rational engineering for strain improvement additionally contributed to high yield amino acid production of L-glutamate (Sawada *et al.*, 2010), L-lysine (Ikeda *et al.*, 2006; Becker *et al.*, 2011), L-alanine (Jojima *et al.*, 2010), L-serine (Lai *et al.*, 2012; Peters-Wendisch *et al.*, 2005), L-valine (Blombach *et al.*, 2008; Hasegawa *et al.*, 2013), aromatic amino acids (Ikeda, 2006; Zhao *et al.*, 2011; Li *et al.*, 2009) and even non-proteinogenic amino acids (Stäbler *et al.*, 2011).

While L-glutamate is mainly used as flavor enhancer and L-aspartic acid together with L-tryptophan for production of the artificial sweetener aspartame, applications of further amino acids are the pharmaceuticals and cosmetics industry as well as the medical sector, where they are mainly supplied in infusion solutions (Leuchtenberger *et al.*, 2005). The largest market of amino acids, however, represents the fast growing animal feed industry. In order to improve feed efficiency and to enhance animal growth, essential amino acids, in particular L-lysine, D/L-methionine, L-threonine, and L-tryptophan, have to be supplied as feed additives in animal farming. Here, L-methionine represents the first limiting amino acid in the nutrition of poultry. On the basis of an increasing consumption of animal protein, poultry in particular, the global world market for L-methionine as a food additive is expected to grow by 2% over the next decade (Novus International, 2010). Currently, about 685-700 kilo metric tons of D/L-methionine are produced on a petrochemical basis (Novus International, 2010). Despite its great demand, no fermentative production process could be established for L-methionine so far, which is in contrast to all other industrially relevant amino acids produced at large-scale. Since *C. glutamicum* proved as versatile cell factory for overproduction of amino acids, several efforts focused on engineering of this organism to set up a competitive biotechnological process for microbial production of L-methionine (Kumar & Gomes, 2005).

2.2. Biosynthesis of L-methionine in *C. glutamicum*

L-methionine synthesis represents a challenging target as it is strictly regulated at the transcriptional as well as at the enzymatic level. Moreover, it demands incorporation of reduced sulfur and precursors from C_1-metabolism which requires high energy cost (7 mol ATP and 8 mol NADPH) and makes it the most expensive amino acid for the cell (Neidhardt *et al.*, 1990; Figge, 2007). In *C. glutamicum* the aspartate family of amino acids comprises L-methionine, L-lysine, L-threonine, and L-isoleucine. The biosynthetic pathway of L-methionine and L-threonine share the first reactions steps transforming L-aspartate to L-

homoserine, which is catalyzed by the aspartate kinase (*lysC*), aspartate semialdehyde dehydrogenase (*asd*) and homoserine dehydrogenase (*hom*) (Figure 1). Homoserine transacetylase (*metX*) catalyzes the first specific reaction towards L-methionine synthesis by activation of the γ-hydroxyl group of L-homoserine *via* acetylation (Park *et al.*, 1998). The next step presents the incorporation of reduced sulfur, which is accomplished in two parallel pathways in *C. glutamicum*. Acetyl-homoserine sulfhydrylase (*metY*) directly catalyzes the synthesis of L-homocysteine from *O*-acetyl-L-homoserine and hydrogen sulfide (Hwang *et al.*, 2002). Alternatively, cystathionine γ-synthase (*metB*) catalyzes the γ-replacement reaction of *O*-acetyl-L-homoserine and L-cysteine, forming γ-cystathionine (Hwang *et al.*, 1999; Hwang *et al.*, 2002). Cystathionine-β-lyase (*aecD/metC*) cleaves the C-S bond of γ-cystathionine yielding L-homocysteine, pyruvate and ammonia (Kim *et al.*, 2001; Rossol & Pühler, 1992). The terminal step in L-methionine synthesis is the transfer of the C_5-methyl group to L-homocysteine, which is catalyzed by cobalamin (B_{12})-independent methionine synthase (*metE*) or alternatively by cobalamin (B_{12})-dependent methionine synthase (*metH*) (Rückert *et al.*, 2003). Methyl groups are provided by N^5,N^{10}-methylenetetrahydrofolate reductase (*metF*) an enzyme that reduces N^5,N^{10}-methylenetetrahydrofolate (CH_2–THF) to CH_3–THF (Rückert *et al.*, 2003). In turn, N^5,N^{10}-methylenetetrahydrofolate is formed by transfer of a methylene group from L-serine to tetrahydrofolate catalyzed by serine hydroxymethyltransferase *(glyA)*.

Apart from its role in protein biosynthesis, L-methionine is degraded to yield *S*-adenosyl-methionine (SAM), which is the central donor for methyl groups in the cell, *e.g.* for methylation of DNA (Schäfer *et al.*, 1997; Cantoni, 1953; Lu, 2000). SAM is formed by adenylation of L-methionine catalyzed by methionine adenosyltransferase encoded by *metK* (Grossmann *et al.*, 2000).

The transport of L-methionine in *C. glutamicum* has been studied in detail by the group of Reinhard Krämer. Import of L-methionine is accomplished by the high affinity ABC transporter MetQNI and a secondary uptake system MetP which is characterized by a lower affinity (Trötschel *et al.*, 2008). BrnFE, originally described for export of the branched-chain amino acids, L-leucine, L-isoleucine, and L-valine (Kennerknecht *et al.*, 2002), was identified as the dominant export system for L-methionine (Trötschel *et al.*, 2005). However, studies provided evidence for a second transporter with low affinity but high capacity, which has not been identified so far.

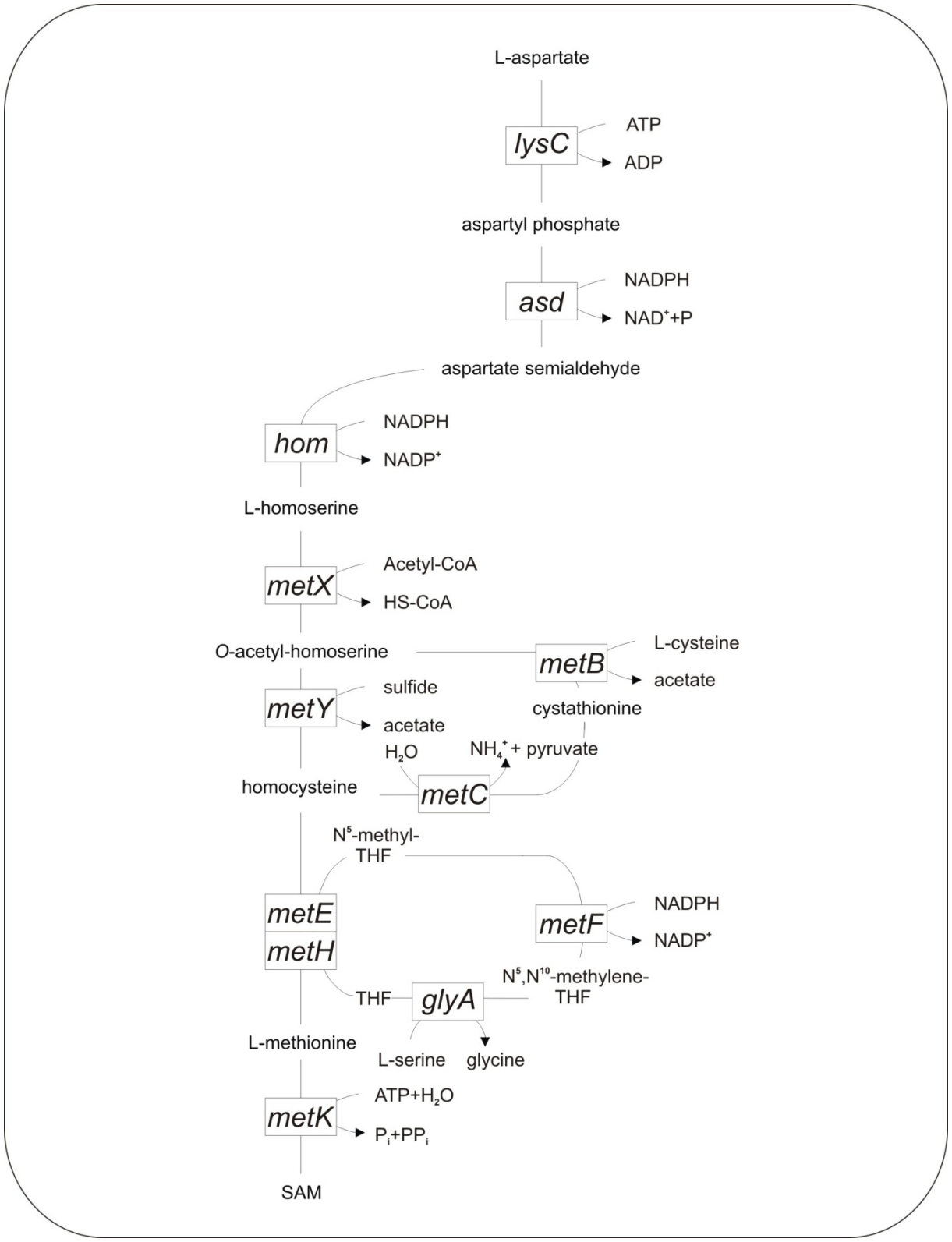

Figure 1. L-methionine biosynthesis in *C. glutamicum.*

2.3. Strategies for strain development

The high diversity of microbes provides a broad spectrum of metabolic pathways and platforms for the production of valuable products. However, naturally or microbially produced metabolite amounts are in general too low and do not exceed levels required for cellular growth and maintenance. Thus, efficient strategies for strain engineering and development are required to enhance metabolic capabilities of microbes for successful overproduction of target metabolites and to establish biotechnological production processes which are economically competitive to petrochemical-based production. Traditionally, approaches for strain improvement relied on random mutagenesis using chemical mutagens (*e.g.* alkylating agents, base analogs) or physical mutagenesis (*e.g.* UV-radiation, X- or gamma rays) and an appropriate and efficient selection strategy for the isolation of promising clones among millions of cells (Parekh *et al.*, 2000). Iterative mutagenesis and screening procedures were applied, until a strain with the maximal, desired productivity and yield was obtained.

Two decades ago advanced genetic engineering methods enabled strategies of strain development to shift to a more rational design, termed metabolic engineering (Bailey, 1991; Stephanopoulos & Vallino, 1991). By definition "*Metabolic engineering is the directed improvement of product formation or cellular properties through the modification of specific biochemical reaction(s) or introduction of new one(s) with the use of recombinant DNA technology*" (Stephanopoulos *et al.*, 1998). In contrast to classical strain development, precise modifications were implemented to construct well-defined genetic backgrounds. Application of molecular biology and DNA recombination techniques allowed the targeted introduction of genetic changes by *e.g.*, heterologous expression of genes in new host organisms, deletion or overexpression of endogenous genes or modulation of enzymatic activities (Koffas *et al.*, 1999; Adrio & Demain, 2006). Further manipulations were carried out once the physiological and biochemical impact of first implemented genetic modifications was thoroughly assessed. In order to redirect or enhance fluxes towards the target metabolite, the focus extended from the analysis of individual reactions to metabolic flux analysis of entire pathways considering pathway synthesis, thermodynamic feasibility, pathway flux and its control (Stephanopoulos, 1999). In the post-genomic era, strain improvement strategies extensively applied powerful *omic*-techniques to consider modifications based on an expanded view of the cell and a systematic understanding of the broad molecular landscape (Yadav *et al.*, 2012; Stephanopoulos *et al.*, 2004; Alper & Stephanopoulos, 2004).

Metabolic engineering as well as classical strain development, including random mutagenesis, screening and selection, have written remarkable success stories represented in the production of antibiotics, amino acids, organic acids, vitamins, nucleotides and biofuels in the last decades (Figure 2) (Wendisch, 2007; Alper & Stephanopoulos, 2009; Leuchtenberger *et al.*, 2005; Lee *et al.*, 2009; Marienhagen & Bott, 2013).

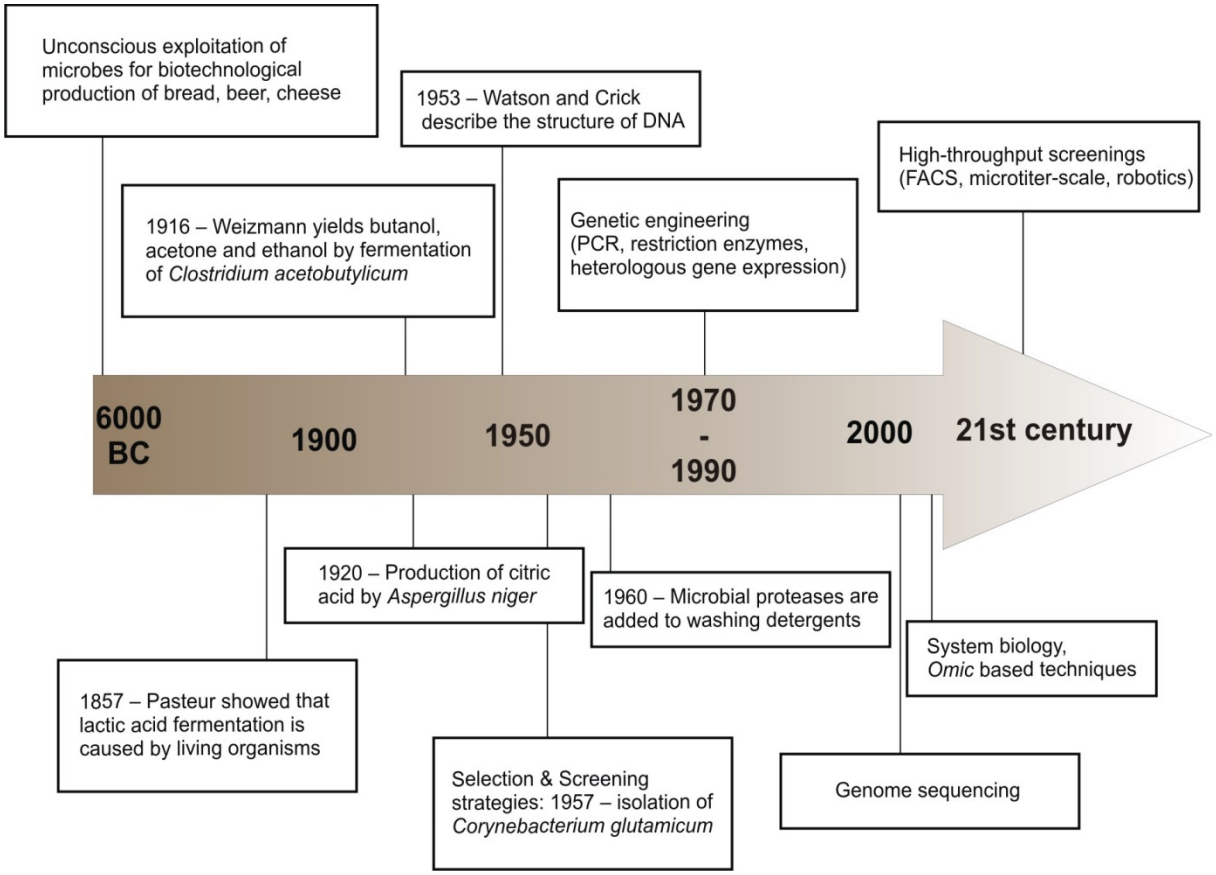

Figure 2. Timeline: Biotechnology.

2.4. Genetically-encoded biosensors

Current efforts in industrial biotechnology aim for the development of new techniques enabling the detection and quantification of specific metabolites at the single cell level. Since the discovery and popularization of autofluorescent proteins two decades ago, significant progress towards single cell interrogation has been made by the use of fluorescent tags enabling the measurement of expression profiles and protein localization with single cell resolution. However, only a few studies report on the visualization of metabolites. This, in fact, represents a unique challenge considering their rapid dynamics compared to proteins in cellular environments. In this context, the use of genetically-encoded biosensors, transforming the specific and sensitive detection of inconspicuous, small molecules into an optical readout (*e.g.* fluorescence output), provides a powerful toolbox for the visualization of metabolites in single bacterial cells. In the last 10-20 years, extensive research contributed to the development of an ever-expanding number of biosensors allowing monitoring of small molecules with single cell resolution. Various classifications of biosensors are described and resumed in several reviews as for example based i) on the source of signal (*e.g.* small or macromolecules, pH, temperature, light) (Zhang & Keasling, 2011), ii) the sensory device used (*e.g.* RNA, proteins) (Michener *et al.*, 2012) or iii) biosensors design and application (van der Meer & Belkin, 2010; Dietrich *et al.*, 2010).

Nature provides an extensive repertoire of sensor devices in form of *e.g.* riboswitches, RNA-aptamers, transcription factors, and enzymes to detect a broad spectrum of metabolites. Sensor constructs which are based on these devices linked to fluorescence proteins enable the detection of small, inconspicuous molecules by providing an optical readout. In the following three categories of genetically-encoded biosensors using different types of sensor devices will be outlined.

RNA-based biosensors use natural or engineered RNA switches as the key biosensor component. Typically, RNA switches consist of an input domain, *i.e.* an RNA aptamer, and an output domain, an RNA gene regulatory component *e.g.* ribozyme. Win *et al.* described a xanthine sensing RNA-switch, which allows correct folding of only one domain at any given time (Win & Smolke, 2007). In response to effector binding, the modular assembly of RNA switches enables stringent control of target gene expression. In principle, the output domain cleaves itself once it is correctly folded. As a result the mRNA of the target gene is degraded. Binding of the effector molecule, however, stabilizes proper folding of the RNA aptamer and prevents folding of the output domain. For biosensor construction the RNA switch can be

placed upstream of a fluorescent reporter gene, thus binding of the effector molecule results in increased reporter gene expression (Michener & Smolke, 2012; Michener *et al.*, 2012).

Biosensors, based on transcriptional regulators, represent a further class of biosensors which can be used for the design of a regulatory circuit where the expression of a reporter gene is under direct control of the metabolite-sensing regulator. Typically, transcription factors undergo a molecular switch upon ligand binding resulting in transcriptional activation of the cognate regulatory DNA element. Transcriptional or translational fusion of the target promoter to a promoterless fluorescent reporter gene provides in turn, a measurable optical readout, which displays cytosolic accumulation of the effector molecule.

FRET-based biosensors (förster (fluorescence) resonance energy transfer) represent well established sensor systems which exploit the molecular recognition specificity of several protein classes. Typically, in FRET-based sensors an acceptor and donor domain within the same protein or of two different proteins are linked to a pair of fluorophores differing in their emission and excitation wavelengths. Binding of the target molecule conducts conformational changes of the sensor domain bringing donor and acceptor fluorophore in close vicinity, and thus leading to FRET (Frommer *et al.*, 2009; Okumoto *et al.*, 2012).

In the last decades, biosensors, based on transcriptional regulators, have been extensively exploited in microbial sensing systems for the detection of environmental pollutants (van der Meer & Belkin, 2010; Harms *et al.*, 2006). Whereas FRET-based or RNA-based biosensors have been applied in studies mainly focusing on fundamental biological questions by specific detection of several molecule classes such as sugars, ions, vitamins, antibiotics and many more not noted herein (Okumoto *et al.*, 2012; Michener *et al.*, 2012). In industrial biotechnology the great potential of biosensors for the detection and quantification of small molecules at single cell resolution has not been harnessed so far. However, some striking studies in the group of C. Smolke highlight RNA-based sensors as powerful tool for screening of biotechnologically interesting molecules (Michener & Smolke, 2012; Michener *et al.*, 2012). Overall, the implementation of the different types of biosensors might facilitate high-throughput screenings in future, and thus contributes to new breakthroughs in microbial strain development.

2.5. Population heterogeneity in bacterial monocultures

Nowadays, phenotypic variation within clonal populations of bacterial cells is a well-described and accepted phenomenon. New technologies facilitating single cell measurement such as flow cytometry and technical advances in automated microscopy and lab-on-chip devices have provided fundamental new insights into population dynamics (Diaz *et al.*, 2010; Tracy *et al.*, 2010; Müller & Nebe-von-Caron, 2010; Schmid *et al.*, 2010; Szita *et al.*, 2010; Gulati *et al.*, 2009; Fritzsch *et al.*, 2012; Vinuselvi *et al.*, 2011). Classical examples for phenotypical heterogeneity observed in bacterial populations are, for example, chemotaxis in *Escherichia coli*, genetic competence, motility and sporulation of *Bacillus subtilis* or the occurrence of persister cells upon antibiotic treatment (Korobkova *et al.*, 2004; Maamar *et al.*, 2007; Haijema *et al.*, 2001; Kearns, 2005; Gonzalez-Pastor *et al.*, 2003; Balaban *et al.*, 2004). Phenotypical heterogeneity can have diverse origins such as differences in cell age or cell cycle, or simply stochastic effects in gene expression (Lidstrom & Konopka, 2010; Elowitz, 2002; Cai *et al.*, 2006; Kærn *et al.*, 2005; Müller *et al.*, 2010).

Random fluctuations in biochemical reactions result in a stochastic variation, so-called noise. Noise is regarded as a key determinant for cell-to-cell variation within clonal populations. Stochastic fluctuations are notably enhanced when the number of involved reactants is small. Therefore, in particular gene expression is influenced by stochasticity, due to the typically low number of transcription factor molecules in the cell (Kærn *et al.*, 2005; Swain *et al.*, 2002). Amplification of a noisy signal by positive feedback can result in bimodal distribution in gene expression referred as bistability. In response to environmental changes, some genes may exhibit a bistable expression resulting in the formation of two distinct subpopulations, which display altered phenotypic traits within a clonal population (Dubnau & Losick, 2006; Veening *et al.*, 2008).

"Randomization of phenotype", *i.e.* cell-to-cell variation within genetically identical populations and occurrence of subpopulations are considered to be beneficial for the population in unpredictable environments, since distinct phenotypes might be pre-adapted or allow rapid adaption to sudden changes in environment (Acar *et al.*, 2008; Kussell & Leibler, 2005). Despite the knowledge of its common occurrence, little attention is paid to the phenomenon of population heterogeneity in biotechnological processes. Obviously, cell-to-cell variation in regard to physiological states and productivity and the formation of inefficient subpopulations within a production culture can adversely affect production processes (Lencastre Fernandes *et al.* 2011; Müller *et al.* 2010). Particularly in large-scale

bioreactors, cell cultures are confronted with environmental heterogeneity during cultivation, such as gradients in oxygen, pH, or carbon source concentration (Lara *et al.*, 2006; Liden, 2002; Takors, 2012; Hewitt & Nienow, 2007; Enfors *et al.*, 2001). Nevertheless, optimization strategies for bioprocesses still rely on the measurement and interpretation of average data, which obviously mask cell-to-cell variation and give no information about the complex phenotypic structure of microbial populations. Thus, biological phenomena might be misinterpreted and result in wrong decisions regarding further improvement strategies for production process and strain engineering (Figure 3) (Lidstrom & Konopka, 2010). The key challenge to finally perform efficient microbial bioprocesses in future, hence, demands on in-depth investigations and detailed understanding of complex phenotypical structures of biotechnological production strains (Müller *et al.*, 2010; Lencastre Fernandes *et al.*, 2011).

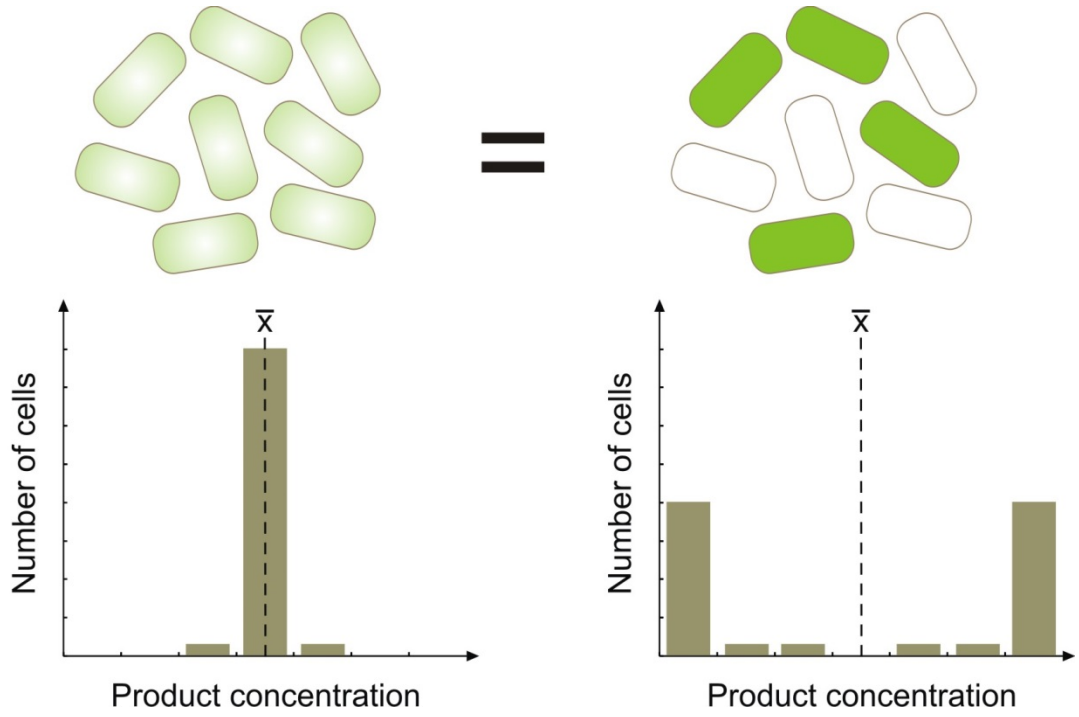

Figure 3. Measurement of populations average does not allow to distinguish between a production process where all cells are averagely producing (left) from one where some cells are highly or not producing (right) (adapted from Lidstrom & Konopka, 2010).

2.6. Aims of this work

The first aim of this work was the development of a single cell biosensor capable of detecting cytosolic amino acid accumulation in *C. glutamicum*. For this purpose, the transcriptional regulator Lrp (leucine-responsive protein) was chosen as a potential "sensor protein". Previous studies suggested that *C. glutamicum* Lrp might respond to elevated cytosolic amounts of the branched-chain amino acids and L-methionine. To provide a basis for sensor construction, promoter binding and effector molecule specificity of Lrp has to be analyzed in detail. Once a convenient sensor is constructed, the capability of the biosensor to distinguish between increased and wild type levels of cytosolic amino acid concentrations has to be assessed. To enhance artificially the intracellular concentration of effector amino acids, the previously well-described feeding strategy can be applied to *C. glutamicum* wild type cells containing the biosensor. Supplied dipeptides are uptaken and hydrolysed by *C. glutamicum* increasing the intracellular pool of free amino acids.

In order determine under which conditions the biosensor performs robust and reproducible measurements, a calibration of the biosensor has to be performed which describes the relation between input, *i.e.* cytosolic amino acid concentration, and output signal, *i.e.* specific fluorescence signal of the cells. Here, again the dipeptide feeding strategy can be applied to calibrate intracellularly different amino acid concentrations. In order to measure the fluorescence output of the cells, experiments could be performed in a microplate reader capable of fluorescence measurements. Various applications of the biosensor are conceivable in approaches aiming for strain development and screening strategies in industrial biotechnology. For example, the biosensor can be implemented in FACS (fluorescence-activated cell sorting) based high-throughput screenings of *C. glutamicum* mutant libraries. Cells which show an increased production of the effector amino acids after *e.g.* random mutagenesis should exhibit a higher fluorescence signal compared to non-producing mutants. Thus, rapid screening of these cells and accurate isolation *via* FACS is enabled. Further, the biosensor can be applied to monitor amino acid formation in *C. glutamicum* production strains in live cell imaging studies. For this, the sensor can be integrated into available L-valine production strains of *C. glutamicum.* Biosensor-based live cell imaging of these strains, cultivated in microfluidic devices, should allow investigation of single cell growth and productivity in a time-resolved manner.

3 Results

The major topic of this PhD thesis was the development and application of a single cell biosensor for detection of L-methionine and branched-chain amino acids in *C. glutamicum*. The results allocated to this research field have been summarized in three publications and two further manuscripts which will be submitted in near future.

The first publication "Lrp of *Corynebacterium glutamicum* controls expression of the *brnFE* operon encoding the export system for L-methionine and branched-chain amino acids" describes the analysis of the transcriptional control of the *brnFE* operon in *C. glutamicum* by the transcriptional regulator Lrp. My contribution to this work was essentially the investigation of the promoter binding of Lrp and the influence of putative effector molecules on Lrp binding affinity. In electrophoretic mobility shift assays, the transcriptional regulator Lrp was shown to bind to the intergenic region between *lrp* and *brnFE* and to activate transcription of *brnFE* in the presence of increased levels of branched-chain amino acids or L-methionine. Thus, Lrp controlled activation of BrnFE avoids inhibitory effects of intracellular amino acid accumulation. These data and further results on expression analysis of *brnFE* obtained in the group of our collaboration partner Prof. V. Wendisch (University of Bielefeld, Germany) were published in the above mentioned publication.

Based on the transcriptional regulator Lrp, a novel single cell biosensor was developed, which enables the intracellular detection of L-methionine and branched-chain amino acids at single cell resolution and transforms this information into an optical readout (eYFP fluorescence). This work was presented in the publication "The development and application of a single-cell biosensor for the detection of L-methionine and branched-chain amino acids". A detailed characterization of the biosensor revealed highest sensitivity for L-methionine followed by L-leucine, L-isoleucine and L-valine; a linear relationship of fluorescence output and intracellular concentrations of the effector amino acids was observed. The biosensor was successfully implemented in FACS-based high-throughput screenings for the enrichment of amino acid producing bacteria and was applied in first live cell imaging studies of *C. glutamicum* in microfluidic chip devices.

Fluorescent proteins are used as versatile tools to report on gene expression or protein localization. However, the extreme high stability of native fluorescent proteins (GFP > 24 h) hampers dynamic measurements. In order to provide valuable tools for the monitoring of dynamic gene expression in *C. glutamicum*, unstable variants of the GFP derivate GFPuv and

eYFP were presented in the article "Destabilized eYFP variants for dynamic gene expression studies in *Corynebacterium glutamicum*". SsrA-mediated peptide tagging was used to construct destabilized fluorescence proteins with significantly reduced half-lives. First application of the unstable eYFP variants in transient gene expression studies showed their general suitability for dynamic measurements. This study was performed under my supervision within the diploma thesis of Eva Hentschel. Results obtained by the group of Prof. A. Burkovski on destabilization of GFP were obtained within the master thesis of Conni Will and also included in the abovementioned report.

Since L-methionine is currently of major interest for biotechnological strain development, further studies focused on adaption of the biosensor-based screening procedure to isolate in particular L-methionine producing mutants. For this reason, mutant libraries based on different strain backgrounds, harboring genetic modifications assumed to be beneficial for L-methionine production, were screened in following studies. The manuscript "L-methionine producing mutants of *Corynebacterium glutamicum* isolated by biosensor-based high-throughput screening" describes the successful isolation of L-methionine producing strains. The best mutant strains were found to accumulate up to 8 mM L-methionine in the supernatant. Whole genome sequencing of selected mutant strains revealed novel mutations in genes of central metabolism and pathways contributing to L-methionine biosynthesis.

First application of the Lrp-biosensor in live cell imaging studies revealed variations in doubling time, cell size, and most interestingly, single cell productivity in *C. glutamicum* Δ*aceE* during L-valine production. The manuscript "Application of a genetically-encoded biosensor for the single cell analysis of *Corynebacterium glutamicum* L-valine production strains" describes in depth investigation of phenotypic structure in gradually engineered *C. glutamicum* L-valine production strains based on *C. glutamicum* Δ*aceE.* In order to access population dynamics during production processes, multiparameter FACS analysis of fed-batch cultures cultivated in lab-scale bioreactors were performed as well as live cell imaging studies of cells grown in microfluidic devices.

The last part of this section is a book chapter with the title "Development and application of genetically-encoded biosensors for strain development and single cell analysis of *Corynebacterium glutamicum*" which will be published in "*Corynebacterium glutamicum*: Systems Biology, Biotechnological Applications and Control" edited by Prof. A. Burkovski. This article introduces the general design and characterization of biosensor performance features focusing on sensors which are based on regulatory circuits. Furthermore, an overview

of currently available *C. glutamicum* biosensors and their application in biosensor-driven strain development and single cell analysis is provided.

Journal of Biotechnology 158 (2012) 231–241

Contents lists available at ScienceDirect

Journal of Biotechnology

journal homepage: www.elsevier.com/locate/jbiotec

Lrp of *Corynebacterium glutamicum* controls expression of the *brnFE* operon encoding the export system for L-methionine and branched-chain amino acids

Christian Lange[a,1], Nurije Mustafi[a], Julia Frunzke[a], Nicole Kennerknecht[a,2], Mirja Wessel[a,3], Michael Bott[a], Volker F. Wendisch[b,*]

[a] Institut für Bio- und Geowissenschaften, IBG-1: Biotechnologie, Forschungszentrum Jülich, D-52425 Jülich, Germany
[b] Chair of Genetics of Prokaryotes, Bielefeld University, D-33615 Bielefeld, Germany

ARTICLE INFO

Article history:
Received 13 January 2011
Received in revised form 13 May 2011
Accepted 1 June 2011
Available online 12 June 2011

Keywords:
Corynebacterium glutamicum
Leucine responsive protein
Amino acid production
Lrp family trasncriptional regulators
Regulation of transport of branched-chain amino acids

ABSTRACT

Corynebacterium glutamicum possesses export systems for various amino acids including BrnFE, a two-component export system for L-methionine and the branched-chain amino acids L-valine, L-isoleucine and L-leucine. A gene for a putative transcriptional regulator of the Lrp family is transcribed divergently to the *brnFE* operon and is required for L-isoleucine export. By comparing global gene expression changes due to L-isoleucine addition we revealed increased *brnFE* expression in response to L-isoleucine in *C. glutamicum* wild type but not in an *lrp* deletion mutant. ChIP-to-chip analysis, band shift experiments and DNAse footprint analysis demonstrated that Lrp binds to the intergenic region between *lrp* and *brnF*. Expression analysis of transcriptional fusions with the *lrp* and *brnFE* promoters indicated that branched-chain amino acids and L-methionine when added to the growth medium stimulated *brnFE* expression in the order L-leucine > L-methionine > L-isoleucine > L-valine and that Lrp was required for activation of *brnFE* expression. Thus, regulation of *brnFE* by Lrp ensures that BrnFE is synthesized only if its substrate amino acids accumulate in cells which is commensurate with its role to counteract such situations of metabolic imbalance.

1. Introduction

The Gram-positive soil bacterium *Corynebacterium glutamicum* is used industrially for the production of over 2,160,000 tons of L-glutamate and over 1,330,000 tons of L-lysine per year (www.ajinomoto.co.jp/ir/pdf/fact/Feed-useAA-Oct2010.pdf). This bacterium has also been engineered for the production of other amino acids such as L-serine (Peters-Wendisch et al., 2005), L-isoleucine (Morbach et al., 1996) or L-valine (Blombach et al., 2007; Radmacher et al., 2002) or of products derived from amino acids and their precursors such as 1,4-diaminobutane (Schneider and Wendisch, 2010) or 1,5-diaminopentane (Kind et al., 2010; Mimitsuka et al., 2007) and 2-ketoisovalerate (Krause et al., 2010). Due to its importance for amino acid production the export of amino acids by *C. glutamicum* has been well characterized on the biochemical and genetic level (Marin and Krämer, 2007). The proteins for export of L-lysine and L-threonine, respectively, were first identified and characterized in *C. glutamicum* and LysE (Vrljic et al., 1996) and ThrE (Simic et al., 2001) are eponymous for the respective protein families (Marin and Krämer, 2007; Vrljic et al., 1999). LysE-mediated export of L-lysine, which cannot be catabolized by *C. glutamicum*, ensures that this amino acid does not accumulate to inhibitory concentrations within the cells (Vrljic et al., 1995; Vrljic et al., 1996). In the absence of LysE, feeding of the dipeptide L-lysyl-L-alanine caused a growth arrest due to intracellular accumulation of L-lysine up to 1.1 M (Vrljic et al., 1996). Under metabolically balanced conditions, i.e. when uptake and synthesis of L-lysine match the anabolic demand for this amino acid, L-lysine excretion would represent wasted metabolic energy. Therefore, synthesis of LysE is controlled by the transcriptional regulator LysG, which is encoded by a gene transcribed divergently to *lysE* (Bellmann et al., 2001). LysG activates expression of *lysE* when the intracellular concentration of one of the basic amino acids L-lysine, L-arginine, L-citrulline or L-histidine exceeds a certain threshold, e.g. a 20-fold activation of *lysE* by LysG was observed at intracellular L-lysine concentrations exceeding 30–40 mM (Bellmann et al., 2001). However, besides L-lysine only L-arginine is a substrate of LysE (Bellmann et al., 2001).

Export of the branched-chain amino acid L-isoleucine has also been characterized in *C. glutamicum* and can be mediated by diffusion or by a proton motive force-driven carrier (Ebbighausen

* Corresponding author at: Chair of Genetics of Prokaryotes, Faculty of Biology & CeBiTec, University of Bielefeld, P.O. Box 100131, D-33501 Bielefeld, Germany. Tel.: +49 521 106 5611; fax: +49 521 106 5626.
E-mail address: volker.wendisch@uni-bielefeld.de (V.F. Wendisch).
[1] Present address: Molekularbiologie, Medizinische Laboratorien Düsseldorf, 40477 Düsseldorf.
[2] Present address: Molekularbiologie, Helios Klinikum, 47805 Krefeld, Germany.
[3] Present address: Evonik, Paul-Baumann-Straße 1, D-45764 Marl, Germany.

0168-1656/$ – see front matter © 2011 Elsevier B.V. All rights reserved.
doi:10.1016/j.jbiotec.2011.06.003

Table 1
Bacterial strains and plasmids used in this study.

Strain or plasmid	Relevant characteristics	Reference
C. glutamicum strains		
ATCC 13032	wild type (WT)	Abe et al. (1967)
C. glutamicum Δ *brnFE*	*brnFE* deletion mutant	Kennerknecht et al. (2002)
C. glutamicum Δ *lrp*	*lrp* deletion mutant	This work
13032*lrp*Strep	WT derivative expressing a C-terminally *Strep*-tagged Lrp obtained by integration of pK19*mobsacB-lrpStrep* into chromosomal *lrp* locus	This work
E. coli strain		
DH5α	F⁻ *thi-1 endA1 hsdr17*(r^-, m^-) *supE44* Δ*lacU169*(*Φ80lacZ*Δ*M15*) *recA1 gyrA96 relA1*	Hanahan (1983)
Plasmids		
pAN3K	Kan^R, derivative of the *E. coli* expression vector pASK-IBA3C (IBA, Göttingen, Germany) for anhydrotetracycline-inducible production of C-terminally Strep-tagged proteins, contains the Kan^R gene and the *C. glutamicum* replicon from pJC1 allowing plasmid replication and gene expression in *C. glutamicum*	Niebisch et al. (2006)
pAN3K-*lrp*	pAN3K derivate for production of C-terminally *Strep*-tagged Lrp	This work
pAN5K	Kan^R, derivative of the *E. coli* expression vector pASK-IBA5C (IBA, Göttingen, Germany) for anhydrotetracycline-inducible production of N-terminally Strep-tagged proteins, contains the Kan^R gene and the *C. glutamicum* replicon from pJC1 allowing plasmid replication and gene expression in *C. glutamicum*	Niebisch et al. (2006)
pAN5K-*lrp*	pAN5K derivate for production of N-terminally *Strep*-tagged Lrp	This work
pET2	promoter probe vector	Vasicova et al. (1998)
pET2-*plrp*	pET2 with a 219 bp fragment of the *lrp–brnF* intergenic region	Kennerknecht et al. (2002)
pET2-*pbrnF*	pET2 with the promoter fragment in divergent orientation to pET2-*plrp*	Kennerknecht et al. (2002)
pK19*mobsacB*	Kan^R, vector for allelic exchange in *C. glutamicum*; (pK19 $oriV_{E.c.}$, *sacB*, *lacZα*)	Schäfer et al. (1994)
pK19*mobsacB*Δ *lrp*	Kan^R, pK19*mobsacB* derivative containing a crossover PCR product covering the up- and downstream regions of *lrp*	This work
pK19*mobsacB-lrpStrep*	pK19*mobsacB* with the C-terminal part (bp 96–bp 453) of *lrp* fused to a C-terminal *Strep*-tag II ([SA]WSHPQFEK)	This work

et al., 1989; Hermann and Krämer, 1996; Kennerknecht et al., 2002; Morbach et al., 1996; Zittrich and Krämer, 1994). This carrier, the two-component permease BrnFE, belongs to the LIV-E transporter family (Eggeling and Sahm, 2003; Marin and Krämer, 2007) together with the AzlCD system for azaleucine-resistance from *B. subtilis* (Belitsky et al., 1997). In *C. glutamicum*, BrnFE is the only carrier for export of L-isoleucine, L-leucine and L-valine (Kennerknecht et al., 2002). BrnFE also exports L-methionine, but is not essential for export of this amino acid in *C. glutamicum* (Trötschel et al., 2005).

Regulation of export of the branched-chain amino acids has not been studied in detail, but is known that high intracellular concentrations of the BrnFE substrate amino acids lead to increased export and *brnF* RNA levels (Hermann and Krämer, 1996; Trötschel et al., 2005). In *Escherichia coli*, export of L-leucine is mediated by *leuE* (Kutukova et al., 2005) and induction of *leuE* by L-leucine is mediated by the leucine-responsive protein Lrp, a global regulator of gene expression in this bacterium (Brinkman et al., 2003; Yokoyama et al., 2006). Whereas Lrp from *E. coli* is a global regulator and its regulon comprises hundreds of genes (Tani et al., 2002), its paralog AsnC in *E. coli* (Kölling and Lother, 1985) and most of its homologs in other organisms such as BkdR in *Pseudomonas putida* (Madhusudhan et al., 1995) are specific regulators of only very few amino acid-metabolism related genes (Brinkman et al., 2003). In *C. glutamicum*, an Lrp-like protein is encoded by a gene transcribed divergently to *brnFE* and the divergent promoters within the 74 bp intergenic region have overlapping −35 promoter regions (Kennerknecht et al., 2002; Patek et al., 2003). For both genes leaderless transcripts are formed as the transcriptional start sites and the first base of the start codon are identical (Patek et al., 2003). Disruption of *lrp* abrogated export of L-isoleucine by *C. glutamicum* (Kennerknecht et al., 2002). While this observation led to the suggestion that Lrp activates BrnFE gene expression (Kennerknecht et al., 2002), gene expression changes due to deletion of *lrp* in *C. glutamicum* could not be observed (Hayashi et al., 2006). Therefore, we aimed at characterizing Lrp-dependent regulation in *C. glutamicum*.

2. Materials and methods

2.1. Bacterial strains, plasmids, media and growth conditions

Bacterial strains and plasmids used in this work are listed in Table 1. *E. coli* was cultivated at 37 °C and *C. glutamicum* at 30 °C. Cultivations in 500-ml baffled shake flasks were agitated at 120 rpm. For the determination of growth rates, chloramphenicol transacetylase (CAT) assays and for analyses of the global gene expression of *C. glutamicum*, a first preculture in 5 ml CGIII medium (Menkel et al., 1989) was inoculated from a fresh LB (Sambrook and Russell, 2001) agar plate and cultivated overnight in a test tube. Cells were harvested and used to inoculate 60 ml CgXII medium (Keilhauer et al., 1993) containing 0.03 g/l protocatechuic acid and 0.2 M glucose. This second preculture was grown overnight in a 500 ml-baffled shake flask. The main culture was inoculated with cells from the second preculture and grown under the same conditions. When indicated, branched-chain amino acids were added to CgXII medium before adjusting the pH and autoclaving. For CAT assays and transcriptome analysis, the CgXII preculture contained the same supplements as the main culture to ensure full adaptation (growth under constant conditions for at least ten generations) and main cultures were harvested in the exponential growth phase as described (Lange et al., 2003). When needed, 25 μg of kanamycin/ml or 20 μg of chloramphenicol/ml was added to the cultivation media.

2.2. Construction of plasmids and strains

E. coli DH5α was used for the construction of plasmids. Genes were amplified by PCR (Expand High Fidelity PCR Kit, Roche, Mannheim, Germany) with genomic DNA of *C. glutamicum* ATCC 13032 as a template (Eikmanns et al., 1994). For ligation of DNA, the Rapid DNA Ligation Kit (Roche, Mannheim, Germany) was used according to the manufacturer's instructions. Plasmids were prepared with the QIAprep Spin Miniprep Kit (Qiagen, Hilden,

Germany) and after checking inserts by DNA sequencing they were transformed to *E. coli* according to (Inoue et al., 1990) or to *C. glutamicum* according to (van der Rest et al., 1999). For the expression of Lrp carrying a C-terminal Strep-tag II (N-(SA)WSHPQFEK-C) in *C. glutamicum* and *E. coli*, the plasmid pAN3K-*lrp* was constructed. For this purpose, *lrp* of *C. glutamicum* was amplified using the primers 5′-ATGGTA**GGTCTCA**AATGAAGCTAGATTCCATTGATCGCGC-3′ (the underlined nt corresponds to nt 276754 of NC003450, the *Bsa*I site is given in bold) and 5′-ATGGTA**GGTCTCA**GCGCTCACCTGGGGGCGAGCTGGTT-3′ (the underlined nt corresponds to nt 276302 of NC003450, the *Bsa*I site is given in bold) and cloned into pAN3K using *Bsa*I sites. Accordingly, pAN5K-*lrp* for the expression of a N-terminally Strep-tagged *lrp* was constructed using the primers 5′-ATGGTA**GGTCTCA**GCGCCATGAAGCTAGATTCCATTGATCGC-3′ and 5′-ATGGTA**GGTCTCA**TATCACACCTGGGGGCGAGCTGGT-3′. For in frame deletion of *lrp* in *C. glutamicum* 13032 the plasmid pK19*mobsacB*Δ*lrp* was constructed according to (Link et al., 1997). The 5′ flanking region of *lrp* was amplified using the primers 5′-GGCG**CCCGGG**GGCGTGCGC-3′ (the underlined nt corresponds to nt 273828 of NC003450, the *Xma*I site is given in bold) and 5′-*CCCATCCACTAAACTTAAACA*AATGGAATCTAGCTTCATATATTGCAC-3′ (the underlined nt corresponds to nt 276737 of NC003450, the linker sequence is given in italics), while primers 5′-*TGTTTAAGTTTAGTGGATGGG*GCTATGAAAGTGGTGAAACCAGCT-3′ (the underlined nt corresponds to nt 276337 of NC003450, the linker sequence is given in italics) and 5′-CCGG**TCTAGA**GGATCCGCAATTCC-3′ (the underlined nt corresponds to nt 275968 of NC003450, the *Xba*I site is given in bold) were used for amplification of the 3′ region of *lrp*. These PCR fragments were amplified in a cross-over-PCR with the shorter primers as described by (Link et al., 1997) and the resulting cross-over-PCR fragment encoding an Lrp derivative with CLSLVDG replacing amino acids 7–139 was cloned into pK19*mobsacB* (Schäfer et al., 1994) using *Xma*I and *Xba*I restriction. Gene deletion mutagenesis with the resulting plasmid pK19*mobsacB*Δ*lrp* was performed as described previously (Peters-Wendisch et al., 1993). PCR with the primers 5′-TTTGCTGCAGGTTTGCGCACCTCAACTAG-3′ (the underlined nt corresponds to nt 276798 of NC003450) and 5′-CATGGGATCCGTCCTTCACTAGATG-3′ (the underlined nt corresponds to nt 276245 of NC003450) was used to verify the deletion of *lrp*. The strain Δ*lrp* was further checked by Southern blot analysis with *Sph*I and *Pst*I fragments of genomic DNA (restriction in the regions flanking *lrp*) and DIG-labelled DNA probes. As expected, an internal *lrp* probe gave a signal in the *C. glutamicum* wild type, not in the *lrp* deletion mutant, while a full-length *lrp* probe detected shorter fragments in Δ*lrp* compared to the wild type (data not shown).

To generate a strain derived from *C. glutamicum* 13032, which expresses C-terminally Strep-tagged Lrp from the genomic *lrp* locus, the plasmid pK19*mobsacB*-*lrp*Strep was constructed. The base pairs 96–453 of *lrp* were amplified using primers 5′-**GAATT**CCGGGACCTTGCTTGAGGAGGG-3′ (the underlined nt corresponds to nt 276659 of NC003450, the *Eco*RI site is given in bold) and 5′-CG**GGATCC***TTATTTTTCGAACTGCGGG-TGGCTCCAAGCGCT*CACCTGGGGGCGA-3′ (the underlined nt corresponds to nt 276302 of NC003450, the *Bam*HI site is given in bold) introducing the Strep-tag II sequence (highlighted in italics). The PCR product was cloned into pK19*mobsacB* using *Eco*RI and *Bam*HI sites. *C. glutamicum* was transformed with the resulting plasmid pK19*mobsacB*-*lrp*Strep, site-specific integration of the plasmid into the *lrp* genomic locus was checked by PCR with the primers 5′-GCGCGAATGCGCGCATCTCA-3′ (the underlined nt corresponds to nt 276711 of NC003450) and 5′-AACTGCGGGTGGCTCCAAGC-3′ which is homologous to the plasmid-encoded Strep-tag II. As expected, only *C. glutamicum* 13032*lrp*Strep yielded a PCR product of the expected size, while no signal was obtained with ATCC 13032 or the plasmid pK19*mobsacB*-*lrp*Strep.

2.3. Global gene expression analysis using C. glutamicum DNA microarrays

The preparation of total RNA was performed as described previously (Lange et al., 2003; Sindelar and Wendisch, 2007; Wendisch, 2003). Isolated RNA samples were analysed for quantity and quality by UV spectrophotometry and denaturing formaldehyde agarose gel electrophoresis (Sambrook et al., 1989), respectively, and stored at −70 °C until use. The production of whole-genome *C. glutamicum* DNA microarrays (Wendisch, 2003), synthesis of fluorescently labelled cDNA from total RNA, hybridization, washing and data analysis were performed as described previously (Ishige et al., 2003; Lange et al., 2003; Polen et al., 2003).

2.4. Identification of DNA sequences bound by Lrp in vivo (ChIP-to-chip analysis)

For the identification of the genomic binding sites of Lrp, we performed *ChIP-to-chip experiments* (Brocker and Bott, 2006; Iyer et al., 2001; Pollack and Iyer, 2002) using *C. glutamicum* 13032*lrp*Strep that expresses a C-terminally Strep-tagged Lrp (LrpStrep) from the genomic *lrp* locus (see above and Table 1). *C. glutamicum* 13032*lrp*Strep and 13032 precultured in 50 ml LB medium in a baffled 500 ml-shake flask overnight were used to inoculate 0.5 l LB in a baffled 2 l-shake flask to a OD_{600} of 0.5. Cells were grown to an OD_{600} of 6.0 and harvested by centrifugation. To crosslink DNA bound by DNA-binding proteins, formaldehyde in a concentration of 1% (v/v) was added to the harvested cells in 10 ml TE buffer (100 mM Tris, 1 mM EDTA, pH 8.0) and the mixture was incubated at room temperature for 20 min under slight agitation. After excessive formaldehyde was inactivated by addition of 125 mM glycine, the formaldehyde-treated cells were collected by centrifugation (10 min, 3500 × *g*, 4 °C), washed twice with 50 ml TE buffer and resuspended in 10 ml TE buffer containing Complete Protease Inhibitor (Roche, Mannheim, Germany). Cell disruption was achieved by 5 passages through a French pressure cell at 172 MPa followed by two sonication steps (30 s, intensity of 1, pulse length of 40%; Sonifier UP200s, Dr. Hielscher GmbH, Teltow, Germany) to reduce the length of protein-bound DNA fragments to about 50–600 bp as judged by gel electrophoresis. Subsequently, Strep-Tactin affinity chromatography was performed for the purification of LrpStrep (see below). The purified, crosslinked DNA–protein complexes in the elution fractions were incubated with 1% (w/v) SDS at 65 °C over night and treated with 20 μg proteinase K (Roche, Mannheim, Germany) at 55 °C for 3 h before DNA was extracted with phenol/chloroform and precipitated with ethanol and sodium acetate (Sambrook and Russell, 2001). The DNA was solved in 100 μl 10 mM Tris–HCl, pH 7.6, 1 mM EDTA, the concentration was determined spectrophotometrically and quality and length of the DNA fragments were checked by agarose gel electrophoresis (Sambrook and Russell, 2001). Two micrograms of DNA purified from 13032*lrp*Strep and from the wild-type control were fluorescently labelled using either FluoroLink Cy3-dUTP or Cy5-dUTP (Amersham Pharmacia, Freiburg, Germany) and the BioPrime DNA Labeling System (Invitrogen, Karlsruhe, Germany) according to the manufacturer's protocol. Inactivation of the enzyme and purification of the labelled DNA probes with Microcon YM-30 filter units (Millipore, Schwalbach, Germany) was performed as described before (Khodursky et al., 2003). Both probes were simultaneously hybridized to a *C. glutamicum* DNA microarray as described before (Lange et al., 2003; Sindelar and Wendisch, 2007; Wendisch, 2003). Higher hybridization signals for the probe obtained from

13032*lrp*Strep than from wild type indicated direct binding of Lrp-Strep to this DNA sequence *in vivo*.

2.5. Purification of Lrp

For the purification of Lrp carrying a C-terminal Strep-tag II (LrpStrep) by Strep-Tactin affinity chromatography (Skerra and Schmidt, 2000), 500 ml LB medium in a 2-l-baffled shake flask was inoculated to an OD_{600} of 0.1 with *E. coli* DH5α(pAN3K-*lrp*) (see above and Table 1) from an overnight pre-culture in 50 ml LB medium (Sambrook and Russell, 2001) in a 500 ml-baffled shake flask. After 2 h at an OD_{600} of 0.5, expression of the plasmid-encoded *lrp* gene under the control of a tet promoter (Ptet) was induced by the addition of 0.2 μg anhydrotetracycline/ml (Skerra, 1994). At an OD_{600} of 1.3 (2 h after induction) 500 ml of the culture were harvested by centrifugation (10 min, 11325 × *g*, 4 °C), washed with 250 ml 100 mM Tris, 1 mM EDTA, pH 8.0 and suspended in 10 ml of this buffer containing Complete Protease Inhibitor (Roche, Mannheim, Germany). Cells were disrupted by 3 passages at 108 MPa through a French pressure cell. The cell-free extract was obtained by centrifugation (20 min, 27000 × g, 4 °C). The cytosolic fraction was separated from the membrane fraction by centrifugation (1 h, 150,000 × *g*, 4 °C) and incubated with 10 μg avidin at 4 °C for 30 min to block biotinylated proteins. The cytosolic fraction was applied onto a column containing 4 ml 50% (w/v) Strep-Tactin sepharose equilibrated with 5 ml 100 mM Tris, 1 mM EDTA, 100 mM NaCl, pH 8.0 (buffer W). The column was washed 5 times with 2 ml of buffer W and bound proteins were eluted in 8 fractions of 1 ml with buffer W containing 2.5 mM desthiobiotin. For regeneration, the column was washed with 30 ml buffer W containing 1 mM 2-(4-hydroxyphenylazo) benzoic acid and subsequently with 16 ml buffer W. The concentration of the isolated protein was determined according to Bradford (1976) using a reagent provided by Sigma (Taufkirchen, Germany), the purity of the protein was checked by SDS polyacrylamide gel electrophoresis (10% NuPAGE Bis–Tris gel system, Invitrogen, Karlsruhe, Germany) and Coomassie staining (Gel Code Blue Stain Reagent, Pierce Chemical Company, Rockford, USA). In two purifications, about 1.5 mg LrpStrep (18 kDa) were purified to more than 95% purity from *E. coli* DH5α(pAN3K-*lrp*). The identity of LrpStrep was verified using StrepTactin-alkaline phosphatase conjugate and colorimetric detection *in gelo* as described for Western blots (Skerra and Schmidt, 2000) as well as by matrix-assisted laser desorption ionization-time of flight mass spectrometry as previously described (Fountoulakis and Langen, 1997; Schaffer et al., 2001).

2.6. Electrophoretic mobility shift assay

To test the binding of Lrp protein to the intergenic region of *lrp–brnFE* purified protein was incubated with the DNA fragment (197 bp, final concentration 100 ng) in a total volume of 20 μl. The binding buffer contained 10 mM Tris/HCl, pH 7.5, 50 mM NaCl, 5 mM $MgCl_2$, 2.5 mM $CaCl_2$, 5% (v/v) glycerol, 0.05% (v/v) Triton X-100, and 0.5 mM EDTA. DTT (0.5 mM final concentration) was freshly added prior incubation. A DNA fragment containing the *gntK* promoter region (100 ng) was used as negative control. The reaction mixtures were incubated at room temperature for 20 min and then loaded onto 10% native polyacrylamide gels. Electrophoresis and staining with SYBR Green I (Sigma–Aldrich) was performed as described previously (Wennerhold et al., 2005). All PCR products used in the gel shift assays were purified with a PCR purification kit (Qiagen) and eluted in EB buffer (10 mM Tris/HCl pH 8.5).

2.7. Gel filtration

For the determination of the molecular weight of LrpStrep purified protein was loaded on a Superdex™ 200 10/300 GL prep grade column (GE Healthcare) using the Äkta FPLC System (Amersham Biosciences) and 50 mM NaH_2PO_4, pH 8.0, 50 mM NaCl with 0.01% Triton X-100 (v/v) as running buffer. Apparent molecular masses were estimated by comparison to a mass standard kit (Kit for Molecular Weights 6500–66,000, Sigma) consisting of aprotinin (6.5 kDa), cytochrome *c* (12.4 kDa), carbonic anhydrase (29 kDa) and bovine serum albumin (66 kDa).

2.8. DNase I footprinting

DNase I footprinting experiments (Galas and Schmitz, 1978) were performed to identify the binding site of Lrp in the *brnF-lrp* promoter region C-terminally Strep-tagged Lrp (LrpStrep) was purified from *E. coli* (pAN3K-*lrp*) as described above. Eluted Lrp-Strep was transferred into 10 mM Tris–HCl, pH 8.0 by gel filtration with Sephadex G-25 columns (PD-10 column; Amersham Pharmacia, Freiburg, Germany). The column was equilibrated with 10 ml Tris–HCl, 2 ml protein solution and 0.5 ml 10 mM Tris–HCl, pH 8.0 were added and the protein was eluted in four fractions of 1 ml 10 mM Tris–HCl, pH 8.0. The protein concentration was determined according to Bradford (1976) using a reagent provided by Sigma (Taufkirchen, Germany).

The sequence about 350 bp upstream to 50 bp downstream of the transcription start site of *lrp* was first amplified using primers 5′-IRD800-ATGTGGTGAGCGCGATGGCG-3′ (the underlined nt corresponds to nt 277129 of NC003450) and 5′-GCACCTTGTCAGCCAGTGCG-3′ (the underlined nt corresponds to nt 276667 of NC003450) or primers CATCTGGTTCCAGGGCTGCC (the underlined nt corresponds to nt 276898 of NC003450) and 5′-IRD800-TCAGCAACGCCGATGCGGAC-3′ (the underlined nt corresponds to nt 276414 of NC003450). The labelled PCR products were purified using Microcon YM-30 columns (Millipore, Schwalbach, Germany). The binding reactions were carried out in a volume of 200 μl and contained 0.6 pmol labelled PCR product, 10 mM Tris–HCl pH 7.5, 0.5 mM EDTA, 5% (v/v) glycerol, 0.5 mM DTT, 0.005% (v/v) Triton X-100, 50 mM NaCl, 5 mM $MgCl_2$, 2.5 mM $CaCl_2$, 6 pmol poly(dI-dC) as a competitor (Sigma, Taufkirchen, Germany), branched-chain amino acids and different amounts of Lrp (0–20 μg) and were incubated for 30 min at room temperature. After Lrp-Strep binding, the DNA probe was partially restricted by addition of 5 μl 0.25 μg/ml DNase I in DNase I buffer (10 mM Tris–HCl pH 8.0, 5 mM $MgCl_2$, 5 mM $CaCl_2$, 50 mM KCl, 1 mM DTT) and 2 min incubation at room temperature. The restriction was stopped by addition of 700 μl cold 88% ethanol (v/v) containing 20 μg salmon sperm DNA and 0.65 M ammonium acetate and the DNA was precipitated over night at -20 °C. After centrifugation (40 min, 14,500 × *g*, 4 °C) and washing with 500 μl 70% ethanol (v/v), the DNA was dried and resolved in 2.5 μl water and 2.5 μl formamide loading buffer (Thermosequenase kit, Amersham Pharmacia, Freiburg). The corresponding unlabelled PCR product was generated and used as template for a sequencing reaction with the respective IRD800 labelled primer using the Thermosequenase kit (Amersham Pharmacia) according to the manufacturer's instructions. A DNase I footprinting reaction together with the corresponding sequencing reactions was separated on a polyacrylamide gel using the LI-COR 4200 DNA sequencer (MWG Biotech, Ebersberg) as indicated by the manufacturer.

2.9. Chloramphenicol acetyltransferase reporter assays

C. glutamicum was grown in CgXII minimal medium as described above, harvested by centrifugation, washed with 50 ml 0.08 M

Tris–HCl pH 7.0 and resolved in 1 ml of this buffer. Cells were disrupted by sonication for 10 min on ice (intensity 20%, pulse length 20%; Sonifier W-250, Branson-Emerson, Danbury, Conn.). The supernatant obtained by centrifugation (1 h, 14,500 × *g*, 4 °C) was used for activity measurements. Chloramphenicol acetyltransferase activity was assayed photometrically at 412 nm as described previously (Shaw, 1975; Wendisch et al., 1997) in 1 ml of a solution of 100 mM Tris–HCl (pH 7.8), 1 mM 5,5′-dithiobis-2-nitrobenzoic acid (ε_{412nm} = 13.6 mM^{-1} cm^{-1}), 0.1 mM acetyl-CoA, and 0.25 mM chloramphenicol. One unit of activity was defined as 1 μmol of chloramphenicol acetylated per min at 37 °C.

3. Results

3.1. L-Isoleucine-dependent gene expression changes in C. glutamicum ATCC 13032 and the lrp deletion mutant C. glutamicum Δlrp

Previous studies revealed that an Lrp-like regulatory gene (*lrp*, NCgl0253) is required for active export of L-isoleucine in *C. glutamicum* as *lrp* mutants did not show L-isoleucine export (Kennerknecht et al., 2002). As L-isoleucine is exported by the two-component permease BrnFE, which is encoded by an operon transcribed divergently to *lrp*, it was suggested that Lrp activates BrnFE gene expression (Kennerknecht et al., 2002). Feeding L-isoleucine dipeptides resulted in high *brnF* RNA levels (Trötschel et al., 2005).

Growth of an in-frame deletion mutant of *lrp* was monitored in glucose minimal medium without and with addition of branched-chain amino acids or L-methionine and compared to growth of the parent strain and of a *brnFE* deletion mutant. While growth of *C. glutamicum* ATCC 13032 was hardly affected by the addition of L-isoleucine, L-leucine, L-valine (Table 2) or L-methionine (data not shown), strains *C. glutamicum* Δ*lrp* and *C. glutamicum* Δ*brnFE* showed slowed growth when branched-chain amino acids were added to the medium (Table 2). Ectopic expression of *lrp* alleviated the growth defect of Δ*lrp* when grown in the presence of L-isoleucine or L-leucine at least partially. Without induction by anhydrotetracycline, *C. glutamicum* Δ*lrp*(pAN5K-*lrp*) showed growth rates of 0.20 h^{-1} and 0.20 h^{-1}, respectively, in the presence of L-isoleucine and L-leucine, respectively, and of 0.31 h^{-1} and 0.26 h^{-1}, respectively, after induction by anhydrotetracycline (Table 2).

DNA microarray experiments were performed to compare global gene expression changes due to addition of L-isoleucine for *C. glutamicum* WT and an *lrp* deletion mutant (see Section 2). For *C. glutamicum* wild type, the addition of L-isoleucine to CgXII glucose minimal medium resulted in significant expression changes of 5 genes: increased RNA levels for *brnF* and *brnE* and decreased transcript levels of 3 other genes (Table 3). In *C. glutamicum* Δ*lrp*, 18 genes were differentially expressed when L-isoleucine was added to the medium including *ripA* and members of the RipA regulon coding for proteins involved in the iron starvation response (Wennerhold et al., 2005). However, RNA levels of *brnF* and *brnE* were unaltered in the *lrp* deletion mutant in response to L-isoleucine addition. Taken together, these results revealed that increased expression of the *brnFE* operon in the presence of L-isoleucine depends on Lrp and suggested that Lrp positively regulates *brnFE* either directly or indirectly.

3.2. Identification of putative Lrp target genes by ChIP-to-chip analysis

For the identification of Lrp binding sites on the *C. glutamicum* chromosome, a variant of the so-called ChIP-to-chip analysis was performed. A *C. glutamicum* strain expressing C-terminally Strep-tagged Lrp from the chromosome was constructed and named *lrp*Strep (see Section 2). To determine if the Strep-tag affects Lrp function, growth of the *C. glutamicum* strains ATCC 13032, Δ*lrp* and 13032*lrp*Strep was compared (Table 2). 13032*lrp*Strep did not show a similar growth defect as described for Δ*lrp* in the presence of branched-chain amino acids, but grew comparably to the wild type ATCC 13032.

C. glutamicum strains ATCC 13032 and 13032*lrp*Strep were cultivated in LB medium and exponentially growing cells were harvested and subjected to ChIP-to-chip analysis (DNA–protein cross-linking, Streptactin affinity purification of DNA–LrpStrep–protein complexes and identification of the DNA in the DNA–LrpStrep–protein complexes by DNA microarray hybridization as described in Section 2). DNA enriched in the DNA–LrpStrep–protein complexes more than 1.5-fold (average of four experiments; two biological and two technical replicates) were *brnF* (3.0-fold), *lrp* (1.8-fold), NCgl1200 (2.1-fold) and *trpA* (1.7-fold). It is not clear whether Lrp binds upstream of NCgl1200 or of the last gene of the *trp* operon, *trpA*, as both genes were not differentially expressed in ATCC 130322 and *C. glutamicum* Δ*lrp* in the presence of L-isoleucine (Table 3). By contrast, enrichment of the divergently transcribed *lrp* and *brnF* in the ChIP-to-chip experiments is in agreement with the results of the gene expression analysis (Table 3) for *brnFE* and suggested that Lrp might bind to the *lrp–brnF* intergenic region to activate expression of *brnFE*.

3.3. Binding of Lrp to the intergenic region of lrp and brnFE

To test for a direct interaction of Lrp with the intergenic region of *lrp–brnFE in vitro* gel shift assays were performed using purified Lrp protein. For this purpose, the Lrp protein containing a carboxy-terminal StrepTag-II was overproduced in *E. coli* BL21 (DE3) and purified to apparent homogeneity by affinity chromatography. DNA fragments covering the intergenic region of *lrp–brnFE* were incubated with increasing concentrations of purified Lrp protein and subsequently separated on a 10% native polyacrylamide gel. As shown in Fig. 1, the intergenic region of *lrp–brnFE* was completely

Table 2
Growth of various *C. glutamicum* strains in glucose minimal medium in the presence or absence of branched-chain amino acids.

C. glutamicum strain	Growth rate [h^{-1}] in glucose minimal medium[a]			
	–	+100 mM L-leucine	+100 mM L-isoleucine	+100 mM L-valine
13032	0.42	0.34	0.35	0.39
Δ*brnFE*	0.41	0.23	0.24	0.34
Δ*lrp*	0.40	0.22	0.22	0.34
Δ*lrp*(pAN5K-*lrp*) without anhydrotetracycline	0.35	0.20	0.20	0.33
Δ*lrp*(pAN5K-*lrp*) + 0.2 mg/l anhydrotetracycline	0.36	0.31	0.26	0.35
13032*lrp*Strep	0.40	0.35	0.33	0.38

[a] Growth rates were determined from triplicate growth experiments with CgXII minimal medium with glucose as carbon source and the indicated concentrations of amino acids and anhydrotetracycline. Where appropriate, 25 μg/ml kanamycin was added. Standard deviations were below 10%.

Table 3
Global gene expression analysis of *C. glutamicum* 13032 and Δ*lrp* in response to L-isoleucine addition.

Gene[a]	Gene name and/or annotation[a]	Relative RNA level ± L-isoleucine	
		C. glutamicum 13032[b]	*C. glutamicum* Δ*lrp*[c]
cg0310	*katA*; catalase	1.5	**2.2**
cg0314	*brnF*; branched-chain amino acid permease	**2.0**	1.1
cg0315	*brnE*; branched-chain amino acid permease	**2.0**	1.0
cg0471	conserved secreted protein	n.d.	**0.4**
cg0588	hypothetical protein	n.d.	**0.5**
cg0589	ABC-type transporter, ATPase	n.d.	**0.4**
cg0590	ABC-type transporter, permease	n.d.	**0.5**
cg0762	*prpC2*; methyl citrate synthase	0.7	**0.4**
cg0768	ABC-type transporter, ATPase	0.7	**0.5**
cg0771	*trp1*; iron responsive protein 1	0.8	**0.4**
cg0928	ABC-type transporter, ATPase component	0.9	**0.5**
cg1120	*ripA*; AraC-type transcriptional regulator	0.7	**0.4**
cg1129	*aroF*; Phospho-2-dehydro-3-deoxyheptonate aldolase	0.7	**0.3**
cg1341	*narI*; nitrate reductase gamma subunit	n.d.	**2.2**
cg1343	*narH*; nitrate reductase beta chain	1.7	**2.3**
cg1376	*ssuD1*; alkanesulfonate monoxygenase	**0.5**	1.0
cg1377	*ssuC*; sulfonate ABC transporter, permease	**0.5**	1.0
cg1376	*ssuB*; sulfonate ABC transporter, ATPase	**0.5**	0.8
cg1737	*acn*; aconitase	1.9	**2.3**
cg2312	*gip*; hydroxypyruvate isomerase	1.0	**0.4**
cg2560	*aceA*; isocitrate lyase	0.6	**0.5**
cg3022	hypothetical protein	1.8	**3.2**
cg3404	ABC-type transporter, binding protein	0.7	**0.4**

[a] Gene identifiers and annotations are given according to BX927147.
[b] The mRNA levels were derived from nine experiments.
[c] The mRNA levels were derived from four experiments. mRNA levels ≥2 or ≤0.5 are shown in bold. Only values for genes whose mRNA ratio was altered significantly ($p < 0.05$), and at least two-fold in one or both of the transcriptome comparisons are shown.

shifted at a 20-fold molar excess of Lrp protein. In contrast, no specific shift was observed with a DNA fragment covering the promoter of *gntK* used as negative control. Addition of putative effectors (L-methionine, L-leucine, L-isoleucine, and L-valine) resulted in a slightly (only recognizable at 10-fold excess of protein, Fig. 1), but not significantly higher affinity of Lrp to the target DNA.

In further experiments, DNase I footprinting was performed to identify the Lrp binding motif within the intergenic region of *lrp–brnF*. Here, Lrp binding was assayed in the presence of the putative effectors L-valine, L-leucine and L-isoleucine (25 mM each). Under the chosen conditions the protected region extended from about −35 nt relative to the transcription start site of *brnF* to +25

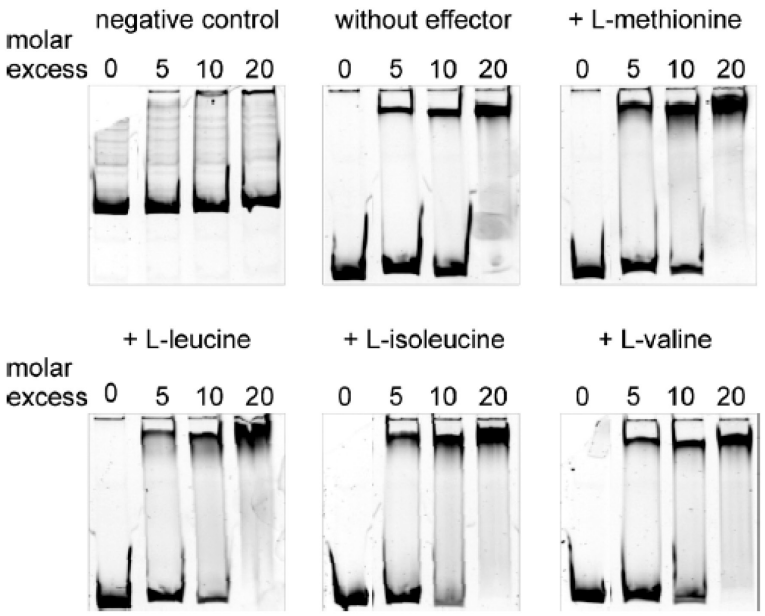

Fig. 1. Electrophoretic mobility shift assays (EMSA) with purified Lrp protein and the intergenic region of *lrp–brnFE*. DNA fragments covering the *lrp–brnFE* intergenic region (197 bp) and the promoter of *gntK* (138 bp) as negative control were incubated without and with increasing amounts of purified Lrp protein. When indicated, 25 mM of the putative effector amino acids L-methionine, L-leucine, L-isoleucine, or L-valine were added. Subsequently, the samples were separated by native polyacrylamide gel electrophoresis (10%), and the DNA was stained with SYBR Green I.

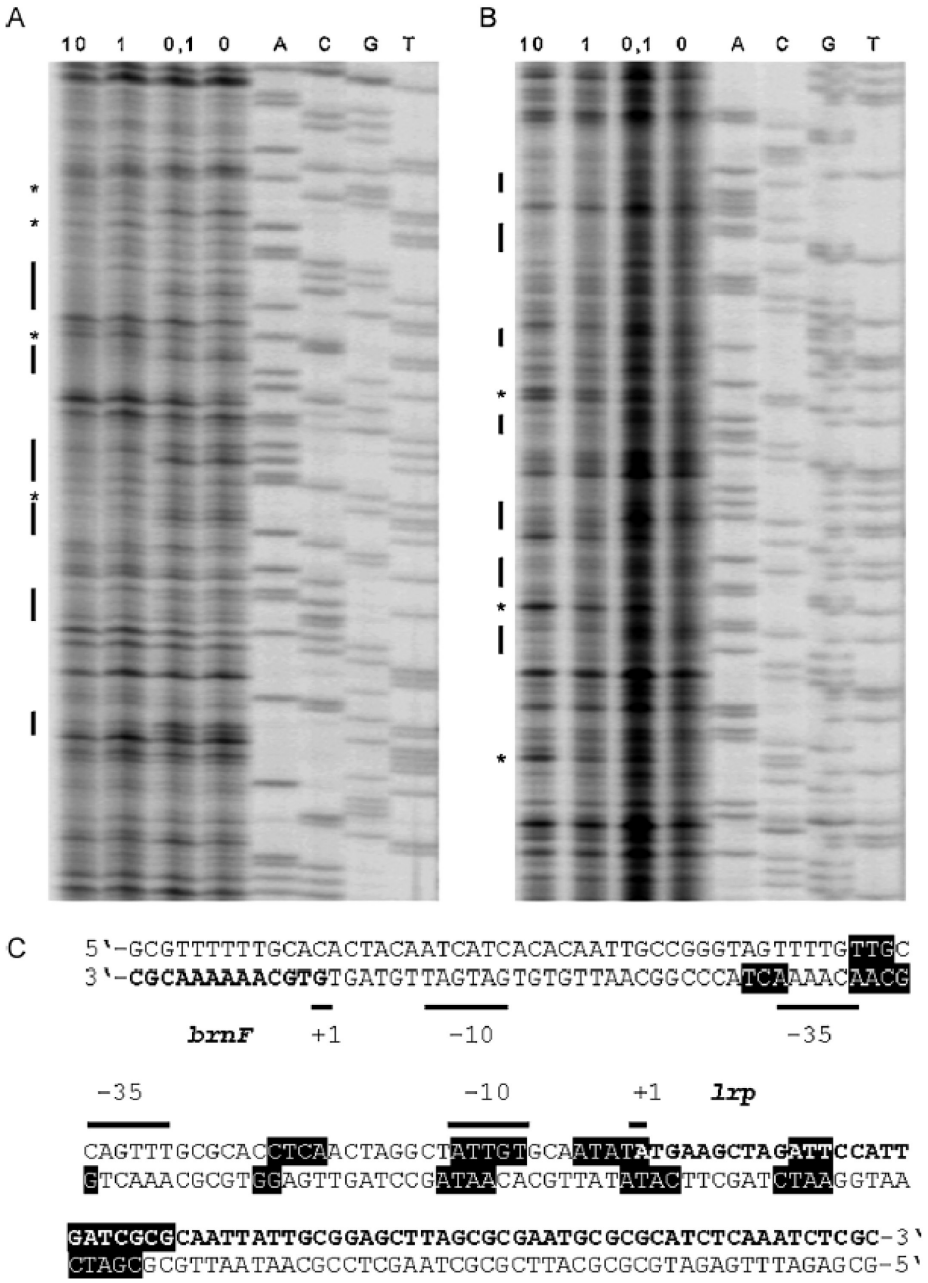

Fig. 2. DNAse footprint analysis of the *lrp–brnF* intergenic region. 0.6 pmol IRD800-labelled DNA of (A) the *lrp* coding strand and (B) the complementary *brnF* coding strand were incubated with different amounts of LrpStrep as indicated above the lanes in the presence of 25 mM each L-valine, L-leucine and L-isoleucine. After DNase I treatment, the resulting DNA fragments were separated on a polyacrylamide gel next to sequencing reactions performed with the corresponding IRD800 labelled primer and ddNTPs. Regions protected from DNase I degradation in the presence of Lrp are marked by lines and hypersensitive regions by asterisks. (C) The intergenic region between the open reading frames (bold) of *brnF* and *lrp* is shown with the start codons, −10 and −35 regions (lines) and the transcriptional start sites (+1) as defined by (Kennerknecht et al., 2002). Sequences protected by Lrp in the DNase I footprints are highlighted by black boxes.

relative to the transcription start site of *lrp*, suggesting activation of *brnF* transcription by Lrp and negative autoregulation of *lrp* itself. Furthermore, distinct hypersensitive sites were detected, indicating DNA bending as a result of Lrp binding. Altogether seven protected regions were present on both strands of DNA, except one region only being present on the *brnF* template strand (Fig. 2). In fact, protection of more than hundreds of nt is a typical feature of representatives of this family of regulators and was reported in several studies to correlate with the formation of multimeric states of Lrp-type regulators (Brinkman et al., 2003). However, the native mass of LrpStrep determined by size exclusion chromatography was found to be ~36 kDa (calculated monomeric mass: 17.8 kDa),

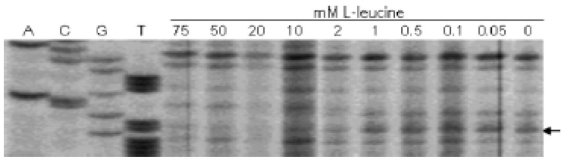

Fig. 3. Effects of L-leucine on binding of Lrp to the *brnF–lrp* intergenic region. DNase I footprinting was performed as in Fig. 2A with 10 μg LrpStrep and 0.6 pmol labelled DNA, but only L-leucine was present in the concentrations indicated above the lanes. The cutout includes the lowest Lrp protected band from Fig. 2A marked by the arrow.

indicating that Lrp in a non-DNA-bound state forms a homodimer in *C. glutamicum* (data not shown). In addition, increasing concentrations of L-leucine were tested to investigate the effector dependent binding of Lrp to DNA. As shown in Fig. 3, at concentrations above 10–20 mM L-leucine protection of distinct DNA regions against DNase I cleavage could be demonstrated.

3.4. Analysis of transcriptional fusions

In order to determine if Lrp activates *brnFE* and if Lrp is subject to autoregulation transcriptional fusions of the promoter regions of *brnFE* and *lrp* were constructed and their expression assayed in *C. glutamicum* WT and *C. glutamicum* Δ*lrp* during growth in glucose minimal medium in the presence or absence of the amino acids L-leucine, L-isoleucine, L-valine and L-methionine. The addition of L-leucine, L-isoleucine, L-valine and L-methionine induced expression of the *brnF'–'cat* fusion (Table 4). Expression of the *brnF'–'cat* fusion was comparably high (0.35–0.41 U/mg) when 200 mM L-valine, 100 mM L-isoleucine or 25 mM L-leucine were added to the medium, while it was two-fold lower when 25 mM L-methionine was added (Table 4). Thus, the inducing effects of these amino acids when added to the growth medium were highest with L-leucine and decreased in the order L-leucine > L-methionine > L-isoleucine > L-valine. Deletion of *lrp* led to very low or undetectable (0.02 or <0.01 U/mg) expression of the *brnF'–'cat* fusion indicating that Lrp activates expression of *brnFE*.

Expression of the *lrp'–'cat* fusion was lower than that of the *brnF'–'cat* fusion and was hardly influenced by the addition of amino acids or by the presence or absence of *lrp* (Table 4). Thus, no indication that expression of *lrp* is subject to autoregulation or is affected by addition of L-methionine or branched-chain amino acids was obtained.

4. Discussion

Lrp from *C. glutamicum* was shown to directly activate *brnFE* expression when branched-chain amino acids or L-methionine were added to the medium. The stimulating effect of amino acids added to the growth medium was ranked in descending order: L-leucine > L-methionine > L-isoleucine > L-valine. Previously, feeding the dipeptide L-methionyl-L-methionine was shown to result in stronger and faster increases of the *brnF* RNA level in *C. glutamicum* wild type than feeding of the dipeptide L-isoleucyl-L-isoleucine (Trötschel et al., 2005). Clearly, further intricate experiments, in which fixed intracellular amino acid concentrations have to be adjusted as e.g. described for LysG (Bellmann et al., 2001), are required to compare the different stimulatory effects of these amino acids under *in vivo* conditions. Moreover, Lrp proteins may respond to a wider range of amino acids than is typically appreciated as e.g. Lrp from *Mycobacterium tuberculosis* also binds L-phenylalanine, L-tyrosine, L-methionine, L-histidine, L-lysine, L-arginine, L-proline, L-threonine and L-glutamine (Shrivastava and Ramachandran, 2007). Similarly, Lrp from *E. coli* also responds to L-alanine and L-methionine, which have been demonstrated to function as corepressors in this bacterium (Hart and Blumenthal, 2011).

E. coli possesses three Lrp-like proteins (Lrp, AsnC and the uncharacterized YbaO) and *B. subtilis* possesses LrpC and six similar proteins. Besides *lrp* (cg0311), *C. glutamicum* possesses only one further gene encoding a putative transcriptional regulator of the Lrp family, cg2942, which is divergently transcribed to gene coding for a putative RhtB-type export system (Marin and Krämer, 2007). *C. glutamicum* also possesses paralogs of *brnF* and *brnE*, cg3412 and cg3413, which, however, are separated from the second *lrp*-like gene (cg2942) by about 460 kb. Neither the function of the Lrp-like protein (cg2942) nor of the BrnFE-like putative transport system has yet been characterized.

DNA-binding sites of Lrp-type transcriptional regulators often exhibit rather low sequence conservation and lack perfect symmetry elements (Cui et al., 1995; Ouhammouch and Geiduschek, 2001; Peeters et al., 2004). In this study, DNase I footprinting experiments revealed binding of Lrp to several AT-rich regions within the intergenic region of *lrp–brnFE* extending over approx. 75 bp but missing obvious inverted repeats. The finding that the binding region overlaps with the −35 promoter region of *brnFE* supports the idea that Lrp activates *brnFE* expression (Table 4). With respect to *lrp* itself, protected regions reach about 25 bp into the orf of the *lrp* gene suggesting a negative autoregulation as a result of promoter exclusion as reported for the Lrp orthologs of *P. putida* and *Agrobacterium tumefaciens* (Jafri et al., 1999; Madhusudhan et al., 1995). However, promoter fusion experiments described in this study do not support the notion of a negative autoregulation of *C. glutamicum lrp* since no significant change in *lrp* expression was observed in an *lrp* deletion mutant or upon addition of amino acids (Table 4). However, the binding site of Lrp was identified by DNase footprinting *in vitro* and, thus, does not reflect the *in vivo* state where binding of Lrp might be influenced by several other factors. In fact, *E. coli* Lrp often acts in concert with other global regulator such as Crp, IHF (integration host factor) or the histone-like protein H-NS (Corcoran and Dorman, 2009; Levinthal et al., 1994; Paul et al., 2001; Weyand et al., 2001). Based on the available data, we can neither rule out nor support the possibility that Lrp also controls transcription of its own gene which necessitates further studies.

Lrp of *E. coli*, LrpC of *B. subtilis* and Lrp of *Neisseria meningitidis* are examples of Lrp proteins functioning as global regulators controlling expression of up to hundreds of genes (Lintner et al., 2008; Ren et al., 2000; Thaw et al., 2006). Reasons contributing the multitude of genes regulated by Lrp of *E. coli* include effects on sigma factor selectivity (Weber et al., 2005) or DNA bending (Wang and Calvo, 1993). On the other hand, AsnC, a paralog of *E. coli* Lrp, is a specific regulator of its own gene and the divergently transcribed asparagine synthetase gene *asnA* (Kölling and Lother, 1985). Many bacteria contain several Lrp-like proteins and the majority of them have been described as specific transcriptional regulators (Brinkman et al., 2003), e.g. the Lrp homologs of *P. putida* and *Streptomyces coelicolor* named BkdR are required for transcriptional regulation of divergently transcribed operons encoding branched-chain amino acid dehydrogenase complex (Madhusudhan et al., 1995; Sprusansky et al., 2005). Similar to Lrp and the amino acid transport system BrnFE in *C. glutamicum*, Lrp of *B. subtilis* is regulating expression of a divergently transcribed operon for transport of the L-leucine analog L-azaleucine (Belitsky et al., 1997). Lrp *from C. glutamicum* is a specific regulator of *brnFE* and growth defects due to branched-chain amino acids added to the growth medium coincide for a mutant either lacking Lrp or its target genes *brnFE* (see Table 2). The affinity of BrnFE for its substrate L-leucine (Kennerknecht et al., 2002) coincides with the L-leucine concentration that was sufficient for a complete protection of distinct DNA regions of the *lrp–brnFE* intergenic region by Lrp against DNase I cleavage (see

Table 4
Expression of the *brnF'–'cat* and *lrp'–'cat* transcriptional fusions.

CGXII glucose minimal medium with	Expression of the *cat* reporter gene fusion[a]			
	C. glutamicum 13032		*C. glutamicum* Δ*lrp*	
	pET2-*pbrnF*	pET2-*plrp*	pET2-*pbrnF*	pET2-*plrp*
–	<0.01	0.02	<0.01	0.03
25 mM L-leucine	0.35	0.03	<0.01	0.04
100 mM L-leucine	1.31	0.06	<0.01	0.07
25 mM L-isoleucine	0.06	0.02	0.02	0.03
100 mM L-isoleucine	0.41	0.02	<0.01	0.03
100 mM L-valine	0.20	0.02	<0.01	0.07
200 mM L-valine	0.41	0.02	<0.01	0.03
25 mM L-methionine	0.20	0.02	<0.01	0.02

[a] Chloramphenicol acetyltransferase specific activity is given in U/mg protein as averages of two independent biological replicates with experimental errors less than 10%. Expression of the *cat* reporter gene fusion in the control strains 13032 (pET2) and Δ*lrp*(pET2) with or without added amino acids could not be detected (<0.01 U/mg protein).

Fig. 3). The fact that addition of L-isoleucine to cultures of *C. glutamicum* Δ*lrp* resulted in more expression changes than observed with *C. glutamicum* WT (see Table 3) might be due to secondary effects. Likely, higher concentrations of branched-chain amino acids pertain when these are added to *C. glutamicum* Δ*lrp* cultures as *brnFE* is not expressed in the absence of Lrp (see Table 4).

As BrnFE is the only export system for L-leucine, L-isoleucine and L-valine (Kennerknecht et al., 2002), but not for L-methionine (Trötschel et al., 2005), production of branched-chain amino acids may benefit from overexpression of *brnFE* or from constitutive activation of *brnFE* by Lrp, a strategy not yet implemented in *C. glutamicum* strain development for production of L-valine or L-isoleucine (Bartek et al., 2010; Blombach et al., 2007, 2008, 2009; Denina et al., 2010; Elisakova et al., 2005; Holatko et al., 2009; Lange et al., 2003; Patek, 2007). Indeed, genetic or flux analysis identified export of L-isoleucine and L-valine, respectively, as limiting step in production of these amino acids by *C. glutamicum* (Magnus et al., 2009; Morbach et al., 1996), while L-methionine production by *C. glutamicum* appears to be limited by precursor supply and/or activity of biosynthetic enzyme(s) (Bolten et al., 2010). So far, transport engineering for the production of branched-chain amino acids or L-methionine by *C. glutamicum* has only been suggested for abolishing re-uptake e.g. of L-methionine (Park et al., 2007b). Whereas L-methionine production by *E. coli* (Figge, 2007) is claimed to be augmented by overexpression of *yjeH*, which encodes a putative export system for L-methionine (EP1445310), and L-valine production by *E. coli* was improved by overexpression of *lrp* and of the valine export genes *ygaZH* (Park et al., 2007a), the potential of BrnFE transport engineering and Lrp regulatory engineering has not yet been tapped for *C. glutamicum*.

Acknowledgements

During the initial phase, this work was supported in part by the European Union within the framework of the VALPAN project (QLK 3-2000-00497). Excellent technical help by Karin Niemann, Westfalian Wilhelms University Münster, Germany, is gratefully acknowledged.

References

Abe, S., Takayama, K.-I., Kinoshita, S., 1967. Taxonomical studies on glutamic acid-producing bacteria. J. Gen. Appl. Microbiol. 13, 279–301.
Bartek, T., Blombach, B., Zonnchen, E., Makus, P., Lang, S., Eikmanns, B.J., Oldiges, M., 2010. Importance of NADPH supply for improved L-valine formation in *Corynebacterium glutamicum*. Biotechnol. Prog. 26, 361–371.
Belitsky, B.R., Gustafsson, M.C., Sonenshein, A.L., Von Wachenfeldt, C., 1997. An *lrp*-like gene of *Bacillus subtilis* involved in branched-chain amino acid transport. J. Bacteriol. 179, 5448–5457.
Bellmann, A., Vrljic, M., Patek, M., Sahm, H., Krämer, R., Eggeling, L., 2001. Expression control and specificity of the basic amino acid exporter LysE of *Corynebacterium glutamicum*. Microbiology 147, 1765–1774.
Blombach, B., Arndt, A., Auchter, M., Eikmanns, B.J., 2009. L-Valine production during growth of pyruvate dehydrogenase complex-deficient *Corynebacterium glutamicum* in the presence of ethanol or by inactivation of the transcriptional regulator SugR. Appl. Environ. Microbiol. 75, 1197–1200.
Blombach, B., Schreiner, M.E., Bartek, T., Oldiges, M., Eikmanns, B.J., 2008. *Corynebacterium glutamicum* tailored for high-yield L-valine production. Appl. Microbiol. Biotechnol. 79, 471–479.
Blombach, B., Schreiner, M.E., Holatko, J., Bartek, T., Oldiges, M., Eikmanns, B.J., 2007. L-valine production with pyruvate dehydrogenase complex-deficient *Corynebacterium glutamicum*. Appl. Environ. Microbiol. 73, 2079–2084.
Bolten, C.J., Schröder, H., Dickschat, J., Wittmann, C., 2010. Towards methionine overproduction in *Corynebacterium glutamicum*—methanethiol and dimethyldisulfide as reduced sulfur sources. J. Microbiol. Biotechnol. 20, 1196–1203.
Bradford, M.M., 1976. A rapid and sensitive method for the quantitation of microgram quantities of protein utilizing the principle of protein–dye binding. Anal. Biochem. 72, 248–254.
Brinkman, A.B., Ettema, T.J., De Vos, W.M., van der Oost, J., 2003. The Lrp family of transcriptional regulators. Mol. Microbiol. 48, 287–294.
Brocker, M., Bott, M., 2006. Evidence for activator and repressor functions of the response regulator MtrA from *Corynebacterium glutamicum*. FEMS Microbiol. Lett. 264, 205–212.
Corcoran, C.P., Dorman, C.J., 2009. DNA relaxation-dependent phase biasing of the fim genetic switch in *Escherichia coli* depends on the interplay of H-NS, IHF and LRP. Mol. Microbiol. 74, 1071–1082.
Cui, Y., Wang, Q., Stormo, G.D., Calvo, J.M., 1995. A consensus sequence for binding of Lrp to DNA. J. Bacteriol. 177, 4872–4880.
Denina, I., Paegle, L., Prouza, M., Holatko, J., Patek, M., Nesvera, J., Ruklisha, M., 2010. Factors enhancing L-valine production by the growth-limited L-isoleucine auxotrophic strain *Corynebacterium glutamicum* Delta*ilvA* Delta*panB ilvNM13* (pECKA*ilvBNC*). J. Ind. Microbiol. Biotechnol. 37, 689–699.
Ebbighausen, H., Weil, B., Krämer, R., 1989. Transport of branched-chain amino acids in *Corynebacterium glutamicum*. Arch. Microbiol. 151, 238–244.
Eggeling, L., Sahm, H., 2003. New ubiquitous translocators: amino acid export by *Corynebacterium glutamicum* and *Escherichia coli*. Arch. Microbiol. 180, 155–160.
Eikmanns, B.J., Thum-Schmitz, N., Eggeling, L., Lüdtke, K.U., Sahm, H., 1994. Nucleotide sequence, expression and transcriptional analysis of the *Corynebacterium glutamicum gltA* gene encoding citrate synthase. Microbiology 140, 1817–1828.
Elisakova, V., Patek, M., Holatko, J., Nesvera, J., Leyval, D., Goergen, J.L., Delaunay, S., 2005. Feedback-resistant acetohydroxy acid synthase increases valine production in *Corynebacterium glutamicum*. Appl. Environ. Microbiol. 71, 207–213.
Figge, R.M., 2007. Methionine biosynthesis in *Escherichia coli* and *Corynebacterium glutamicum*. In: Wendisch, V.F. (Ed.), Amino Acid Biosynthesis – Pathways, Regulation and Metabolic Engineering. Springer, Heidelberg, Germany.
Fountoulakis, M., Langen, H., 1997. Identification of proteins by matrix-assisted laser desorption ionization-mass spectrometry following in-gel digestion in low-salt, nonvolatile buffer and simplified peptide recovery. Anal. Biochem. 250, 153–156.
Galas, D.J., Schmitz, A., 1978. DNAse footprinting: a simple method for the detection of protein–DNA binding specificity. Nucl. Acids Res. 5, 3157–3170.
Hanahan, D., 1983. Studies on transformation of *Escherichia coli* with plasmids. J. Mol. Biol. 166, 557–580.
Hart, B.R., Blumenthal, R.M., 2011. Unexpected coregulator range in the global regulator Lrp of Escherichia coli and Proteus mirabilis. J. Bacteriol. 193, 1054–1064.
Hayashi, M., Mizoguchi, H., Ohnishi, J., Mitsuhashi, S., Yonetani, Y., Hashimoto, S., Ikeda, M., 2006. A *leuC* mutation leading to increased L-lysine production and *rel*-independent global expression changes in *Corynebacterium glutamicum*. Appl. Microbiol. Biotechnol. 72, 783–789.
Hermann, T., Krämer, R., 1996. Mechanism and regulation of isoleucine excretion in *Corynebacterium glutamicum*. Appl. Environ. Microbiol. 62, 3238–3244.

Holatko, J., Elisakova, V., Prouza, M., Sobotka, M., Nesvera, J., Patek, M., 2009. Metabolic engineering of the L-valine biosynthesis pathway in *Corynebacterium glutamicum* using promoter activity modulation. J. Biotechnol. 139, 203–210.

Inoue, H., Nojima, H., Okayama, H., 1990. High efficiency transformation of *Escherichia coli* with plasmids. Gene 96, 23–28.

Ishige, T., Krause, M., Bott, M., Wendisch, V.F., Sahm, H., 2003. The phosphate starvation stimulon of *Corynebacterium glutamicum* determined by DNA microarray analyses. J. Bacteriol. 185, 4519–4529.

Iyer, V.R., Horak, C.E., Scafe, C.S., Botstein, D., Snyder, M., Brown, P.O., 2001. Genomic binding sites of the yeast cell-cycle transcription factors SBF and MBF. Nature 409, 533–538.

Jafri, S., Evoy, S., Cho, K., Craighead, H.G., Winans, S.C., 1999. An Lrp-type transcriptional regulator from *Agrobacterium tumefaciens* condenses more than 100 nucleotides of DNA into globular nucleoprotein complexes. J. Mol. Biol. 288, 811–824.

Keilhauer, C., Eggeling, L., Sahm, H., 1993. Isoleucine synthesis in *Corynebacterium glutamicum*: molecular analysis of the *ilvB-ilvN-ilvC* operon. J. Bacteriol. 175, 5595–5603.

Kennerknecht, N., Sahm, H., Yen, M.R., Patek, M., Saier Jr.JJr., M.H., Eggeling, L., 2002. Export of L-isoleucine from *Corynebacterium glutamicum*: a two-gene-encoded member of a new translocator family. J. Bacteriol. 184, 3947–3956.

Khodursky, A.B., Bernstein, J.A., Peter, B.J., Rhodius, V., Wendisch, V.F., Zimmer, D.P., 2003. *Escherichia coli* spotted double-strand DNA microarrays: RNA extraction, labeling, hybridization, quality control, and data management. Methods Mol. Biol. 224, 61–78.

Kind, S., Jeong, W.K., Schröder, H., Zelder, O., Wittmann, C., 2010. Identification and elimination of the competing N-acetyldiaminopentane pathway for improved production of diaminopentane by *Corynebacterium glutamicum*. Appl. Environ. Microbiol. 76, 5175–5180.

Kölling, R., Lother, H., 1985. AsnC: an autogenously regulated activator of asparagine synthetase A transcription in *Escherichia coli*. J. Bacteriol. 164, 310–315.

Krause, F.S., Blombach, B., Eikmanns, B.J., 2010. Metabolic engineering of *Corynebacterium glutamicum* for 2-ketoisovalerate production. Appl. Environ. Microbiol. 76, 8053–8061.

Kutukova, E.A., Livshits, V.A., Altman, I.P., Ptitsyn, L.R., Zyiatdinov, M.H., Tokmakova, I.L., Zakataeva, N.P., 2005. The *yeaS (leuE)* gene of *Escherichia coli* encodes an exporter of leucine, and the Lrp protein regulates its expression. FEBS Lett. 579, 4629–4634.

Lange, C., Rittmann, D., Wendisch, V.F., Bott, M., Sahm, H., 2003. Global expression profiling and physiological characterization of *Corynebacterium glutamicum* grown in the presence of L-valine. Appl. Environ. Microbiol. 69, 2521–2532.

Levinthal, M., Lejeune, P., Danchin, A., 1994. The H-NS protein modulates the activation of the *ilvIH* operon of *Escherichia coli* K12 by Lrp, the leucine regulatory protein. Mol. Gen. Genet. 242, 736–743.

Link, A.J., Phillips, D., Church, G.M., 1997. Methods for generating precise deletions and insertions in the genome of wild-type *Escherichia coli*: application to open reading frame characterization. J. Bacteriol. 179, 6228–6237.

Lintner, R.E., Mishra, P.K., Srivastava, P., Martinez-Vaz, B.M., Khodursky, A.B., Blumenthal, R.M., 2008. Limited functional conservation of a global regulator among related bacterial genera: Lrp in *Escherichia*, *Proteus* and *Vibrio*. BMC Microbiol. 8, 60.

Madhusudhan, K.T., Huang, N., Sokatch, J.R., 1995. Characterization of BkdR-DNA binding in the expression of the *bkd* operon of *Pseudomonas putida*. J. Bacteriol. 177, 636–641.

Magnus, J.B., Oldiges, M., Takors, R., 2009. The identification of enzyme targets for the optimization of a valine producing *Corynebacterium glutamicum* strain using a kinetic model. Biotechnol. Prog. 25, 754–762.

Marin, K., Krämer, R., 2007. Amino acid transport systems in biotechnologically relevant bacteria. In: Wendisch, V.F. (Ed.), Amino Acid Biosynthesis – Pathways, Regulation and Metabolic Engineering. Springer, Heidelberg, Germany.

Menkel, E., Thierbach, G., Eggeling, L., Sahm, H., 1989. Influence of increased aspartate availability on lysine formation by a recombinant strain of *Corynebacterium glutamicum* and utilization of fumarate. Appl. Environ. Microbiol. 55, 684–688.

Mimitsuka, T., Sawai, H., Hatsu, M., Yamada, K., 2007. Metabolic engineering of *Corynebacterium glutamicum* for cadaverine fermentation. Biosci. Biotechnol. Biochem. 71, 2130–2135.

Morbach, S., Sahm, H., Eggeling, L., 1996. L-Isoleucine production with *Corynebacterium glutamicum*: Further flux increase and limitation of export. Appl. Environ. Microbiol. 62, 4345–4351.

Niebisch, A., Kabus, A., Schultz, C., Weil, B., Bott, M., 2006. Corynebacterial protein kinase G controls 2-oxoglutarate dehydrogenase activity via the phosphorylation status of the OdhI protein. J. Biol. Chem. 281, 12300–12307.

Ouhammouch, M., Geiduschek, E.P., 2001. A thermostable platform for transcriptional regulation: the DNA-binding properties of two Lrp homologs from the hyperthermophilic archaeon *Methanococcus jannaschii*. EMBO J. 20, 146–156.

Park, J.H., Lee, K.H., Kim, T.Y., Lee, S.Y., 2007a. Metabolic engineering of *Escherichia coli* for the production of L-valine based on transcriptome analysis and in silico gene knockout simulation. Proc. Natl. Acad. Sci. U.S.A. 104, 7797–7802.

Park, S.D., Lee, J.Y., Sim, S.Y., Kim, Y., Lee, H.S., 2007b. Characteristics of methionine production by an engineered *Corynebacterium glutamicum* strain. Metab. Eng. 9, 327–336.

Patek, M., 2007. Branched-chain amino acids. In: Wendisch, V.F. (Ed.), Amino Acid Biosynthesis – Pathways, Regulation and Metabolic Engineering. Springer, Heidelberg, Germany.

Patek, M., Nesvera, J., Guyonvarch, A., Reyes, O., Leblon, G., 2003. Promoters of *Corynebacterium glutamicum*. J. Biotechnol. 104, 311–323.

Paul, L., Blumenthal, R.M., Matthews, R.G., 2001. Activation from a distance: roles of Lrp and integration host factor in transcriptional activation of *gltBDF*. J. Bacteriol. 183, 3910–3918.

Peeters, E., Thia-Toong, T.L., Gigot, D., Maes, D., Charlier, D., 2004. Ss-LrpB, a novel Lrp-like regulator of *Sulfolobus solfataricus* P2, binds cooperatively to three conserved targets in its own control region. Mol. Microbiol. 54, 321–336.

Peters-Wendisch, P., Stolz, M., Etterich, H., Kennerknecht, N., Sahm, H., Eggeling, L., 2005. Metabolic engineering of *Corynebacterium glutamicum* for L-serine production. Appl. Environ. Microbiol. 71, 7139–7144.

Peters-Wendisch, P.G., Eikmanns, B.J., Thierbach, G., Bachmann, B., Sahm, H., 1993. Phosphoenolpyruvate carboxylase in *Corynebacterium glutamicum* is dispensable for growth and lysine production. FEMS Microbiol. Lett. 112, 269–274.

Polen, T., Rittmann, D., Wendisch, V.F., Sahm, H., 2003. DNA microarray analyses of the long-term adaptive response of *Escherichia coli* to acetate and propionate. Appl. Environ. Microbiol. 69, 1759–1774.

Pollack, J.R., Iyer, V.R., 2002. Characterizing the physical genome. Nat. Genet. 32, 515–521.

Radmacher, E., Vaitsikova, A., Burger, U., Krumbach, K., Sahm, H., Eggeling, L., 2002. Linking central metabolism with increased pathway flux: L-valine accumulation by *Corynebacterium glutamicum*. Appl. Environ. Microbiol. 68, 2246–2250.

Ren, B., Robert, F., Wyrick, J.J., Aparicio, O., Jennings, E.G., Simon, I., Zeitlinger, J., Schreiber, J., Hannett, N., Kanin, E., Volkert, T.L., Wilson, C.J., Bell, S.P., Young, R.A., 2000. Genome-wide location and function of DNA binding proteins. Science 290, 2306–2309.

Sambrook, J., Fritsch, E.F., Maniatis, T., 1989. Molecular Cloning. A Laboratory Manual, 2nd ed. Cold Spring Harbor Laboratoy Press, New York.

Sambrook, J., Russell, D.W., 2001. Molecular Cloning – A Laboratory Manual, 3rd ed. Cold Spring Harbor Laboratory Press, New York.

Schäfer, A., Tauch, A., Jäger, W., Kalinowski, J., Thierbach, G., Pühler, A., 1994. Small mobilizable multi-purpose cloning vectors derived from the *Escherichia coli* plasmids pK18 and pK19: selection of defined deletions in the chromosome of *Corynebacterium glutamicum*. Gene 145, 69–73.

Schaffer, S., Weil, B., Nguyen, V.D., Dongmann, G., Günther, K., Nickolaus, M., Hermann, T., Bott, M., 2001. A high-resolution reference map for cytoplasmic and membrane-associated proteins of *Corynebacterium glutamicum*. Electrophoresis 22, 4404–4422.

Schneider, J., Wendisch, V.F., 2010. Putrescine production by engineered *Corynebacterium glutamicum*. Appl. Microbiol. Biotechnol. 88, 859–868.

Shaw, W.V., 1975. Chloramphenicol acetyltransferase from chloramphenicol-resistant bacteria. Methods Enzymol. 43, 737–755.

Shrivastava, T., Ramachandran, R., 2007. Mechanistic insights from the crystal structures of a feast/famine regulatory protein from *Mycobacterium tuberculosis* H37Rv. Nucleic Acids Res. 35, 7324–7335.

Simic, P., Sahm, H., Eggeling, L., 2001. L-Threonine export: use of peptides to identify a new translocator from *Corynebacterium glutamicum*. J. Bacteriol. 183, 5317–5324.

Sindelar, G., Wendisch, V.F., 2007. Improving lysine production by Corynebacterium glutamicum through DNA microarray-based identification of novel target genes. Appl. Microbiol. Biotechnol. 76, 677–689.

Skerra, A., 1994. Use of the tetracycline promoter for the tightly regulated production of a murine antibody fragment in *Escherichia coli*. Gene 151, 131–135.

Skerra, A., Schmidt, T.G., 2000. Use of the *Strep*-Tag and streptavidin for detection and purification of recombinant proteins. Methods Enzymol. 326, 271–304.

Sprusansky, O., Stirrett, K., Skinner, D., Denoya, C., Westpheling, J., 2005. The *bkdR* gene of *Streptomyces coelicolor* is required for morphogenesis and antibiotic production and encodes a transcriptional regulator of a branched-chain amino acid dehydrogenase complex. J. Bacteriol. 187, 664–671.

Tani, T.H., Khodursky, A., Blumenthal, R.M., Brown, P.O., Matthews, R.G., 2002. Adaptation to famine: a family of stationary-phase genes revealed by microarray analysis. Proc. Natl. Acad. Sci. U.S.A. 99, 13471–13476.

Thaw, P., Sedelnikova, S.E., Muranova, T., Wiese, S., Ayora, S., Alonso, J.C., Brinkman, A.B., Akerboom, J., van der Oost, J., Rafferty, J.B., 2006. Structural insight into gene transcriptional regulation and effector binding by the Lrp/AsnC family. Nucleic Acids Res. 34, 1439–1449.

Trötschel, C., Deutenberg, D., Bathe, B., Burkovski, A., Krämer, R., 2005. Characterization of methionine export in *Corynebacterium glutamicum*. J. Bacteriol. 187, 3786–3794.

van der Rest, M.E., Lange, C., Molenaar, D., 1999. A heat shock following electroporation induces highly efficient transformation of *Corynebacterium glutamicum* with xenogeneic plasmid DNA. Appl. Microbiol. Biotechnol. 52, 541–545.

Vasicova, P., Abrhamova, Z., Nesvera, J., Patek, M., Sahm, H., Eikmanns, B., 1998. Integrative and autonomously replicating vectors for analysis of promoters in *Corynebacterium glutamicum*. Biotechnol. Tech. 12, 743–746.

Vrljic, M., Garg, J., Bellmann, A., Wachi, S., Freudl, R., Malecki, M.J., Sahm, H., Kozina, V.J., Eggeling, L., Saier Jr., M.H., 1999. The LysE superfamily: topology of the lysine exporter LysE of *Corynebacterium glutamicum*, a paradyme for a novel superfamily of transmembrane solute translocators. J. Mol. Microbiol. Biotechnol. 1, 327–336.

Vrljic, M., Kronemeyer, W., Sahm, H., Eggeling, L., 1995. Unbalance of L-lysine flux in *Corynebacterium glutamicum* and its use for the isolation of excretion-defective mutants. J. Bacteriol. 177, 4021–4027.

Vrljic, M., Sahm, H., Eggeling, L., 1996. A new type of transporter with a new type of cellular function: L-lysine export from *Corynebacterium glutamicum*. Mol. Microbiol. 22, 815–826.

Wang, Q., Calvo, J.M., 1993. Lrp, a global regulatory protein of *Escherichia coli*, binds co-operatively to multiple sites and activates transcription of *tlvIH*. J. Mol. Biol. 229, 306–318.

Weber, H., Polen, T., Heuveling, J., Wendisch, V.F., Hengge, R., 2005. Genome-wide analysis of the general stress response network in *Escherichia coli*: sigmaS-dependent genes, promoters, and sigma factor selectivity. J. Bacteriol. 187, 1591–1603.

Wendisch, V.F., 2003. Genome-wide expression analysis in *Corynebacterium glutamicum* using DNA microarrays. J. Biotechnol. 104, 273–285.

Wendisch, V.F., Spies, M., Reinscheid, D.J., Schnicke, S., Sahm, H., Eikmanns, B.J., 1997. Regulation of acetate metabolism in *Corynebacterium glutamicum*: transcriptional control of the isocitrate lyase and malate synthase genes. Arch. Microbiol. 168, 262–269.

Wennerhold, J., Krug, A., Bott, M., 2005. The AraC-type regulator RipA represses aconitase and other iron proteins from *Corynebacterium* under iron limitation and is itself repressed by DtxR. J. Biol. Chem. 280, 40500–40508.

Weyand, N.J., Braaten, B.A., van der Woude, M., Tucker, J., Low, D.A., 2001. The essential role of the promoter-proximal subunit of CAP in *pap* phase variation: Lrp- and helical phase-dependent activation of *papBA* transcription by CAP from -215. Mol. Microbiol. 39, 1504–1522.

Yokoyama, K., Ishijima, S.A., Clowney, L., Koike, H., Aramaki, H., Tanaka, C., Makino, K., Suzuki, M., 2006. Feast/famine regulatory proteins (FFRPs): *Escherichia coli* Lrp, AsnC and related archaeal transcription factors. FEMS Microbiol. Rev. 30, 89–108.

Zittrich, S., Krämer, R., 1994. Quantitative discrimination of carrier-mediated excretion of isoleucine from uptake and diffusion in *Corynebacterium glutamicum*. J. Bacteriol. 176, 6892–6899.

Name of the journal:	Journal of Biotechnology
Impact factor:	3.045
Contribution of own work:	20%
2. author:	Experimental work and writing of the manuscript

Metabolic Engineering 14 (2012) 449–457

Contents lists available at SciVerse ScienceDirect

Metabolic Engineering

journal homepage: www.elsevier.com/locate/ymben

The development and application of a single-cell biosensor for the detection of L-methionine and branched-chain amino acids

Nurije Mustafi, Alexander Grünberger, Dietrich Kohlheyer, Michael Bott, Julia Frunzke *

Institut für Bio- und Geowissenschaften, IBG-1: Biotechnologie, Forschungszentrum Jülich, Leo-Brandt-Straße, 52425 Jülich, Germany

ARTICLE INFO

Article history:
Received 19 October 2011
Received in revised form
30 January 2012
Accepted 6 February 2012
Available online 15 February 2012

Keywords:
Corynebacterium glutamicum
Lrp
GFP
amino acids
L-valine

ABSTRACT

The detection and quantification of specific metabolites in single bacterial cells is a major goal for industrial biotechnology. We have developed a biosensor based on the transcriptional regulator Lrp that detects intracellular L-methionine and branched-chain amino acids in *Corynebacterium glutamicum*. In assays, fluorescence output showed a linear relationship with cytoplasmic concentrations of the effector amino acids. In increasing order, the affinity of Lrp for the amino acids is L-valine, L-isoleucine, L-leucine and L-methionine. The sensor was applied for online monitoring and analysis of cell-to-cell variability of L-valine production by the pyruvate dehydrogenase-deficient *C. glutamicum* strain Δ*aceE*. Finally, the sensor system was successfully used in a high-throughput (HT) FACS screen for the isolation of amino acid-producing mutants after random mutagenesis of a non-producing wild type strain. These applications illustrate how one of nature's sensor devices – transcriptional regulators – can be used for the analysis, directed evolution and HT screening for microbial strain development.

1. Introduction

Improvements to microbial production of biological molecules represent a key goal for industrial biotechnology. Traditional approaches for strain development include random mutagenesis followed by selection or screening, and the rational design of metabolic pathways to redirect or enhance metabolic flux, optimize precursor supply or tune metabolic regulation (Bailey, 1991). These methods take time, require bulk sampling and do not interface with high-throughput technologies. New techniques that detect and quantify specific metabolites in single cells have the potential to dramatically improve efficiency. They allow the analysis of productivity of a given strain at the single-cell level and offer the potential for high-throughput screening to isolate strains that produce the desired metabolite (Bailey, 1991).

Recent advances in mass spectrometry and next generation sequencing technologies have opened up new ways to analyze and screen production strains. However, they focus mostly on easily accessible phenotypes, while the majority of desirable bacterial products are small, rather inconspicuous molecules that cannot easily be detected at the single-cell level. For such low-profile molecules, genetically-encoded biosensors offer the potential to transform information about a specific metabolite into an optical output. Recently, a range of sensors have been used, including enzymes or multistep enzymatic pathways, inducible expression systems and whole organisms (Dietrich et al., 2010; Michener et al., in press; van der Meer and Belkin, 2010; Zhang and Keasling, 2011). These systems facilitate small-molecule detection through colorimetric assays, fluorescence readout or growth-coupled screening techniques based on auxotrophic growth. However, for the most biotechnology-relevant compounds, notably amino acids, organic acids or polymer precursors, no appropriate optical sensors are currently available.

The Gram-positive soil bacterium *Corynebacterium glutamicum* is an important platform organism for industrial biotechnology (Kinoshita et al., 1957). It is used, for example, for the large-scale production of more than two million tons of L-glutamate and L-lysine per year (Burkovski, 2008; Eggeling and Bott, 2005) and for the production of a few thousand tons each of L-threonine, L-leucine and L-valine, which are essential amino acids for all vertebrates (Eggeling, 2001; Leuchtenberger, 1996). Applications for the branched-chain amino acid L-valine include artificial nutrition and the synthesis of antiviral drugs and herbicides (Bartek et al., 2011; Blombach et al., 2008; Park et al., 2007). The development of strains for the production of L-methionine is of major interest as around 500 kt are produced annually from petrochemicals at present (Ikeda, 2003).

Here, we present a biosensor system that can enhance strain development by detecting intracellular L-methionine and the branched-chain amino acids L-valine, L-leucine and L-isoleucine. The biosensor uses the transcriptional regulator Lrp of *C. glutamicum*, which activates the expression of the *brnFE* operon in the presence of

* Corresponding author. Fax: +49 2461 61 2710.
E-mail address: j.frunzke@fz-juelich.de (J. Frunzke).

1096-7176/$ - see front matter © 2012 Elsevier Inc. All rights reserved.
doi:10.1016/j.ymben.2012.02.002

increased levels of branched-chain amino acids or L-methionine (Lange et al., 2011). BrnFE, a two-component permease belonging to the LIV-E transporter family, facilitates the export of these amino acids, thus avoiding the inhibitory effects of intracellular amino acid accumulation (Kennerknecht et al., 2002; Trötschel et al., 2005). The export of amino acids is usually tightly regulated to avoid wasting metabolic energy. Lrp binds the intergenic region of *lrp-brnFE* and activates expression in the presence of elevated concentrations of the appropriate amino acids.

We report on the construction of a novel amino acid biosensor based on the transcriptional regulator Lrp, which allows the intracellular detection and quantification of branched-chain amino acids and L-methionine at single-cell resolution. We present this sensor technology as a simple and convenient tool for the analysis of biotechnological production strains and for the establishment of novel high-throughput screening approaches.

2. Material and methods

2.1. Bacterial strains, media and growth conditions

Bacterial strains and plasmids are listed in Table 1. Unless stated otherwise, cultures of *C. glutamicum* were inoculated to an OD_{600} of 1 and grown in CGXII minimal medium with 4% (w/v) glucose as carbon source. For the dipeptide feeding assay, the main culture was inoculated to an OD_{600} of ~3 and cultivated in a BioLector microbioreactor system (Kensy et al., 2009). For random mutagenesis of *C. glutamicum* ATCC 13032 cells were grown to an OD_{600} of 5 in BHIS medium (BHI with 0.5 M sorbitol) and subsequently incubated with N′-methyl-N′-nitro-N-nitrosoguanidine (0.125 mg/ml) for 15 min. After mutagenesis the cells were washed twice with 50 ml 0.9% (w/v) saline and cultivated in BHIS medium for 1 h, after which kanamycin (25 μg ml^{-1}) was added. *Escherichia coli* DH5α was grown aerobically in LB medium on a rotary shaker (120 rpm) or on LB agar plates at 37 °C (Sambrook et al., 2001). Where appropriate, the media contained kanamycin (25 μg ml^{-1} for *C. glutamicum* or 50 μg ml^{-1} for *E. coli*).

2.2. Recombinant DNA work

Standard methods including PCR, DNA restriction or ligation were carried out according to standard protocols (Sambrook et al., 2001). Oligonucleotides were synthesized by Eurofins MWG Operon (Ebersfeld, Germany) and are listed in Table 1. For construction of the biosensor, the fragment containing the *C. glutamicum lrp* open reading frame, the intergenic region of *lrp-brnF*, the first 30 nucleotides of *brnF*, and the ribosomal binding site of the pET-16b Vector (Novagen, Darmstadt, Germany) were amplified using oligonucleotides Lrp-fw-A-BamHI and Lrp-brnF-rv-I-NdeI introducing a BamHI and NdeI restriction site, respectively. Additionally, *eyfp* was amplified by PCR with oligonucleotides eYFP-fw-H-NdeI and eYFP-rv-D-SalI using the vector pEKEx2-yfp-tetR as template, thereby introducing restriction sites for NdeI and SalI digestion (Frunzke et al., 2008). Both PCR products were cloned into the vector pJC1 (Schäfer et al., 1997), resulting in plasmid pJC1-*lrp-brnF′-eyfp*.

2.3. Fluorescence microscopy and spectroscopy

For phase contrast and fluorescence microscopy, samples were placed on a microscope slide coated with a thin aqueous Poly-L-lysine solution of 0.1% (w/v, Sigma-Aldrich GmbH, Munich, Germany) and covered by a coverslip. Images were taken on a Zeiss Axioplan 2 imaging microscope that was equipped with an AxioCam MRm camera and a Plan-Apochromat 100x, 1.40 Oil DIC oil-Immersion objective. Digital images were acquired and analyzed with AxioVision 4.6 software (Zeiss, Göttingen, Germany).

Fluorescence spectrometry measurements of *C. glutamicum* strains were carried out using a JASCO FP-6500/6600 spectrofluorometer (JASCO GmbH, Gross-Umstadt, Germany) in 3 ml QS fluorescence cells (Hellma GmbH, Müllheim, Germany). Final documentation of the recorded spectra was performed using Spectra-Manager Software (JASCO).

2.4. Adjustment and determination of intracellular amino acid concentrations

To adjust the intracellular amino acid concentration, dipeptides were added to preincubated cells (60 min at 30 °C, 1200 rpm) using different ratios of the corresponding dipeptides at a final concentration of 3 mM. To adjust internal effector levels, the following dipeptides were added: L-methionine: alanyl-methionine (Ala-Met) or methionyl-methionine (Met-Met) with alanyl-alanine (Ala-Ala); L-leucine: alanyl-leucine (Ala-Leu) with Ala-Ala; L-isoleucine: alanyl-isoleucine (Ala-Ile) with Ala-Ala;

Table 1
Bacterial strains, plasmids and oligonucleotides.

Strains or plasmids	Relevant characteristics	Source or reference
Strains		
***C. glutamicum* ATCC 13032**	Biotin-auxotrophic wild type	(Kinoshita et al., 1957)
C. glutamicum* Δ*aceE	In-frame deletion of cg2466	(Schreiner et al., 2005)
***E. coli* DH5α**	*supE44 ΔlacU169* (ϕ80*lacZ*ΔM15) *hsdR17 recA1 endA1 gyrA96 thi-1 relA1*	Invitrogen
Plasmids		
pJC1	*E. coli-C. glutamicum* shuttle vector, Kan^R $oriV_{Ec}$ $oriV_{Cg}$	(Schäfer et al., 1997)
pJC1-*lrp-brnF′-eyfp*	Kan^R; pJC1 derivative containing *lrp* (cg0313), the intergenic region of *lrp brnF* (cg0314) and a transcriptional fusion of *brnF* with *eyfp*	This study
pEKEx2-*yfp-tetR*	Kan^R; pEKEx2 derivative containing *eyfp-tetR*, encoding an eYFP-TetR fusion protein under the control of the *tac* promoter	(Frunzke et al., 2008)
Oligonucleotides	**Sequence (5′→3′) and properties**[a]	
Lrp-fw-A-BamHI	GCGCGGATCCTCACACCTGGGGGCGAGCTG (BamHI)	
Lrp-brnF-rv-I-NdeI	GCGCCATATGATATCTCCTTCTTAAAGTTCAGCTTGAATGAATCTCTTGCG (NdeI)	
EYfp-fw-H-NdeI	GCGCCATATGGTGAGCAAGGGCGAGGAG (NdeI)	
EYfp-rv-D-SalI	GCGCGTCGACTTATCTAGACTTGTACAGCTCGTC (SalI)	
aceE-out-fw	CACTTCGGCGTGTCACAATTAGG	
aceE-out-rv	GTCTGACAAGGCGTTCCTCGG	

[a] In some cases oligonucleotides were designed to introduce recognition sites for restriction endonucleases (recognition sites underlined, restriction endonucleases indicated in parentheses).

L-valine: alanyl-valine (Ala-Val) with Ala-Ala (Fig. S1). The internal level of the respective effector amino acid forms a distinct peak within minutes after addition of the dipeptide mixture (Trötschel et al., 2005). This time point was determined to be after 7 min in case of L-methionine and L-leucine, 10 min for L-isoleucine and 20 min for L-valine (see Fig. S1). Intracellular amino acid concentrations were measured in three samples of 200 µl taken from the cell suspension when maximal internal amino acid concentration was reached. The cells were quickly separated from the surrounding medium and extracted in perchloric acid (20%) by silicone oil centrifugation as described previously (Ebbighausen et al., 1989). Amino acids were quantified as their ortho-phthaldialdehyde derivatives using ultra-high pressure liquid chromatography by automatic pre-column derivatization and separation by reversed-phase chromatography on an Agilent 1290 Infinity LC ChemStation (Agilent, Santa Clara, USA) with fluorescence detection. The intracellular volume used to calculate the internal amino acid concentration was 1.7 µl mg (dry weight)$^{-1}$ (Ruffert et al., 1997).

2.5. Microfluidic chip fabrication and imaging

Microfluidic chips based on a disposable transparent poly (dimethylsiloxane) (PDMS) (Sylgard 184 Silicone Elastomer, Dow Corning Corp., Midland, MI, USA) were fabricated as described in SI Experimental Procedures (Xia and Whitesides, 1998). For imaging, the device was placed on a fully motorized inverted microscope (Nikon Eclipse Ti, Nikon Instruments Europe). For the study of microcolonies, single *C. glutamicum* Δ*aceE* cells (Schreiner et al., 2005) were seeded into the chip device by flushing the cell suspension (OD_{600} ~4) through the channels with ~25 nl/min (calculated flow in one channel; 300 ml/min for the whole chip device). Once single cells were trapped, CGXII medium with 4% glucose (w/v) and 1.5% (w/v) potassium acetate was infused by a syringe pump with a flow rate of ~25 nl/min. Colony growth was followed by time lapse microscopy for approximately five generations. In order to initiate the L-valine production phase, the medium was switched after 15 h to medium containing 4% glucose (w/v) (Blombach et al., 2007). Images were acquired at 15 min intervals. Fluorescence emission was quantified through mean intensity of every defined region of interest (ROIs), which encompasses the cell area.

2.6. Microtiter plate cultivation

Online monitoring of growth and fluorescence was conducted in 48-well microtiter Flowerplates (MFPs) with the BioLector cultivation system (m2p-labs GmbH, Aachen, Germany). 48-well MFPs containing 750 µl medium per well were inoculated with *C. glutamicum* cells from a preculture (see Section 2.1) and grown at 30 °C, a shaking frequency of 1200 rpm, and a shaking diameter of 3 mm. During cultivation the production of biomass was measured as the backscattered light intensity of sent light with a wavelength of 620 nm (signal gain factor of 10), the eYFP fluorescence of the cultures was measured at an excitation of 510 nm and an emission of 532 nm (signal gain factor of 60). The specific fluorescence for the cells is defined as eYFP fluorescence per scattered light intensity (given in a.u.) (Kensy et al., 2009).

2.7. Flow cytometry

Flow cytometric measurements and sorting were performed on a FACSAria II (Becton Dickinson, San Jose, USA) with 488 nm excitation from a blue solid-state laser. Forward-scatter characteristics (FSC) and side-scatter characteristics (SSC) were detected as small- and large-angle scatters of the 488-nm laser, respectively. EYFP fluorescence was detected using a 502-nm long-pass and a 530/30-nm band-pass filter set. Sorting was performed with four-way purity as the precision mode at a threshold rate up to 10,000 events/s. Cells were sorted on BHI agar plates containing 25 µg ml^{-1} kanamycin or in a tube containing CGXII medium.

2.8. Determination of pyruvate dehydrogenase activity

For enzyme assays, *C. glutamicum* WT and mutant cells were grown in the main culture in CGXII minimal medium with 4% (w/v) glucose, 1.5% (w/v) potassium acetate and 0.1% (w/v) yeast extract and harvested at OD_{600} of ~5. Cells were disrupted by sonication in 0.1 mM TES([*N*-tris(hydroxymethyl)methyl-2-aminoethanesulfonic acid), pH 7.2, 10 mM $MgCl_2$, 3 mM L-cysteine, and 30% (w/v) glycerol. Crude extract was prepared by subsequent centrifugation and gel-filtrated in the same buffer on PD10 columns (GE Healthcare, Buckinghamshire, UK). Ultracentrifugation of the crude extract and finally the pyruvate dehydrogenase assay were performed as described previously (Hoffelder et al., 2010).

3. Results

3.1. Biosensor construction and proof of principle

To design a biosensor that responds to elevated intracellular concentrations of L-methionine or branched-chain amino acids, we constructed a module based on the transcriptional regulator Lrp (leucine-responsive protein) of *C. glutamicum*. The genomic region containing the open-reading frame of *lrp* and the intergenic region of *lrp-brnF*, which contains the promoter of *brnF*, were cloned in front of *eyfp*, thereby setting *eyfp* expression under the control of P_{brnF} (Fig. 1A). The resulting sensor plasmid was transformed into *C. glutamicum* wild type (WT) strain. In a first set

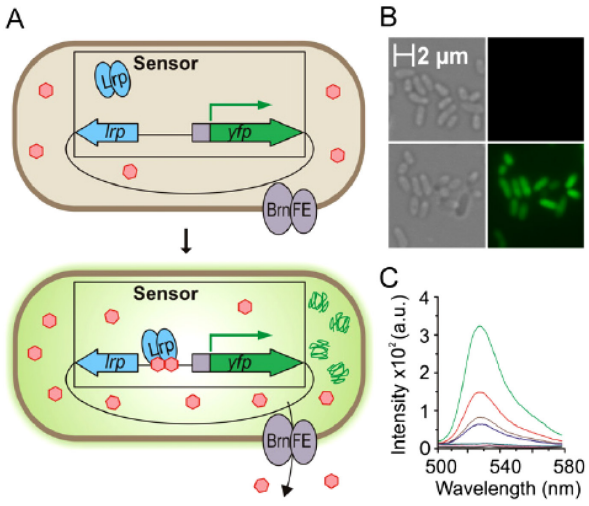

Fig. 1. Construction and verification of the Lrp-based biosensor. (A) A sensor cell with wild type levels of the effector amino acids exhibits background levels of eYFP fluorescence (upper panel). Increased intracellular concentration of the respective amino acids induces *eyfp* expression in sensor cells (lower panel). (B) Phase contrast and fluorescence microscopy images of *C. glutamicum* sensor cells fed with 3 mM Lys-Ala (upper row) or Ala-Met (lower row) dipeptide. (C) Fluorescence spectrometry (488 nm excitation) of *C. glutamicum* sensor cells fed with 3 mM Ala-Met (green), Ala-Leu (red), Ala-Ile (brown), Ala-Val (purple). Controls include CGXII minimal medium (black), *C. glutamicum* WT cells (pink), sensor cells (blue) and sensor cells fed with Lys-Ala (dark red). (For interpretation of the references to color in this figure legend, the reader is referred to the web version of this article.)

of experiments, the capability of the system to monitor the intracellular accumulation of the respective amino acids was confirmed by fluorescence microscopy and spectroscopy. To artificially increase the intracellular concentration of specific amino acids, we used the dipeptide feeding strategy described previously (Vrljic et al., 1996). Dipeptides containing the amino acid under study were added to the growth medium; the uptake and subsequent hydrolysis of these dipeptides by cytoplasmic hydrolases leads to an increased pool of the respective amino acids.

C. glutamicum wild type cells transformed with the biosensor showed no discernable fluorescence signal above the autofluorescence of *C. glutamicum* wild type. When the intracellular concentration of L-methionine was increased by the addition of the dipeptide alanyl-methionine (Ala-Met), a significant increase in eYFP fluorescence resulted (Fig. 1B). As expected, elevated intracellular L-leucine, L-isoleucine or L-valine levels, achieved by feeding with Ala-Leu, Ala-Ile or Ala-Val, respectively, also resulted in higher fluorescent output by the biosensor cells, as shown by fluorescence spectroscopy (488 nm excitation). No significant signal was obtained upon addition of Ala-Ala or Ala-Lys or with cells containing the empty vector pJC1. The highest intensity of fluorescence was observed for L-methionine, and decreased from L-leucine to L-isoleucine to L-valine (Fig. 1C). These results demonstrate the functionality of the biosensor: Intracellular detection of elevated levels of L-methionine and branched-chain amino acids is transformed into an optical readout.

3.2. Quantitative characterization of the biosensor response

One prerequisite for the application of biosensors is an accurate description of the relationship between effector input and reporter output. To assess this, we established a competitive dipeptide feeding assay to generate defined intracellular concentrations of amino acids. The approach is based on the principle that a competitor dipeptide, for example, Ala-Ala, competes with an effector-containing dipeptide, for example Ala-Met, for uptake by the cell, allowing internal effector levels to be regulated (see Section 2.4 and SI).

After the addition of dipeptide mixtures, the internal concentrations of amino acids reach distinct maxima within minutes (Fig. S1) (Trötschel et al., 2005). Thus, the approach provides a system to study the correlation between internal amino acid concentration and the resulting reporter output. Effector input and eYFP output was correlated for each Lrp effector amino acid, shown in Fig. 2A. There were linear fluorescence responses to the internal concentration of the amino acids across the concentration ranges tested.

The biosensor displayed highest sensitivity for L-methionine followed by L-leucine, L-isoleucine and L-valine (Fig. 2A, Table 2). Maximal induction in response to L-methionine accumulation was 78-fold, thereby defining the minimal dynamic range of the biosensor. However, due to restrictions in the kinetic properties of the system, such as dipeptide uptake and hydrolysis, the highest internal concentration achieved was 25 mM in *C. glutamicum* wild type. Consequently, the dynamic range and minimal linear detection range given in Table 2 represent minimal values but demonstrate the analog response of the biosensor in the low to medium mM range.

Next, the suitability of the biosensor system for FACS-based screening approaches was tested. Cells fed with dipeptides (containing one of the four Lrp effector amino acids) to the previously determined maximal internal amino acid concentration were sampled two hours after addition of the dipeptides (the time point with the highest fluorescence signal). Then, three or four samples of cells each containing a different internal concentration of a particular amino acid were mixed in a ratio of 1:1:1(:1) and immediately analyzed by flow cytometry. (Fig. 2B–E). Distinct populations of cells with increased internal effector concentrations were found, although these displayed no differences in terms of morphological parameters (side scatter, SSC and forward scatter, FSC, see raw data used for color accentuation in Fig. S2). In the case of L-methionine, concentrations below 1 mM generated a population clearly distinguishable from wild type with respect to eYFP fluorescence. Thus, the biosensor-flow cytometry combination can discriminate subpopulations of cells that exhibit slight differences in the internal accumulation of amino acids in the low to medium mM range – the concentration range relevant to the development of production strains.

3.3. Biosensor-based online monitoring of production strains

To further assess the performance of the biosensor in online monitoring of production strains, we chose the *C. glutamicum* strain Δ*aceE*. This strain lacks the E1p enzyme of the pyruvate dehydrogenase complex and excretes low amounts of L-valine when cultivated in minimal medium with 4% glucose and 1.5% acetate. Production of L-valine *via* the metabolization of glucose has been shown to begin after all of the acetate is consumed (Blombach et al., 2007).

In accordance with published data, *C. glutamicum* Δ*aceE* containing the biosensor grew exponentially without producing L-valine for the first ten hours. Once acetate was depleted, the cells stopped growing and started to produce L-valine. The sensor responded with eYFP fluorescence that correlated with the increased production of L-valine (Fig. 3A). Three hours after the start of L-valine production the signal reached a maximum value, suggesting that a constant internal L-valine concentration is reached and maintained. In contrast, *C. glutamicum* wild type containing the sensor plasmid showed no significant eYFP emission.

3.4. Analysis of L-valine production by C. glutamicum ΔaceE at the single-cell level

As the Lrp-based biosensor allows the visualization of internal amino acid levels in single cells, we analyzed L-valine production by *C. glutamicum* Δ*aceE* cells in isogenic microcolonies. For this purpose, cells were cultivated in PDMS-based microfluidic devices. In contrast to microcolony growth on agar pads, as commonly used, cultivation in microfluidic chips offers the advantage of continuous supply of medium, oxygen, constant temperature and pH, and the ability to switch between different cultivation media.

Initially, single *C. glutamicum* Δ*aceE* sensor cells were tracked in the microfluidic chamber and isogenic microcolonies were grown in minimal medium with 4% glucose and 1.5% acetate. After 15 h the medium was switched to conditions supporting L-valine production and the fluorescent output was measured (Fig. 3B). Significant variations in fluorescence intensity were observed between single cells, indicating different production levels of L-valine. A lineage tree based on the growth of the microcolony revealed another level of heterogeneity, namely variation in cell size and interdivision intervals among single cells (Fig. 3C). Doubling times for single duplication events ranged from 0.5–5 h. In comparison, the parental *C. glutamicum* wild type has an average doubling time of about 70 min in the microfluidic system, with a range of 40–110 min (data not shown).

When an average growth rate was calculated from the lineage tree, the result ($0.24\ h^{-1}$) was comparable to the growth rate of Δ*aceE* in shake flask cultures. We stopped medium flux through the microfluidic device, thereby simulating batch culture

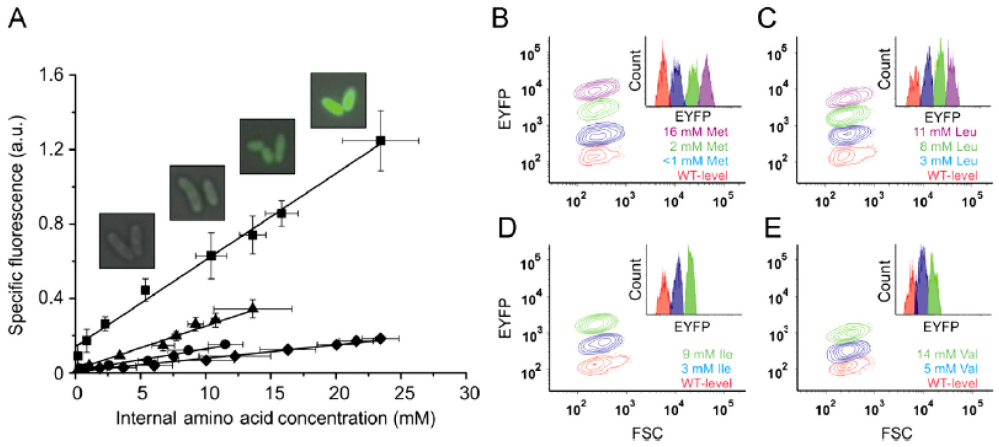

Fig. 2. Characterization of the specificity and affinity of the biosensor. (A) Relationship between intracellular concentrations of effector amino acids L-methionine (■), L-leucine (▲), L-isoleucine (●) and L-valine (♦) and specific fluorescence outputs in *C. glutamicum* cells. Data represent the average values of three independent measurements. The fluorescence microscopy images show *C. glutamicum* sensor cells with increasing internal concentrations of L-methionine (1–20 mM). (B)–(E): FACS-generated contour plots and histograms displaying the FSC signal (forward scatter) and/or the eYFP signal of mixed *C. glutamicum* populations differing in their intracellular amino acid concentrations of (B) Met, (C) Leu, (D) Ile and (E) Val. No variation in terms of morphology parameters (forward scatter (FSC) and side scatter (SSC)) was observed for the populations. For analysis cells fed with dipeptides to the known internal amino acid concentration were mixed and immediately analyzed by flow cytometry. See Fig. S2 for FSC/SSC plots and gating strategy used for color accentuation.

Table 2
Performance parameters for the biosensor ($n=3$).

Effector	Minimal dynamic range (fold increase)	Minimal linear detection range (mM)
L-methionine	>78	>0.2–23.5
L-leucine	>22	>0.2–13.6
L-isoleucine	>10	>0.4–11.5
L-valine	>12	>1.5–23.4

conditions in which secreted L-valine accumulates extracellularly. Under these conditions, cell-to-cell variation decreased significantly as cells within the microcolony with low fluorescent signals caught up (Fig. S3). Thus, this sensor-based analysis of an L-valine producer uncovers phenotypic heterogeneity at the single-cell level which is masked by typical bulk measurements.

3.5. Sorting efficiency

In further experiments, the strain Δ*aceE* was used to examine the sensor-based sorting efficiency of the FACS system. Mixtures of *C. glutamicum* wildtype and fluorescing *C. glutamicum* Δ*aceE* cells (1% *vs.* 99% and *vice versa*) were analyzed after 24 h of cultivation by FACS and single cells were sorted on agar plates (1500 cells in total). The two strains could be distinguished by the small colony phenotype of Δ*aceE*. Colony PCR analysis of the sorted cells revealed a >95% correct sorting efficiency and a survival rate of *ca.* 96%. This demonstrates the suitability of the system for isolating single mutants/cells which exhibit increased amino acid production out of a mixture of non-producing cells.

3.6. Biosensor-based FACS high-throughput screen

We next developed a high-throughput-compatible sensor system to screen large mutant libraries in order to detect cells with increased levels of L-methionine or branched-chain amino acids. For a primary screen, wild type cells containing the sensor plasmid were chemically mutagenized by incubation with N′-methyl-N′-nitro-N-nitrosoguanidine, as described in Section 2.1. Subsequent to mutagenesis, *C. glutamicum* cells were incubated in BHIS medium for 6 h and then analyzed and sorted by FACS. As depicted in Fig. 4A, parallel approaches were taken. In screen S1, 150 mutants that exhibited significantly increased fluorescence were sorted out of *ca.* 6 million cells from gate S1-P1 on BHI plates (survival rate: 60%, Fig. 4D). 48 colony forming mutants were used to inoculate a 48-well plate containing CGXII medium with 4% glucose, 1.5% acetate and 0.1% yeast extract. Acetate was added to the screening medium to support growth of L-valine producing mutants with decreased pyruvate dehydrogenase activity. After 48 h of cultivation in microtiter plates, amino acid concentrations in the supernatant were assayed by uHPLC. This approach (S1 in Fig. 4A) yielded 23% positive clones (11 out of 48). *Via* the chosen screening conditions especially L-valine-excreting mutants were obtained – all positive clones produced significant amounts of this amino acid. 10% of the mutants also produced up to 2 mM L-leucine and L-isoleucine (for an overview of all screened mutants, see Table S1). An iterative approach was developed (S2) to screen for clones that do not have significant growth defects under the chosen conditions. In screen S2, cells were cultivated for 24 h after mutagenesis and mutants with increased eYFP emission were sorted into liquid BHIS complex medium and grown at 30 °C. After 24 h 10,000 cells with most enhanced fluorescence emission were again sorted into a BHIS containing tube and cultivated for 24 h. This procedure of isolating and cultivating the upper 10,000 fluorescence cells was repeated three times.

The iterative screen resulted in an up-shift of eYFP fluorescence in the whole population (Fig. 4C). Due to the wide distribution of the fluorescence signal, the cells were subdivided into three populations: S2-P1 (highest fluorescence), S2-P2 (medium fluorescence) and S2-P3 (low fluorescence). A clear pattern was observed in these subpopulations: in the groups of cells exhibiting middle (S2-P2) and low levels of fluorescence (S2-P3), 6% and 2% of the tested clones excreted significant amounts of L-valine, respectively; within the subpopulation that produced high levels of fluorescence (S2-P1), 25% excreted significant amounts of L-valine (Fig. 4D). The survival rate of the sorted cells increased significantly from 59% (S1) to almost 96% on the fourth day of the iterative screen (S2).

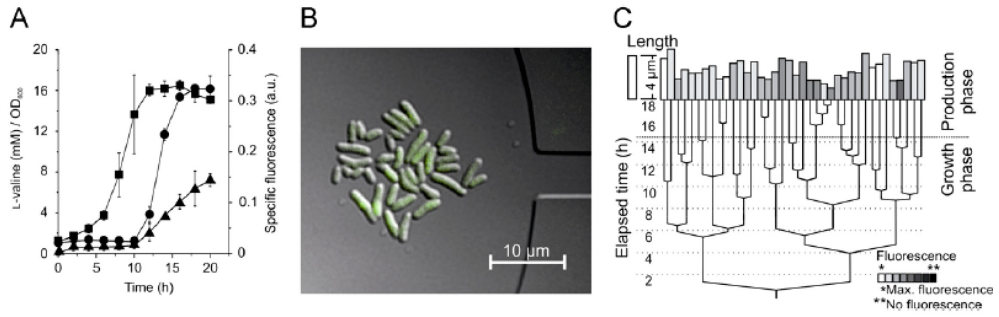

Fig. 3. Biosensor-based analysis of *C. glutamicum* Δ*aceE*. (A) Growth (■), eYFP fluorescence (●) and L-valine production (▲) of *C. glutamicum* Δ*aceE* cultivated in minimal medium containing 4% glucose and 1.5% acetate. Data represent average values of three independent cultivations. (B) A microcolony and (C) respective lineage tree of *C. glutamicum* Δ*aceE* containing the biosensor plasmid grown in a microfluidic chamber, illustrating variation at the single-cell level. Growth phase: minimal medium containing 4% glucose and 1.5% acetate. Production phase: minimal medium with 4% glucose. EYFP fluorescence was quantified in single cells after 18 h. The length of the boxes corresponds to the length of the cells at the time of fluorescence measurement. The lineage tree is based on Video S1 (growth phase).

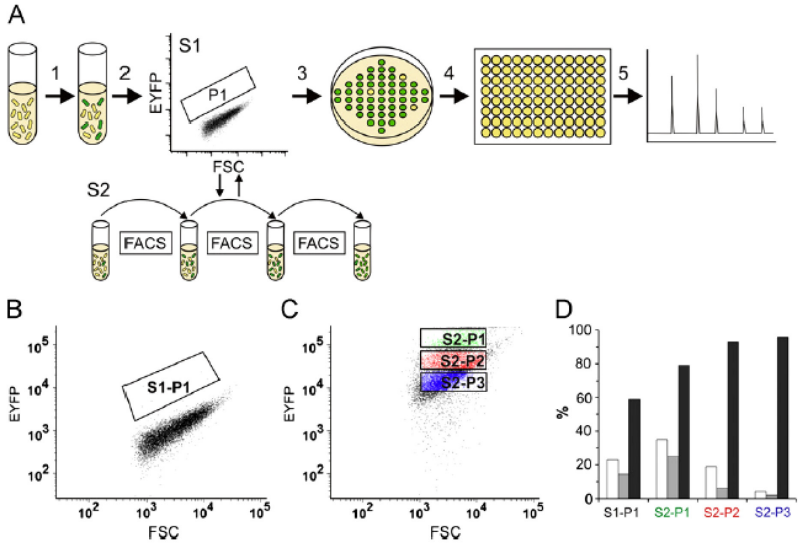

Fig. 4. Biosensor-based FACS high-throughput screening. (A) Schematic diagram of FACS screening: (1) Mutagenesis, (2) Screening approach S1: fluorescent cells were sorted by FACS, Screening approach S2: The 10,000 mutants with highest levels of eYFP emission were sorted in liquid medium, isolated and re-cultivated; this procedure of sorting and re-cultivation was repeated three times. (3) Sorting on plates, (4) cultivation in microtiter plates (48 h) and (5) uHPLC analysis of supernatant. (B) Dot plot displaying the FCS signal against the eYFP signal of mutagenized *C. glutamicum* cells six hours after mutagenesis and subsequent incubation in BHIS medium. Cells were sorted from gate S1-P1. (C) Dot plot (FSC/eYFP) of mutagenized cells on the fourth day of the iterative screen. Cells were sorted on BHI agar plates from gates S2-P1, S2-P2, and S2-P3. (D) The percentage of positive clones (white bars), those excreting > 2 mM effector amino acids (gray bars) and viability of clones after sorting (black bars).

Overall, the top five mutants obtained from FACS screening (S1 and S2) produced up to 8 mM L-valine, up to 2 mM of L-isoleucine and up to1 mM L-isoleucine after 48 h in minimal medium with 4% glucose, 1.5% acetate and 0.1% yeast extract (Table 3). Growth and sensor output of the top five mutants are shown in Fig. S4. In two of the top five mutants PDH activity was about twofold decreased in comparison to the WT (mutant 2: 0.049 ± 0.001 U/mg, mutant 4: 0.043 ± 0.007 U/mg, WT: 0.082 ± 0.01 U/mg), which could be a reason for L-valine excretion. However, no mutation in the gene sequence of *aceE* could be identified in these mutants.

Table 3
Top five mutants excreting branched-chain amino acids (n=2).

Mutant no.	L-valine (mM)	L-leucine (mM)	L-isoleucine (mM)
1	8.7	1.3	0.9
2	5.1	1.0	1.3
3	4.8	1.0	1.0
4	4.6	n.d.	2.1
5	4.6	1.2	1.2

4. Discussion

Nature has evolved versatile sensor devices for small molecules, metabolites and physical parameters in the form of proteins, RNA and DNA. We harnessed the functionality of one of these – the transcriptional regulator Lrp – to report on *in vivo* amino acid production in *C. glutamicum*, an organism of considerable importance to the biotechnology industry. This Lrp-based biosensor detects intracellular L-methionine and the branched-chain amino acids L-leucine, L-isoleucine and L-valine by transforming the information into a fluorescent output signal.

Screening and analysis of production strains using a biosensor requires that the relationship between the effector molecule input and reporter output is well understood. To achieve this,

we favoured an *in vivo* determination of the sensor transfer curve. Although the dipeptide feeding approach that we used was restricted by the kinetics of peptide uptake and hydrolysis, the minimal dynamic range and linear detection range (described in Table 2) covers the low to medium mM range. This range makes the system suitable for the analysis and screening of production strains as it allows the discrimination of strains with significantly elevated intracellular amino acid levels (mM range) from wild type level (nM to high μM range). A few studies report on the intracellular concentration of amino acids in production strains, but the high external accumulation of the respective metabolite often makes an exact determination difficult. Eggeling and co-workers reported an accumulation of up to 110 mM isoleucine in the isoleucine-producing strain *C. glutamicum* SM13 (Morbach et al., 1996). In-house measurements of the internal L-lysine concentration of several lysine production strains revealed a concentration ranging from 5–30 mM L-lysine, depending on the strain background (Eggeling, unpublished). In the case of the PDHC-deficient L-valine producers *C. glutamicum* Δ*aceE* and Δ*aceE*(pJC4-ilvBNCE), the internal concentration of the L-valine precursor pyruvate amounts to 25 and 2.3 mM, respectively (Blombach et al., 2007). If the assessment of higher accumulations of internal amino acids with the described sensor system is desired, exporter deletion strains could be used, which have been reported to accumulate up to 0.5–1 M of the respective amino acids (Kennerknecht et al., 2002; Vrljic et al., 1996). However, this approach seems inappropriate, since comparability to the wild type strain in regard to the formation of a distinct internal amino acid peak is hardly given.

The sensor technology was used in an ultra high-throughput FACS screen (10,000 cells per second) to isolate cells with increased intracellular concentrations of the effector amino acids following random mutagenesis. Our first screening approach resulted in the isolation of about 40 mutants that produced branched-chain amino acids, out of 192 screened by uHPLC (Fig. 4, Table S1). Among these, the top five mutants produced up to 8 mM L-valine, up to 2 mM of L-leucine and up to 1 mM L-isoleucine. As known from previous studies, the activity of the PDH complex is crucial for the production of L-valine (Bartek et al., 2011; Blombach et al., 2007). Indeed, two of the top five mutants showed a reduced PDH activity, but sequencing of the *aceE* revealed wild type situation in all of the top five mutants. Further reasons for a reduced PDH activity might be for example an impaired cofactor biosynthesis or mutations in genes encoding regulatory proteins (Bartek et al., 2010). For detailed insights genomic analysis of promising mutants is required for identification of novel and unexpected targets for strain improvement. For example, a melanin-based screen for L-tyrosine led to the identification of mutants in unknown proteins which could not have been predicted by rational strain design (Santos and Stephanopoulos, 2008).

As far as we are aware, this is the first biosensor-based FACS screen for the *in vivo* detection of inconspicuous, biotechnologically-relevant products, such as amino acids, in single bacterial cells (Dietrich et al., 2010). Previously, targets for FACS screenings have included metabolites that are natural or synthetic photophores, such as carotenoids (Albrecht et al., 2000; An et al., 1991), the antibiotic gramicidin S (Azuma et al., 1992) or polyhydroxyalkanoates (Vidal-Mas et al., 2001). A common problem of FACS screenings is the high rate of false positives, in some cases beyond 99% (Sitnikov et al., 1995). In our Lrp biosensor-based screening, secondary screening revealed that 20–30% (depending on the gating strategy) of the isolated mutants excreted significant amounts of the effector amino acids. Among so-called "false-positive" clones we will certainly find several mutants which intracellularly accumulate high amounts of the respective amino acids, but might have a defect in export of those (*e.g.* mutation of *brnFE* itself). Thus, we emphasize this system also for the identification of transport systems. This could, for example, easily be realized by screening transposon-mutagenized sensor cells for cells with significantly increased fluorescent output.

In these experiments, the screening conditions led to isolation of mutants producing branched-chain amino acids. However, the outcome of screens can be influenced by several factors, including cultivation conditions, the original strain used for mutagenesis and the gating strategy used in FACS. As L-methionine is currently of major interest for biotechnological strain development, future work will adapt the screening procedure for the isolation of L-methionine-producing mutants. Prevention of reuptake (Δ*metNI* and Δ*metP*) (Trötschel et al., 2008), derepression of L-methionine biosynthesis genes (Rey et al., 2003) and the addition of reduced sulfur compounds such as methanethiol or dimethyldisulfide, might be important prerequisites for the successful isolation of L-methionine producing mutants in future screening approaches (Bolten et al., 2010).

The intracellular, rather than extracellular, detection of a specific metabolite is a prerequisite for a biosensor system compatible with high-throughput FACS screening or single cell analysis of production strains. Systems, such as the one described in this study, allow the rapid isolation of mutations, but cannot provide information with respect to the excretion of the particular metabolite. Thus, a quantitative analysis of the extracellular metabolite concentrations by uHPLC or mass spectrometry is required to determine whether the isolated mutants excrete the respective metabolite in the supernatant. As the described biosensor system depends on the use of a transcriptional regulator (Lrp) as the sensor device, specificity and dynamic range of the respective system depends on the biochemical characteristics of the chosen regulator. These can, in principle, be optimized by protein engineering and/or evolution. However, in many cases more than one specific effector metabolite influences the activity of a given regulator; in case of Lrp four amino acids (L-methionine and the branched-chain amino acids) have been described (Lange et al., 2011). Thus, the intracellular detection of more than one effector metabolite as well as the typically high rate of false positive clones in FACS screenings clearly necessitates secondary screening, for example, uHPLC, for reliable mutant analysis. The use of GFP-based autofluorescent proteins as reporter proteins also have some pros and cons. The stable, non-cytotoxic expression of *gfp* and its derivatives, plus their outstanding brightness, make them a favorable option (Chudakov et al., 2005; Frommer et al., 2009; Giepmans et al., 2006). However, signal delay due to chromophor maturation or the dependency on molecular oxygen are drawbacks (Shaner et al., 2005; Tsien, 1998).

It has long been known that clonal populations of microorganisms display substantial variation in phenotypic traits. Reasons for this population heterogeneity include micro-environmental differences, variations in cell age, stages in the cell cycle and stochastic effects (Elowitz et al., 2002; Lidstrom and Konopka, 2010). Cell-to-cell variation with regard to promoter activity or protein abundance is easily detected using autofluorescent proteins but there has been little study of single-cell quantification of metabolites (Heinemann and Zenobi, 2011). Biosensors, in the form of FRET sensors, and regulatory circuits do provide powerful tools for single-cell resolution (Deuschle et al., 2005; Michener et al., in press; van der Meer and Belkin, 2010; Zhang and Keasling, 2011). In this study, we achieved a first glimpse of variation in productivity using the PDHC-deficient L-valine producer *C. glutamicum* Δ*aceE*. Our analysis of microcolonies grown from one single cell revealed variations in doubling time, cell size and, most interestingly, single-cell fluorescence. Such effects could not be detected in shake flask experiments where L-valine

accumulates in the supernatant and in turn influences internal levels of L-valine. Indeed, stopping the flow of medium through the microfluidic chamber almost completely masked cell-to-cell variation (Fig. S3). The origin of the variability in internal L-valine accumulation among Δ*aceE* cells will be assessed in future studies. Factors reported to influence L-valine production in *C. glutamicum* include the expression level of L-valine biosynthesic genes, the activity of the PDHC by-pass pyruvate:quinone oxidoreductase, as well as the supply of NADH, depending on the flux through the pentose phosphate pathway (Bartek et al., 2010; Blombach et al., 2008).

5. Conclusions

Biosensors based on transcriptional regulators have a successful history in bioengineering, where they are used to detect environmental pollutants including antibiotics, carcinogens and heavy metals (van der Meer and Belkin, 2010; Zhang and Keasling, 2011). However, the great potential of transcription factor-based sensor technologies for strain development and screening strategies in industrial biotechnology has not been exploited at all so far. The technology described here initiatives that process: it can be applied to an extensive repertoire of natural sensor devices for the design of biosensors that detect a broad spectrum of important biotechnological metabolites.

Acknowledgments

We thank Reinhard Krämer for helpful advice on dipeptide feeding, Lothar Eggeling for discussion, Georg Schendzielorz, Stephan Binder and Janko Potzkei (University of Düsseldorf) for technical assistance, and Arun Nanda for critical reading of the manuscript. This work was supported by the German ministry of Education and Research (BMBF, funding of NM) and the Helmholtz Gemeinschaft (Helmholtz YIG to JF).

Appendix A. Supporting information

Supplementary data associated with this article can be found in the online version at doi:10.1016/j.ymben.2012.02.002.

References

Albrecht, M., Takaichi, S., Steiger, S., Wang, Z.Y., Sandmann, G., 2000. Novel hydroxycarotenoids with improved antioxidative properties produced by gene combination in *Escherichia coli*. Nat. Biotechnol. 18, 843–846.

An, G.H., Bielich, J., Auerbach, R., Johnson, E.A., 1991. Isolation and characterization of carotenoid hyperproducing mutants of yeast by flow cytometry and cell sorting. Biotechnology (NY) 9, 70–73.

Azuma, T., Harrison, G.I., Demain, A., 1992. Isolation of a gramicidin S hyperproducing strain of *Bacillus brevis* by use of a fluorescence activated cell sorting system. Appl. Microbiol. Biotechnol. 38, 173–178.

Bailey, J.E., 1991. Toward a science of metabolic engineering. Science 252, 1668–1675.

Bartek, T., Blombach, B., Lang, S., Eikmanns, B.J., Wiechert, W., Oldiges, M., Nöh, K., Noack, S., 2011. Comparative (13)C metabolic flux analysis of pyruvate dehydrogenase complex-deficient, L-valine-producing *Corynebacterium glutamicum*. Appl. Environ. Microbiol. 77, 6644–6652.

Bartek, T., Blombach, B., Zonnchen, E., Makus, P., Lang, S., Eikmanns, B.J., Oldiges, M., 2010. Importance of NADPH supply for improved L-valine formation in *Corynebacterium glutamicum*. Biotechnol. Prog. 26, 361–371.

Blombach, B., Schreiner, M., Holatko, J., Bartek, T., Oldiges, M., Eikmanns, B., 2007. L-valine production with pyruvate dehydrogenase complex-deficient *Corynebacterium glutamicum*. Appl. Environ. Microbiol. 73, 2079–2084.

Blombach, B., Schreiner, M.E., Bartek, T., Oldiges, M., Eikmanns, B.J., 2008. *Corynebacterium glutamicum* tailored for high-yield L-valine production. Appl. Microbiol. Biotechnol. 79, 471–479.

Bolten, C.J., Schröder, H., Dickschat, J., Wittmann, C., 2010. Towards methionine overproduction in *Corynebacterium glutamicum*—methanethiol and dimethyldisulfide as reduced sulfur sources. J. Microbiol. Biotechnol. 20, 1196–1203.

Burkovski, A., 2008. Corynebacteria: Genomics and Molecular Biology. Caister Academic Press, Norfolk UK.

Chudakov, D.M., Lukyanov, S., Lukyanov, K.A., 2005. Fluorescent proteins as a toolkit for *in vivo* imaging. Trends Biotechnol. 23, 605–613.

Deuschle, K., Fehr, M., Hilpert, M., Lager, I., Lalonde, S., Looger, L.L., Okumoto, S., Persson, J., Schmidt, A., Frommer, W.B., 2005. Genetically encoded sensors for metabolites. Cytometry A 64, 3–9.

Dietrich, J.A., McKee, A.E., Keasling, J.D., 2010. High-throughput metabolic engineering: advances in small-molecule screening and selection. Annu. Rev. Biochem. 79, 563–590.

Ebbighausen, H., Weil, B., Krämer, R., 1989. Isoleucine excretion in *Corynebacterium glutamicum*: evidence for a specific efflux carrier system. Appl. Microbiol. Biotechnol. 31, 184–190.

Eggeling, L., 2001. Amino acids. In: Ratledge, C., Kristiansen, B. (Eds.), Basic Biotechnology. Cambridge University Press, London, pp. 281–303.

Eggeling, L., Bott, M., 2005. Handbook of *Corynebacterium glutamicum*. Academic Press, Inc., Boca Raton, FL.

Elowitz, M.B., Levine, A.J., Siggia, E.D., Swain, P.S., 2002. Stochastic gene expression in a single cell. Science 297, 1183–1186.

Frommer, W.B., Davidson, M.W., Campbell, R.E., 2009. Genetically encoded biosensors based on engineered fluorescent proteins. Chem. Soc. Rev. 38, 2833–2841.

Frunzke, J., Bramkamp, M., Schweitzer, J.E., Bott, M., 2008. Population heterogeneity in *Corynebacterium glutamicum* ATCC 13032 caused by prophage CGP3. J. Bacteriol. 190, 5111–5119.

Giepmans, B.N.G., Adams, S.R., Ellisman, M.H., Tsien, R.Y., 2006. The fluorescent toolbox for assessing protein location and function. Science 312, 217–224.

Heinemann, M., Zenobi, R., 2011. Single cell metabolomics. Curr. Opin. Biotechnol. 22, 26–31.

Hoffelder, M., Raasch, K., van Ooyen, J., Eggeling, L., 2010. The E2 domain of OdhA of *Corynebacterium glutamicum* has succinyltransferase activity dependent on lipoyl residues of the acetyltransferase AceF. J. Bacteriol 192, 5203–5211.

Ikeda, M., 2003. Amino acid production processes. Adv. Biochem. Eng. Biotechnol. 79, 1–35.

Kensy, F., Zang, E., Faulhammer, C., Tan, R.K., Büchs, J., 2009. Validation of a high-throughput fermentation system based on online monitoring of biomass and fluorescence in continuously shaken microtiter plates. Microb. Cell Factories 8, (31).

Kennerknecht, N., Sahm, H., Yen, M.R., Patek, M., Saier Jr., M.H., Eggeling, L., 2002. Export of L-isoleucine from *Corynebacterium glutamicum*: a two-gene-encoded member of a new translocator family. J. Bacteriol. 184, 3947–3956.

Kinoshita, S., Udaka, S., Shimono, M., 1957. Studies on the amino acid fermentation: I. Production of L-glutamic acid by various microorganisms. J. Gen. Appl. Microbiol. 3, 193–205.

Lange, C., Mustafi, N., Frunzke, J., Kennerknecht, N., Wessel, M., Bott, M., Wendisch, V.F., 2011. Lrp of *Corynebacterium glutamicum* controls expression of the *brnFE* operon encoding the export system for L-methionine and branched-chain amino acids. J. Biotechnol.

Leuchtenberger, W., 1996. Amino acids—technical production and use. In: Rehm, H., et al. (Eds.), Biotechnology, vol. 6. VCH, Weinheim, pp. 465–502.

Lidstrom, M.E., Konopka, M.C., 2010. The role of physiological heterogeneity in microbial population behavior. Nat. Chem. Biol. 6, 705–712.

Michener, J.K., Thodey, K., Liang, J.C., Smolke, C.D. Applications of genetically-encoded biosensors for the construction and control of biosynthetic pathways. Metab. Eng., doi:10.1016/j.ymben.2011.09.004, in press.

Morbach, S., Sahm, H., Eggeling, L., 1996. L-isoleucine production with *Corynebacterium glutamicum*: Further flux increase and limitation of export. Appl. Environ. Microbiol. 62, 4345–4351.

Park, J.H., Lee, K.H., Kim, T.Y., Lee, S.Y., 2007. Metabolic engineering of *Escherichia coli* for the production of L-valine based on transcriptome analysis and in silico gene knockout simulation. Proc. Natl. Acad. Sci. USA 104, 7797–7802.

Rey, D.A., Pühler, A., Kalinowski, J., 2003. The putative transcriptional repressor McbR, member of the TetR-family, is involved in the regulation of the metabolic network directing the synthesis of sulfur containing amino acids in *Corynebacterium glutamicum*. J. Biotechnol. 103, 51–65.

Ruffert, S., Lambert, C., Peter, H., Wendisch, V.F., Krämer, R., 1997. Efflux of compatible solutes in *Corynebacterium glutamicum* mediated by osmoregulated channel activity. Eur. J. Biochem. 247, 572–580.

Sambrook, J., MacCallum, P., Russell, D., 2001. Molecular Cloning. A Laboratory Manual. Cold Spring Harbor Laboratory Press, New York.

Santos, C.N., Stephanopoulos, G., 2008. Melanin-based high-throughput screen for L-tyrosine production in *Escherichia coli*. Appl. Environ. Microbiol. 74, 1190–1197.

Schäfer, A., Tauch, A., Droste, N., Pühler, A., Kalinowski, J., 1997. The *Corynebacterium glutamicum cglIM* gene encoding a 5-cytosine methyltransferase enzyme confers a specific DNA methylation pattern in an McrBC-deficient *Escherichia coli* strain. Gene 203, 95–101.

Schreiner, M.E., Fiur, D., Holatko, J., Patek, M., Eikmanns, B.J., 2005. E1 enzyme of the pyruvate dehydrogenase complex in *Corynebacterium glutamicum*: molecular analysis of the gene and phylogenetic aspects. J. Bacteriol. 187, 6005–6018.

Shaner, N.C., Steinbach, P.A., Tsien, R.Y., 2005. A guide to choosing fluorescent proteins. Nat. Methods. 2, 905–909.

Sitnikov, D.M., Schineller, J.B., Baldwin, T.O., 1995. Transcriptional regulation of bioluminesence genes from *Vibrio fischeri*. Mol. Microbiol. 17, 801–812.
Trötschel, C., Deutenberg, D., Bathe, B., Burkovski, A., Krämer, R., 2005. Characterization of methionine export in *Corynebacterium glutamicum*. J. Bacteriol. 187, 3786–3794.
Trötschel, C., Follmann, M., Nettekoven, J.A., Mohrbach, T., Forrest, L.R., Burkovski, A., Marin, K., Krämer, R., 2008. Methionine uptake in *Corynebacterium glutamicum* by MetQNI and by MetPS, a novel methionine and alanine importer of the NSS neurotransmitter transporter family. Biochemistry 47, 12698–12709.
Tsien, R.Y., 1998. The green fluorescent protein. Annu. Rev. Biochem. 67, 509–544.
van der Meer, J.R., Belkin, S., 2010. Where microbiology meets microengineering: design and applications of reporter bacteria. Nat. Rev. Microbiol. 8, 511–522.
Vidal-Mas, J., Resina, P., Haba, E., Comas, J., Manresa, A., Vives-Rego, J., 2001. Rapid flow cytometry—Nile red assessment of PHA cellular content and heterogeneity in cultures of *Pseudomonas aeruginosa* 47T2 (NCIB 40044) grown in waste frying oil. Antonie Van Leeuwenhoek 80, 57–63.
Vrljic, M., Sahm, H., Eggeling, L., 1996. A new type of transporter with a new type of cellular function: L-lysine export from *Corynebacterium glutamicum*. Mol. Microbiol. 22, 815–826.
Xia, Y.N., Whitesides, G.M., 1998. Soft lithography. Angew. Chem. Int. Ed. 37, 551–575.
Zhang, F., Keasling, J., 2011. Biosensors and their applications in microbial metabolic engineering. Trends Microbiol. 19, 323–329.

Name of the journal:	Metabolic Engineering
Impact factor:	5.614
Contribution of own work:	80%
1. author:	Experimental work and writing of the manuscript

microbial biotechnology

Open Access

Brief report

Destabilized eYFP variants for dynamic gene expression studies in *Corynebacterium glutamicum*

Eva Hentschel,[1†] Cornelia Will,[2†] Nurije Mustafi,[1] Andreas Burkovski,[2] Nadine Rehm[2] and Julia Frunzke[1*]

[1]*Institut für Bio- und Geowissenschaften, IBG-1: Biotechnologie, Forschungszentrum Jülich, Germany.*
[2]*Lehrstuhl für Mikrobiologie, Friedrich-Alexander-Universität Erlangen-Nürnberg, Erlangen, Germany.*

Summary

Fluorescent reporter proteins are widely used for the non-invasive monitoring of gene expression patterns, but dynamic measurements are hampered by the extremely high stability of GFP and homologue proteins. In this study, we used SsrA-mediated peptide tagging for the construction of unstable variants of the GFP derivative eYFP (enhanced yellow fluorescent protein) and applied those for transient gene expression analysis in the industrial platform organism *Corynebacterium glutamicum*.

The Gram-positive soil bacterium *Corynebacterium glutamicum* was isolated in 1957 in Japan due to its ability to excrete large amounts of the amino acid L-glutamate (Kinoshita, 1957). Within the last decades *C. glutamicum* was proven to be an excellent production platform not only for amino acids, but also for a variety of other metabolites, including organic acids, vitamins and polymer precursors (Leuchtenberger, 1996; Eggeling and Bott, 2005; Burkovski, 2008). Efficient metabolic engineering, however, depends on a detailed understanding of gene expression patterns and adaptive responses of the respective organism. Reporter proteins, such as β-galactosidase (*lacZ*), bacterial luciferase (*luxCDABE*), and autofluorescent proteins (*gfp*, *yfp*, etc.) represent convenient tools for the detection and quantification of molecular and genetic events (Ghim *et al*., 2010). Among these, fluorescent proteins offer the advantage of broad-host applicability, no need for substrate addition, and a non-destructive measurement at the single cell level (Chalfie *et al*., 1994; Tsien, 1998). A major drawback of several reporter proteins is, however, their extremely long half-life (GFP > 24 h), which leads to accumulation of the protein within the cell and hampers the study of transient changes in gene expression. To address this issue, Andersen and co-workers used C-terminal SsrA peptide tagging for destabilization of GFP in *Escherichia coli* and *Pseudomonas putida* (Andersen *et al*., 1998). This approach was in the following successfully applied to generate unstable GFP variants in, e.g. *Mycobacterium* species or for destabilization of the *Photorhabdus luminescens* luciferase (Triccas *et al*., 2002; Blokpoel *et al*., 2003; Allen *et al*., 2007).

The SsrA tag is encoded by the tmRNA (tmRNA, *ssrA* or 10Sa RNA), which functions as both transfer and messenger RNA and acts as a rescue system of ribosomes stalled on broken or damaged mRNA (Keiler, 2008). By translation of the messenger part of tmRNA a peptide tag of 11 amino acids is added to the C-terminus of the premature protein (*E. coli* SsrA tag: AANDENYALAA), thereby rendering it susceptible for tail-specific proteases, such as ClpXP, ClpAP or FtsH (Gottesman *et al*., 1998; Herman *et al*., 1998). Previous studies showed that variation of the terminal three amino acids of the tag can be used to generate variants of different protein stability (Andersen *et al*., 1998).

The *ssrA* gene is highly conserved in bacterial genomes and a homologue was also annotated in the *C. glutamicum* genome (Kalinowski *et al*., 2003). In this study we used SsrA peptide tagging to construct a set of destabilized fluorescent protein variants (eYFP and GFPuv) with significantly reduced half-lives, compared with the native proteins. These proteins represent valuable tools for the monitoring of dynamic gene expression patterns in the biotechnological organism *C. glutamicum*.

For construction of unstable fluorescent protein variants the native *E. coli* (AANDENYALAA) and *C. glutamicum* SsrA tag (AAEKSQRDYALAA) or tags varying in their terminal three amino acids of the corynebacterial tag (in the

Received 31 May, 2012; revised 1 August, 2012; accepted 3 August, 2012. *For correspondence. E-mail j.frunzke@fz-juelich.de; Tel. (+49) 2461 61 5430; Fax (+49) 2461 61 2710. †Both authors contributed equally to this work.
doi:10.1111/j.1751-7915.2012.00360.x
Funding Information This work was supported by the Helmholtz Association (Helmholtz Grant VH-NG-716 to J.F.) and by the BMBF in frame of the SysMo2 programme.

Table 1. Plasmids and oligonucleotides used in this study.

Plasmid	Properties	Reference
pEKEx2	Kan^R; expression vector with *lacI*^{q}, P_{tac} and pUC18 multiple cloning site	Eikmanns *et al.* (1991)
pEKEx2-*eyfp*	Kan^R, pEKEx2 containing *eyfp* with artificial RBS, under control of P_{tac}	This study
pEKEx2-*eyfp*-asv	Kan^R, pEKEx2 containing *eyfp*, with artificial RBS, under control of P_{tac}, modified to include the gene sequence for the C-terminal *C. glutamicum* SsrA tag variation AAEKSQRDYAASV	This study
pEKEx2-*eyfp*-aav	Similar to pEKEx2-*eyfp*-ASV using the alternative tag AAEKSQRDYAAAV	This study
pEKEx2-*eyfp*-lva	Similar to pEKEx2-*eyfp*-ASV using the alternative tag AAEKSQRDYALVA	This study
pEKEx2-*eyfp*-laa	Similar to pEKEx2-*eyfp*-ASV using the native *C. glutamicum* tag AAEKSQRDYALAA	This study
pEKEx2-*eyfp*-Ec_laa	Similar to pEKEx2-*eyfp*-ASV using the native *E. coli* tag AANDENYALAA	This study
pJC1	Kan^R, Amp^R; *C. glutamicum* shuttle vector	Cremer *et al.* (1991)
pJC1-P_{gntK}-*eyfp*	Kan^R, pJC1 containing *eyfp* under control of the promoter of *gntK* (153 bp)	This study
pJC1-P_{gntK}-*eyfp*-asv	Similar to pJC1-P_{gntK}-*eyfp* using *eyfp* modified to include the gene sequence for the C-terminal *C. glutamicum* SsrA tag AAEKSQRDYAASV	This study
pEKEx2-*eyfp*-*tetR*	Kan^R, pEKEx2 derivative containing *yfp*-*tetR*, encoding a eYFP–TetR fusion protein under the control of the P_{tac}	Frunzke *et al.* (2008a)
pEKEx2-*gfp*	Kan^R pEKEx2 containing *gfpuv* with artificial RBS, under control of P_{tac}	This study
pEKEx2-*gfp*-asv	Kan^R, pEKEx2 containing *gfpuv*, with artificial RBS, under control of P_{tac}, modified to include the gene sequence for the C-terminal *C. glutamicum* SsrA tag variation AAEKSQRDYAASV	This study
pEKEx2-*gfp*-aav	Similar to pEKEx2-*gfpuv*-ASV using the alternative tag AAEKSQRDYAAAV	This study
pEPR1-*gfp*	*gfpuv*, Kan^R, *rep*, *per*, T1 (T-*trpE*) (T-*trpA*), T2 (T-*rmB*) (T-*leuB*); promoter probe vector	Knoppova *et al.* (2007)

Oligonucleotide	Sequence 5′ -> 3′[a]	Application[b]
eYFP-ASV-*C.g.*-EcoRI-rv	CGCGAATTCTTA*AACTGATGCAGCGTAATCACGTTGGCTCTTTTCTGCTGC*TCTAGACTTGTACAGCTCGTC (EcoRI)	Rv for *eyfp-Cg*-ASV
eYFP-AAV-*C.g.*-EcoRI-rv	CGCGAATTCTTA*AACAGCTGCTGCGTAATCACGTTGGCTCTTTTCTGCTGC*TCTAGACTTGTACAGCTCGTC (EcoRI)	Rv for *eyfp-Cg*-AAV
eYFP-LVA-*C.g.*-EcoRI-rv	CGCGAATTCTTA*AGCTACTAAAGCGTAATCACGTTGGCTCTTTTCTGCTGC*TCTAGACTTGTACAGCTCGTC (EcoRI)	Rv for *eyfp-Cg*-LVA
eYFP-LAA-*C.g.*-EcoRI-rv	CGCGAATTCTTA*AGCTGCTAAAGCGTAATCACGTTGGCTCTTTTCTGCTGC*TCTAGACTTGTACAGCTCGTC (EcoRI)	Rv for *eyfp-Cg*-LAA
eYFP-LAA-*E.c.*-EcoRI-rv	CGCGAATTCTTA*AGCTGCTAAAGCGTAGTTTTCGTCGTTTGCTGC*TCTAGACTTGTACAGCTCGTC (EcoRI)	Rv for *eyfp-Ec*-LAA
eYFP-EcoRI-rv	CGCGAATTCTTATCTAGACTTGTACAGCTCGTC (EcoRI)	Rv for *eyfp*
eYFP-RBS-BamHI-fw	CGCGGATCC**AAGGAGATATGAT**ATGGTGAGCAAGGGCGAGGAG (BamHI)	Fw for *eyfp* and destabilized variants
eYFP-ASV-*C.g.*-SalI-rv	CGCGTCGACTTA*AACTGATGCAGCGTAATCACG* (SalI)	Rv for *eyfp-Cg*-ASV
eYFP-AAV-*C.g.*-SalI-rv	CGCGTCGACTTA*AACAGCTGCTGCGTAATCACG* (SalI)	Rv for *eyfp-Cg*-AAV
eYFP-NdeI-fw	CGCCATATGGTGAGCAAGGGCGAGGAG (NdeI)	Fw for *eyfp* and destabilized variants
P_{gntK}-BamHI-fw	CGCGGATCCACATACAGTCCCCGTGATGTGAC (BamHI)	Fw for promoter region of *gntK*
P_{gntK}-NdeI-rv	CGC CATATG GTCTTATCCTTTCTTTGGTGGCG (NdeI)	Rv for promotor region of *gntK*
GFPuv-AAV-*C.g.*-EcoRI-rv	GCGCGATATCGAATTCTCATTA*AACAGCTGCTGCGTAATCACGTTGGCTCTTTTCTGCTGC*TTTGTAGAGCT CATCCATGCCATG (EcoRI)	Rv for *gfpuv-Cg*-AAV
GFPuv-ASV-*C.g.*-EcoRI-rv	GCGCGATATCGAATTCTCATTA*AACTGATGCAGCGTAATCACGTTGGCTCTTTTCTGCTGC*TTTGTAGAGCTC ATCCATGCCATG (EcoRI)	Rv for *gfpuv-Cg*-ASV
GFPuv-Acc65I-fw	GCGCGGTACCGGTAGAAAAAATGAG (Acc65I)	Fw for *gfpuv* and destabilized variants
GFPuv-EcoRI-rv	GCGCGCGAATTCGAGAGTTATCTCGGCCAGCCAC (EcoRI)	Rv for *gfpuv*

a. Some oligonucleotides were designed with restriction sites (underlined), ribosome binding sites (bold) and include SsrA-tag sequences (italic) as indicated.
b. Rv, reverse primer; Fw, forward primer for amplification.

Table 2. Overview of SsrA tag variants.

SsrA-tag	Amino acid sequence	Half-life (min)[a]	Signal intensity (%)[b]
E. c. LAA-tag native	AANDENYA**LAA**	n.d.	n.d.
C. g. LAA-tag native	AAEKSQRDYA**LAA**	n.d.	n.d.
C. g. LVA-tag variation	AAEKSQRDYA**LVA**	n.d.	n.d.
C. g. ASV-tag variation	AAEKSQRDYA**ASV**	22 ± 4	46
C. g. AAV-tag variation	AAEKSQRDYA**AAV**	8 ± 3	20

a. Protein half-lives were calculated from Western blot analysis (Fig. 1C) corresponding to the decay law $\lambda = \frac{\ln\left(\frac{N_{(0)}}{N_{(t)}}\right)}{t}$ $T_{1/2} = \frac{\ln(2)}{\lambda}$. Given values represent the average values with standard deviation of three independent experiments. For indicated constructs rapid degradation occurred and half-lives could not be determined (n.d.).
b. Signal intensity relative to native eYFP at the time of measurement.

following designated as ASV, AAV and LVA) were fused to the C-terminus of eYFP and GFPuv, which are both commonly used as reporter proteins in *C. glutamicum*. The fusion variants were cloned into the vector pEKEx2, under control of P_{tac}, and transferred into *C. glutamicum* ATCC 13032 by electroporation (Table 1). For fluorescence measurements cells were grown in 48-well microtiter Flowerplates containing CGXII minimal medium with 4% glucose in a BioLector microbioreactor system (m2p labs, Germany) (Kensy *et al.*, 2009); gene expression was induced by addition of 1 mM IPTG. In case of the eYFP variants we observed significant fluorescent signals for fusion constructs with ASV tag (46% of native eYFP) and AAV tag (20% of native eYFP) (Table 2). No signal was detected for the eYFP variants fused either to the native SsrA tag (*E. coli* or *C. glutamicum*) or to the LVA modified version (data not shown). To assess the stability of the ASV and AAV variants, transcription and translation of the

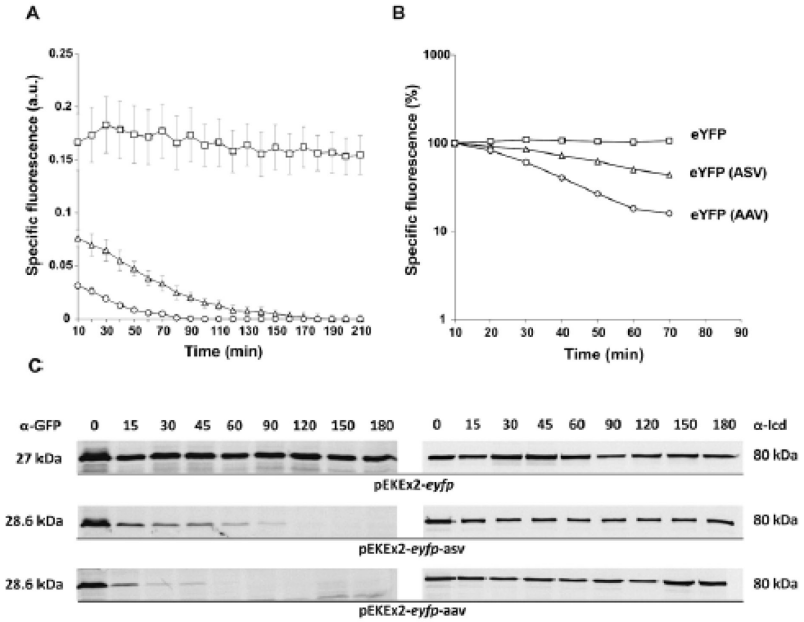

Fig. 1. Stability of eYFP variants in *C. glutamicum*. (A) Fluorescence of recombinant *C. glutamicum* ATCC 13032 strains expressing *eyfp* variants: ATCC 13032/pEKEx2-*eyfp* (squares), ATCC 13032/pEKEx2-*eyfp*-asv (triangles), ATCC 13032/pEKEx2-*eyfp*-aav (circles). Prior induction, cells were inoculated to an OD_{600} of 1 in 750 µl of CGXII minimal medium containing 4% glucose and cultivated in 48-well microtiter plates in the BioLector system (m2p labs, Germany). Gene expression was induced by addition of 1 mM IPTG. To estimate the stability of the eYFP variants 250 µg ml^{-1} rifampicin (Rif) and 100 µg ml^{-1} tetracycline (Tet) were added 1.5 h after induction to stop the transcription and translation. In the BioLector system the growth (backscatter signal of 620 nm light) and eYFP fluorescence (excitation 510 nm/emission 532 nm) were monitored in 10 min intervals. The specific fluorescence was calculated as fluorescence signal per backscatter signal (given in arbitrary units, a.u.). Results represent average values with standard deviation of three independent experiments. (B) Logarithmic scale blotting of data shown in 1A. Specific fluorescence of each strain to the time of antibiotic addition was set to 100%. (C) Determination of half-lives via Western blot analysis of eYFP (27.0 kDa), eYFP-ASV (28.6 kDa) and eYFP-AAV (28.6 kDa). Cells were cultivated in 70 ml of BHI medium with 2% glucose to an OD_{600} of 3–4. Prior and after addition of Tet and Rif (addition of antibiotics after 1.5 h) 5 ml of cells were harvested by centrifugation and subsequently frozen in liquid nitrogen. For isolation of crude extract cells were ruptured with glass beads in TE buffer (10 mM Tris, 1 mM EDTA, pH 8) with complete protease inhibitor (Roche, Germany). Samples (25 µg) were loaded on two identical SDS gels and proteins were separated by SDS-PAGE and analysed via Western blot analysis using anti-GFP (cross-reacting to eYFP) and anti-lcd for referencing (80 kDa). The intensity of bands was analysed with the AIDA software version 4.15 (Raytest GmbH, Germany). The images are representative ones out of three independent biological replicates.

respective strains were inhibited by the addition of tetracycline and rifampicin (100 μg ml^{-1} and 250 μg ml^{-1}, respectively) to the culture medium. Both antibiotics were added 1.5 h after induction with IPTG. The decrease in fluorescence was measured in 10 min intervals in the BioLector system (Fig. 1A and B). In the course of these measurements, a stable signal was observed for native eYFP for > 24 h whereas a rapid decrease in signal was observed for eYFP-ASV and eYFP-AAV. The half-life of both variants was determined via Western blot analysis using anti-GFP antibodies cross-reacting towards eYFP. A rapid decrease in eYFP protein level was detected for both, ASV and AAV, tagged variants and half-lives of 22 ± 4 min (ASV) and 8 ± 3 min (AAV) were calculated (Fig. 1C and Table 2). The reference protein, isocitrate dehydrogenase (Icd), exhibited a stable signal in Western blot analysis within the period of measurement (Fig. 1C). These data are in agreement with studies of SsrA-tagged variants in *E. coli* or *Mycobacterium* species. In almost all cases ASV and AAV variants resulted in a moderate destabilization of reporter proteins, whereas the native tag and the LVA variant are very unstable and hardly useful for the study of expression kinetics (Andersen *et al.*, 1998; Triccas *et al.*, 2002; Blokpoel *et al.*, 2003; Allen *et al.*, 2007).

We also investigated the suitability of SsrA-tagged GFPuv variants as reporters for transient gene expression, since GFPuv has been used as an appropriate reporter for *C. glutamicum* promoters in previous studies (Knoppová *et al.*, 2007; Hänßler *et al.*, 2009). As observed for the eYFP variants, no signal was detectable for proteins fused to the native SsrA tag or the LVA version whereas for GFPuv tagged with either ASV or AAV, fluorescence could be monitored (Fig. 2). However, in contrast to eYFP, tagging of GFPuv led to an immense loss in fluorescent signal with a very low residual fluorescence of 10% (AAV) and 12% (ASV) compared with native GFPuv. Since these fluorescence levels were only slightly above background level, determination of reporter half-lives was hardly feasible (Fig. 2).

The results observed for eYFP and GFPuv show that the destabilizing effect conferred by a specific degradation tag depends very much on the protein it is fused to. In fact, when fusing the same SsrA tag variants (ASV and AAV) to the far-red dsRed derivative E2-Crimson (Strack *et al.*, 2009), only a slightly decreased protein stability was obtained, whereas a major fraction of the proteins seemed stable after blocking translation and transcription with antibiotics (data not shown). This effect might be due to the tetrameric structure of E2-Crimson masking the SsrA tag towards recognition by tail-specific proteases. A similar assumption was made by Allen and co-workers who constructed an SsrA-tagged version of the luciferase subunits LuxB and LuxA, respectively (Allen *et al.*, 2007). In their study, tagging of LuxB did not result in significant

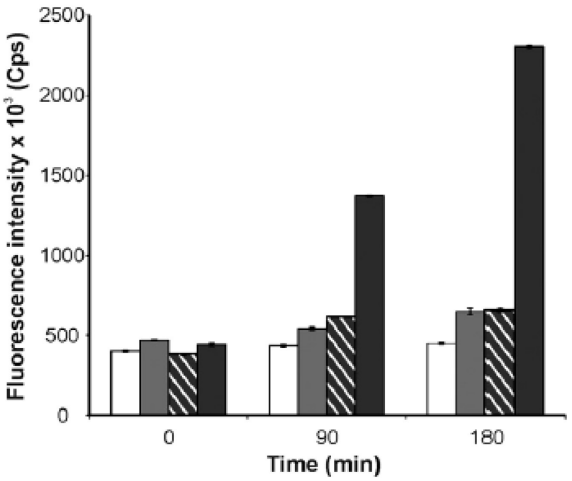

Fig. 2. Fluorescence of recombinant *C. glutamicum* strains expressing *gfp* variants. Shown is ATCC 13032/pEKEx2-*gfpuv* (black), ATCC 13032/pEKEx2-*gfpuv*-aav (patterned), ATCC 13032/pEKEx2-*gfpuv*-asv (grey) and ATCC 13032/pEKEx2 (white) as control. Cells were cultivated in CGXII minimal medium containing 1 mM IPTG to an OD_{600} of 3–5; 2 ml of cells were harvested by centrifugation and subsequently frozen in liquid nitrogen. Fluorescence was determined using Fluorolog 3 Double Spectrometer (Spex, USA). For this purpose, cells were thawed on ice, resuspended in 10 ml of cold TE buffer (10 mM Tris, 1 mM EDTA, pH 7.5) and the OD_{600} was determined. GFPuv fluorescence was carried out in triplicates using an excitation wavelength of 395 nm and recording emission at 509 nm. The graph shows the mean maximum fluorescence referred to the cell dry weight (1 ml of cell suspension of an OD_{600} of 1 corresponds to 0.36 mg of dry weight).

protein degradation; modification of both subunits, LuxA and LuxB, resulted in a rapid decay of bioluminescence. Therefore, a masking of the SsrA tag within a protein complex is an aspect which has to be considered for the destabilization of multimeric proteins.

As proof of principle we applied the eYFP-ASV variant to study the dynamic expression of the *gntK* gene in *C. glutamicum*. Expression of *gntK*, encoding gluconate kinase, is stringently regulated by the transcriptional regulators GntR1 and GntR2 in response to carbon source availability (Frunzke *et al.*, 2008b). When gluconate, the substrate of GntK, is present, repression of *gntK* by GntR1/2 is relieved and expression of *gntK* is strongly induced in the exponential growth phase. To assess the suitability of the unstable eYFP-ASV variant, fusions of the P_{gntK} promoter with *eyfp* or *eyfp*-asv, respectively, were constructed and cloned into the vector pJC1. As expected, both promoter fusions gave rise to a significant fluorescent signal when the cells were cultivated in minimal medium containing gluconate as carbon source (Fig. 3A: 100 mM gluconate; Fig. 3B: 50 mM of glucose and gluconate). No signal was observed in minimal medium with 100 mM glucose (data not shown). In contrast to the reporter with native eYFP, the signal of the

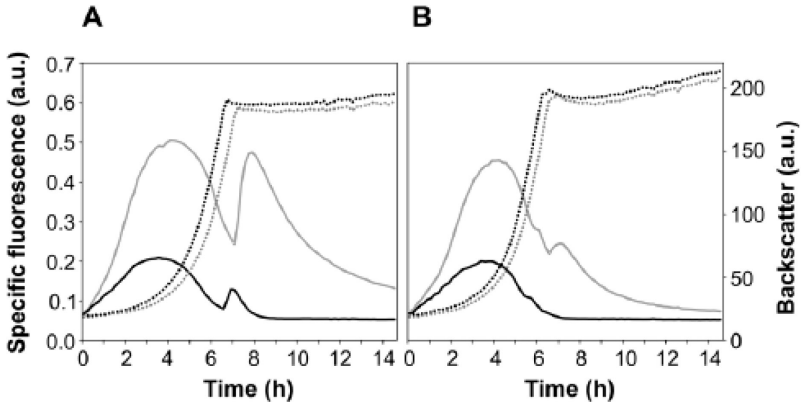

Fig. 3. Application of eYFP (grey) and destabilized eYFP-ASV (black) for dynamic gene expression analysis of *gntK* in *C. glutamicum*. Cells were inoculated to an OD_{600} of 1 in 750 µl of CGXII minimal medium containing either 100 mM gluconate (A) or 50 mM glucose and gluconate (B) in 48-well microtiter plates in the BioLector cultivation system (m2p labs, Germany). The final backscatter corresponds to a maximum OD_{600} of 35 and 38 for growth on 100 mM gluconate and 50 mM glucose plus gluconate, respectively. For pre-cultures, cells were cultivated in CGXII with 100 mM glucose. Growth (dashed line) and fluorescence (solid line) were recorded in 15 min intervals (for details see Fig. 1).

eYFP-ASV variant dropped back to zero when entering the stationary phase which is in agreement with enzyme activity measurements of GntK (Frunzke *et al.*, 2008b). The signal of native eYFP, however, did not reach background level within 24 h of measurement. This illustrates the suitability of unstable reporter variants to mirror the dynamic expression pattern of a gene of interest. Notably, the kink in specific fluorescence residing at the entrance into the stationary phase is due to delayed chromophore maturation in the log phase caused by oxygen limitation (Tsien, 1998; Shaner *et al.*, 2005; Drepper *et al.*, 2010). This effect is most likely less distinct for the unstable variant due to a lower amount of protein requiring oxygen for chromophore maturation. The kink in fluorescence was not observed with carbon source concentrations lower than 50 mM (data not shown). Interestingly, *C. glutamicum* expressing native *eyfp* showed a slight delay in growth in comparison with cells expressing the *eyfp*-asv variant. This indicates that expression of unstable reporter protein variants might even diminish the burden for the cell due to a rapid protein turnover and the avoidance of protein accumulation. A drawback of unstable variants is, however, the lowered reporter output (about twofold lower for eYFP-ASV) compared with the native reporter protein, which might lead to problems when monitoring genes with a low expression level. Consequently, the choice of the fluorescent protein variant, regarding spectral properties and protein half-life, clearly depends on the strength and dynamics of the promoter to be measured. Enlarging the tool box of reporter protein variants is required for optimal experimental design and output.

In a recent study, introduction of an SsrA-tagged variant of the enzyme TyrA into a phenylalanine producing *E. coli* strain was an elegant approach to improve the accumulation of phenylalanine (Doroshenko *et al.*, 2010). Our data reveal the applicability of corynebacterial SsrA tags and variants thereof for the efficient destabilization of eYFP and GFPuv in *C. glutamicum*. The use of SsrA peptide tagging is, yet, not limited to reporter proteins, but can be a valuable tool for the engineering of synthetic gene circuits (Elowitz and Leibler, 2000) or fine-tuning of protein levels in metabolic engineering of this important platform organism.

Conflict of interest

None declared.

References

Allen, S.A., Wilgus, J.R., Chewning, C.S., Sayler, G.S., and Simpson, M.L. (2007) A destabilized bacterial luciferase for dynamic gene expression studies. *Syst Synth Biol* **1:** 3–9.

Andersen, J.B., Sternberg, C., Poulsen, L.K., Bjorn, S.P., Givskov, M., and Molin, S. (1998) New unstable variants of green fluorescent protein for studies of transient gene expression in bacteria. *Appl Environ Microbiol* **64:** 2240–2246.

Blokpoel, M.C.J., O'Toole, R., Smeulders, M.J., and Williams, H.D. (2003) Development and application of unstable GFP variants to kinetic studies of mycobacterial gene expression. *J Microbiol Methods* **54:** 203–211.

Burkovski, A. (2008) *Corynebacteria: Genomics and Molecular Biology*. Norfolk, UK: Caister Academic Press.

Chalfie, M., Tu, Y., Euskirchen, G., Ward, W.W., and Prasher, D.C. (1994) Green fluorescent protein as a marker for gene expression. *Science* **263:** 802–805.

Cremer, J., Eggeling, L., and Sahm, H. (1991) Control of the lysine biosynthesis in *Corynebacterium glutamicum* as analyzed by overexpression of the individual corresponding genes. *Appl Environ Microbiol* **57:** 1746–1752.

Doroshenko, V.G., Shakulov, R.S., Kazakova, S.M., Kivero, A.D., Yampolskaya, T.A., and Mashko, S.V. (2010) Construction of an l-phenylalanine-producing tyrosine-prototrophic *Escherichia coli* strain using *tyrA* ssrA-like tagged alleles. *Biotechnol Lett* **32:** 1117–1121.

Drepper, T., Huber, R., Heck, A., Circolone, F., Hillmer, A.K., Büchs, J., and Jaeger, K.E. (2010) Flavin mononucleotide-based fluorescent reporter proteins outperform green fluorescent protein-like proteins as quantitative in vivo real-time reporters. *Appl Environ Microbiol* **76:** 5990–5994.

Eggeling, L., and Bott, M. (2005) *Handbook of* Corynebacterium glutamicum. Boca Raton, FL, USA: Academic Press.

Eikmanns, B.J., Kleinertz, E., Liebl, W., and Sahm, H. (1991) A family of *Corynebacterium glutamicum*/*Escherichia coli* shuttle vectors for cloning, controlled gene expression, and promoter probing. *Gene* **102:** 93–98.

Elowitz, M.B., and Leibler, S. (2000) A synthetic oscillatory network of transcriptional regulators. *Nature* **403:** 335–338.

Frunzke, J., Bramkamp, M., Schweitzer, J.E., and Bott, M. (2008a) Population heterogeneity in *Corynebacterium glutamicum* ATCC 13032 caused by prophage CGP3. *J Bacteriol* **190:** 5111–5119.

Frunzke, J., Engels, V., Hasenbein, S., Gätgens, C., and Bott, M. (2008b) Co-ordinated regulation of gluconate catabolism and glucose uptake in *Corynebacterium glutamicum* by two functionally equivalent transcriptional regulators, GntR1 and GntR2. *Mol Microbiol* **67:** 305–322.

Ghim, C.M., Lee, S.K., Takayama, S., and Mitchell, R.J. (2010) The art of reporter proteins in science: past, present and future applications. *BMB Rep* **43:** 451–460.

Gottesman, S., Roche, E., Zhou, Y.N., and Sauer, R.T. (1998) The ClpXP and ClpAP proteases degrade proteins with carboxy-terminal peptide tails added by the SsrA-tagging system. *Genes Dev* **12:** 1338–1347.

Hänßler, E., Müller, T., Palumbo, K., Patek, M., Brocker, M., Krämer, R., and Burkovski, A. (2009) A game with many players: control of *gdh* transcription in *Corynebacterium glutamicum*. *J Biotechnol* **142:** 114–122.

Herman, C., Thevenet, D., Bouloc, P., Walker, G.C., and D'Ari, R. (1998) Degradation of carboxy-terminal-tagged cytoplasmic proteins by the *Escherichia coli* protease HflB (FtsH). *Genes Dev* **12:** 1348–1355.

Kalinowski, J., Bathe, B., Bartels, D., Bischoff, N., Bott, M., Burkovski, A., *et al.* (2003) The complete *Corynebacterium glutamicum* ATCC 13032 genome sequence and its impact on the production of L-aspartate-derived amino acids and vitamins. *J Biotechnol* **104:** 5–25.

Keiler, K.C. (2008) Biology of trans-translation. *Annu Rev Microbiol* **62:** 133–151.

Kensy, F., Zang, E., Faulhammer, C., Tan, R.K., and Buchs, J. (2009) Validation of a high-throughput fermentation system based on online monitoring of biomass and fluorescence in continuously shaken microtiter plates. *Microb Cell Fact* **8:** 31.

Kinoshita, J.H. (1957) The stimulation of the phosphogluconate oxidation pathway by pyruvate in bovine corneal epithelium. *J Biol Chem* **228:** 247–253.

Knoppová, M., Phensaijai, M., Veselý, M., Zemanova, M., Nešvera, J., and Paték, M. (2007) Plasmid vectors for testing *in vivo* promoter activities in *Corynebacterium glutamicum* and *Rhodococcus erythropolis*. *Curr Microbiol* **55:** 234–239.

Leuchtenberger, W. (1996) Amino acids – technical production and use. In *Biotechnology*. Rehm, H., Reed, G., Pühler, A., and Stadler, P. (eds). Weinheim: VCH, pp. 465–502.

Shaner, N.C., Steinbach, P.A., and Tsien, R.Y. (2005) A guide to choosing fluorescent proteins. *Nat Methods* **2:** 905–909.

Strack, R.L., Hein, B., Bhattacharyya, D., Hell, S.W., Keenan, R.J., and Glick, B.S. (2009) A rapidly maturing far-red derivative of dsRed-Express2 for whole-cell labeling. *Biochemistry* **48:** 8279–8281.

Triccas, J.A., Pinto, R., and Britton, W.J. (2002) Destabilized green fluorescent protein for monitoring transient changes in mycobacterial gene expression. *Res Microbiol* **153:** 379–383.

Tsien, R.Y. (1998) The green fluorescent protein. *Annu Rev Biochem* **67:** 509–544.

Name of the journal:	Microbial Biotechnology
Impact factor:	2.534
Contribution of own work:	30%
3. author:	Supervision of the study

L-methionine producing mutants of *Corynebacterium glutamicum* isolated by biosensor-based high-throughput screening

Nurije Mustafi*[1], *Christian* Rückert[2], Jörn Kalinowski[2], Michael Bott[1], and Julia Frunzke[1]
[1]*Institute of Bio- and Geosciences, IBG-1: Biotechnology, Research Centre Jülich, Germany.*
[2]*Center for Biotechnology, CeBiTec, University of Bielefeld,Germany.*
∗*Corresponding author, j.frunzke@fz-juelich.de*

Summary

Currently, the development of strains for the production of L-methionine is of major interest for industrial biotechnology. In the present work, we isolated L-methionine producing strains by high-throughput screening of *Corynebacterium glutamicum* mutant libraries using fluorescence-activated cell sorting (FACS). The screening approach relied on implementation of the recently presented Lrp-biosensor, which enables the intracellular detection of L-methionine and branched-chain amino acids at single cell resolution transforming this information into an optical readout (eYFP fluorescence). The outcome of the screen was significantly influenced by the genetic background of the strain used for mutant library construction and cultivation conditions of the mutants. The isolated strains produced up to 7.6 mM L-methionine after 48 h cultivation in microtiter plates. Whole genome sequencing of the best producing mutants revealed novel mutations in genes of the central metabolism and pathways contributing to L-methionine biosynthesis as well as in genes encoding transcriptional regulators involved in sulfur utilization, SsuR and CysR, and genes coding for proteins of the L-methionine transport, BrnFE. Overall, this study illustrates how biosensor-based high-throughput screening combined with whole genome sequencing enables efficient isolation of L-methionine producing strains and rapid access to novel mutations, thus, contributing successfully to microbial strain development.

Introduction

The Gram-positive soil bacterium *Corynebacterium glutamicum* represents nowadays one of the most important platform organisms of industrial biotechnology dominating the global large-scale production with more than three million tons of L-glutamate and L-lysine per year (Eggeling & Bott, 2005; Burkovski, 2008). Increased meat consumption and the fast growth of the poultry segment are predicted to drive the consumption of amino acids in the near future. In particular, there is a high demand of L-methionine being the first limiting amino acid in poultry farming. Currently, about 685-700 kilo metric tons of the racemic mixture D/L-methionine are produced. But in contrast to other industrial relevant amino acids, it is still produced on petrochemical basis (Novus International, 2010). Despite several efforts to set up a competitive biotechnological process for microbial production, a breakthrough towards commercial relevant yield levels has not been achieved so far (Kumar & Gomes, 2005). Currently available strains were obtained traditionally by random mutagenesis and subsequent selection using L-methionine analogues. Park *et al.* harnessed successful overproduction of L-lysine, which shares the common precursor L-aspartate, by redirecting carbon flux of the genetically undefined L-lysine producer *C. glutamicum* MH20-22B towards L-methionine synthesis, yielding production of 2.9 g l^{-1} L-methionine (Park *et al.*, 2007; Menkel *et al.*, 1989). Elementary flux mode analysis predicted a high metabolic potential of *C. glutamicum* for L-methionine production (0.49 (C-mol) $(C\text{-mol})^{-1}$) (Krömer *et al.*, 2006). Recently, we reported on a novel biosensor-based high-throughput screening approach for the isolation of amino acid producing mutants of *C. glutamicum* (Mustafi *et al.*, 2012). The presented biosensor is based on the transcriptional regulator Lrp (leucine-responsive protein) of *C. glutamicum*, which was shown to activate the expression of *brnFE* encoding an amino acid export system in the presence of increased levels of the branched-chain amino acids (L-leucine, L-isoleucine and L-valine) or L-methionine (Lange *et al.*, 2012; Trötschel *et al.*, 2005; Kennerknecht *et al.*, 2002). By setting *eyfp* expression under the control of P_{brnFE} the sensor transforms the intracellular levels of the effector amino acids into an optical readout (eYFP fluorescence). Visualization of amino acid production at the single cell level combined with flow cytometrical high-throughput techniques enabled rapid screening of large *C. glutamicum* mutant libraries and resulted in the successful isolation of numerous mutants producing branched-chain amino acids. Binder *et al.* reported on a similar approach using a biosensor for L-lysine detection, which resulted in effective isolation of L-lysine production strains and the identification of novel mutations serving to increase L-lysine production in *C. glutamicum* (Binder *et al.*, 2012). However, no L-methionine producing mutants were obtained in the initial screening using the Lrp-biosensor, thus, we focused in this study on adaption of the high-throughput screening procedure to isolate in particular L-methionine producing mutants.

Results and discussion

Alternative cultivation conditions and strain backgrounds

Typically, product formation strongly depends on the medium composition used for cultivation. Studies by Krömer *et al.* predicted a strongly increased theoretical potential for L-methionine production when alternative sulfur sources are provided. Basically, the assimilation of conventionally used sulfate requires 2 ATP and 4 NADPH. In contrast, sulfur compounds with a high degree of reduction, such as thiosulfate (+II) or sulfide (-II) offer a reduced NADPH demand. In the case of methanethiol (-II) or its dimeric form dimethlyldisulfide (-II), additionally the terminal methylation step is avoided resulting in an increase of the theoretical L-methionine yield (Krömer *et al.*, 2006). However, comparatively high costs, inefficient MetY activity catalyzing their incorporation, and depletion of the MetY substrate *O*-acetylhomoserine make methanethiol and dimethyldisulfide less suitable as sulfur source in screening media (Bolten *et al.*, 2010). In our studies, we used alternatively sulfate in combination with thiosulfate as sulfur source. Unless stated otherwise, all cultivations within the screening system were performed in $CaCO_3$-buffered medium containing glucose. Further nutrients and compounds were based on reported media composition for L-methionine production (Kase & Nakayama, 1974; Deutenberg, 2003; Reershemius, 2008).

Besides the cultivation conditions, the background strain used for library construction can have a strong impact on the screening outcome. First screenings based on the Lrp-sensor used the *C. glutamicum* wild type strain as parental background and resulted in the isolation of mutants producing exclusively the branched-chain amino acids (Mustafi *et al.*, 2012). Hence, we started following screenings based on *C. glutamicum* strains harboring genetic modifications assumed to be beneficial for L-methionine production. McbR, a TetR-type regulator, acts as global repressor of L-methionine and L-cysteine synthesis in *C. glutamicum* (Rey *et al.*, 2003; Rey *et al.*, 2005). Due to its stringent transcriptional control on biosynthesis genes, deletion of *mcbR* is regarded as important prerequisite for the successful overproduction of L-methionine. Further deletions of *metQNI* and *metP* coding for the described L-methionine uptake systems were proposed to enhance L-methionine yield, since reuptake of L-methionine is prevented (Trötschel *et al.*, 2008). In previous studies, Park *et al.* could show that excreted extracellular L-methionine is depleted, when the carbon source in the media is consumed, indicating a reuptake of L-methionine (Park *et al.*, 2007).

In *C. glutamicum* biosynthesis of L-methionine branches from L-lysine synthesis at the shared precursor L-aspartate with the transformation of aspartate semialdehyde to L-homoserine. The biosynthetic pathway of L-lysine and L-threonine share the same first reactions steps, catalyzed by the L-lysine and L-threonine feedback controlled aspartate kinase (*lysC*), aspartate semialdehyde dehydrogenase (*asd*) and homoserine dehydrogenase (*hom*) (Kalinowski *et al.*, 1991; Cremer *et al.*, 1988). Successful overproduction of L-lysine in *C. glutamicum* was achieved by abolishing feedback inhibition of the respective enzymes ($lysC^{T311I}$, hom^{V59A}, hom^{G378Q}) (Ohnishi *et al.*, 2002; Reinscheid *et al.*, 1991). Further strain modifications for L-lysine production focused on the increased supply with oxaloacetate as direct precursor of L-aspartate. This was realized by point mutation in *pyc* (pyc^{P458S}) encoding pyruvate carboxylase, the major anapleurotic enzyme in *C. glutamicum*, and deletion of *pck* coding for PEP-carboxykinase, which uses oxaloacetate as substrate and, thus, competes with synthesis of L-aspartate-derived amino acids (Ohnishi *et al.*, 2002; Petersen *et al.*, 2001).

Since L-lysine and L-methionine derive from the same precursor L-aspartate, successful engineering of the L-lysine producer *C. glutamicum* MH20-22B towards L-methionine synthesis showed that available L-lysine producers represent a well-founded starting point for construction of L-methionine production strains (Park *et al.*, 2007). Therefore, Rückert *et al.* constructed different basic strains for the overproduction of L-methionine based on the described modifications for L-lysine synthesis and deletions of *mcbR*, *metQNI,* and *metP* (Rückert *et al.*, unpublished). Furthermore, the activity of *S*-adenosylmethionine (SAM)-synthetase (*metK*) was reduced in order to decrease conversion of L-methionine to SAM (Deutenberg, 2003). Two strains harboring the listed modifications, termed CgN371 and CgN373, were implemented in following biosensor-based screenings for mutants with increased L-methionine productivity. In order to understand to what extent rational metabolic engineering prior to random mutagenesis influences screening outcomes, *C. glutamicum* Δ*mcbR*, *C. glutamicum* Δ*metP* Δ*metQNI* and the L-lysine producer *C. glutamicum* DM1730 were used additionally as parental strains. Another approach focused on the effector sensitivity of the biosensor by utilizing *C. glutamicum* Δ*ilvE* Δ*avtA*, a strain auxotrophic for branched-chain amino acids (Marienhagen *et al.*, 2005). Mutant library construction based on this strain should significantly reduce the isolation of mutants accumulating L-valine, L-isoleucine or L-leucine and, thus, was proposed to lead to an enrichment of L-methionine producing mutants. To provide a basis for the following experiments, we first measured L-methionine production of all strains used for mutagenesis and screening. Under chosen cultivation conditions (48 h, 30°C, microtiter plate, 990 rpm) *C. glutamicum* Δ*mcbR* showed a production of 0.9 mM and CgN371 of 1.7 mM L-methionine, whereas CgN373 did not accumulate L-methionine. In the

supernatant of *C. glutamicum* Δ*metP* Δ*metQNI*, *C. glutamicum* Δ*ilvE* Δ*avtA* and DM1730, L-methionine was not detected after 48 hours of cultivation.

Screening of mutant libraries

The plasmid-encoded Lrp-sensor was transformed into the different background strains described above. Resulting strains were randomly mutagenized using *N*-methyl-*N'*-nitro-*N*-nitrosoguanidine (MNNG). According to the selection strategy presented in Mustafi *et al.*, cells of the constructed mutant libraries were screened for their fluorescence output *via* FACS. Cells with enhanced fluorescence emission displaying enhanced cytosolic accumulation of the effector amino acids were sorted on agar plates and re-cultivated in minimal medium in microtiter plates (Mustafi *et al.*, 2012). After 48 h of cultivation, amino acid concentrations of the supernatant were assayed by uHPLC analysis. Mutants producing 20% more L-methionine than the parental strain were defined as positive clones. Further, positive clones had to show at least 20% more L-methionine in the supernatant than provided by the yeast extract component in the medium (at the beginning of cultivation).

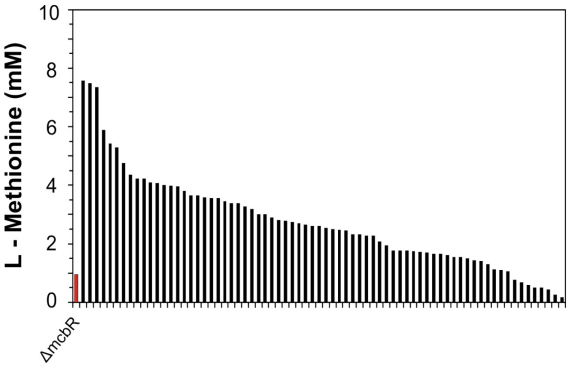

Figure 1. L-methionine production of isolated *C. glutamicum* Δ*mcbR* mutants. For random mutagenesis, *C. glutamicum* Δ*mcbR* containing the Lrp-sensor was grown in complex medium (brain heart infusion with 0.5 M sorbitol, BHIS) to an OD_{600} of 5 and subsequently incubated with *N*-methyl-*N'*-nitro-*N*-nitrosoguanidine (MNNG, 0.125 mg ml^{-1}) for 15 minutes. After mutagenesis, the cells were cultivated in BHIS medium for 24 h and then analyzed by FACS. Mutants exhibiting enhanced fluorescence emission compared to *C. glutamicum* Δ*mcbR* untreated cells were sorted on BHI agar plates. 96 mutants were used to inoculate a microtiter plate (Flowerplate, m2p-labs GmbH, Aachen, Germany) containing 1 ml minimal medium with 7% (w/v) glucose and 1% (w/v) yeast extract. After 48 h, amino acid concentrations in the supernatant were measured by uHPLC (Agilent 1290 Infinity LC ChemStation, Santa Clara, USA). The diagram shows L-methionine production of 72 mutants (black bars) (96 analyzed in total) and the parental strain *C. glutamicum* Δ*mcbR* (red bar).

The screening approach based on *C. glutamicum* Δ*mcbR,* CgN371 and CgN373 resulted in 63.5%, 8.3% and 12.5% positive clones, respectively. Mutants derived from *C. glutamicum* Δ*mcbR* produced up to 7.6 mM L-methionine, mutants of CgN371 up to 5.9 mM, and mutants of CgN373 up to 3.4 mM L-methionine (Table 1). Taken together, about 50% of *C. glutamicum* Δ*mcbR* mutants produced twice as much L-methionine as the parental strain (Figure 1). Screening of libraries based on *C. glutamicum* Δ*metP* Δ*metQNI* resulted in isolation of only two positive clones which produced up to 0.8 mM L-methionine. No positive clones were obtained after mutagenesis of *C. glutamicum* Δ*ilvE* Δ*avtA* and DM1730. All analyzed mutants accumulated the branched-chain amino acids (Table 1). Remarkably, mutants derived from the auxotrophic strain *C. glutamicum* Δ*ilvE* Δ*avtA* showed low accumulation of branched-chain amino acids. To exclude that the isolated clones represent revertant mutants, growth assays were performed on defined CGXII agar plates. None of the 96 analyzed mutants showed growth without the supplementation of the branched-chain amino acids, thus, revertant mutations can be precluded. In this case, it seems highly probable that isolated mutants represented false positive clones with defects in export (*brnFE*), detection of amino acids (*lrp*) or reporter output (*eyfp*). Figure 2 summarizes the screening outcomes and the viability after sorting of the different strain backgrounds. Mutants originating from *C. glutamicum* Δ*mcbR* (5.6%) and CgN373 (1.7%) featured a considerably low survival rate. This was ascribed to the deletion of *mcbR*, which was reported to have a 50% reduced growth rate (Krömer *et al.*, 2008). Additionally, CgN371 mutants showed a strong decreased viability (6.0%), which might be caused by the deregulated SAM-synthetase of this strain (Satishchandran *et al.*, 1990). However, the reduced survival rate of *C. glutamicum* Δ*metP* Δ*metQNI* remains unexplained, since no effect on growth was reported for the deletion of the importer proteins (Trötschel *et al.*, 2008). The described results clearly emphasize a strong impact of the parental background on the success, *e.g.* isolation of L-methionine producing mutants. Overall, the screen of *C. glutamicum* Δ*metP* Δ*metQNI, C. glutamicum* Δ*ilvE* Δ*avtA* and the previously reported screen of the wild type demonstrate that isolation of L-methionine producing mutants is almost impossible without previous modifications on the biosynthesis genes in the strain background (Mustafi *et al.*, 2012). Modifications beneficial for L-lysine production, as present in DM1730, did not have a positive impact on the screening achievements. Only when combined with further strain engineering towards regulation of L-methionine biosynthesis, as in CgN371 and CgN373,

Table 1: Maximal amino acid production of mutants of the respective *C. glutamicum* strain.

Strain	L-Met (mM)	L-Val (mM)	L-Leu (mM)	L-Ile (mM)
Δ*mcbR*	7.6	n.d.	19.9	27.1
Δ*metP* Δ*metQNI*	0.8	13.2	4.4	4.0
Δ*ilvE* Δ*avtA*	0	n.d.	3.7	2.4
CgN371	5.9	10.0	3.8	10.0
CgN373	3.4	13.0	4.1	6.0
DM1730	0	13.9	3.3	5.1

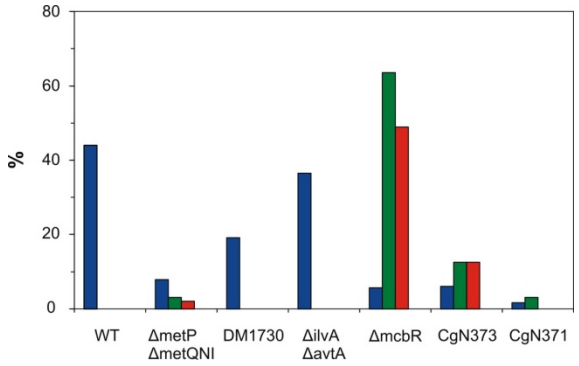

Figure 2. Impact of the strain background on the survival rate and isolation of positive clones in biosensor-based FACS screenings. Shown is the percentage of positive clones (green bars), those excreting minimally twofold higher L-methionine concentrations than the parental strain (red bars) and the survival rate of mutants after sorting (blue bars). Mutagenesis of the different *C. glutamicum* strains, screening and cultivation of mutants, and amino acid determination were performed as described for *C. glutamicum* Δ*mcbR* in the legend of Figure 1.

positive clones were obtained. However, the best screening results were achieved with the strain harboring exclusively the single deletion of *mcbR*, thus, underlying the importance of removing transcriptional repression of the biosynthesis genes for overproduction of L-methionine in *C. glutamicum*.

Verification of isolated producers

Re-cultivation (n=3) of 24 positively tested *C. glutamicum* Δ*mcbR* mutants revealed significant variations in L-methionine production, as it was described in previous studies (Deutenberg, 2003). In total, only 12 of 24 reanalyzed mutants reconfirmed L-methionine accumulation. In some cases, L-methionine production was about twofold decreased compared to the yields obtained in the first screening. In five independent cultivations, clones of mutant no. 62, for example, showed an L-methionine titer ranging from 1.7 mM to 7.5 mM L-methionine. Among all isolated mutants, no. 62 and no. 58 showed the highest production on average. For a detailed characterization, mutant no. 62 and no. 58 were cultivated in 50 ml shake flasks and amino acid concentrations were assayed after 24 h and 48 h (Figure 3). Both mutants showed strongly affected growth rate and a lower final OD_{600} of 43.6 (no. 62) and 20.8 (no. 58), respectively. This is in accordance with published data of *C. glutamicum* Δ*mcbR* exhibiting a 30% reduced biomass yield compared to the wild type (Krömer *et al.*, 2008). However, L-methionine could not be detected in culture supernatant of mutant no. 58 when cultivated in shake flasks, whereas mutant no. 62 produced 2.3 mM L-methionine and 1 mM L-valine within 24 h. Further cultivation for 24 h did not result in a higher L-methionine accumulation (2.1 mM). In contrast, re-cultivation (n=3) of selected CgN373 mutants, showed a lower variability in L-methionine accumulation. Mutant no. 16 (1.3 mM), 33 (2.5 mM) and 75 (3.0 mM) showed the highest titer after 48 h. Remarkably, no L-methionine accumulation could be detected when the mutants were cultivated in CGXII minimal medium or modified CGXII medium containing $CaCO_3$ instead of MOPS (data not shown). This proved to be true for all tested mutants independent of the strain background.

Genome sequence of *C. glutamicum* Δ*mcbR* and CgN373 mutants

Whole genome sequencing of the best producing mutants, *C. glutamicum* Δ*mcbR* mutant no. 58, 62, and 63, as well as of CgN373 mutant no. 16, 33, and 75 (Table 2) was performed on a Illumina Miseq sequencing platform yielding a total of 8,434,942 reads. Mapping was performed using the program SARUMAN with an error rate of 8% allowing ~95% of the reads to be mapped to the reference genome of *C. glutamicum* ATCC 13032 (Blom *et al.*, 2011).

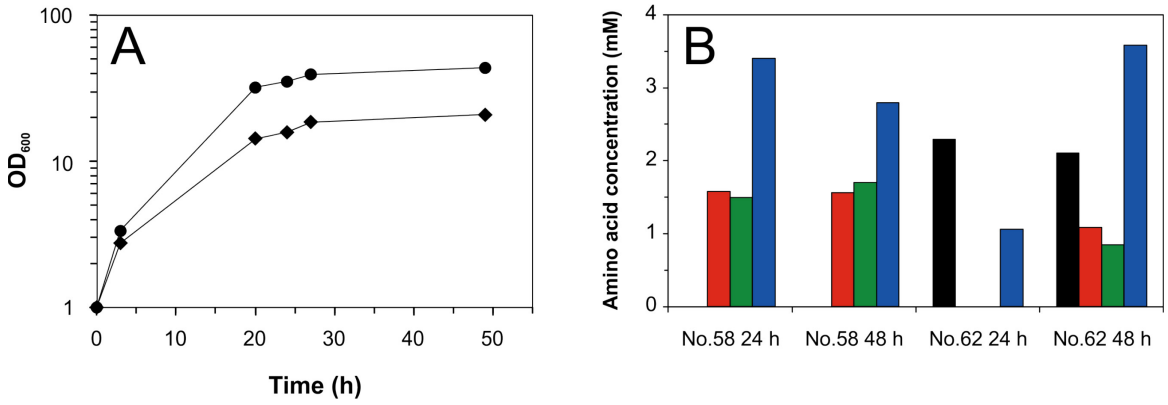

Figure 3. Characterization of *C. glutamicum* Δ*mcbR* mutants. (A) Growth of *C. glutamicum* Δ*mcbR* mutant no. 58 (●) and no. 62 (♦) in $CaCO_3$-buffered medium containing 7% (w/v) glucose and 1% (w/v) yeast extract. Cells were pre-cultivated in BHI complex medium for 24 h and used to inoculate 50 ml minimal medium in shake flasks to an OD_{600} of 1. **(B)** Amino acid concentrations of the respective strains were assayed after 24 h and 48 h cultivation, L-methionine (black bars), L-isoleucine (red bars), L-leucine (green bars), and L-valine (blue bars).

This resulted in a mean coverage of the reference genome of 35.6- to 60.1-fold with 99.8% of the reference genome covered at least tenfold. In total, the analysis revealed a genome-wide distribution of up to 459 single-nucleotide polymorphisms (SNPs), two deletions, and six insertions within CgN373 mutants. Moreover, up to 332 SNPs, two deletions and one insertion were detected within *C. glutamicum* Δ*mcbR* mutants (see Figure S1 in SI). The majority of SNPs consisted of transitions (G·C→A·T), as it is expected when using MNNG for mutagenesis (Ohnishi *et al.*, 2008). We screened the sequencing data for mutations in genes specific for L-methionine biosynthesis as well as pathways supplying building blocks, precursors and redox power (Figure 4). *In silico* analysis for rational design of L-methionine production predicted a high flux through pentose phosphate pathway (PPP) to generate the required high amount of NADPH (8 mol NADPH *per* mol L-methionine) (Krömer *et al.*, 2006). Mutations in the PPP gene *gnd* (6-phosphogluconate dehydrogenase) making it less sensitive to feedback inhibition, as well as overexpression of the entire transketolase (*tkt*) operon (*zwf, opcA, tkt* and *tal*) has already been proven to be of benefit for L-lysine overproduction (Becker *et al.*, 2011; Ohnishi *et al.*, 2005). Sequencing revealed undescribed mutations in *gnd*^{R376C}, *tkt*^{A191T}, and *tkt*^{G415D}. Enhanced activities of anapleurotic or glyoxylate shunt enzymes improve the availability of oxaloacetate, the direct precursor of L-aspartate. This can strongly increase the production of the L-aspartate-derived amino acids (Sauer & Eikmanns, 2005; Peters-Wendisch *et al.*, 2001; Litsanov *et al.*, 2012). Several mutations in *pyc* (*pyc*^{G1133D}, *pyc*^{S1070F}), *ppc* coding for phospho-enolpyruvate carboxylase (*ppc*^{A543V}, *ppc*^{R6C}, *ppc*^{T432I}), *aceA* coding for isocitrate lyase (*aceA*^{L216F}, *aceA*^{G197D}) and *odx* encoding a putative oxaloacetate decarboxylase (*odx*^{E114K}, *odx*^{G158D}, *odx*^{A224T}) were found in the sequenced mutants. Reducing feedback control of aspartate kinase (*lysC*) has been proven to be an important prerequisite for L-lysine production in *C. glutamicum*. Various mutations of *lysC* are reported; our sequencing revealed a novel one (*lysC*^{P276S}) in the regulatory subunit of aspartate kinase (Cremer *et al.*, 1991; Follettie *et al.*, 1993; Kalinowski *et al.*, 1991; Sugimoto *et al.*, 1997; Yoshida *et al.*, 2010). In the pathway leading from L-homoserine to L-methionine, mutations resulting in amino acid exchange occurred only in *metH* (*metH*^{A740V}) encoding a vitamin B12-dependent methionine synthase, which incorporates the methyl group into homocysteine yielding L-methionine (Rückert *et al.*, 2003). Mutations in SAM and L-methionine feedback controlled *metX* (homoserine *O*-acetyltransferase), *metY* (*O*-acetyl-homoserine sulfhydrylase) and *metB* (cystathionine *γ*-synthase) were not found. However, a mutation was identified in cg2344 (cg2344^{V54A}) coding for a hypothetical cystathionine β-synthase, which is proposed to be involved in a pathway degrading L-methionine to L-cysteine by converting homocysteine to L-cystathionine (Rückert & Kalinowski, 2008). Furthermore, several mutations in genes involved in sulfur metabolism were identified: *e.g.* in *seuA* (*seuA*^{P162L}) and *seuC* (*seuC*^{R393H}) encoding FMNH2-dependent monooxygenases involved in sulfonate ester utilization (Koch *et al.*, 2005b); *cysH* (*cysH*^{T201I}) encoding an adenosine phosphosulfate reductase involved in reduction of sulfate to sulfite; in *fpr1* (*fpr1*^{S213F}) and *fpr2* (*fpr2*^{E184K}) encoding putative NADP(+)–ferredoxin reductases, described to be involved in reduction of sulfite to sulfide; and in *cysG* (*cysG*^{G91E}, *cysG*^{G47E}), a putative uroporphyrinogen III synthase, and *thtR* (*thtR*^{A229T}), a thiosulfate sulfurtransferase, described to be involved in siroheme biosynthesis, which is an essential cofactor of sulfite reductase (Rückert & Kalinowski, 2008). In the pathway of L-serine synthesis, two mutations were revealed in *serC* (*serC*^{V274I}, *serC*^{A152V}) (phosphoserine transaminase) catalyzing the amino transfer from L-glutamate to generate 3-phosphoserine (Peters-Wendisch *et al.*, 2002). L-serine plays an important role in L-methionine biosynthesis since it represents the direct precursor of L-cysteine and acts as donor of the methyl group for formation of methyl-tetrahydrofolate (THF). In the downstream pathway leading from L-serine to L-cysteine, mutations in *cysK* (*cysK*^{E193K}) encoding cysteine synthase, which catalyzes L-cysteine formation by sulfhydrylation of *O*-acetyl-L-serine, were identified (Wada *et al.*, 2004). Additionally, mutations in genes coding for the L-methionine export system *brnFE* (*brnF*^{P48S}, *brnE*^{G97D}) were found. Manipulated transport systems increasing the export of target amino acids proved to enhance significantly L-isoleucine yields in *C. glutamicum* (Xie *et al.*, 2012). However, identified modifications relied on deletion or overexpression of the respective genes. Mutations affecting transport rates are not described for BrnFE so far. As increased concentrations of intermediates of the sulfur metabolism can be toxic to the cell and as L-methionine biosynthesis demands on high energy costs, pathways involved in sulfur metabolism are tightly regulated on the transcriptional level (Rückert & Kalinowski, 2008). Besides McbR acting as master regulator of L-methionine and

Table 2: L-methionine production of selected mutant strains and the respective parental strains CgN373 and *C. glutamicum* Δ*mcbR* which were analyzed by whole genome sequencing.

Strain	L-Met (mM)
CgN373	0
CgN373 mutant no. 16	1.3
CgN373 mutant no. 33	2.5
CgN373 mutant no. 75	3.4
C. glutamicum Δ*mcbR*	1.0
C. glutamicum Δ*mcbR* mutant no. 58	7.6
C. glutamicum Δ*mcbR* mutant no. 62	7.5
C. glutamicum Δ*mcbR* mutant no. 63	3.3

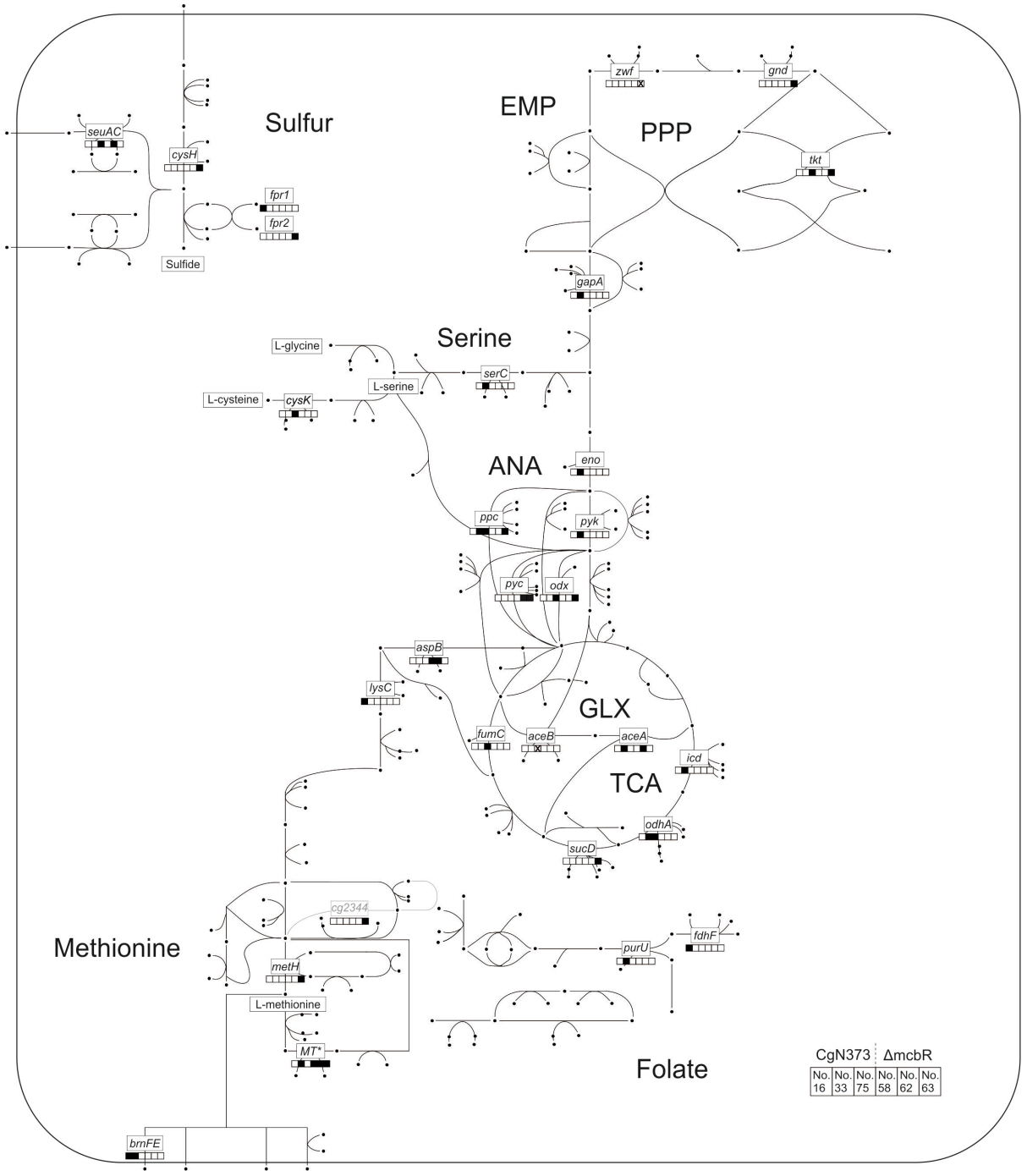

Figure 4. Schematic illustration of central metabolism and pathways involved in L-methionine biosynthesis in *C. glutamicum*. Pathways are shown according to Droste *et al.* including glycolysis (EMP), pentose-phosphate pathway (PPP), tricarboxylic acid cycle (TCA), glyoxylate cycle (GLX), and anaplerotic fluxes (ANA) (Droste *et al.*, 2011). Mutations resulting in amino acid exchanges (■) or stop codons (x) in genes of the respective genome are indicated. Silent mutations are not implemented. The sequencing libraries were created from 50 ng genomic DNA *per* sample using the Nextera library preparation kit (Epicentre Biotechnologies, Madison, WI, USA) according to the manufacturer's protocol, including the introduction of a barcode for each sample. Afterwards, equal molar amounts of the eight libraries were pooled and this pool was used for sequencing on a Illumina Miseq sequencing platform. The run (151+8+151 bp) yielded a total of 8,434,942 reads post filtering and de-multiplexing (2x 4,217,471 read pairs). *Per* sample, 825k to 1,389k were obtained corresponding to 247.6 to 416.9 Mbases of data. Mapping was performed using the program SARUMAN with an error rate of 8% allowing ~95% of the reads to be mapped to the reference genome (*C. glutamicum* ATCC 13032) (Blom *et al.*, 2011). This resulted in a mean coverage of the reference genome of 35.6- to 60.1-fold with 99.8% of the reference genome covered at least tenfold. MT*=SAM-dependent methyltransferases.

L-cysteine biosynthesis, two further regulators of the ROK-type family were identified in *C. glutamicum*, SsuR and CysR. Both regulators control a subset of genes of the McbR regulon involved in sulfonate (ester) utilization (SsuR) and sulfate reduction in response to the availability of sulfide acceptor molecules (CysR) (Koch *et al.*, 2005a; Rückert *et al.*, 2008). Mutations were identified in *ssuR* (*ssuR*^{P143L}, *ssuR*^{S230N}) as well as in *cysR* (*cysR*^{A5V}, *cysR*^{G161D}). Though, no mutations were found in the *mcbR* gene itself or in identified binding sites of McbR target genes (Rey *et al.*, 2005). Mampel *et al.* isolated a cg3031 deficient strain by transposon mutagenesis and reported on a twofold improved L-methionine production compared to the wild type strain (Mampel *et al.*, 2005). Cg3031 was postulated to act as regulatory element on expression of the *cys*-operon. However, direct transcriptional regulation could not be proven and no transcriptional regulatory domains were predicted for this protein. Interestingly, cg3031 mutations in three sequenced mutants were found: two resulting in a stop codon (cg3031^{Q348}, cg30131^{W125}) and cg3031^{G241D}. Table 1 in SI summarizes all mutations which were identified in (putative) transcriptional regulators in our screenings.

Concluding remarks and future perspectives

Biosensor-based FACS high-throughput screening of *C. glutamicum* mutant libraries enabled rapid isolation of L-methionine producing mutants. Different strain backgrounds used for mutant library construction revealed deletion of *mcbR* as key modification for overproduction in *C. glutamicum*. Sequencing analysis of the isolated mutants provided first insights into genomic constitution of L-methionine producing strains. Overall, a large number of novel mutations was revealed, distributed in metabolic pathways channeling carbon flux from central metabolism to L-aspartate and finally to L-methionine, as well as in genes encoding regulatory proteins. Future studies will focus on transcriptome analysis of the isolated mutants in order to analyze the impact of the identified mutations on the global gene expression pattern of sulfur metabolism. In order to gain a defined L-methionine production strain, harboring only biotechnologically useful mutations without accumulation of undefined ones, selected mutations will systematically be introduced into the wild type strain and analyzed for their individual influence on L-methionine production.

The successful isolation of L-methionine producing mutants by implementation of the Lrp-sensor in fluorescence-activated cell sorting, proved the sensor technology as powerful tool for novel high-throughput screenings of bacterial production strains. So far, our studies focused on screening of mutant libraries derived from *C. glutamicum*. *In silico* analysis of metabolic pathways for L-methionine production revealed an even higher theoretical, optimal L-methionine yield of *Escherichia coli* compared to *C. glutamicum* (Krömer *et al.*, 2006). Thus, future work will focus on the development of a suitable biosensor for *E. coli* and its application in high-throughput screenings of *E. coli* based mutant libraries. Detailed genomic and transcriptome analysis of new mutants should permit targeted engineering of L-methionine overproducing strains viable in commercial production processes in the near future.

References

Becker, J., Zelder, O., Häfner, S., Schröder, H. & Wittmann, C. (2011) From zero to hero - design-based systems metabolic engineering of *Corynebacterium glutamicum* for L-lysine production. *Metabolic Engineering* 13: 159-168.

Binder, S., Schendzielorz, G., Stäbler, N., Krumbach, K., Hoffmann, K., Bott, M. & Eggeling, L. (2012) A high-throughput approach to identify genomic variants of bacterial metabolite producers at the single-cell level. *Genome Biology* 13: R40.

Blom, J., Jakobi, T., Doppmeier, D., Jänicke, S., Kalinowski, J., Stoye, J. & Gösmann, A. (2011) Exact and complete short-read alignment to microbial genomes using graphics processing unit programming. *Bioinformatics* 27: 1351-1358.

Bolten, C.J., Schröder. H, Dickschat. J & C., W. (2010) Towards methionine overproduction in *Corynebacterium glutamicum* - methanethiol and dimethyldisulfide as reduced sulfur sources. *Journal of Microbiology and Biotechnology* 20: 1196-1203.

Burkovski, A., (2008) *Corynebacteria: genomics and molecular biology*. Caister Academic Press, Norfolk UK.

Cremer, J., Eggeling, L. & Sahm, H. (1991) Control of the lysine biosynthesis sequence in *Corynebacterium glutamicum* as analyzed by overexpression of the individual corresponding genes. *Applied and Environmental Microbiology* 57: 1746-1752.

Cremer, J., Treptow, C., Eggeling, L. & Sahm, H. (1988) Regulation of enzymes of lysine biosynthesis in *Corynebacterium glutamicum*. *Journal of General Microbiology* 134: 3221-3229.

Deutenberg, D. (2003) Genetische Optimierung der Methioninproduktion in *Corynebacterium glutamicum* ATCC 13032. Diploma thesis, University of Bielefeld, Bielefeld, Germany.

Droste, P., Miebach, S., Niedenführ, S., Wiechert, W. & Nöh, K. (2011) Visualizing *multi-omics* data in

metabolic networks with the software Omix-a case study. *Biosystems* 105: 154-161.

Eggeling, L. & Bott, M., (2005) *Handbook of Corynebacterium glutamicum*. Academic Press, Inc., Boca Raton, FL: CRC Press.

Follettie, M.T., Peoples, O.P., Agoropoulou, C. & Sinskey, A.J. (1993) Gene structure and expression of the *Corynebacterium flavum* N13 *ask-asd* operon. *Journal of Bacteriology* 175: 4096-4103.

Kalinowski, J., Cremer, J., Bachmann, B., Eggeling, L., Sahm, H. & Pühler, A. (1991) Genetic and biochemical analysis of the aspartokinase from *Corynebacterium glutamicum*. *Molecular Microbiology* 5: 1197-1204.

Kase, H. & Nakayama, K. (1974) Production of *O*-acetyl-L-homoserine by methionine analog-resistant mutants and regulation of homoserine-*O*-transacetylase in *Corynebacterium glutamicum*. *Agricultural and Biological Chemistry* 38: 2021-2030.

Kennerknecht, N., Sahm, H., Yen, M.R., Patek, M., Saier, M.H. & Eggeling, L. (2002) Export of L-isoleucine from *Corynebacterium glutamicum*: a two-gene-encoded member of a new translocator family. *Journal of Bacteriology* 184: 3947-3956.

Koch, D.J., Rückert, C., Albersmeier, A., Hüser, A.T., Tauch, A., Pühler, A. & Kalinowski, J. (2005a) The transcriptional regulator SsuR activates expression of the *Corynebacterium glutamicum* sulphonate utilization genes in the absence of sulphate. *Molecular Microbiology* 58: 480-494.

Koch, D.J., Rückert, C., Rey, D.A., Mix, A., Pühler, A. & Kalinowski, J. (2005b) Role of the *ssu* and *seu* genes of *Corynebacterium glutamicum* ATCC 13032 in utilization of sulfonates and sulfonate esters as sulfur sources. *Applied and Environmental Microbiology* 71: 6104-6114.

Krömer, J.O., Bolten, C.J., Heinzle, E., Schröder, H. & Wittmann, C. (2008) Physiological response of *Corynebacterium glutamicum* to oxidative stress induced by deletion of the transcriptional repressor McbR. *Microbiology* 154: 3917-3930.

Krömer, J.O., Wittmann, C., Schröder, H. & Heinzle, E. (2006) Metabolic pathway analysis for rational design of L-methionine production by *Escherichia coli* and *Corynebacterium glutamicum*. *Metabolic Engineering* 8: 353-369.

Kumar, D. & Gomes, J. (2005) Methionine production by fermentation. *Biotechnology Advances* 23: 41-61.

Lange, C., Mustafi, N., Frunzke, J., Kennerknecht, N., Wessel, M., Bott, M. & Wendisch, V.F. (2012) Lrp of *Corynebacterium glutamicum* controls expression of the *brnFE* operon encoding the export system for L-methionine and branched-chain amino acids. *Journal of Biotechnology* 158: 231-241.

Litsanov, B., Kabus, A., Brocker, M. & Bott, M. (2012) Efficient aerobic succinate production from glucose in minimal medium with *Corynebacterium glutamicum*. *Microbial Biotechnology* 5: 116-128.

Mampel, J., Schröder, H., Haefner, S. & Sauer, U. (2005) Single-gene knockout of a novel regulatory element confers ethionine resistance and elevates methionine production in *Corynebacterium glutamicum*. *Applied Microbiology and Biotechnology* 68: 228-236.

Marienhagen, J., Kennerknecht, N., Sahm, H. & Eggeling, L. (2005) Functional analysis of all aminotransferase proteins inferred from the genome sequence of *Corynebacterium glutamicum*. *Journal of Bacteriology* 187: 7639-7646.

Menkel, E., Thierbach, G., Eggeling, L. & Sahm, H. (1989) Influence of increased aspartate availability on lysine formation by a recombinant strain of *Corynebacterium glutamicum* and utilization of fumarate. *Applied and Environmental Microbiology* 55: 684-688.

Mustafi, N., Grünberger, A., Kohlheyer, D., Bott, M. & Frunzke, J. (2012) The development and application of a single-cell biosensor for the detection of L-methionine and branched-chain amino acids. *Metabolic Engineering* 14: 449-457.

Novus International, I. (2010) Methionine global outlook: the next decade. *http://www.novusint.com/portals/0/v2/multimedia/pdf/whitepapers/Methionine_Global_Outlook.pdf*.

Ohnishi, J., Katahira, R., Mitsuhashi, S., Kakita, S. & Ikeda, M. (2005) A novel *gnd* mutation leading to increased L-lysine production in *Corynebacterium glutamicum*. *FEMS Microbiology Letters.* 242: 265-274.

Ohnishi, J., Mitsuhashi, S., Hayashi, M., Ando, S., Yokoi, H., Ochiai, K. & Ikeda, M. (2002) A novel methodology employing *Corynebacterium glutamicum* genome information to generate a new L-lysine-producing mutant. *Applied Microbiology and Biotechnology* 58: 217-223.

Ohnishi, J., Mizoguchi, H., Takeno, S. & Ikeda, M. (2008) Characterization of mutations induced by *N*-methyl-*N'*-nitro-*N*-nitrosoguanidine in an industrial *Corynebacterium glutamicum* strain. *Mutation Research-Genetic Toxicology and Environmental Mutagenesis* 649: 239-244.

Park, S.-D., Lee, J.-Y., Sim, S.-Y., Kim, Y. & Lee, H.-S. (2007) Characteristics of methionine production by an engineered *Corynebacterium glutamicum* strain. *Metabolic Engineering* 9: 327-336.

Peters-Wendisch, P., Netzer, R., Eggeling, L. & Sahm, H. (2002) 3-phosphoglycerate dehydrogenase from

Corynebacterium glutamicum: the C-terminal domain is not essential for activity but is required for inhibition by L-serine. *Applied Microbiology and Biotechnology* 60: 437-441.

Peters-Wendisch, P.G., Schiel, B., Wendisch, V.F., Katsoulidis, E., Mockel, B., Sahm, H. & Eikmanns, B.J. (2001) Pyruvate carboxylase is a major bottleneck for glutamate and lysine production by *Corynebacterium glutamicum*. *Journal of Molecular Microbiology and Biotechnology* 3: 295-300.

Petersen, S., Mack, C., de Graaf, A.A., Riedel, C., Eikmanns, B.J. & Sahm, H. (2001) Metabolic consequences of altered phosphoenolpyruvate carboxykinase activity in *Corynebacterium glutamicum* reveal anaplerotic regulation mechanisms *in vivo*. *Metabolic Engineering* 3: 344-361.

Reershemius, H.J. (2008) Production of L-methionine with *Corynebacterium glutamicum*. Disserataion, Technical University Braunschweig, Braunschweig, Germany.

Reinscheid, D.J., Eikmanns, B.J. & Sahm, H. (1991) Analysis of a *Corynebacterium glutamicum hom* gene coding for a feedback-resistant homoserine dehydrogenase. *Journal of Bacteriology* 173: 3228-3230.

Rey, D.A., Nentwich, S.S., Koch, D.J., Rückert, C., Pühler, A., Tauch, A. & Kalinowski, J. (2005) The McbR repressor modulated by the effector substance *S*-adenosylhomocysteine controls directly the transcription of a regulon involved in sulphur metabolism of *Corynebacterium glutamicum* ATCC 13032. *Molecular Microbiology* 56: 871-887.

Rey, D.A., Pühler, A. & Kalinowski, J. (2003) The putative transcriptional repressor McbR, member of the TetR-family, is involved in the regulation of the metabolic network directing the synthesis of sulfur containing amino acids in *Corynebacterium glutamicum*. *Journal of Biotechnology* 103: 51-65.

Rückert, C. & Kalinowski, J., (2008) Sulfur metabolism in *Corynebacterium glutamicum*. In: Corynebacteria: genomics and molecular biology. Burkovski, A. (ed). Caister Academic Press, Norfolk UK, pp.

Rückert, C., Milse, J., Albersmeier, A., Koch, D.J., Pühler, A. & Kalinowski, J. (2008) The dual transcriptional regulator CysR in *Corynebacterium glutamicum* ATCC 13032 controls a subset of genes of the McbR regulon in response to the availability of sulphide acceptor molecules. *BMC Genomics* 9: 483.

Rückert, C., Pühler, A. & Kalinowski, J. (2003) Genome-wide analysis of the L-methionine biosynthetic pathway in *Corynebacterium glutamicum* by targeted gene deletion and homologous complementation. *Journal of Biotechnology* 104: 213-228.

Satishchandran, C., Taylor, J.C. & Markham, G.D. (1990) Novel *Escherichia coli* K-12-mutants impaired in *S*-adenosylmethionine synthesis. *Journal of Bacteriology* 172: 4489-4496.

Sauer, U. & Eikmanns, B.J. (2005) The PEP-pyruvate-oxaloacetate node as the switch point for carbon flux distribution in bacteria. *FEMS Microbiology Reviews* 29: 765-794.

Sugimoto, M., Tanaka, A., Suzuki, T., Matsui, H., Nakamori, S. & Takagi, H. (1997) Sequence analysis of functional regions of homoserine dehydrogenase genes from L-lysine and L-threonine-producing mutants of *Brevibacterium lactofermentum*. *Bioscience, Biotechnology, and Biochemistry* 61: 1760-1762.

Trötschel, C., Deutenberg, D., Bathe, B., Burkovski, A. & Krämer, R. (2005) Characterization of methionine export in *Corynebacterium glutamicum*. *Journal of Bacteriology* 187: 3786-3794.

Trötschel, C., Follmann, M., Nettekoven, J.A., Mohrbach, T., Forrest, L.R., Burkovski, A., Marin, K. & Krämer, R. (2008) Methionine uptake in *Corynebacterium glutamicum* by MetQNI and by MetPS, a novel methionine and alanine importer of the NSS neurotransmitter transporter family. *Biochemistry* 47: 12698-12709.

Wada, M., Awano, N., Yamazawa, H., Takagi, H. & Nakamori, S. (2004) Purification and characterization of *O*-acetylserine sulfhydrylase of *Corynebacterium glutamicum*. *Bioscience, Biotechnology, and Biochemistry* 68: 1581-1583.

Xie, X., Xu, L., Shi, J., Xu, Q. & Chen, N. (2012) Effect of transport proteins on L-isoleucine production with the L-isoleucine-producing strain *Corynebacterium glutamicum* YILW. *Journal of Industrial Microbiology & Biotechnology* 39: 1549-1556.

Yoshida, A., Tomita, T., Kuzuyama, T. & Nishiyama, M. (2010) Mechanism of concerted inhibition of $\alpha_2\beta_2$-type hetero-oligomeric aspartate kinase from *Corynebacterium glutamicum*. *Journal of Biological Chemistry* 285: 27477-27486.

Application of a genetically-encoded biosensor for the single cell analysis of *Corynebacterium glutamicum* L-valine production strains

Nurije Mustafi[1§], Alexander Grünberger[1§], Regina Mahr[1], Stefan Helfrich[1], Katharina Nöh[1], Bastian Blombach[2], Dietrich Kohlheyer[1], Michael Bott[1], Julia Frunzke[1]*

[1]IBG-1: Biotechnology, Forschungszentrum Jülich GmbH (Research Centre Jülich), 52425 Jülich, Germany
[2]Institute of Biochemical Engineering, University of Stuttgart, 70569 Stuttgart, Germany

Abstract

Metabolite sensing biosensors transforming the detection of inconspicuous, small molecules into an optical readout (*e.g.* fluorescence) present powerful tools for single cell quantification of metabolites. However, their versatile potential for analysis of metabolite production in biotechnological processes has rarely been exploited so far. In this study, the recently developed Lrp-biosensor, capable of monitoring amino acid production in single bacterial cells, was applied to investigate population dynamics of gradually engineered L-valine producing *Corynebacterium glutamicum* strains. Strains under study are based on the pyruvate dehydrogenase complex-deficient strain *C. glutamicum* Δ*aceE*. Multiparameter flow cytometry analysis of lab-scale fed-batch cultures revealed not only differences in single cell productivity, but also showed the occurrence of several subpopulations with significant loss in metabolic activity and viability during the cultivation process. To study these observations in a time-resolved manner, we performed growth and production studies of single cells in microfluidic systems, providing constant environmental cultivation conditions. These investigations revealed typical Gaussian distribution regarding single cell fluorescence. However, live cell imaging studies displayed the appearance of different types of non-producing cells within isogenic microcolonies. These findings prove the Lrp-biosensor as a valuable tool for single cell monitoring and quantification of phenotypic variability in production processes.

1. Introduction

Often isogenic bacterial cultures are regarded as homogenous populations, neglecting upcoming evidence for substantial variation in diverse phenotypical traits. This common occurrence of multimodal heterogeneity can originate, for example from differences in cell age or cell cycle, epigenetic variation or simply stochastic effects in gene expression (Lidstrom & Konopka, 2010; Elowitz *et al.*, 2002; Cai *et al.*, 2006; Kærn *et al.*, 2005). In recent literature, examples of population heterogeneity include heterologous protein expression in *e.g. Bacillus megaterium*, occurrence of subpopulations in batch cultures of *Lactobacillus rhamnosus, Bacillus licheniformis*, and *Pseudomonas taetrolens* (David *et al.*, 2011; da Silva *et al.*, 2009; Alonso *et al.*, 2012). In natural environments inherent cell-to-cell variation within isogenic populations and resulting formation of subpopulations are considered to be beneficial, as their occurrence allows rapid adaption to sudden changes in environment (Kussell & Leibler, 2005; Acar *et al.*, 2008; Veening *et al.*, 2008). In regard to biotechnological systems, however, arising phenotypic variation and resulting formation of insufficient producing subpopulations can adversely affect the entire production process (Müller *et al.*, 2010; Lencastre Fernandes *et al.*, 2011). Besides its biological origin heterogeneity within cultivation processes is enforced by microenvironmental variations in *e.g.* dissolved gases, pH and nutrient concentrations caused by insufficient mixing or formation of biofilms (Lara *et al.*, 2006; Liden, 2002; Takors, 2012). This occurs even in well-mixed laboratory scale-cultures, and can severely impact large-scale cultivations (Hewitt & Nienow, 2007; Enfors *et al.*, 2001; Brognaux *et al.*, 2013; Brognaux

*Corresponding author. Phone: +492461615430.
E-Mail adress: j.frunzke@fz-juelich.de (J.Frunzke).
§Both authors contributed equally to this work.

et al., 2012). However, in most bioprocesses monitoring is typically restricted to bulk approaches delivering average values for the whole population, but masking occurring variations at the single cell level and thus possibly resulting in incorrect interpretations of biological phenomena (Lidstrom & Konopka, 2010).

In depth investigations and detailed understanding of heterogeneity and its impact on the efficiency and metabolite productivity of microbial productions strains would therefore be the first goal for finally performing efficient bioprocesses (Müller *et al.*, 2010). Especially, the investigation of cell-to-cell heterogeneity in regard to metabolite production is of major interest. However, this demands on the development of novel tools and techniques for single cell quantification and real-time monitoring of inconspicuous, small metabolites (Fritzsch *et al.*, 2012; Heinemann & Zenobi, 2011; Müller & Hiller, 2013; Dietrich *et al.*, 2010). In this context, the application of genetically-encoded biosensors capable of detecting molecules and transforming this information into an optical readout can provide valuable insights into production process with single cell resolution (Lencastre Fernandes *et al.*, 2011; Zhang & Keasling, 2011; Dietrich *et al.*, 2010). Flow cytometry proved as valuable technique to access multiple parameters in single cells, such as cell size, cell granularity, DNA content, membrane potential and integrity (Díaz *et al.*, 2010; Tracy *et al.*, 2010; Müller & Nebe-von-Caron, 2010; Brehm-Stecher & Johnson, 2004). The application of metabolite sensing biosensors in flow cytometrical studies thus, provides a powerful tool to investigate population heterogeneities regarding productivity and physiological states of single cells by high throughput analysis of large cell populations (Hewitt & Nebe-Von-Caron, 2001; Lewis *et al.*, 2004; Nebe-von-Caron *et al.*, 2000). While flow cytometry based analysis provide a snapshot, the implementation of metabolite biosensors in live cell imaging studies offers the advantage of long time observation of single cell growth and productivity with high temporal resolution (Locke & Elowitz, 2009). Novel microfluidic reactor systems enable bacterial cultivation at environmental constant and defined conditions, hence allowing in particular investigation of biological heterogeneity, excluding cell-to-cell variability caused by highly fluctuating cultivations conditions using lab-scale reactors or shake-flasks (Schmid *et al.*, 2010; Szita *et al.*, 2010; Gulati *et al.*, 2009; Fritzsch *et al.*, 2012; Vinuselvi *et al.*, 2011; Grünberger *et al.*, 2012).

Corynebacterium glutamicum represents one of the most important platform organisms in industrial biotechnology; dominating the global, large-scale production of amino acids (*e.g.* L-glutamate, L-lysine, and L-valine) (Eggeling & Bott, 2005; Burkovski, 2008; Wendisch, 2007). Studies of our lab using multiparameter flow cytometry revealed phenotypic heterogeneity in terms of viability, membrane potential and growth activity of *C. glutamicum* wild type cells (Neumeyer *et al.*, 2013). However, population heterogeneity in particular during production processes has not been studied in detail for this species yet. Recently, our group reported on the development of a genetically-encoded biosensor (Lrp-sensor), which enables the cytosolic detection of branched-chain amino acids or L-methionine in *C. glutamicum*. The sensor was successfully applied in FACS (fluorescence-activated cell sorting) high throughput (HT) screenings for the isolation of amino acid producing mutants (Mustafi *et al.*, 2012) and in first live cell imaging studies of the L-valine production strain *C. glutamicum* Δ*aceE*. Deletion of the *aceE* gene, coding for E1p subunit of the pyruvate dehydrogenase complex (PDHC) in *C. glutamicum* results in acetate-dependent growth of this strain and growth-decoupled L-valine production. Blombach *et al.* showed that enhanced precursor availability, *i.e.* pyruvate, achieved by deletion of the genes encoding pyruvate:quinone oxidoreductase (*pqo*) and pyruvate carboxylase (*pyc*) further increased L-valine production in *C. glutamicum* (Blombach *et al.*, 2008). Enhanced supply with NADPH obtained by deletion of *pgi* (phosphoglucose isomerase), redirecting carbon flux from glycolysis to the pentose phosphate pathway, and plasmid-bound overexpression of the L-valine biosynthesis genes (*ilvBNCE*) resulted in a drastic increased L-valine production and yields achieving maximal theoretical $Y_{P/S}$.

In this work, we assessed the performance of the Lrp-biosensor to investigate population dynamics with respect to single cell productivity, plasmid content and viability in *C. glutamicum* production strains. Therefore, the biosensor was implemented in multiparameter FACS analysis and live cell imaging studies of gradually engineered *C. glutamicum* L-valine production strains, cultivated at different scales, ranging from lab-scale bioreactors, cultivation in microtiter plates to cultivation in microfluidic picoliter bioreactors (PLBR).

2. Material and methods

2.1. Bacterial strains, media, and growth conditions

Bacterial strains and plasmids used or constructed in this work are listed in Table 1. Unless stated otherwise, pre-cultures of *C. glutamicum* were inoculated with single colonies from a fresh brain heart infusion (BHI) agar plate containing 51 mM acetate and incubated in 4 ml BHI complex medium with 51 mM acetate for 6 h at 30°C and 170 rpm. This first pre-culture was used to inoculate a 100 ml shake flask containing 20 ml CGXII minimal medium with 222 mM glucose and 154 mM acetate added as carbon source (Keilhauer *et al.*, 1993). The cells of the second pre-culture were cultivated overnight at 30°C and 120 rpm, washed twice with 0.9% (w/v) saline and then used to inoculate the main culture to an optical density at 600 nm (OD_{600}) of 1. If not stated different, cells in the main culture were cultivated under the same conditions as in the pre-culture. *Escherichia coli* DH5 was grown aerobically in LB medium on a rotary shaker (120 rpm) or on LB agar plates at 37°C (Sambrook *et al.*, 2001). Where appropriate, the media contained kanamycin (25 µg ml^{-1} for *C. glutamicum* or 50 µg ml^{-1} for *E. coli*) or isopropyl β-D-1-thiogalactopyranoside (IPTG). Culture conditions in microtiter plate cultivations in the BioLector (m2p-labs GmbH, Aachen, Germany) system for online monitoring of growth and fluorescence were performed as described before (Kensy *et al.*, 2009; Mustafi *et al.*, 2012).

2.2. Recombinant DNA work

Standard methods like PCR, DNA restriction or ligation were carried out according to standard protocols (Sambrook *et al.*, 2001). Synthesis of oligonucleotides and sequencing analysis have been performed by Eurofins MWG Operon (Ebersfeld, Germany). The vector pE2-Crimson was derived by Clontech Laboratories (Mountain View, CA, USA). For the construction of pJC4-ilvBNCE-E2-Crimson *e2-crimson* under transcriptional control of P_{tac} was amplified using oligonucleotides lacI-fw and E2-Crimson-rv (Strack *et al.*, 2009). The PCR product was cloned into the vector pJC4-ilvBNCE by using the Bst1107I restriction site (Radmacher *et al.*, 2002). For chromosomal integration of the Lrp-sensor, the sensor cassette was cloned into the intergenic region of *cg1121, cg1122* by using pK18-mobsacB-cg1121,cg1122 (Mustafi *et al.*, 2012). The transfer of the integration plasmid into *C. glutamicum* and selection of the first and second recombination events were performed as described previously (Niebisch & Bott, 2001). The integration at the chromosomal locus was verified by colony PCR using primers Int-cg1121-fw and Int-cg1122-rv.

2.3. L-valine production in fed-batch mode

Fed-batch fermentations were performed at 30°C in a 1.4 l glass bioreactor (Multifors Multi-Fermenter System) with six independently controllable bio-reactors (Infors, Einsbach, Germany). Cells of an 50 ml overnight pre-culture grown in BHI complex medium supplemented with 85 mM acetate in 500 ml shake flasks were harvested, washed twice with 0.9% (w/v) saline and then used to inoculate 450 ml CGXII minimal medium containing 0.5% BHI, 254 mM acetate and 222 mM glucose to an OD_{600} of 1. The bioreactors were sparged with 0.9 l min^{-1} air. Oxygen saturation was measured online using a polarimetric oxygen electrode (Mettler Toledo, Giessen, Germany) and adjusted permanently to 30% by gradually increasing stirrer speed from 600 rpm up to 1000 rpm. The pH was online measured using a standard pH electrode (Mettler Toledo, Gießen, Deutschland) and adjusted to pH 7 with 4 M potassium hydroxide and 4 M hydrochloric acid. Foam development was suppressed automatically by titration of 25% (v/v) silicon antifoam 204/water suspension (Sigma Aldrich, Steinheim, Germany). During the fed-batch processes, adequate amounts of 50% (w/v) glucose and 50% (w/v) acetate were injected.

2.4. Quantification of amino acids, glucose, and acetate

For determination of amino acids, glucose and acetate concentrations in the supernatant, samples of the cultures were harvested by centrifugation (13,000 rpm, 10 min, 4°C). Amino acids were quantified as their *ortho*-phthalaldehyde derivatives *via* ultra-high pressure liquid chromatography by automatic pre-column derivatization and separation by reversed-phase chromatography on an Agilent 1290 Infinity LC ChemStation (Santa Clara, USA) with fluorescence detection (λ_{ex}=230 nm and λ_{em}=450 nm). As eluent, a gradient of 0.01 M Na_2HPO_4, 0.01 M $Na_2B_4O_7$ buffer pH 8.2 with increasing concentrations of methanol was used. Glucose and acetate concentrations were quantified using an Agilent 1100 liquid chromatogra-phy (LC) system (Santa Clara, USA). Isocratic elution was performed with 100 mM sulfuric acid. Glucose was detected *via* an Agilent 1100 refractive index detector, and acetate was detected *via* an Agilent 1100 diode array detector at 215 nm.

2.5. Microfluidic chip cultivation

Microfluidic PDMS-glass chips were fabricated according to Grünberger *et al.* (Grünberger *et al.*, 2012). The microfluidic picoliter bioreactor system (PLBR) used in this study is intended for microcolony growth and growth-coupled phenotypic studies at the single cell level (Grünberger *et al.*, 2013; Grünberger *et al.*, 2012). The device features several arrays of PLBRs (1 µm x 40 µm x 40 µm) allowing for high-throughput observation of cells grown in a monolayer under environmental constant conditions. The principle is similar to the previous reported systems by Grünberger *et al.* and was adapted in particular to trap efficiency and reduced convectional flow within the chambers (Grünberger *et al.*, 2012). The microfluidic PDMS-glass chip was placed inside an in-house manufactured incubator for temperature and atmosphere control and connected to 1 ml disposable plastic syringes (Omnifix 40 Duo, B. Braun Melsungen AG, Melsungen, Germany) for continuous media supply. Media flow was controlled with high precision syringe pumps (neMESYS, Cetoni GmbH, Korbussen, Germany). The incubator was mounted onto a fully motorized inverted Nikon Eclipse Ti microscope (Nikon GmbH, Düsseldorf, Germany) suitable for time-lapse live cell imaging. In detail, the setup was equipped with a focus assistant (Nikon PFS) compensating for thermal drift during long term microscopy. The CFI Plan Apo Lambda DM 100X Oil phase contrast objective was additionally heated with an objective heater (ALA OBJ-Heater, Ala Scientific Instruments, USA). A cell suspension with an OD_{600} between 0.5 and 1, transferred from a pre-culture at exponential growth phase, was infused to the system. After successful cell seeding with bacteria suspension, the growth medium was infused at approx. 100 nl min^{1} per channel to initiate the cultivation. If not stated differently, cells were grown for around 5 to 20 h in standard CGXII medium.

2.6. Live cell imaging and image analysis

For image analysis, the system was equipped with ANDOR LUCA R DL604 camera (Andor Technology plc., Belfast, UK) and a Xenon fluorescence light source for fluorescence excitation. The YFP filters used were HQ 500/20 (excitation filter; Chroma), Q515 (dichroic; Chroma), and HQ 535/30 (emission; Chroma). The E2-Crimson filters used were HQ 600/37 (excitation filter; Chroma), Q630 (dichroic; Chroma), and Q675/67 (emission; Chroma). If not stated differently, the fluorescence exposure time was 200 ms for E2-Crimson and 200 ms for eYFP with a fluorescence intensity set to 100% of maximal power. Phase contrast and fluorescence microscopy images of several arrays of cells were captured in 15 min time intervals and resulting time-lapse images were recorded. The fluorescence exposure time and frame rate was chosen in that way that the illumination did not cause noticeable effects on cellular growth over cultivation period. Typically between 10 and 20 colonies of the same experimental setting were followed in one experiment. Only isogenic colonies originating from one single cell, which did not lose cells during cultivation, were taken for analysis; reactors filled with more than one cell were excluded. Differences of colony size to the time of medium change could not be prevented, as they originated from single cell variations in individual lag-phase and growth rate. For fluorescence analysis (Figure 3, 4, 6) the mean fluorescence value (eYFP and/or E2-Crimson) for each cell was measured at distinct times. For all obtained fluorescence values the background fluorescence (measured at the cell-free space between different PLBRs) of the same frame was subtracted. Image analysis was performed with the Nikon NIS Elements AR software package. The visualization of the lineage tree (Figure 6B) was realized using in-house Python based software.

2.7. Flow cytometry

Flow cytometrical measurements and sorting were performed on a FACSAria II (Becton Dickinson, San Jose, USA) with excitation at 488 nm from a blue solid-state laser or at 633 nm from a red-diode laser at 13 mW. Forward scatter characteristics (FSC) and side scatter characteristics (SSC) were detected as small- and large-angle scatters of the 488 nm laser, respectively. Fluorescence was detected using following filter sets, eYFP (502 nm long-pass and a 530/30 nm band-pass filter), PI (595 nm long-pass and a 610/20 nm band-pass filter), and E2-Crimson (660/20 nm band-pass filter) (Neumeyer *et al.*, 2013). All analyses were performed while thresholding on FSC to remove noise. For flow cytometry (FC) analysis, *C. glutamicum* culture samples were diluted to an OD_{600} of 0.05 in FACSFlow™ sheath fluid buffer (BD, Heidelberg, Germany). For analysis of cell viability, cell samples diluted to an OD_{600} of 0.05 were incubated with 20 µM propidium iodide (PI) (Molecular Probes, Leiden, Netherlands) for 15 min at room temperature. Sorting was performed with 4-way purity as the precision mode at a threshold rate up to 10,000 events/sec. Cells were sorted on BHI agar plates supplemented with 51 mM acetate and 25 µg ml^{-1} kanamycin.

3. Results

3.1. Online monitoring of L-valine production

Previously, we presented the Lrp-biosensor as convenient tool to discriminate between low yield L-valine production strains (<30 mM), such as Δ*aceE,* and non-producing wild type cells. In this study, we assessed the performance of the biosensor to monitor the course of L-valine production over time and to differentiate between high yield and basic production of gradually engineered *C. glutamicum* L-valine production strains. For this purpose, the Lrp-sensor was chromosomally integrated in the different strains in order to avoid plasmid-bound effects, such as fluctuating copy numbers or plasmid loss. Strains under study were Δ*aceE*::Lrp-sensor/pJC4-ilvBNCE-E2-Crimson, Δ*aceE* Δ*pqo*::Lrp-sensor/pJC4-ilvBNCE-E2-Crimson, Δ*aceE* Δ*pqo* Δ*pgi*::Lrp-sensor/pJC4-ilvBNCE-E2-Crimson, and Δ*aceE* Δ*pqo* Δ*pgi* Δ*pyc*::Lrp-sensor/pJC4-ilvBNCE-E2-Crimson, henceforth referred to as Δ*aceE*/pJC4-ilvBNCE-E2-Crimson, Δ*aceE* Δ*pqo*/pJC4-ilvBNCE-E2-Crimson, Δ*aceE* Δ*pqo* Δ*pgi*/pJC4-ilvBNCE-E2-Crimson, and Δ*aceE* Δ*pqo* Δ*pgi* Δ*pyc*/pJC4-ilvBNCE-E2-Crimson. The strains were cultivated in CGXII minimal medium supplied with 154 mM acetate and 222 mM glucose in microtiter plates (0.75 ml filling volume) in the BioLector cultivation system, enabling online measurement of biomass (backscatter, given in a.u.) and eYFP fluorescence (Kensy *et al.*, 2009). The strains grew exponentially within the first 12 to 15 hours, exhibiting decreasing fluorescence in time (Figure 1A, B). Since the cells where pre-cultivated over night in CGXII minimal medium containing 222 mM glucose and 254 mM acetate, the residual fluorescence signal resulted from L-valine production in the pre-cultures and is subsequently diluted by cell growth in the log phase. *C. glutamicum* Δ*aceE*/pJC4-ilvBNCE-E2-Crimson (μ_{max}=0.32) and Δ*aceE* Δ*pqo*/pJC4-ilvBNCE-E2-Crimson (μ_{max}=0.29) showed comparatively faster growth; Δ*aceE* Δ*pqo* Δ*pgi*/pJC4-ilvBNCE-E2-Crimson (μ_{max}=0.27) and Δ*aceE* Δ*pqo* Δ*pgi* Δ*pyc*/pJC4-ilvBNCE-E2-Crimson (μ_{max}=0.24) exhibited a lower growth rate. As soon as cells entered the stationary phase, eYFP fluorescence was detected indicating initiation of the growth-decoupled L-valine production of the strains (Figure 1B). In previous studies, the fluorescence output was shown to correlate with increasing L-valine production of Δ*aceE* (Mustafi *et al.*, 2012). At the early production phase, all strains exhibited similar fluorescence of the

Table 1: Bacterial strains, plasmids and oligonucleotides used in this study.

Strains, plasmids	Relevant characteristics	Source or reference
Strains		
E. coli DH5α	*supE44, ΔlacU169* (*ϕ*80*lacZ*ΔM15), *hsdR17, recA1, endA1, gyrA96,thi1,relA1*	Invitrogen
C. glutamicum ATCC13032	Biotin-auxotrophic wild type	(Kinoshita *et al.*, 1957)
Δ*aceE*::Lrp-sensor	*C. glutamicum* wild type with deletion of the *aceE* gene, coding for the E1p subunit of the pyruvate dehydrogenase complex (PDHC)	(Schreiner *et al.*, 2005)
Δ*aceE* Δ*pqo*::Lrp-sensor	Δ*aceE* strain with deletion of the *pqo* gene, coding for pyruvate:quinone oxidoreductase	(Schreiner *et al.*, 2006)
Δ*aceE* Δ*pqo* Δ*pgi*::Lrp-sensor	Δ*aceE* Δ*pqo* strain with deletion of the *pgi* gene, coding for the phosphoglucose isomerase	(Blombach *et al.*, 2008)
Δ*aceE* Δ*pqo* Δ*pgi* Δ*pyc*::Lrp-sensor	Δ*aceE* Δ*pqo* Δ*pgi* strain with deletion of the *pyc* gene, coding for the pyruvate carboxylase	(Blombach *et al.*, 2008)
Plasmids		
pJC1	*E. coli-C. glutamicum* shuttle vector, Kan^R, $ori V_{Ec}$, $ori V_{Cg}$.	(Schäfer *et al.*, 1997)
pJC1-lrp-brnF'-eyfp	Kan^R; pJC1derivative containing Lrp-sensor cassette, which consists of *lrp* (cg0313), the intergenic region of *lrp brnF* (cg0314) and a transcriptional fusion of *brnF* with *eyfp.*	(Mustafi *et al.*, 2012)
pJC4-ilvBNCE	Kan^R; pJC1derivative carrying the *ilvBNCE* genes coding for the L-valine biosynthetic enzymes acetohydroxyacid synthase, isomeroreductase and transaminase B.	(Radmacher *et al.*, 2002)
pJC4-ilvBNCE-E2-Crimson	Similiar to pJC4-ilvBNCE, containing *e2-crimson* under transcriptional control of P_{tac}.	This work
pK18-mobsacB-cg1121,cg1122-Lrp-sensor	Kan^R; $ori V_{Ec}$ *sacB lacZα*; vector for genomic integration of the Lrp-sensor in the intergenic region of cg1121-cg1122 in *C. glutamicum.*	This work
Oligonucleotides	Sequence (5` → 3`)	
lacI-fw	TCAAGCCTTCGTCACTGGTCC	This work
E2-Crimson-rv	CTACTGGAACAGGTGGTGGCG	This work
Int-cg1121-fw	TTGGCGTGTGGTTGGTTAG	This work
Int-cg1122-rv	CGCATCAAGCAGATCTCTG	This work

L-valine biosensor, but split up in the course of cultivation and differed significantly between high yield producers Δ*aceE* Δ*pqo* Δ*pgi*/pJC4-ilvBNCE-E2-Crimson, Δ*aceE* Δ*pqo* Δ*pgi* Δ*pyc*/pJC4-ilvBNCE-E2-Crimson and basic producers Δ*aceE*/pJC4-ilvBNCE-E2-Crimson, Δ*aceE* Δ*pqo*/pJC4-ilvBNCE-E2-Crimson twelve hours after entrance into the production phase (Figure 1B, C). While fluorescence outputs of Δ*aceE*/pJC4-ilvBNCE-E2-Crimson and Δ*aceE* Δ*pqo*/pJC4-ilvBNCE-E2-Crimson reached within three hours a maximum value, suggesting constant internal L-valine concentrations, fluorescence intensities of Δ*aceE* Δ*pqo* Δ*pgi*/pJC4-ilvBNCE-E2-Crimson and Δ*aceE* Δ*pqo* Δ*pgi* Δ*pyc*/pJC4-ilvBNCE-E2-Crimson increased for about ten hours, thus, displaying the higher potential for L-valine production of these strains. Determination of amino acid concentrations in the supernatant confirmed different levels of L-valine production, ranging from 30 mM L-valine in average for Δ*aceE* Δ*pqo* Δ*pgi*/pJC4-ilvBNCE-E2-Crimson and Δ*aceE* Δ*pqo* Δ*pgi* Δ*pyc*/pJC4-ilvBNCE-E2-Crimson to 23 mM in average for Δ*aceE*/pJC4-ilvBNCE-E2-Crimson and Δ*aceE* Δ*pqo*/pJC4-ilvBNCE-E2-Crimson (Figure 1C). These results show that the Lrp-sensor is suitable to discriminate not only a ON/OFF response (wild type *versus* production strain), but can be applied for online monitoring of production processes in basic as well as high yield production strains, since (i) information about initiation of the production process is provided, (ii) the course of metabolite production process is displayed over time, and (iii) different levels of productivity are revealed.

3.2. FACS-based multiparameter analysis of Δ*aceE*/pJC4-ilvBNCE-E2-Crimson and Δ*aceE* Δ*pqo* Δ*pgi*/pJC4-ilvBNCE-E2-Crimson

In the following, the sensor was applied to display population dynamics of *C. glutamicum* strains during large-scale production processes at the single cell level. In order to compare population structures of basic and high yield production strains, we choose Δ*aceE*/pJC4-ilvBNCE-E2-Crimson and Δ*aceE* Δ*pqo* Δ*pgi*/pJC4-ilvBNCE-E2-Crimson for investigation. FACS analysis of the strains were performed during fed-batch cultivations in lab-scaled bioreactors (450 ml filling volume) with 25 µM IPTG, 222 mM glucose, 254 mM acetate, and 0.5% (w/v) BHI. To allow growth to high cell densities, adequate amounts of acetate were added two times to the growing cells. *C. glutamicum* Δ*aceE*/pJC4-ilvBNCE-E2-Crimson showed linear growth to an OD_{600} of 40 within 14 h cultivation (μ_{max}=0.35); Δ*aceE* Δ*pqo* Δ*pgi*/pJC4-ilvBNCE-E2-Crimson reached within 21 hours an OD_{600} of 40 (μ_{max}=0.24) (Figure 2A, B).

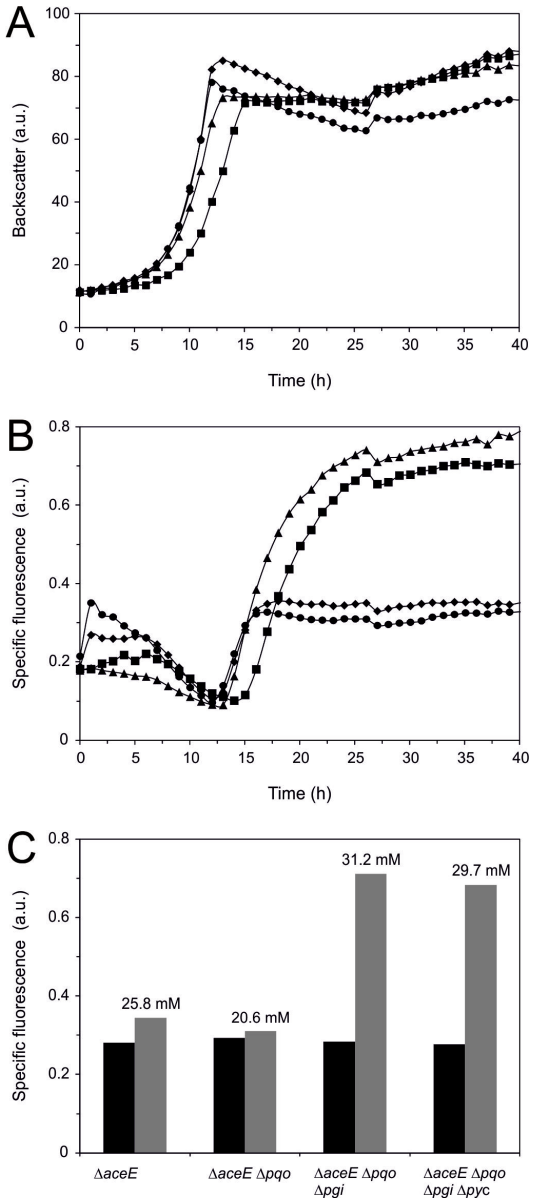

Figure 1. Biosensor-based online monitoring of L-valine production in *C. glutamicum* L-valine production strains with chromosomally integrated Lrp-sensor. Growth **(A)** and Lrp-sensor output, eYFP fluorescence, **(B)** of Δ*aceE*/pJC4-ilvBNCE-E2-Crimson (diamond), Δ*aceE* Δ*pqo*/pJC4-ilvBNCE-E2-Crimson (circle), Δ*aceE* Δ*pqo* Δ*pgi*/pJC4-ilvBNCE-E2-Crimson (triangle), and Δ*aceE* Δ*pqo* Δ*pgi* Δ*pyc*/pJC4-ilvBNCE-E2-Crimson (square) cultivated in CGXII minimal medium containing 222 mM glucose and 254 mM acetate. Data represent average values of two independent cultivations. **(C)** EYFP fluorescence of respective strains at the beginning of the production phase (black bars) and twelve hours after the initiation of L-valine production (grey bars). L-valine concentration (mM) in the supernatant of the respective strain 26.5 h after beginning of cultivation is indicated above the grey bars.

In addition to acetate and BHI, about 13 g glucose/l was consumed during the growth phase by Δ*aceE*/pJC4-ilvBNCE-E2-Crimson and about 6 g glucose/l by Δ*aceE* Δ*pqo* Δ*pgi*/pJC4-ilvBNCE-E2-Crimson. Immediately after the depletion of the last acetate pulse, both strains stopped growing and started to produce L-valine. Three pulses of 222 mM glucose to time points 15 h, 30 h and 50 h were added to the stationary cells to allow high productivity by providing the cells with sufficient carbon source. In comparison to the published data of Blombach *et al.* both strains showed a more than twofold reduced L-valine production, Δ*aceE*/pJC4-ilvBNCE-E2-Crimson accumulated about 73 mM L-valine within 49 h and Δ*aceE* Δ*pqo* Δ*pgi*/pJC4-ilvBNCE-E2-Crimson about 77 mM (Blombach *et al.*, 2008). Additionally, both strains showed a significantly decreased glucose consumption rate compared to the previously reported data.

Multiparameter FACS analysis was applied to provide detailed insights into phenotypic traits of the cells during production process. The analysis included measurements of morphological characteristics as the relative cell size (forward scatter=FSC) and the relative cell granularity (side scatter=SSC), fluorescence measurements of eYFP, displaying biosensor detected L-valine production of the cells and fluorescence measurement of propidium iodide (PI) to label cells with an impaired membrane integrity. In order to gain information about plasmid content, *e2-crimson* coding for far-red fluorescing E2-Crimson was inserted under control of P_{tac} into the vector pJC4-ilvBNCE (Strack *et al.*, 2009). This vector, encoding L-valine biosynthesis genes *ilvBNCE* for overexpression, was introduced into all strains under study. Thus, fluorescence measurements of E2-Crimson, displayed presence of pJC4-ilvBNCE-E2-Crimson in the cells. As it is demonstrated in Figure 2C, F immediately after the depletion of acetate and the start of L-valine production (Δ*aceE*/pJC4-ilvBNCE-E2-Crimson, 20 h; Δ*aceE* Δ*pqo* Δ*pgi*/pJC4-ilvBNCE-E2-Crimson, 24 h) cells exhibited an increased eYFP signal. Due the rather low L-valine production of Δ*aceE* Δ*pqo* Δ*pgi*/pJC4-ilvBNCE-E2-Crimson, no significant difference in fluorescence output compared to Δ*aceE*/pJC4-ilvBNCE-E2-Crimson was detected over time (Figure 2C, F). Interestingly, measuring eYFP and E2-Crimson fluorescence revealed the occurrence of several subpopulations within the fermentation culture of Δ*aceE*/pJC4-ilvBNCE-E2-Crimson and Δ*aceE* Δ*pqo* Δ*pgi*/pJC4-ilvBNCE-E2-Crimson (Figure 2E, H). Obviously, cells displaying a high eYFP and E2-Crimson signal represented the productive subpopulation (12-14% for Δ*aceE*/pJC4-ilvBNCE-E2-Crimson, 7% for Δ*aceE* Δ*pqo* Δ*pgi*/pJC4-ilvBNCE-E2-Crimson) within the culture. Sorting of these cells on agar plates revealed a high survival rate of 91% for Δ*aceE*/pJC4-ilvBNCE-E2-Crimson cells and of 80% for Δ*aceE* Δ*pqo* Δ*pgi*/pJC4-ilvBNCE-E2-Crimson cells. The largest population (83-85% for Δ*aceE*/pJC4-ilvBNCE-E2-Crimson, ~90% for Δ*aceE* Δ*pqo* Δ*pgi*/pJC4-ilvBNCE-E2-Crimson) was represented by cells showing a relatively low eYFP signal, indicating a low internal L-valine level, despite presence of pJC4-ilvBNCE-E2-Crimson and thus, overexpression of L-valine biosynthesis genes in the cells, which was displayed by a high E2-Crimson fluorescence. The relative low survival rates of 59% for Δ*aceE*/pJC4-ilvBNCE-E2-Crimson and 32% for Δ*aceE* Δ*pqo* Δ*pgi*/pJC4-ilvBNCE-E2-Crimson suggest, that this population represented energetically exhausted cells, being partially metabolic active. In addition, a subpopulation of E2-Crimson negative cells was observed and cells of this population showed almost no growth on plates. Strikingly, decrease in E2-Crimson fluorescence was accompanied by a strongly decreased eYFP signal, hence indicating a correlation between the biosensor signal and the plasmid marker. A fraction of this population (≤ 14% for Δ*aceE*/pJC4-ilvBNCE-E2-Crimson, ≤ 28% for Δ*aceE* Δ*pqo* Δ*pgi*/pJC4-ilvBNCE-E2-Crimson) displayed higher density compared to the main population in FSC *vs*. SSC plots, indicating shrinkage of cells. However, a small number of E2-Crimson negative cells showed high eYFP fluorescence. Since these cells formed no viable colonies after sorting, they rather represented eYFP fluorescing cell debris of lysed cells than metabolic active cells with a disturbed E2-Crimson synthesis. Yet, they showed no variations in FCS and SSC signals compared to the majority of the culture. The results obtained by measuring eYFP and E2-Crimson fluorescence were well supported by staining of the cells with the fluorescent dye PI, a commonly accepted marker indicating loss of membrane integrity and viability. In the production phase a large PI positive subpopulation (about 10% of the entire population) was detected, which was less pronounced in the log phase (Figure 2D, G). In fact, all PI positive cells were also eYFP negative, but negative and positive for E2-Crimson (data not shown).

3.3. Live cell imaging of L-valine production

We presented the Lrp-biosensor as versatile tool for online monitoring of L-valine production processes performed at different scales. However, results

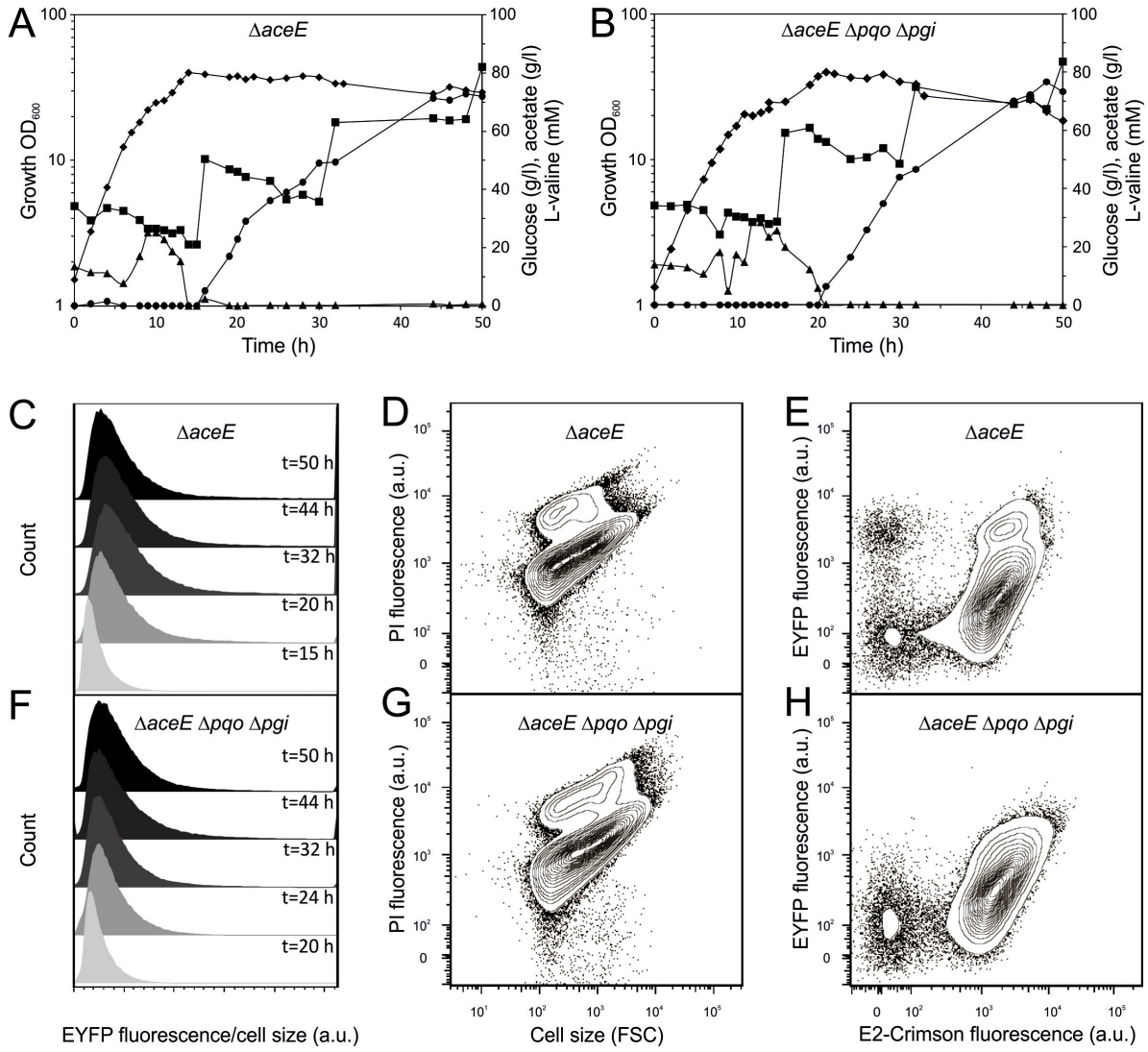

Figure 2. Multiparameter FACS analysis of Δ*aceE*/pJC4-ilvBNCE-E2-Crimson and Δ*aceE* Δ*pqo* Δ*pgi*/pJC4-ilvBNCE-E2-Crimson with chromosomally integrated Lrp-sensor in lab-scale bioreactor cultivation. Representative fed-batch cultivation of Δ*aceE*/pJC4-ilvBNCE-E2-Crimson **(A)** and Δ*aceE* Δ*pqo* Δ*pgi*/pJC4-ilvBNCE-E2-Crimson **(B)**, showing growth of the cells (diamonds), glucose (squares), acetate (triangles), and L-valine (circles) concentrations in the supernatant. FACS generated histograms displaying eYFP fluorescence (ratio eYFP/FSC) of Δ*aceE*/pJC4-ilvBNCE-E2-Crimson **(C)** and Δ*aceE* Δ*pqo* Δ*pgi*/pJC4-ilvBNCE-E2-Crimson **(F)** to different times, density plots displaying FSC and PI signal of Δ*aceE*/pJC4-ilvBNCE-E2-Crimson **(D)** and Δ*aceE* Δ*pqo* Δ*pgi*/pJC4-ilvBNCE-E2-Crimson **(G)** in the production phase (t=32 h), and density plots displaying E2-Crimson and eYFP signal of Δ*aceE*/pJC4-ilvBNCE-E2-Crimson **(E)** and Δ*aceE* Δ*pqo* Δ*pgi*/pJC4-ilvBNCE-E2-Crimson **(H)** in the production phase (t=32 h).

obtained from cultivation in microtiter-based cultivation systems (*e.g.* BioLector system) provide average data for the entire culture. In contrast, FACS measurements allow the HT analysis of the respective population at single cell resolution, but provide a snapshot insight into the phenotypic distribution. To investigate growth, physiology, and productivity states of single cells in a time-resolved manner, *C. glutamicum* L-valine production stains were cultivated in microfluidic PLBR chambers under constant environmental conditions (Grünberger *et al.*, 2012). Therefore, Δ*aceE*/pJC4-ilvBNCE-E2-Crimson and Δ*aceE* Δ*pqo* Δ*pgi*/pJC4-ilvBNCE-E2-Crimson were grown in CGXII minimal medium, containing 154 mM acetate, 222 mM glucose in growth and 222 mM glucose in production phase on a microfluidic chip system, consisting of arrays of picoliter cultivation chambers (Figure 3A). Using automated time-lapse microscopy growth and production studies were performed in parallel manner.

Figure 3C shows two representative colonies of Δ*aceE*/pJC4-ilvBNCE-E2-Crimson and Δ*aceE* Δ*pqo* Δ*pgi*/pJC4-ilvBNCE-E2-Crimson during growth (t_1, t_2) and L-valine production phase (t_3-t_5). In general, Δ*aceE*/pJC4-ilvBNCE-E2-Crimson showed a higher

growth rate (μ_{max}=0.21+/-0.02 (n=12)) than Δ*aceE* Δ*pqo* Δ*pgi*/pJC4-ilvBNCE-E2-Crimson (μ_{max}= 0.15+/-0.02 (n=12)). In order to initiate L-valine production, the carbon source in the medium, *i.e.* acetate (154 mM), was replaced by glucose (222 mM) after 18.5 hours. After medium switch cells gradually stopped growing and simultaneously exhibited progressively increasing eYFP fluorescence. The average fluorescence signal of three microcolonies (fluorescence signal *per* colony area) of Δ*aceE*/pJC4-ilvBNCE-E2-Crimson and Δ*aceE* Δ*pqo* Δ*pgi*/pJC4-ilvBNCE-E2-Crimson during growth and production phase is depicted in Figure 3B. In contrast to Δ*aceE* Δ*pqo* Δ*pgi*/pJC4-ilvBNCE-E2-Crimson colonies of Δ*aceE*/pJC4-ilvBNCE-E2-Crimson displayed a low eYFP signal already during the growth phase. As soon as the medium was changed and the cells were supplied with glucose, the eYFP signal increased in colonies of both strains, indicating growth-decoupled L-valine production. Although Δ*aceE* Δ*pqo* Δ*pgi*/pJC4-ilvBNCE-E2-Crimson colonies displayed lower fluorescence emission compared to Δ*aceE*/pJC4-ilvBNCE-E2-Crimson colonies before the beginning of the production phase (t=18.5 h), levels of fluorescence intensities increased comparable when L-valine production was initiated. In agreement with the results obtained by cultivations in the BioLector system (see Figure 1) colonies of the high yield producer Δ*aceE* Δ*pqo* Δ*pgi*/pJC4-ilvBNCE-E2-Crimson showed an overall higher, final fluorescence signal in comparison to colonies of Δ*aceE*/pJC4-ilvBNCE-E2-Crimson. Interestingly, the time until the strains exhibited maximal fluorescence was about two to three times higher during cultivation in the microfluidic system. In addition to average measurements of colony growth and productivity, monolayer cultivation systems allow investigation of individual cells within the entire population. As a proof of principle we measured the fluorescence development of single cells during the production phase (Figure 3D), which revealed typical Gaussian distribution regarding single cell fluorescence of the respective strains. Similarly to results shown in Figure 3C Δ*aceE* Δ*pqo* Δ*pgi*/pJC4-ilvBNCE-E2-Crimson exhibited higher fluorescence emission in average on single cell level.

3.4. Correlation of single cell biosensor (eYFP fluorescence) and plasmid marker (E2-Crimson fluorescence)

Plasmid instability in production strains represents an obstacle in particular during large-scale bioprocesses, where cultures pass a high number of generations. In our studies, the insertion of the plasmid marker E2-Crimson into pJC4-ilvBNCE enabled monitoring of plasmid content in single cells during cultivation. In order to assess the correlation of plasmid content and L-valine production in basic and high yield production strains, we analyzed eYFP and E2-Crimson fluorescence emission at the single cell level in Δ*aceE*/pJC4-ilvBNCE-E2-Crimson and Δ*aceE* Δ*pqo* Δ*pgi*/pJC4-ilvBNCE-E2-Crimson cultivated in microfluidic systems. Figure 4A shows representative colonies of Δ*aceE*/pJC4-ilvBNCE-E2-Crimson and Δ*aceE* Δ*pqo* Δ*pgi*/pJC4-ilvBNCE-E2-Crimson at the end of the production phase (~46h) from the same experiment discussed in section 3.4. Overall, a strong correlation between eYFP and E2-Crimson signal was observed for Δ*aceE* Δ*pqo* Δ*pgi*/pJC4-ilvBNCE-E2-Crimson (r=0.73+/-0.09 (n=3)) in contrast to Δ*aceE*/pJC4-ilvBNCE-E2-Crimson (r=0.16+/-0.09 (n=3)) (Figure 4B). By analogy with FACS generated dot plots, displaying eYFP/E2-Crimson signal ratio, eYFP and E2-Crimson fluorescence of single cells within the colonies was evaluated. Remarkably, colonies of the respective strain showed in general the same eYFP/E2-Crimson distribution. Only a minor amount of cells (<1 %) displayed a high E2-Crimson, but low eYFP signal (Figure 4A, B). Dead cells (low signal for eYFP and E2-Crimson) were rarely detected. However, their occurrence strongly depended on the chosen colony and time point during cultivation (see section 3.5). Generally, cells of Δ*aceE* Δ*pqo* Δ*pgi*/pJC4-ilvBNCE-E2-Crimson exhibited significant higher E2-Crimson fluorescence compared to cells of Δ*aceE*/ pJC4-ilvBNCE-E2-Crimson. This is exemplary shown for one colony of Δ*aceE*/pJC4-ilvBNCE-E2-Crimson and Δ*aceE* Δ*pqo* Δ*pgi*/pJC4-ilvBNCE-E2-Crimson in Figure 4C. Channeling the carbon flux through pentose phosphate pathway by deletion of *pgi* significantly enhances intracellular NADPH concentrations in Δ*aceE* Δ*pqo* Δ*pgi*/pJC4-ilvBNCE-E2-Crimson compared to Δ*aceE*/pJC4-ilvBNCE-E2-Crimson (sevenfold increase) (Bartek *et al.*, 2010). Thus, the high energy level available in Δ*aceE* Δ*pqo* Δ*pgi*/pJC4-ilvBNCE-E2-Crimson might result in an increased protein synthesis, which is the most energy-consuming process in bacterial cells. In turn, this would result in an increased E2-Crimson production which could explain the higher fluorescence signal and the strong correlation between E2-Crimson and eYFP signal observed for Δ*aceE* Δ*pqo* Δ*pgi*/pJC4-ilvBNCE-E2-Crimson.

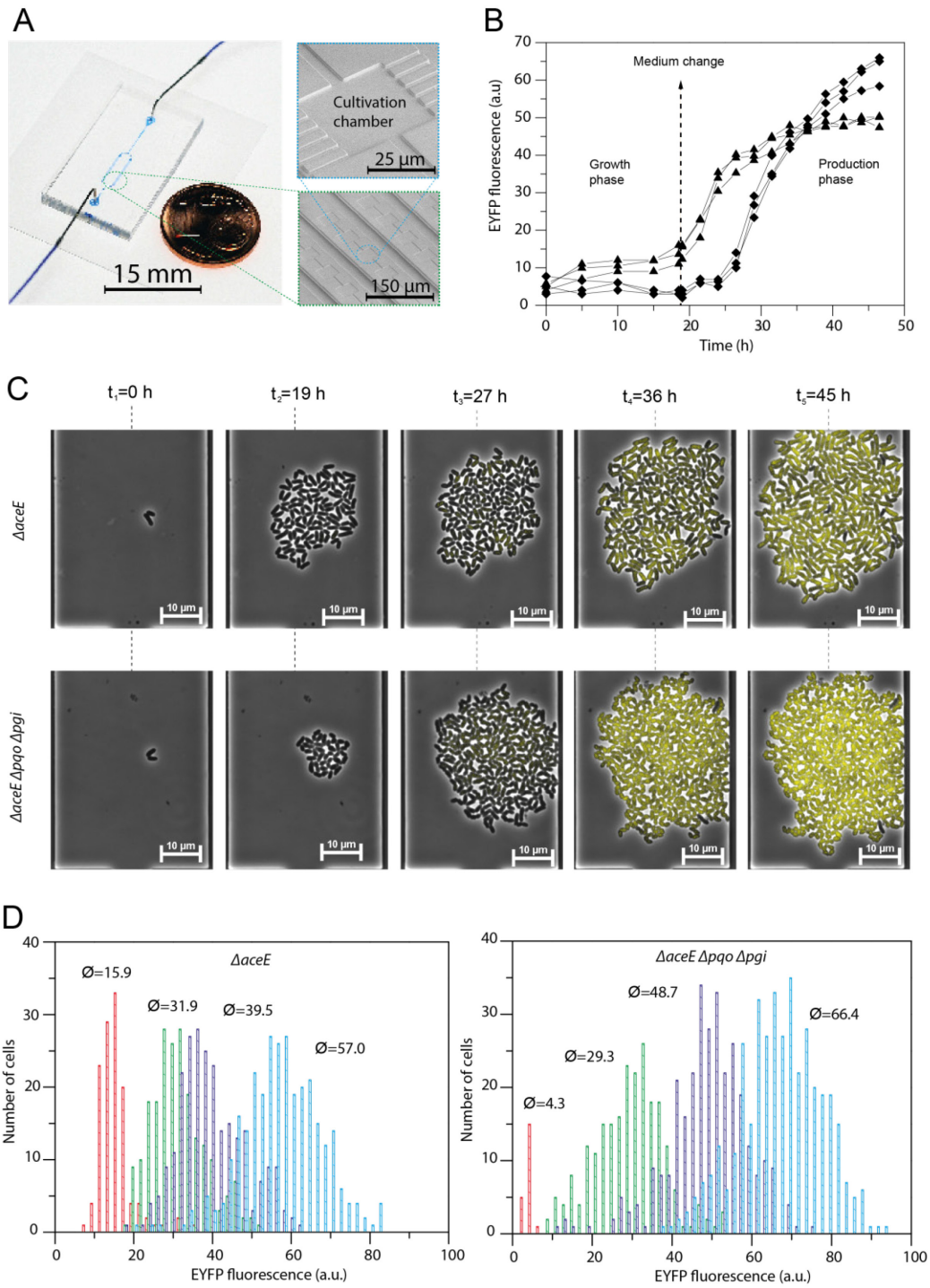

Figure 3. Single cell growth and production studies of *C. glutamicum* Δ*aceE*/pJC4-ilvBNCE-E2-Crimson and Δ*aceE* Δ*pqo* Δ*pgi*/pJC4-ilvBNCE-E2-Crimson with chromosomally integrated Lrp-sensor in microfluidic PLBR at environmental defined conditions. **(A)** Illustration of the microfluidic picoliter bioreactor (PLBR) system. The system consists of several arrays of monolayer picoliter sized cultivation chambers. High magnification time-lapse microscopy can capture several microcolonies in parallel during single cell cultivation. **(B)** Fluorescence emission of three entire microcolonies (average eYFP signal *per* colony area) of Δ*aceE*/pJC4-ilvBNCE-E2-Crimson (triangles) and Δ*aceE* Δ*pqo* Δ*pgi*/pJC4-ilvBNCE-E2-Crimson (diamonds) over time. For evaluation, every 2.5 h the fluorescence was measured. **(C)** Growth (t_1-t_2) and production phase (t_3-t_5) of isogenic microcolonies of Δ*aceE*/pJC4-ilvBNCE-E2-Crimson (upper row) and Δ*aceE* Δ*pqo* Δ*pgi*/pJC4-ilvBNCE-E2-Crimson (lower row). **(D)** Histograms illustrating fluorescence signal distribution within a representative microcolony of Δ*aceE*/pJC4-ilvBNCE-E2-Crimson (left) and Δ*aceE* Δ*pqo* Δ*pgi*/pJC4-ilvBNCE-E2-Crimson (right). EYFP signal of single cells was measured at distinct times, t=19 h (red), t=26 h (green), t=34 h (purple), and t=46 h (blue). Average fluorescence values at these times are indicated above the respective peaks. All cultivations were performed in microfluidic chambers shown in (A) in CGXII minimal medium containing 154 mM acetate, 222 mM glucose during growth phase or 222 mM glucose and 25 µmol IPTG during the production phase, respectively.

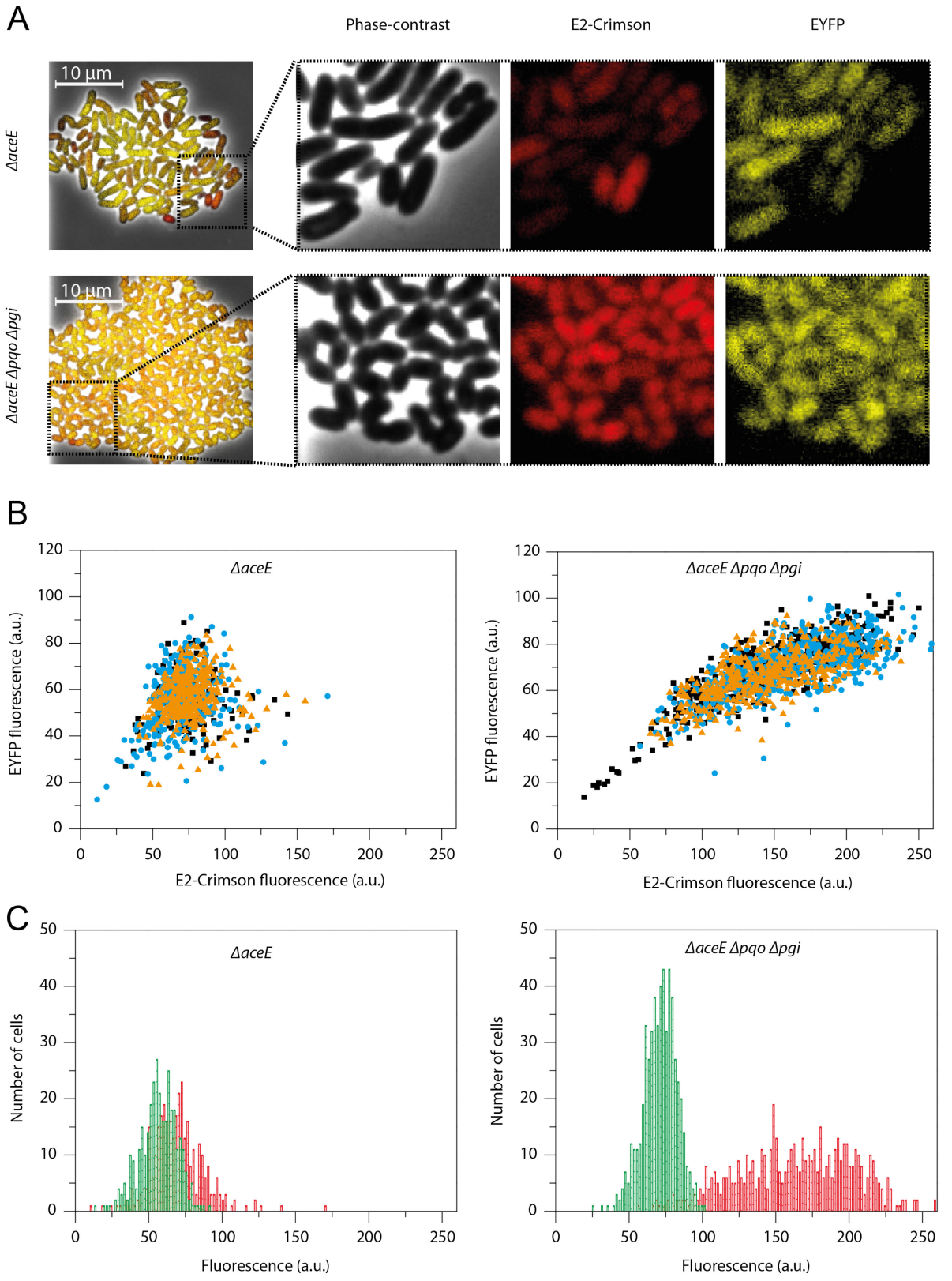

Figure 4. Correlation of chromosomally integrated Lrp-sensor (eYFP) and plasmid marker (E2-Crimson) in Δ*aceE*/pJC4-ilvBNCE-E2-Crimson and Δ*aceE* Δ*pqo* Δ*pgi*/pJC4-ilvBNCE-E2-Crimson. (A) Overlay plot of phase-contrast, eYFP and E2-Crimson signal of isogenic Δ*aceE*/pJC4-ilvBNCE-E2-Crimson (upper panel) and Δ*aceE* Δ*pqo* Δ*pgi*/pJC4-ilvBNCE-E2-Crimson (lower panel) microcolony at the end (~46h) of the single cell cultivation shown in Figure 3C. For better comparability, the same LUT were chosen for both colonies. **(B)** Dot plots displaying eYFP and E2-Crimson signal of single cells of three isogenic microcolonies (triangles, circles, and diamonds) of Δ*aceE*/pJC4-ilvBNCE-E2-Crimson (left) and Δ*aceE* Δ*pqo* Δ*pgi*/pJC4-ilvBNCE-E2-Crimson (right). **(C)** EYFP (green) and E2-Crimson (red) fluorescence signal distribution of a microcolony of Δ*aceE*/pJC4-ilvBNCE-E2-Crimson (left) and Δ*aceE* Δ*pqo* Δ*pgi*/pJC4-ilvBNCE-E2-Crimson (right) 27.5 hours after entrance into the production phase (see Figure 3C). All cultivations were performed as described in the legend of Figure 3.

3.5. How dead is dead?

Strikingly, flow cytometry and microscopy revealed the presence of a non-viable, *i.e.* PI fluorescing, cell fraction (~10%) during the production phase of cells cultivated in lab-scale bioreactors. Although to a minor extent (<1%), we observed the occurrence of non-fluorescent cells also in well-controlled small scale cultivations performed in the microfluidic system. In contrast to FACS, live cell imaging studies offer the advantage to investigate this phenomenon in a time-resolved manner and to discriminate between different types of non-fluorescent cells: *e.g.* lysed dead cells or dormant forms which resume growth after a while.

Under conditions described in section 3.3, we usually observed colonies showing a typical Gaussian distribution of eYFP; occasionally colonies with an increased number of non-fluorescing cells were found (<1% of cells) (Figure 5). We tracked different cells in several colonies, clustered the "dark" cells and found four different types of non-producing cells (Figure 5). The majority of cells, which undergo transition from growth to production, will not be discussed here. The first type of non-producing cells initiated L-valine production, but showed at a later time sudden cell lysis (Figure 5I, II). These cells were rarely seen at environmental constant conditions, but have been more frequently observed, when colony growth exceeded chamber size leading to densely packed colonies, thus, eventually causing unfavorable gradients within the chambers (data not shown). A second fraction of cells showed progressively decreasing fluorescence signal over time, potentially caused by a permeabilized or compromised membrane (Figure 5V). Both such types most likely represent dead cells and none of those were found to resume growth and production later in our experiment. Further, we observed cells, which neither initiated L-valine production nor showed growth after medium change. These cells might either represent cells, which already died or lysed in the growth phase or cells in a kind of dormant state (Figure 5III). The fourth class of non-producing cells did not enter into the production phase as well, but continued to grow (Figure 5V), although no carbon source for growth, *i.e.* acetate, was provided in the medium. In this context, the question arises whether the cells might have adapted growth utilizing glucose as carbon source.

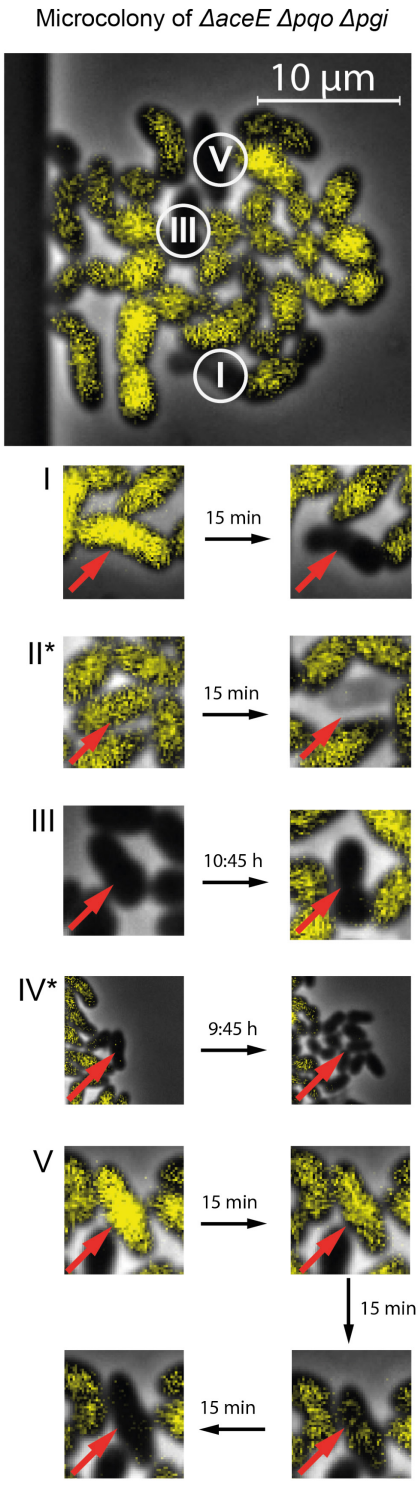

Figure 5. How dead is dead - Different types of non-fluorescent cells during the production phase. The image at the top shows a microcolony of Δ*aceE* Δ*pqo* Δ*pgi*/pJC4-ilvBNCE-E2-Crimson (Lrp-sensor chromosomally integrated) with a considerably high number of non or low eYFP fluorescing cells. **(I+II)** Lysing **(III)** and dormant cells, which does not switch from growth to production. **(IV*)** Cells showing a slow growth, but no production. **(V)** Leaky cells that show progressively decreasing fluorescence signal over time, potentially caused by a permeabilized cell membrane. Images marked with an asterisk show cells of another microcolony of Δ*aceE* Δ*pqo* Δ*pgi*/pJC4-ilvBNCE-E2-Crimson, not shown here. Cultivation was performed as described in the legend of Figure 3, but without addition of IPTG.

3.6. Bistability in *C. glutamicum* L-valine production strains

Homogenous environmental conditions as given in the microfluidic setup are fictional and far away from fluctuations in bioreactor processes at larger scale. To simulate environmental heterogeneities, in particular those triggering transition of L-valine production strains from growth to production phase, we performed cultivation with constant, but non-defined (several carbon sources) conditions by adding complex medium compounds (BHI). Starting from a single cell growth of an isogenic microcolony of Δ*aceE*/pJC4-ilvBNCE-E2-Crimson in minimal medium with 154 mM acetate, 222 mM glucose and 0.5% BHI in the microfluidic cultivation system was followed. To trigger L-valine production, the primary carbon source utilized for growth, acetate, was removed and cells were supplied with 222 mM glucose and additionally 0.5% BHI. Although most of the cells followed the switch from growth to production, surprisingly in approximately 50% of the recorded colonies one single cell continued growing after medium switch (Figure 6A). Figure 6 shows exemplary two cells originating from the same mother cell where one cell (marked in green) divided for the last time and initiated L-valine production directly after the medium switch, while the sister cell (marked in blue) continued cell growth. In the following, some of the descendants of the blue cell also switched to L-valine production (marked in orange and purple) or continued growth throughout the course of the experiment (marked in cyan). This experiment illustrates that under these conditions looking at the average fluorescent emission of the entire microcolony masks the significant variation at the single cell level (Figure 6C). This bistability in the decision of switching from growth to production was observed for all L-valine producing strains under study when the cells were grown in the presence of low amounts of BHI. In contrast, a continuous, homogenous switching behavior was observed when only glucose was present in the production medium illustrating the strong impact of slight changes in medium composition on the phenotypic structure of a particular population.

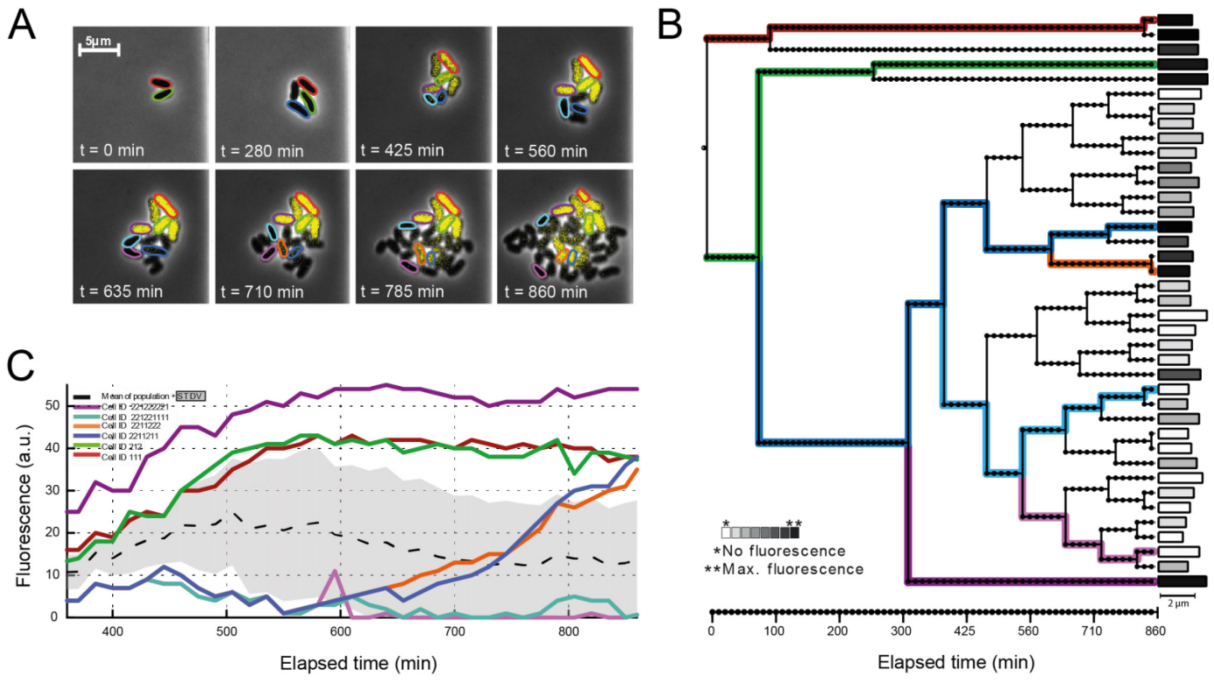

Figure 6. Bistability of Δ*aceE*/pJC4-ilvBNCE-E2-Crimson with chromosomally integrated Lrp-sensor upon switch from growth to production phase. (A) Growth and production phase (initiated after 340 min) of an isogenic microcolony under carbon-source limiting conditions, **(B)** and lineage tree of the respective microcolony highlighting several single cell traces. EYFP fluorescence was quantified in single cells after 860 min. The length of the boxes indicates the length of the cells at the time of fluorescence measurement. **(C)** Single cell traces of fluorescence output of marked cells (B) and average emission of the whole colony (black, dashed line, SD=grey shading). Cultivation was performed in CGXII minimal medium containing 154 mM acetate, 222 mM glucose and 0.5% BHI during growth phase or 222 mM glucose and 0.5% BHI during production phase, respectively.

4. Discussion

Quantifying and understanding the origin and impact of cell-to-cell heterogeneity in microbial bioprocesses remains one major challenge for future bioprocess optimization (Müller *et al.*, 2010; Lencastre Fernandes *et al.*, 2011). First investigations of the basic L-valine production strain Δ*aceE* indicated cell-to-cell variations in respect to L-valine production in isogenic microcolonies (Mustafi *et al.*, 2012). Nevertheless, studies aiming for detailed single cell analysis of population dynamics in *C. glutamicum* based bioprocesses have not been described yet. Technological limitations and a lack of convenient tools for accurate single cell analysis prevented systematic studies until now. In this work, we present the recently described Lrp-sensor, capable of detecting cytosolic accumulation of amino acids, as a powerful tool for monitoring and single cell analysis of biotechnological production processes.

Proof of principle experiments assessing the performance of the biosensor in gradually engineered L-valine production strains, revealed significant differences in fluorescence output of basic producers Δ*aceE*/pJC4-ilvBNCE-E2-Crimson and Δ*aceE* Δ*pqo*/pJC4-ilvBNCE-E2-Crimson and high yield producers Δ*aceE* Δ*pqo* Δ*pgi*/pJC4-ilvBNCE-E2-Crimson and Δ*aceE* Δ*pqo* Δ*pgi* Δ*pyc*/pJC4-ilvBNCE-E2-Crimson. This was in agreement with different levels of final L-valine production, as it was shown by HPLC measurements of L-valine concentrations in the supernatant of the respective strains (Blombach *et al.*, 2008). Thus, the biosensor proved as convenient tool for online monitoring of metabolite production, what makes it highly suitable for screening of different cultivation conditions in order to optimize production processes. Further, the biosensor can be implemented in screening procedures aiming for the isolation of amino acid producing strains (Mustafi *et al.*, 2012; Binder *et al.*, 2012). However, online measurements of fluorescence during cultivation in microtiter plates provide information on productivity of the whole population, but mask variation at the single cell level. Here, multiparameter flow cytometry was applied to access population dynamics of *C. glutamicum* L-valine producers during fed-batch cultivation in a bioreactor. PI measurements displayed a progressive loss of cellular membrane integrity during the production phase, resulting in a non-viable subpopulation of up to 10% of the entire culture. PI positive cells showed no eYFP signal, which might be caused by leakage of intracellular eYFP protein. This strong inverse correlation between PI and eYFP indicates that already the signal of the Lrp-biosensor provides sufficient insights into the metabolic activity and viability of the population and that additional staining procedures (here PI) are basically not required. Similar correlations were recently also described for studies based on a GFP-sensor enabling the detection of carbon-limited conditions in *E. coli* as well as for a reporter system in yeast, where expression of *gfp* was set under control of a ribosomal protein promoter (Delvigne *et al.*, 2011; Carlquist *et al.*, 2012).

In order to investigate population dynamics of the *C. glutamicum* production strains in a time-resolved manner, live cell imaging studies were performed during defined and well-controlled cultivation conditions in microfluidic devices (Grünberger *et al.*, 2012). Strikingly, we observed a fraction of "dark", non-fluorescing cells during the cultivation of the four different strains. Tracking of these cells by time-lapse microscopy, revealed different types of non-producing cells besides the productive main population. Sudden and progressive cell lysis and cells in a kind of dormant state were observed. Further, some cells showed no switch from growth to production phase, although no carbon source for growth was provided in the medium. Two potential reasons explaining this phenomenon can be considered. First cells might utilize low concentrated, but by flow continuously supplied carbon sources. This might be carbon impurities in the minimal medium or carbon-containing substances such as protocatechuic acid or MOPS. Alternatively, cellular metabolism might have been adapted to overflow of glucose; bypassing deletion of E1p subunit of the PDH complex *(aceE)* and pyruvate:menaquinone oxidoreductase *(pqo)* and providing acetyl-CoA as precursor for TCA-cycle. Studies of Litsanov *et al.* described that despite deletions of the genes for the known acetate-forming pathways in *C. glutamicum*, residual acetate formation in strains engineered for aerobic succinate production was still observed (Litsanov *et al.*, 2012).

Our studies revealed, depending on the medium composition, the emergence of non-productive, but growing subpopulations. These might overgrow the entire culture in the course of time and thus, might have a tremendous, negative impact on production process, since resources are depleted for biomass formation instead of being converted to the final product. We mimicked in microfluidic cultivations the actual short time of transition from growth to production phase in fermentation processes, where cells are confronted with depleting acetate

concentrations, the primary carbon source used for growth, by supplying cells with low concentrations of non-defined alternative carbon sources (*e.g.* BHI). Overall, these studies revealed bistability regarding initiation of L-valine production within the different production strains. Besides the expected switch from growth to production, cells showed either unhampered growth and cell division, or a time-delayed switch to L-valine production. This demonstrates that despite targeted, genetic manipulation on cells to work as efficient, uniform microbial factory, phenotypic variation might lead to the occurrence of drastic differences in cellular productivity even under well-controlled cultivation conditions. In fact, further growth of particular cells might be based on different energetic states of the cells or a higher abundance of transporter proteins, enabling a more efficient uptake of residual carbon sources.

However, in contrast to bioreactor experiments the majority of the population transitioned from growth into the production phase during cultivation in the PLBR. Here cells of Δ*aceE*/pJC4-ilvBNCE-E2-Crimson displayed a low eYFP signal already during the growth phase, which could be explained by increased glucose uptake of this strain resulting in basal levels of L-valine production, *i.e.* low fluorescence output. This is well supported by the observed twofold higher glucose consumption of Δ*aceE*/pJC4-ilvBNCE-E2-Crimson during growth in bioreactor experiments, which has also been described by Blombach *et al.* (Blombach *et al.*, 2008). Interestingly the strains required significantly more time (two- to threefold) to reach the maximal fluorescence during cultivation in the microfluidic system compared to batch cultivation in microtiter plate. This can be explained in two ways: first, microfluidic is a perfusion system, removing all secreted L-valine, which prevents an accumulation in the supernatant and in turn, a feasible uptake by the cells. This could lead to a longer time until constant internal L-valine concentrations are reached. Furthermore, in the microfluidic system cells are continuously supplied with growth medium. Necessary nutrients that might not be available for production processes in batch fermentation could be available in the microfluidic system, leading to a prolonged and/or higher productivity of L-valine. In fact, *C. glutamicum* wild type cells showed a 50% higher growth rate during cultivation in PLBRs compared to cultivation in shake flasks.

The development of a predominant population, exhibiting high E2-Crimson, but no eYFP fluorescence signal, as it was the case during large-scale fermentation was not observed during cultivation in the microfluidic system. However, when expression of *e2-crimson* was strongly increased by the addition of IPTG, cells showed neither growth nor L-valine production, instead a high E2-Crimson signal during cultivation in the microfluidic system (data not shown). Referring to the results obtained by the bioreactor experiment, we postulate that the predominant E2-Crimson positive population during large-scale fermentation represented cells with reduced metabolic activity. Several studies described that expression of fluorescence proteins can provide a significant burden on cells, affecting particularly bacterial functions which demand high energy costs (Rang *et al.*, 2003; Knodler *et al.*, 2005; Flores *et al.*, 2004). Yet, we observed no influence of eYFP-expression or Lrp-biosensor production on metabolism of *C. glutamicum*. In contrast to *eyfp*, which was chromosomally integrated with one copy *per* cell, plasmid-bound *e2-crimson* (~10 copies *per* cell) was expressed in high levels in the cells. Chromosomal integration of *gfp* was reported to overcome adverse impact of plasmid-encoded *gfp* expression on invasion of *Salmonella enterica* (Clark *et al.*, 2009). Further, red fluorescent chromophores compared to eYFP require an additional equivalent of molecular oxygen for maturation (Gross *et al.*, 2000). Thus, too high induction levels of *e2-crimson* expression might have placed a substantial burden on energetically stressed cells during L-valine production, resulting in the development of a predominant subpopulation of non-producing cells in the bioreactor experiment. However, we observed no negative influence of *e2-crimson* expression on cellular physiology, when induced in lower amounts during cultivation in the microfluidic system or BioLector. Initially, we introduced this second marker protein (E2-Crimson) in our studies, to assess correlation in single cells between L-valine production and overexpression of L-valine biosynthesis genes *(ilvBNCE), i.e.* eYFP fluorescence emission of the Lrp-sensor and E2-Crimson fluorescence of the plasmid marker. However, this has to be critically examined when studies under physiological conditions are aimed, since our results indicate that a second marker can provide significant metabolic burden for the cells, which might significantly impact the phenotypic pattern of the population. This aspect has to be addressed in future studies.

We presented the amino acid sensing Lrp-sensor as valuable, non-invasive tool to access information of *C. glutamicum* populations in regard to productivity

and physiology of single cells during production processes. This biosensor-based approach represents a first step towards a better understanding of population dynamics in production processes of *C. glutamicum*. Future studies will aim to unravel the underlying molecular mechanisms of the observed phenotypic variation, benchmarking this approach for analysis and improvement of strains and biotechnological production processes. Promising advances are currently made in the development of downstream methods to profile subpopulations, *e.g.* combination of FACS cell sorting with mass spectrometry based proteomic analysis, so-called *Cytomics*, for the analysis of subpopulations (Jehmlich *et al.*, 2010; Müller & Hiller, 2013).

5. References

Acar, M., Mettetal, J.T. & van Oudenaarden, A. (2008) Stochastic switching as a survival strategy in fluctuating environments. *Nature Genetics* 40: 471-475.

Alonso, S., Rendueles, M. & Díaz, M. (2012) Physiological heterogeneity of *Pseudomonas taetrolens* during lactobionic acid production. *Applied Microbiology and Biotechnology* 96: 1465-1477.

Bartek, T., Blombach, B., Zönnchen, E., Makus, P., Lang, S., Eikmanns, B.J. & Oldiges, M. (2010) Importance of NADPH supply for improved L-valine formation in *Corynebacterium glutamicum*. *Biotechnology Progress* 26: 361-371.

Binder, S., Schendzielorz, G., Stäbler, N., Krumbach, K., Hoffmann, K., Bott, M. & Eggeling, L. (2012) A high-throughput approach to identify genomic variants of bacterial metabolite producers at the single-cell level. *Genome Biology* 13.

Blombach, B., Schreiner, M.E., Bartek, T., Oldiges, M. & Eikmanns, B.J. (2008) *Corynebacterium glutamicum* tailored for high-yield L-valine production. *Applied Microbiology and Biotechnology* 79: 471-479.

Brehm-Stecher, B.F. & Johnson, E.A. (2004) Single-cell microbiology: tools, technologies, and applications. *Microbiology and Molecular Biology Reviews* 68: 538-559.

Brognaux, A., Neubauer, P., Twizere, J.-C., Thonart, P. & Delvigne, F. (2012) Potentiality of using microbial biosensors for the detection of substrate heterogeneities and the assessment of microbial viability in industrial bioreactors: a complete set of experiments in chemostat and scale down reactors, and elaboration of a mini scale-down platform. *Communications in agricultural and applied biological sciences* 77: 3-7.

Brognaux, A., Thonart, P., Delvigne, F., Neubauer, P., Twizere, J.-C., Francis, F. & Gorret, N. (2013) Direct and indirect use of GFP whole cell biosensors for the assessment of bioprocess performances: design of milliliter scale-down bioreactors. *Biotechnology Progress* 29: 48-59.

Burkovski, A., (2008) *Corynebacteria: genomics and molecular biology*. Caister Academic Press, Norfolk UK.

Cai, L., Friedman, N. & Xie, X.S. (2006) Stochastic protein expression in individual cells at the single molecule level. *Nature* 440: 358-362.

Carlquist, M., Fernandes, R., Helmark, S., Heins, A.-L., Lundin, L., Sørensen, S.J., Gernaey, K.V. & Lantz, A. (2012) Physiological heterogeneities in microbial populations and implications for physical stress tolerance. *Microbial Cell Factories* 11: 94.

Clark, L., Martinez-Argudo, I., Humphrey, T.J. & Jepson, M.A. (2009) GFP plasmid-induced defects in *Salmonella* invasion depend on plasmid architecture, not protein expression. *Microbiology* 155: 461-467.

da Silva, T.L., Piekova, L., Mileu, J. & Roseiro, J.C. (2009) A comparative study using the dual staining flow cytometric protocol applied to *Lactobacillus rhamnosus* and *Bacillus licheniformis* batch cultures. *Enzyme and Microbial Technology* 45: 134-138.

David, F., Berger, A., Hänsch, R., Rohde, M. & Franco-Lara, E. (2011) Single cell analysis applied to antibody fragment production with *Bacillus megaterium*: development of advanced physiology and bioprocess state estimation tools. *Microbial Cell Factories* 10: 23.

Delvigne, F., Brognaux, A., Francis, F., Twizere, J.-C., Gorret, N., Sorensen, S.J. & Thonart, P. (2011) Green fluorescent protein (GFP) leakage from microbial biosensors provides useful information for the evaluation of the scale-down effect. *Biotechnology Journal* 6: 968-978.

Díaz, M., Herrero, M., García, L.A. & Quirós, C. (2010) Application of flow cytometry to industrial microbial bioprocesses. *Biochem. Eng. J.* 48: 385-407.

Dietrich, J.A., McKee, A.E. & Keasling, J.D. (2010) High-throughput metabolic engineering: advances in small-molecule screening and selection. *Annual Review of Biochemistry* 79: 563-590.

Eggeling, L. & Bott, M., (2005) *Handbook of Corynebacterium glutamicum*. Academic Press, Inc., Boca Raton, FL: CRC Press.

Elowitz, M.B., Levine, A.J., Siggia, E.D. & Swain, P.S. (2002) Stochastic gene expression in a single cell. *Science* 297: 1183-1186.

Enfors, S.O., Jahic, M., Rozkov, A., Xu, B., Hecker, M., Jurgen, B., Kruger, E., Schweder, T., Hamer, G., O'Beirne, D., *et al.* (2001) Physiological responses to mixing in large scale bioreactors. *Journal of Biotechnology* 85: 175-185.

Flores, S., de Anda-Herrera, R., Gosset, G. & Bolivar, F.G. (2004) Growth-rate recovery of *Escherichia coli* cultures carrying a multicopy plasmid, by engineering of the pentose-phosphate pathway. *Biotechnology and Bioengineering* 87: 485-494.

Fritzsch, F.S.O., Dusny, C., Frick, O. & Schmid, A. (2012) Single-cell analysis in biotechnology, systems biology, and biocatalysis. *Annual Review of Chemical and Biomolecular Engineering* 3: 129-155.

Gross, L.A., Baird, G.S., Hoffman, R.C., Baldridge, K.K. & Tsien, R.Y. (2000) The structure of the chromophore within DsRed, a red fluorescent protein from coral. *Proceedings of the National Academy of Sciences of the United States of America* 97: 11990-11995.

Grünberger, A., Paczia, N., Probst, C., Schendzielorz, G., Eggeling, L., Noack, S., Wiechert, W. & Kohlheyer, D. (2012) A disposable picolitre bioreactor for cultivation and investigation of industrially relevant bacteria on the single cell level. *Lab on a Chip* 12: 2060.

Grünberger, A., van Ooyen, J., Paczia, N., Rohe, P., Schiendzielorz, G., Eggeling, L., Wiechert, W., Kohlheyer, D. & Noack, S. (2013) Beyond growth rate 0.6: *Corynebacterium glutamicum* cultivated in highly diluted environments. *Biotechnology and Bioengineering* 110: 220-228.

Gulati, S., Rouilly, V., Niu, X., Chappell, J., Kitney, R.I., Edel, J.B., Freemont, P.S. & de Mello, A.J. (2009) Opportunities for microfluidic technologies in synthetic biology. *Journal of The Royal Society Interface* 6: S493-S506.

Heinemann, M. & Zenobi, R. (2011) Single cell metabolomics. *Current Opinion in Biotechnology* 22: 26-31.

Hewitt, C. & Nienow, A. (2007) The scale-up of microbial batch and fed-batch fermentation processes. *Journal of Biotechnology* 131: S134-S135.

Hewitt, C.J. & Nebe-Von-Caron, G. (2001) An industrial application of multiparameter flow cytometry: assessment of cell physiological state and its application to the study of microbial fermentations. *Cytometry* 44: 179-187.

Jehmlich, N., Hübschmann, T., Salazar, M.G., Völker, U., Benndorf, D., Müller, S., von Bergen, M. & Schmidt, F. (2010) Advanced tool for characterization of microbial cultures by combining cytomics and proteomics. *Applied Microbiology and Biotechnology* 88: 575-584.

Kærn, M., Elston, T.C., Blake, W.J. & Collins, J.J. (2005) Stochasticity in gene expression: from theories to phenotypes. *Nature Reviews Genetics* 6: 451-464.

Keilhauer, C., Eggeling, L. & Sahm, H. (1993) Isoleucine synthesis in *Corynebacterium glutamicum* - molecular analysis of the *ilvb-ilvn-ilvc* operon. *Journal of Bacteriology* 175: 5595-5603.

Kensy, F., Zang, E., Faulhammer, C., Tan, R.-K. & Büchs, J. (2009) Validation of a high-throughput fermentation system based on online monitoring of biomass and fluorescence in continuously shaken microtiter plates. *Microbial Cell Factories* 8.

Kinoshita, S., Udaka, S. & Shimono, M. (1957) Studies on the amino acid fermentation: I. Production of L-glutamic acid by various microorganisms. *The Journal of General and Applied Microbiology* 3: 193–205.

Knodler, L.A., Bestor, A., Ma, C.X., Hansen-Wester, I., Hensel, M., Vallance, B.A. & Steele-Mortimer, O. (2005) Cloning vectors and fluorescent proteins can significantly inhibit *Salmonella enterica* virulence in both epithelial cells and macrophages: implications for bacterial pathogenesis studies. *Infection and Immunity* 73: 7027-7031.

Kussell, E. & Leibler, S. (2005) Phenotypic diversity, population growth, and information in fluctuating environments. *Science* 309: 2075-2078.

Lara, A.R., Galindo, E., Ramirez, O.T. & Palomares, L.A. (2006) Living with heterogeneities in bioreactors. *Molecular Biotechnology* 34: 355-381.

Lencastre Fernandes, R., Nierychlo, M., Lundin, L., Pedersen, A.E., Puentes Tellez, P.E., Dutta, A., Carlquist, M., Bolic, A., Schäpper, D., Brunetti, A.C., *et al.* (2011) Experimental methods and modeling techniques for description of cell population heterogeneity. *Biotechnology Advances* 29: 575-599.

Lewis, G., Taylor, I., Nienow, A. & Hewitt, C. (2004) The application of multi-parameter flow cytometry to the study of recombinant *Escherichia coli* batch fermentation processes. *Journal of Industrial Microbiology & Biotechnology* 31.

Liden, G. (2002) Understanding the bioreactor. *Bioprocess and Biosystems Engineering* 24: 273-279.

Lidstrom, M.E. & Konopka, M.C. (2010) The role of physiological heterogeneity in microbial population behavior. *Nature Chemical Biology* 6: 705-712.

Litsanov, B., Kabus, A., Brocker, M. & Bott, M. (2012) Efficient aerobic succinate production from glucose in minimal medium with *Corynebacterium glutamicum*. *Microbial Biotechnology* 5: 116-128.

Locke, J.C.W. & Elowitz, M.B. (2009) Using movies to analyse gene circuit dynamics in single cells. *Nature Reviews Microbiology* 7: 383-392.

Müller, S., Harms, H. & Bley, T. (2010) Origin and analysis of microbial population heterogeneity in bioprocesses. *Current Opinion in Biotechnology* 21: 100-113.

Müller, S. & Hiller, K. (2013) From multi-*omics* to basic structures of biological systems. *Current Opinion in Biotechnology* 24: 1-3.

Müller, S. & Nebe-von-Caron, G. (2010) Functional single-cell analyses: flow cytometry and cell sorting of microbial populations and communities. *Fems Microbiology Reviews* 34: 554-587.

Mustafi, N., Grünberger, A., Kohlheyer, D., Bott, M. & Frunzke, J. (2012) The development and application of a single-cell biosensor for the detection of L-methionine and branched-chain amino acids. *Metabolic engineering* 14: 449-457.

Nebe-von-Caron, G., Stephens, P.J., Hewitt, C.J., Powell, J.R. & Badley, R.A. (2000) Analysis of bacterial function by multi-colour fluorescence flow cytometry and single cell sorting. *Journal of Microbiological Methods* 42: 97-114.

Neumeyer, A., Hübschmann, T., Müller, S. & Frunzke, J. (2013) Monitoring of population dynamics of *Corynebacterium glutamicum* by multiparameter flow cytometry. *Microbial Biotechnology* 6 (2): 157-167.

Niebisch, A. & Bott, M. (2001) Molecular analysis of the cytochrome bc_1-aa_3 branch of the *Corynebacterium glutamicum* respiratory chain containing an unusual diheme cytochrome c_1. *Archives of Microbiology* 175: 282-294.

Radmacher, E., Vaitsikova, A., Burger, U., Krumbach, K., Sahm, H. & Eggeling, L. (2002) Linking central metabolism with increased pathway flux: L-valine accumulation by *Corynebacterium glutamicum*. *Applied and Environmental Microbiology* 68: 2246-2250.

Rang, C., Galen, J.E., Kaper, J.B. & Chao, L. (2003) Fitness cost of the green fluorescent protein in gastrointestinal bacteria. *Canadian Journal of Microbiology* 49: 531-537.

Sambrook, J., MacCallum, P. & Russell, D., (2001) *Molecular cloning: a laboratory manual*. Cold Spring Harbor Laboratory Press, NewYork.

Schäfer, A., Tauch, A., Droste, N., Pühler, A. & Kalinowski, J. (1997) The *Corynebacterium glutamicum cglIM* gene encoding a 5-cytosine methyltransferase enzyme confers a specific DNA methylation pattern in an McrBC-deficient *Escherichia coli* strain. *Gene* 203: 95-101.

Schmid, A., Kortmann, H., Dittrich, P.S. & Blank, L.M. (2010) Chemical and biological single cell analysis. *Current Opinion in Biotechnology* 21: 12-20.

Schreiner, M.E., Fiur, D., Holatkoj, J., Patek, M. & Eikmanns, B.J. (2005) E1 enzyme of the pyruvate dehydrogenase complex in *Corynebactetium glutamicum*: molecular analysis of the gene and phylogenetic aspects. *Journal of Bacteriology* 187: 6005-6018.

Schreiner, M.E., Riedel, C., Holatko, J., Patek, M. & Eikmanns, B.J. (2006) Pyruvate:quinone oxidoreductase in *Corynebacterium glutamicum:* molecular analysis of the *pqo* gene, significance of the enzyme, and phylogenetic aspects. *Journal of Bacteriology* 188: 1341-1350.

Strack, R.L., Hein, B., Bhattacharyya, D., Hell, S.W., Keenan, R.J. & Glick, B.S. (2009) A rapidly maturing far-red derivative of DsRed-Express2 for whole-cell labeling *Biochemistry* 48: 9704-9704.

Szita, N., Polizzi, K., Jaccard, N. & Baganz, F. (2010) Microfluidic approaches for systems and synthetic biology. *Current Opinion in Biotechnology* 21: 517-523.

Takors, R. (2012) Scale-up of microbial processes: impacts, tools and open questions. *Journal of Biotechnology* 160: 3-9.

Tracy, B.P., Gaida, S.M. & Papoutsakis, E.T. (2010) Flow cytometry for bacteria: enabling metabolic engineering, synthetic biology and the elucidation of complex phenotypes. *Current Opinion in Biotechnology* 21: 85-99.

Veening, J.-W., Igoshin, O.A., Eijlander, R.T., Nijland, R., Hamoen, L.W. & Kuipers, O.P. (2008) Transient heterogeneity in extracellular protease production by *Bacillus subtilis*. *Molecular Systems Biology* 4.

Vinuselvi, P., Park, S., Kim, M., Park, J.M., Kim, T. & Lee, S.K. (2011) Microfluidic technologies for synthetic biology. *International Journal of Molecular Sciences* 12: 3576-3593.

Wendisch, V.F., (2007) *Amino acid biosynthesis - pathways, regulation and metabolic engineering*. Microbiol Monographs, Springer-Verlag.

Zhang, F. & Keasling, J. (2011) Biosensors and their applications in microbial metabolic engineering. *Trends in Microbiology* 19: 323-329

Development and application of genetically-encoded biosensors for strain development and single cell analysis of *Corynebacterium glutamicum*

Nurije Mustafi, Michael Bott, and Julia Frunzke*

Institute of Bio- and Geosciences, IBG-1: Biotechnology,
Research Centre Jülich, 52425 Germany

Corresponding author: Dr. Julia Frunzke, Institute of Bio- and Geosciences, IBG-1: Biotechnology, Research Centre Jülich, 52425 Germany. Phone +49 2461 615430. Fax +49 2461 612710. E-mail: j.frunzke@fz-juelich.de

Abstract

Genetically-encoded single cell biosensors have long been used for the detection of pollutants and stress stimuli in the field of microengineering and bioremediation. In industrial microbiology their potential for the detection of various small molecules at single cell resolution and their implementation in strain development and high-throughput (HT) screenings has rarely been exploited so far. However, several recent studies revealed suchlike sensor systems, which transform the production of inconspicuous small molecules into an optical readout (*e.g.* fluorescence), as a powerful tool for single cell quantification of metabolites. Recently, two studies reported on the construction of transcription factor-based biosensors for the intracellular detection of amino acid production in *Corynebacterium glutamicum.* These biosensors were successfully applied for real-time monitoring of metabolite production and were implemented in first HT screenings for the isolation of amino acid producing mutants of *C. glutamicum*. In this chapter we will introduce the general design and characterization of biosensor performance features focusing on sensors based on regulatory circuits. Furthermore, an overview of all currently available *C. glutamicum* biosensors is provided, including several sensors for the detection of amino acids and stress stimuli in single cells. Finally, we introduce the emerging field of applications for metabolite biosensors including flow cytometry-based HT screening approaches and live cell imaging of metabolite production using microfluidic lab-on-a-chip devices. First results, outlined in this chapter, already highlight the great potential of biosensor-driven strain development and single cell analysis and promise the revolution of traditional approaches towards a "bright" future of industrial microbiology.

1. Introduction-Biosensors

Corynebacterium glutamicum, isolated in 1957 due to its capability to secrete L-glutamate, represents nowadays one of the most important platform organisms in industrial biotechnology (Eggeling & Sahm, 1999; Eggeling & Bott, 2005; Burkovski, 2008; Wendisch, 2007; Kinoshita *et al.*, 1957). During the last decades, metabolic engineering of *C. glutamicum* revealed the great potential of this species not only for amino acid production, but also for the production of organic acids, polymer precursors and biofuels (Becker & Wittmann, 2012; Blombach & Eikmanns, 2011; Wieschalka *et al.*, 2012). Traditional ways of strain development include random mutagenesis followed by diverse strategies for selection and screening for the desired traits, or rational approaches involving the targeted alteration of specific genetic elements (Bailey, 1991). The key issue of almost all these approaches is the detection and quantification of the particular metabolite of interest. A readily accessible phenotype, linked to product formation, significantly impacts success and throughput of the respective procedure (Dietrich *et al.*, 2010). This is, however, given only for a minor fraction of small molecules such as, for instance, some antibiotics or carotenoids (Albrecht *et al.*, 2000; An *et al.*, 1991; Azuma *et al.*, 1992). In these cases product formation can be directly observed by the production of a chromophore. The majority of biotechnologically-relevant metabolites are, however, inconspicuous small molecules, which are classically assayed by low-throughput bulk techniques such as liquid or gas chromatography or NMR providing average data for the microbial population. Measurement of metabolite production at single cell resolution is still hardly feasible (Kalisky & Quake, 2011; Leslie, 2011; Müller *et al.*, 2010; Heinemann & Zenobi, 2011).

In this context, the application of biosensors converting metabolite production into an optical readout has the potential to revolutionize the *status quo* of strain development and analysis in the field of biotechnology. During the last ten to twenty years a variety of biosensors based on cellular regulatory elements has been developed, allowing high temporal and spatial resolution of metabolites at the single cell level. Various classifications of biosensors are described and resumed in several excellent reviews (Dietrich *et al.*, 2010; Michener *et al.*, 2012; van der Meer & Belkin, 2010; Zhang & Keasling, 2011). In the following, we would like to highlight especially four different categories of biosensors designs and architecture, namely whole-cell biosensors, biosensors including single enzymes or multistep enzymatic pathways, FRET-based sensors and sensors based on genetic regulatory circuits.

Natural or engineered auxotrophic strains for specific molecules represent whole-cell biosensors providing an easy accessible phenotype: cellular growth (Figure 1A) (Burkholder, 1951; Payne *et al.*, 1977). Several studies addressed this idea and developed whole-cell biosensors by introducing constitutively expressed reporter genes (*e.g. gfp)* into auxotrophic bacterial strains (Chalova *et al.*, 2007; Bertels *et al.*, 2012; Erickson *et al.*, 2000; Kim *et al.*, 2010). This approach enables a direct correlation of reporter output (*e.g.* fluorescence) to the concentration of the molecule of interest in the environment of the sensor strain. The second class of biosensors is based on *in vivo* single- or multistep enzymatic pathways which transform the presence of a colorless molecule of interest into a detectable optical readout of the cell (Figure 1B). In most cases, this is linked to the synthesis of natural chromophores as end or intermediate product of the enzymatic pathway (Bernhardt *et al.*, 2007; de la Pena Mattozzi *et al.*, 2006; Santos & Stephanopoulos, 2007). Here, in contrast to other biosensor constructs, no classical reporter markers (such as fluorescence proteins) are required to access a phenotype for small molecule detection. Despite the successful application of the described biosensors in various studies, several drawbacks remain unsolved. One major bottleneck is the limited versatility of these biosensor constructs. In fact, a rather small

fraction of biological, biotechnological, or medical interesting molecules is essential for cellular growth, represents natural chromophores or can be linked to the synthesis of ones.

A broad spectrum of metabolites is detected *in vivo* by an extensive repertoire of natural sensor devices (*e.g.* riboswitches, RNA-aptamers, transcription factors, enzymes, or periplasmic-binding proteins). Molecular constructs which make use of these biological molecules, linked to the optical readout of fluorescence proteins, represent versatile tools for small molecule detection. One approach to exploit the molecular recognition specificity of several protein classes is the development of FRET-based metabolite sensors. The modular architecture of FRET-sensors consists of an acceptor and a donor domain linked to a pair of fluorescent proteins differing in their emission and excitation wavelengths. Binding of a molecule to the acceptor or sensor domain conducts a conformational change which brings the chromophores of the fluorescence proteins into close proximity and enables Förster (fluorescence) resonance energy transfer (FRET) from the donor chromophore to the acceptor chromophore (Figure 1C). Thus, effector binding can be detected and measured as change in the ratio of the emitted fluorescence intensities. Nowadays, a large diversity of FRET-based sensors is available for imaging of intrinsic and extrinsic conditions, such as pH, redox potential, ATP:ADP ratio, several sugars and metabolites, various ions, kinase activities and many more (Frommer *et al.*, 2009). However, a major drawback of FRET-based sensors is their inherent high sensitivity towards ionic strength and pH, which can significantly influence affinity parameters and fluorescence response of the sensor (Okumoto *et al.*, 2012).

Finally, genetic regulatory circuits have been extensively exploited for the construction of biosensors especially in the field of microengineering and bioremediation (van der Meer, 2010; van der Meer & Belkin, 2010). Classically, the construction of these sensors is based on i) a sensor protein, *e.g.* a transcription factor, ii) a molecular switch which occurs upon ligand binding and results in transcriptional activation of the cognate regulatory DNA element of the transcription factor, and iii) production of a reporter protein (*e.g.* GFP) as sensor readout (Figure 1D) (van der Meer & Belkin, 2010). This type of biosensors has a long tradition in microbial sensing systems for the detection of environmental pollutants (Belkin, 2003; van der Meer & Belkin, 2010; Harms *et al.*, 2006). For example, a biosensor for toluene-based environmental contaminants was developed by putting the *luc* gene for firefly luciferase under the control of the transcriptional activator XylR. In field tests, the sensor was shown to accurately detect the pollutants on deep aquifer water and soil samples with a sensitivity of about 40 µM (Willardson *et al.*, 1998). Despite the versatile applications in the field of chemical compounds and toxicity detection, only a few studies describe the use of transcription factor based biosensors to report on production of industrially important metabolites.

Two recent studies presented the construction of transcription factor-based biosensors for monitoring of amino acid production in *C. glutamicum* (Binder *et al.*, 2012; Mustafi *et al.*, 2012). These studies represent the first examples of the use of genetically-encoded biosensors for this important platform organism and indicate the high potential of this novel approach for strain development, HT screening and single cell analysis. In the following chapter, we provide an overview of the recently developed *C. glutamicum* sensor systems and briefly sketch current efforts on single cell analysis including live cell imaging and flow cytometry-based approaches.

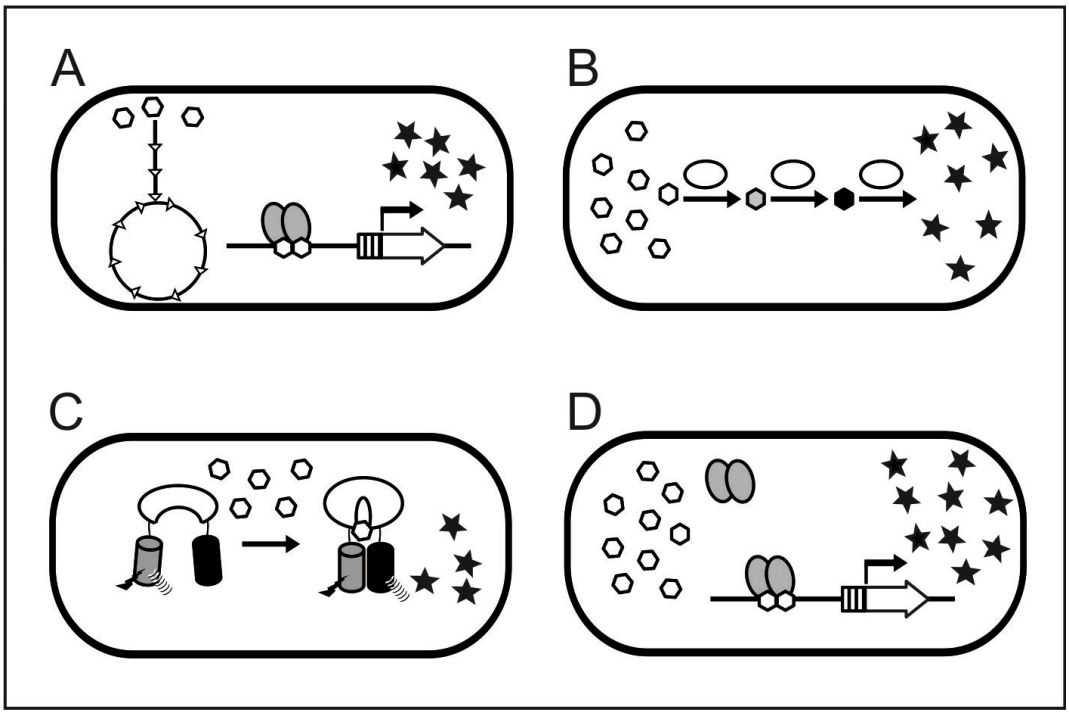

Figure 1. Categories of biosensors design. (A) Cellular growth of auxotrophic whole-cell biosensors reports on the bio-availability of the target molecule**. (B)** In biosensors based on single- or multistep enzyme pathways detection of the target molecule and reporter output is provided through enzymatic activities. **(C)** In FRET-based sensors binding of the target molecule conducts conformational changes of the sensor domain which enables a fluorescence readout by energy transfer from the donor to the acceptor chromophore. **(D)** In sensors based on genetic regulatory circuits the target molecule is detected by a sensor molecule (RNA, DNA or protein) which in turn induces expression of its target gene fused to a reporter gene (adapted from Dietrich *et al.*, 2010).

2. Design of Biosensors Based on Regulatory Circuits

Biosensors based on regulatory circuits essentially consist of a target promoter responsive to a specific stimulus of interest fused to a promoterless reporter protein, which turns the particular response into a measurable output. The input signal can either be recognized by a single sensor protein or RNA or the promoter underlies control from a complex signal transduction network acting as an integral part of the particular cellular response. The latter principle has been successfully applied *e.g.* for the construction of stress-responsive bioreporters (see section 4.2.) (van der Meer & Belkin, 2010).

2.1. Signal integration

In this section, we want to highlight particularly the use of transcription factors as versatile molecular devices to report on small molecule production in *C. glutamicum*. In fact nature provides a variety of appropriate sensor devices in form of transcription factors. Typically, transcriptional regulators undergo a conformational change upon binding of their effector molecules which in turn results in an altered binding affinity of the regulator for its target DNA sequence. Depending on the biosensors final application, the affinity of the sensor element towards its effector molecule is of major importance for assay design. In some cases, however, specificity and/or ligand affinity are not directly suitable for biosensor construction. Here, synthetic biology approaches can be applied to generate variants with

altered specificity or transfer parameters (section 5.1.2.). This has been, for example, demonstrated by the work of Galvao *et al.* who were able to select mutated variants of the transcriptional regulator XylR, sensing toluene in its native form, that are responsive to 2,4-dinitrotoluene (DNT) for the detection of explosives (Galvao *et al.*, 2007). Even sensors with completely new effector specificities can be engineered as proven by the example of AraC, which was switched from a L-arabinose-induced regulator into a mevalonate-responsive protein (Tang & Cirino, 2011). Thus, the multitude of naturally available sensor devices in combination with current achievements in synthetic biology offers a broad, but almost unexploited spectrum of opportunities for biosensor construction.

In order to decrease the rate of false-positives, a positive readout is desirable for the implementation of biosensors in FACS-(fluorescence-activated cell sorting) screenings. This can be easily achieved by setting the expression of the reporter protein under the control of a transcriptional activator. However, the response of a repressor protein can also be easily converted into a positive readout *via* the design of a coupled sensor. Here, the insertion of a strong, non-native repressor and its tightly regulated promoter can be used to invert the signal polarity. A striking example was reported by Ohlendorf *et al.* who inverted the native light-repressed gene expression of the photoreceptor system YF1/FixK by the insertion of the λ phage repressor cI and promoter pR in front of the respective target gene *fixK* (Ohlendorf *et al.*, 2012).

2.2. Promoter fusion

A detailed knowledge of promoter architecture, transcription factor binding sites and translation start is an important prerequisite for successful sensor design. In general the level of reporter gene expression and thus, reporter output can strongly be influenced by transcription and translation initiation rates. Therefore, choosing an adequate type of fusion between target promoter and reporter gene is a further crucial aspect. In general two types of reporter gene fusions can be distinguished: In **transcriptional fusions**, a promoterless reporter gene is fused to the target promoter of the transcription factor. An effective ribosome binding (native or artificial) site is included in the construct (Figure 2A). Thus, reporter output ideally reflects the transcriptional regulation of the target gene. In a **translational fusion**, the promoterless reporter gene is fused in frame to the target gene (first 5-10 codons or even whole open reading frame (orf) and its upstream genomic region (Figure 2B). This design principle is especially of relevance when dealing with the high frequency of leaderless transcripts (approx. 30%) which are present in *C. glutamicum* (Patek, 2005). In these cases, the mRNA completely lacks the binding region of the 16rRNA of the ribosomes, the so called Shine-Dalgarno sequence, which is normally located 5-13 base pairs upstream of the initiation codon in the untranslated mRNA sequence. In leaderless transcripts, as it is the case for example for the mRNA of *brnF* and *lysE* in *C. glutamicum*, the transcriptional start point is either identical with the first nucleotide of the start codon or is located in close proximity (1-3 bases). Regions downstream of the initiation codon were assumed to interact with the 16rRNA of the ribosomes (Moll *et al.*, 2002; Giliberti *et al.*, 2012; Patek, 2005). For this reason, the biosensor constructs of pSenLys and the Lrp-sensor, two recently described *C. glutamicum* sensors (see section 4.1.1. and 4.1.2.), were designed including the upstream promoter region, the first few codons of the respective orf (*lysE* and *brnF*, respectively) and a linker sequence introducing a ribosome binding side in front of the reporter gene *eyfp* (Figure 2C) (Binder *et al.*, 2012; Mustafi *et al.*, 2012).

2.3. Choice of reporter protein

Finally, the construction of a biosensor demands an appropriate reporter protein, that provides an easy measureable signal output and is, ideally, compatible with single cell

analysis (van der Meer & Belkin, 2010). In order to prevent a high background signal, a non-toxic reporter protein should be chosen which is not naturally occurring in the host cell, and which is not interfering with cellular reactions. Several reviews outline the variety of available reporter proteins, their applications and characteristics, their advantages and disadvantages (Hakkila *et al.*, 2002; Daunert *et al.*, 2000; Ghim *et al.*, 2010; Shaner *et al.*, 2005). Classical reporter systems which have been used in numerous promoter studies in *C. glutamicum* are, for example β-galactosidase (Cho *et al.*, 2012) and chloramphenicol acetyltransferase (Vasicova *et al.*, 1999). In recent years, autofluorescent proteins proved in practice as appropriate reporters for monitoring gene expression patterns in *C. glutamicum*. Among others, this has successfully been shown for GFP, CFP, and eYFP in studies of protein localization and interaction with DNA (Donovan *et al.*, 2010; Burmann *et al.*, 2012; Frunzke *et al.*, 2008), protein secretion (Teramoto *et al.*, 2011), and for eYFP and E2-Crimson in biosensors reporting on amino acid production (Binder *et al.*, 2012; Mustafi *et al.*, 2012; Strack *et al.*, 2009). Recently, Hentschel *et al.* described the construction of unstable variants of eYFP and GFP_{uv} by using SsrA-mediated peptide tagging (Hentschel *et al.*, 2012; Keiler, 2008; Andersen *et al.*, 1998). In comparison to the extremely long half-life of native fluorescent proteins (GFP>24 h), the two presented eYFP-variants revealed protein half-lives of 22 and 8 min, respectively. First applications in transient gene expression analysis showed the general suitability of the destabilized eYFP variants for dynamic measurements in *C. glutamicum*.

A drawback of GFP-derived fluorescent reporter proteins is their dependency on molecular oxygen for chromophore maturation as well as time-consuming protein folding. Recently, flavin mononucleotide (FMN)-binding fluorescent proteins (FbFPs) were described as alternative option allowing quantitative real-time *in vivo* assays (Drepper *et al.*, 2007; Drepper *et al.*, 2010). These novel class of reporter proteins exhibits cyan-green fluorescence and does not depend on oxygen for chromophore formation. First proof of principle studies revealed their general suitability for *in vivo* studies in *C. glutamicum* (Nanda and Frunzke, unpublished).

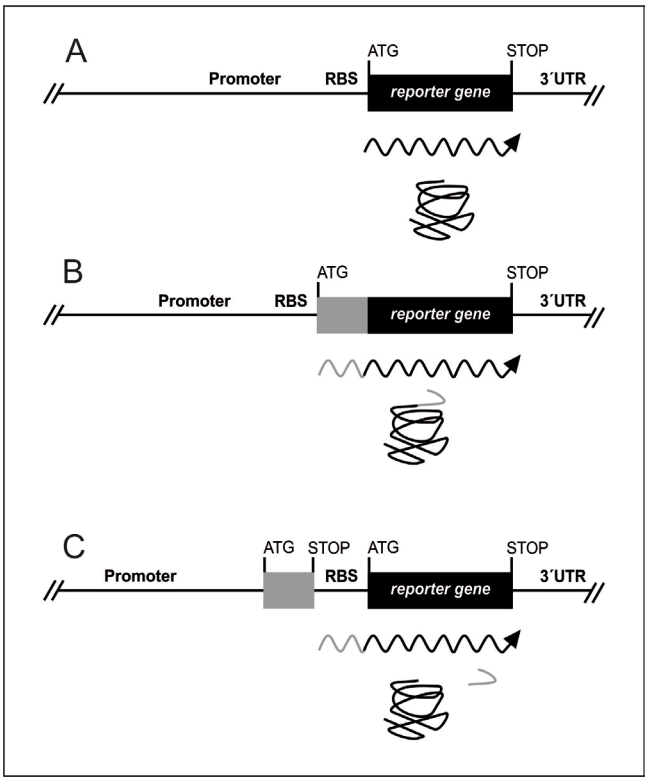

Figure 2. Architecture of reporter gene constructs. (A) Transcriptional fusion of reporter gene and target promoter. **(B)** Translational fusion of reporter (black) and target gene (grey) resulting in the production of hybrid fusion proteins. **(C)** Transcriptional fusion design used for the construction of pSenLys and the Lrp-Sensor, which are based on the leaderless transcripts of *lysE* and *brnF*, respectively.

3. Characterization of Biosensor Performance Parameters

The final application of biosensors for process monitoring or in screening studies requires a detailed understanding and characterization of the sensor performance features. In simple terms, this is represented by an accurate description of the relationship between the effector molecule input and reporter output (*e.g.* fluorescence). This mathematical relationship, termed as transfer function, provides information on the biosensors sensitivity, the dynamic and linear range of detection as well as the detection threshold (Figure 3). The **sensitivity** of a biosensor is described by the rate of increase in reporter output, which is depicted by the slope of the transfer curve within the linear range of detection (see below). The **dynamic range** of a sensor is defined by the maximum fold change of the reporter output resulting from a given sensory input. Furthermore, every sensor construct exhibits a detection window where signal input and sensor output display a linear correlation, the so-called **linear detection range** (Bintu *et al.*, 2005a; Bintu *et al.*, 2005b; Dietrich *et al.*, 2010; Wall *et al.*, 2004; Tabor *et al.* 2009).

A detailed knowledge of the respective biosensor performance parameters is an important prerequisite for assay design since they illustrate the conditions under which the biosensor performs robust and reproducible measurements. In general, biosensor output can be classified as a digital on/off type behavior or an analog-like response. The digital sensor type is characterized by a low detection threshold, a small-linear induction window, a large dynamic range and a high sensitivity. This tight control of response is typical for genetic circuits involved in antibiotic or quorum sensing (Dietrich *et al.*, 2010). One of the most widely used sensors, TetR, represents in its native form a good example for digital response behavior. Lutz and Bujard engineered the already strong target promoter of the TetR repressor by adding further operator sides upstream of the native promoter version. This resulted in a tightly regulated promoter of TetR, showing no expression of target genes when the effector molecule anhydrotetracycline is absent and exhibits an up to ~5000-fold dynamic range (Lutz & Bujard, 1997). In contrast, a low affinity for the effector molecule is often characteristic for an analog-like response showing a sigmoidal function as response to sensory input. Low levels of the effector molecule cause effectively no changes in reporter output signal. Increasing concentrations near the K_D of the sensor-element are responded by a linear increasing output. Through further increasing effector concentrations the sensor is saturated and a constant level of the output signal is reached (Tabor *et al.* 2009). A linear correlation between input and output signal allows discrimination of cells or populations differing in their input concentrations. This performance feature makes analog type biosensors more suitable for applications in screening studies for directed evolution of product yields for example.

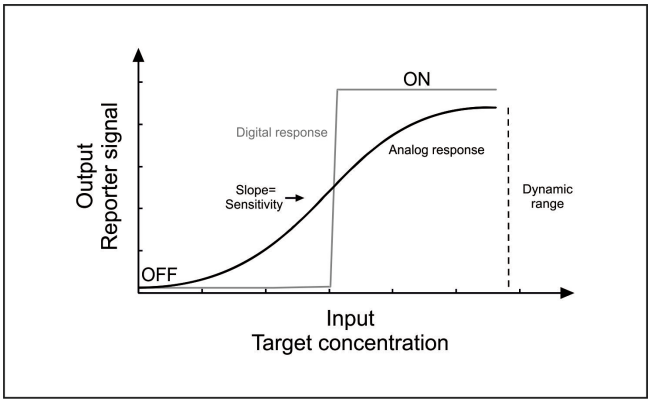

Figure 3. Biosensors transfer curve. The mathematical relationship of biosensors input and output signal provides characteristic information of the biosensor (adapted from Dietrich *et al.*, 2010).

4. Biosensors in *C. glutamicum*

The use of biosensors for process monitoring or strain development in *C. glutamicum* is still in its infancy. In 2012, two publications reporting on construction and application of *C. glutamicum* amino acid biosensors, highlighted the potential of this novel approach for single cell studies and implementation in HT screenings.

4.1. Biosensors for the detection of amino acids

Amino acids represent the most important product class produced at large-scale with *C. glutamicum* and the global market is constantly growing. In the last decades strain development and analysis followed traditional ways in terms of screening, selection and rational engineering. Amino acids are themselves inconspicuous small molecules. Together, these features makes them ideal targets for biosensor design in order to convert product formation into an easily accessible phenotype, which interfaces with FACS HT screenings and allows single cell analysis of populations. Recently, two studies described the development and application of novel single cell biosensors for the detection of several industrially important amino acids, such as L-lysine, L-serine, and L-methionine in *C. glutamicum* (Table 1) (Mustafi *et al.*, 2012; Binder *et al.*, 2012; Burkovski, 2008; Eggeling & Bott, 2005; Ikeda, 2003). The biosensors exploit the exquisite sensitivity of *C. glutamicum* transcriptional regulators as natural sensor devices responding to elevated intracellular concentrations of the respective effector amino acids (Lange *et al.*, 2012; Bellmann *et al.*, 2001).

4.1.1. Basic amino acids

The export of amino acids is usually tightly regulated in order to avoid both wasting of metabolic energy and inhibitory effects of intracellular high amino acid concentrations. The recently described pSenLys biosensor uses the natural specificity and affinity of the *C. glutamicum* transcriptional regulator LysG to report on the production of the basic amino acids, L-lysine, L-histidine, L-arginine and L-citrulline. LysG was shown in previous studies to activate the expression of the *lysE* operon in the presence of increasing levels of the respective effector amino acids (Vrljic *et al.*, 1996). The transporter encoded by this operon, LysE, represents the first amino acid exporter described in literature and was shown to facilitate the specific export of L-lysine and L-arginine (Bellmann *et al.*, 2001). The key features of the LysG-LysE module make it highly suitable for biosensor design ensuring intrinsic molecular recognition specificity combined with appropriate substrate affinity in the low to medium mM range. In general, the sensor module of pSenLys consists of the genomic region encoding the regulator *lysG,* the intergenic region of *lysG* and *lysE* including the regulator binding site, and the first 23 codons of *lysE* fused to *eyfp* (for details on sensor design see section 2.2. and Figure 2C). By this means, eYFP production reflects the transcriptional control of *lysE via* LysG. First proof of principle experiments revealed the general capability of the system to monitor the intracellular accumulation of the basic amino acids L-lysine, L-arginine and L-histidine. For the characterization of pSenLys *C. glutamicum* WT, which does not produce or excrete L-lysine in remarkable concentrations, as well as a set of defined mutant strains varying in their L-lysine productivity (DM1920, DM1919, DM1730, DM1800, and DM1728) were transformed with the plasmid-encoded sensor (Ohnishi *et al.*, 2002). In contrast to the wild type cells, which showed no discernable fluorescence, L-lysine production strains exhibited a significant increase in eYFP fluorescence emission, which correlated with increased extracellular L-lysine concentrations of the respective strains. Remarkably, strain DM1920, which produces comparable amounts of L-lysine to DM1919, displayed a comparatively lower fluorescence signal. In contrast to the other strains, DM1920 harbors two copies of the L-lysine exporter *lysE*, and thus accumulates lower cytosolic L-lysine concentrations due to an increased export. This observation

demonstrates the adjustment of the reporter output due to varying effector input concentrations. The use of production strains differing in their cytosolic L-lysine concentration revealed a dynamic range of pSenLys of about threefold for this particular effector amino acid.

4.1.2. L-methionine and branched-chain amino acids

Lrp represents a further, well-characterized amino acid-sensing transcriptional regulator in *C. glutamicum*, which is therefore also well suitable as sensor device for the design of biosensors (Lange *et al.*, 2012). In response to increasing cytoplasmic concentrations of L-methionine or the branched-chain amino acids, L-leucine, L-isoleucine and L-valine, Lrp activates the expression of the *brnFE* operon, encoding the proton motive force-driven secondary transport system BrnFE involved in export of the respective amino acids (Figure 4A) (Kennerknecht *et al.*, 2002; Trötschel *et al.*, 2005; Lange *et al.*, 2012). For the development of a sensor based on the native Lrp-BrnFE module of *C. glutamicum,* a sensor cassette including *lrp,* the intergenic region of *lrp* and *brnF*, and the first 10 codons of *brnF* fused to *eyfp,* was constructed (see Figure 2C).

As outlined in section 3, biosensor assay design requires a detailed characterization of the relationship between effector input and reporter output. For the characterization of the Lrp-sensor transfer parameters defined intracellular amino acid concentrations were adjusted using the previously well described dipeptide feeding strategy for *C. glutamicum* (Vrljic *et al.*, 1996). The addition of dipeptides (*e.g.* Ala-Met) to the growth medium results in the uptake and subsequent hydrolysis of the dipeptides by cytoplasmic hydrolases and, thus, increases the intracellular concentration of the respective amino acids. To deviate the transfer parameters, the intracellular amino acid concentrations were measured by silicon oil centrifugation and HPLC for all four effector amino acids (Met, Ile, Leu and Val) and set into relation with the maximal reporter output (eYFP fluorescence) (Mustafi *et al.*, 2012). The biosensor revealed highest sensitivity for L-methionine followed by L-leucine, L-isoleucine and L-valine (Figur 4B). No signal was observed for any other amino acid tested. Due to the restrictions in the kinetic properties, the system did not reach saturation. Thus, the presented values reveal only the biosensors minimal dynamic and linear range of detection, which extends from the detection of less than 1 mM up to 25 mM in the case of L-methionine and displays a 78-fold dynamic range for this effector amino acid (Mustafi *et al.*, 2012). In fact, the observed analog-like response of the Lrp biosensor makes it highly suitable for the biosensor-driven optimization of product yields.

To assess the performance of the Lrp-sensor for online monitoring of amino acid formation in production strains, the sensor was tested in the L-valine producer *C. glutamicum* Δ*aceE,* lacking the E1 enzyme of the pyruvate dehydrogenase complex (Blombach *et al.*, 2007). For this purpose cultivations were performed in 48-well microtiter Flowerplates in the BioLector cultivation system (m2p-labs GmbH, Aachen, Germany), enabling the online measurement of growth as backscattered light and fluorescence. Cells transformed with the sensor plasmid displayed fluorescence emission as soon as L-valine production started after consumption of the primary carbon-source acetate (Mustafi *et al.*, 2012). Thus, the biosensor can be applied as convenient device to visualize the course of amino acid production in real-time using *e.g.* microcultivation systems, such as the BioLector or microfluidic chip devices (see below).

4.1.3. L-Serine and *O*-acetyl-L-serine

Besides pSenLys, Binder *et al.* reported on the construction and first proof of principle experiments of further metabolite sensors in *C. glutamicum* (pSenOAS and pSenSer) suitable

for the detection of *O*-acetyl-L-serine and L-serine, respectively (Table 1) (Binder *et al.*, 2012). The pSenOAS sensor exploits the sensitivity of the dual regulator CysR, a member of the ROK family, towards *O*-acetyl-L-serine (OAS) and *O*-acetyl-L-homoserine (OAH). Among several other genes involved in the pathway for assimilatory sulfate reduction in *C. glutamicum,* CysR activates transcription of *cysI*, encoding sulfite reductase, in response to OAS and OAH (Rückert *et al.*, 2008).

The pSenSer sensor is based on the so far not characterized regulatory protein of the LysR superfamily NCgl0581 (cg0702) and its target gene, encoding NCgl0580 (cg0701) a carrier protein with about 40% homology to RhtA (YbiF, b0813), which has been characterized as exporter of L-threonine and L-homoserine in *E. coli* (Livshits *et al.*, 2003; Marin & Krämer, 2007).

4.2. Stress response

Cellular stress responses have long been exploited for the design of bacterial bioreporters used in assays exploring the toxicity or mutagenicity of specific chemicals or to monitor environmental contamination (van der Meer & Belkin, 2010). Many of these systems are directly or indirectly based on the bacterial SOS response, the cellular response to DNA damage conserved throughout all bacterial *phyla* (Storz & Hengge, 2011; Friedberg *et al.*, 2005). Here, the recombination and repair protein RecA functions as a direct sensor for single-stranded DNA, which occurs as a result of DNA damage, and activates autoproteolysis of the central repressor protein LexA. Proteolysis of LexA relieves repression of the SOS regulon, which typically comprises several genes and operons involved in DNA repair, error-prone polymerases, and cell division inhibitor proteins. For the construction of bacterial stress reporters, promoter fusions of prominent SOS genes, such as *recA* itself, *umuC* or *sulA*, and an appropriate reporter protein (*e.g. lacZ* or *gfp*) have been used in several studies. A similar approach has also been applied to assay for spontaneous DNA breakage in *E. coli*, which frequently occurs during DNA replication and is an important cause of genomic rearrangements (Pennington & Rosenberg, 2007).

In recent studies of our lab, aiming at the investigation of single cell dynamics of the SOS response, we analyzed *C. glutamicum* populations containing a plasmid-based or genomically integrated reporter gene fusion of P_{recA} and further SOS target promoters to genes encoding autofluorescent proteins. Flow cytometry analyses and fluorescence microscopy revealed that a fraction of 0.1-0.3% of analyzed single cells exhibited an up to 40-fold higher induction of the SOS response than the main population (Nanda and Frunzke, unpublished). The rate of this spontaneous SOS induction was shown to depend on the growth medium and the particular growth phase of the population. Induced cells exhibited a significantly decreased survival rate (40-60%) when sorted onto agar plates by FACS. Overall, this approach represents a convenient tool to assay for stress response induction and can be applied to optimize cultivation conditions in bioprocesses.

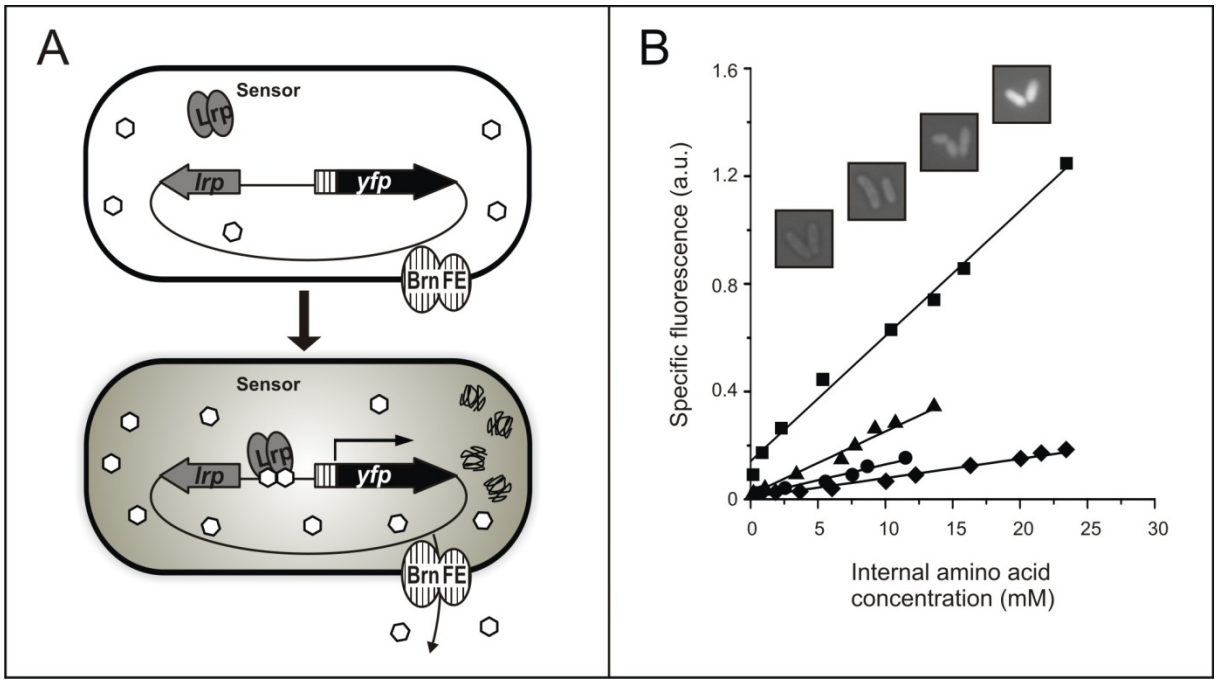

Figure 4. Lrp-biosensor for amino acid detection. (A) A sensor cell with wild type levels of the effector amino acids exhibits background levels of eYFP fluorescence (upper panel). Increased intracellular concentrations of the respective amino acids are sensed by the transcriptional regulator Lrp, which in turn induces *eyfp* expression from the promoter P_{brnF} resulting in fluorescence emission of the sensor cell (lower panel). **(B)** Characterization of the specificity and affinity of the Lrp-biosensor. The transfer curve displays the relationship between intracellular concentration of the effector amino acids L-methionine (■), L-leucine (▲), L-isoleucine (●), and L-valine (♦) and specific fluorescence output. The fluorescence microscopy images show *C. glutamicum* sensor cells with increasing internal concentrations of L-methionine (1-20 mM) (adapted from Mustafi *et al.*, 2012).

Table 1: Overview of *C. glutamicum* biosensors.

Sensor name	Sensor protein	Type of regulator	Targets	Promoter -reporter fusion	Sensi-tivity (n_{app})	Dynamic range (fold increase)	Linear range of detection (mM)	Reference
Lrp-Sensor	Lrp	Lrp-type	L-Met*, L-Ile L-Val, L-Leu	P_{brnF}-*eyfp*	2.6-2	>78	>0.2-23.5	Mustafi *et al.*, 2012
pSenLys	LysG	LysR-type	L-Lys*, L-His, L-Arg	P_{lysE}-*eyfp*	1.6-2	2.6	7.2-12.0	Binder *et al.*, 2012
pSenSer	NCgl 0581	LysR-type	L-Ser	$P_{NCgl0580}$-*eyfp*	n.d.	n.d.	n.d.	Binder *et al.*, 2012
pSenOAS	CysR	ROK-type	*O*-acetyl-L-serine	P_{cysI}-*eyfp*	n.d.	n.d.	n.d.	Binder *et al.*, 2012
SOS sensor	RecA-LexA	LexA repressor	Single-stranded DNA	P_{recA}-*e2-crimson*	n.d.	n.d.	n.d.	Nanda & Frunzke, unpub-lished

* Performance features given in the table refer to the effector amino acid marked with an asterisk.

5. Application of Biosensors in Screening and Single Cell Analysis

In section 4 several genetically-encoded *C. glutamicum* biosensors, which have been developed in recent years, were described. Current efforts aim at the application and evaluation of this type of sensors in strain analysis and development of *C. glutamicum*. The central feature, namely the detection of a particular stimulus of interest (metabolite production, stress response, *etc.*) in single bacterial cells and the conversion thereof into an optical readout opens the way for several new applications, such as:

- Implementation in FACS HT screenings for the isolation of metabolite producing bacteria
- Biosensor-driven enzyme evolution/engineering
- Analysis of the complex phenotypic structure of microbial populations at single cell resolution
- Live cell imaging of metabolite production – the study of single cell dynamics in real-time

The following section summarizes the outcome of first biosensor applications in library screening and single cell analysis of *C. glutamicum*.

5.1. Implementation of biosensors in FACS-based HT screenings

Often the last but crucial step in directed evolution is screening and selection (Dietrich *et al.*, 2010). The success thereof clearly depends on the accessibility of the particular phenotype of interest. However, the majority of biotechnological-relevant molecules and products do not *per se* exhibit a conspicuous phenotype interfacing with HT screening methods. In traditional approaches, gas and liquid chromatography as well as NMR techniques have been ubiquitously applied for small molecule detection and quantification. These techniques are, however, tremendously limited in throughput. Genetically-encoded biosensors can significantly improve screening throughput by converting an inconspicuous phenotype into a screenable output, *e.g.* fluorescence, enabling implementation in FACS HT screenings.

5.1.1. FACS HT screenings based on pSenLys and the Lrp-sensor

The *C. glutamicum* biosensors pSenLys and the Lrp-sensor have both already been applied in first screening approaches aiming at the isolation of amino acid producing mutants (Binder *et al.*, 2012; Mustafi *et al.*, 2012). Due to the activity of the respective biosensors, cells with enhanced cytosolic levels of the effector amino acid could easily be distinguished from cells with wild type level. Experiments testing sensor-based sorting efficiency of the FACS system, revealed a >90% correct sorting efficiency and a survival rate of about 96 and 84% in case of the Lrp-sensor and the pSenLys sensor, respectively. These features allowed the implementation of the sensor systems in FACS HT screenings for amino acid producing cells. Figure 5 provides a schematic overview of the different steps of the biosensor-based HT screen carried out with pSenLys and the Lrp-sensor.

For the generation of genetic diversity, *C. glutamicum* ATCC 13032 carrying a sensor plasmid (either pSenLys or the Lrp-sensor) was mutagenized by treatment with the chemical mutagen MNNG (*N*-methyl-*N'*-nitro-*N*-nitrosoguanidine). Subsequently, the obtained libraries were screened *via* FACS for cells showing a significantly increased fluorescent signal (Figure 5). For pSenLys, the authors introduced an intermediate cultivation step and a second marker protein for screening (E2-crimson) to increase the percentage of viable clones; for details see Binder *et al.* (Binder *et al.*, 2012). As both sensors report exclusively on cytosolic accumulation of the respective amino acids, information with respect to the excretion thereof is not provided. Therefore, a second screen was introduced to measure amino acid

accumulation in the supernatant. This step is crucial in order to discriminate "false positive" clones, which only internally accumulate high concentrations of the amino acids (*e.g.* defects in export), from clones excreting significant amounts of the effector amino acids. Finally, either selected target genes or the whole genome of selected mutants were sequenced to identify novel and unexpected targets for strain development. In the following the results of these first screening attempts are summarized.

The screening approach using pSenLys started with chemically mutagenized *C. glutamicum* wild type and resulted in the isolation of 69% positive mutants (185 of 270 clones analyzed *via* HPLC) accumulating L-lysine in the supernatant after 48 h cultivation in CGXII minimal medium. Re-cultivation of 120 positively tested clones showed L-lysine concentrations ranging from 0.2 to 37 mM. Sequence analysis of selected genes revealed several mutations in *lysC*, of which some were already known to prevent feedback inhibition of aspartate kinase activity. Besides, four new mutations in the regulatory subunit of the aspartate kinase, seven novel mutations in the *hom* gene, encoding the homoserine dehydrogenase and four new mutations in genes coding for L-threonine synthesis, *thrB* and *thrC*, were identified. Whole genome sequencing of selected mutants revealed a novel target gene of particular interest, namely *murE*, encoding UDP-*N*-acetylmuramyl-tripeptide synthetase. This enzyme utilizes the direct precursor of L-lysine D, L-diaminopimelate as substrate and channels it towards cell wall synthesis. Genomic replacement of the *murE* mutation in defined producer strains resulted in a significant increase of L-lysine production, *i.e.* up to 27% in the best producer DM 1933.

The first screening approach using the Lrp-sensor was also started from randomly mutagenized *C. glutamicum* wild type cells. This first attempt resulted in the isolation of 21% (40 of 192 clones) positive clones that produced branched-chain amino acids. Among these the top five mutants produced up to 8 mM L-valine, up to 2 mM of L-leucine and up to 1 mM L-isoleucine after 48 h cultivation in CGXII minimal medium. The conditions chosen for this initial screening obviously favored the isolation of branched-chain amino acid producing mutants. None of the mutants accumulated significant amounts of L-methionine, which is surely a challenging target as it demands sulfur incorporation and precursors from C1-metabolism requiring high energy cost (7 mol ATP and 8 mol NADPH) which makes it the most expensive amino acid for the cell (Neidhardt *et al.*, 1990). As L-methionine is currently of major interest for biotechnological strain development, following experiments aimed at the adaptation of the screen towards the isolation of L-methionine producing mutants. First studies revealed that the outcome of biosensor-based screenings depends on several aspects, including (i) cultivation conditions, (ii) the background strain used for mutagenesis, and (iii) the gating strategy of FACS (Mustafi & Frunzke, unpublished). For this reason mutant libraries based on *C. glutamicum* Δ*mcbR*, lacking the master regulator McbR of L-methionine and L-cysteine biosynthesis in *C. glutamicum* were screened in following studies (Rey *et al.*, 2003). Due to the tight regulation on biosynthesis genes, mediated by McbR, removing transcriptional repression is suggested to be an important prerequisite for the isolation of L-methionine producing mutants. Overall, this screen resulted in 49% (47 of 96 clones) positive clones producing significant amounts of L-methionine (at least twofold more than the parental strain *C. glutamicum* Δ*mcbR*. Among these the top three mutants produced up to 8 mM L-methionine after 48 h cultivation in minimal medium (Mustafi & Frunzke, unpublished).

5.1.2. Further screening applications of single cell biosensors

Further applications of the sensor system to optimize production strains include adaptive laboratory evolution approaches. In the last decades laboratory evolution has proven to be a suitable tool *e.g.* to adapt microorganisms to different environmental conditions as well as to

make them utilize non-native substrates (Portnoy *et al.*, 2011). In this context, the fluorescence readout of sensor cells provides an accessible phenotypic trait which can impose a selective pressure in *e.g.* FACS-based screenings. In suchlike experiments clones with increased productivity compared to the ancestor strain should predominate after several rounds of FACS sorting and re-cultivation.

As mentioned above, the described sensor systems enable the intracellular measurement of amino acid concentrations in *C. glutamicum* cells. This feature can also be of benefit in a screening set up for the identification of novel transport systems. For instance in the case of L-methionine the existence of a second low affinity transport system besides BrnFE has been postulated by Krämer and coworkers in 2005, but it has not been identified to date (Trötschel *et al.*, 2005). Using the sensor system, mutant strains with defects in the export of the particular effector amino acid (*e.g.* mutation of LysE or BrnFE) will accumulate significantly increased internal amounts of the respective amino acids leading to a high fluorescence readout of the sensor. Indeed, detailed characterization of L-lysine producing mutants (n=40) using an expectation maximization algorithm revealed one cluster of mutants exhibiting extreme high fluorescence, but comparatively low L-lysine accumulation (Binder *et al.*, 2012). Targeted isolation of such mutants in screenings might be a promising approach for the identification of novel transport systems for the effector amino acids of the applied sensor.

For production of a specific metabolite of interest, researchers often rely on the performance of heterologously expressed pathways or enzymes. Directed evolution approaches have been used to optimize enzyme activity and specificity of a variety of different enzymes. Most assays are, however, carried out *in vitro* and cannot be adapted for enzyme evolution using whole cells (Arnold & Georgiou, 2003). As metabolite biosensors allow specific detection of small molecules, suchlike sensor systems can also be applied for *in vivo* enzyme evolution. The workflow for such an approach comprises the construction of an enzyme library using *e.g.* error-prone PCR, transformation of sensor cells with the resulting library, and finally FACS screening and validation of obtained variants. A striking example was recently reported by Michener *et al.* who developed a RNA aptamer-based sensor system to screen for improved enzyme activities of caffeine demethylase (Michener & Smolke, 2012). In contrast to conventional direct evolution techniques, this approach allows high throughput analysis of mutant enzyme libraries, where enzyme activity is assayed *in vivo*.

5.2. Biosensor-based single cell analysis

Nowadays, there is increasing evidence that apparent clonal microbial populations display substantial variation in phenotypic traits. This common occurrence of multimodal heterogeneity can originate, for example, from microenvironmental variations, differences in cell age or cell cycle, epigenetic variation or simply stochastic effects in gene expression (Elowitz, 2002; Lidstrom & Konopka, 2010). However, the aspect of population heterogeneity has hardly been studied in industrial productions strains, although inefficient subpopulations within a production culture might have a significant negative impact on the whole bioprocess (Müller *et al.*, 2010). To understand the actual impact of individual cells on population average and heterogeneity the development of novel techniques is required, which enable quantification and real-time monitoring of metabolites at the single cell level (Schmid *et al.*, 2010; Amantonico *et al.*, 2010; Heinemann & Zenobi, 2011; Müller & Hiller, 2012). In this context, the implementation of biosensors capable of detecting molecules with single cell resolution in studies based on flow cytometry, lab-on-a-chip devices, and time-lapse microscopy provides a powerful tool to analyze metabolic productivity differences in individual cells.

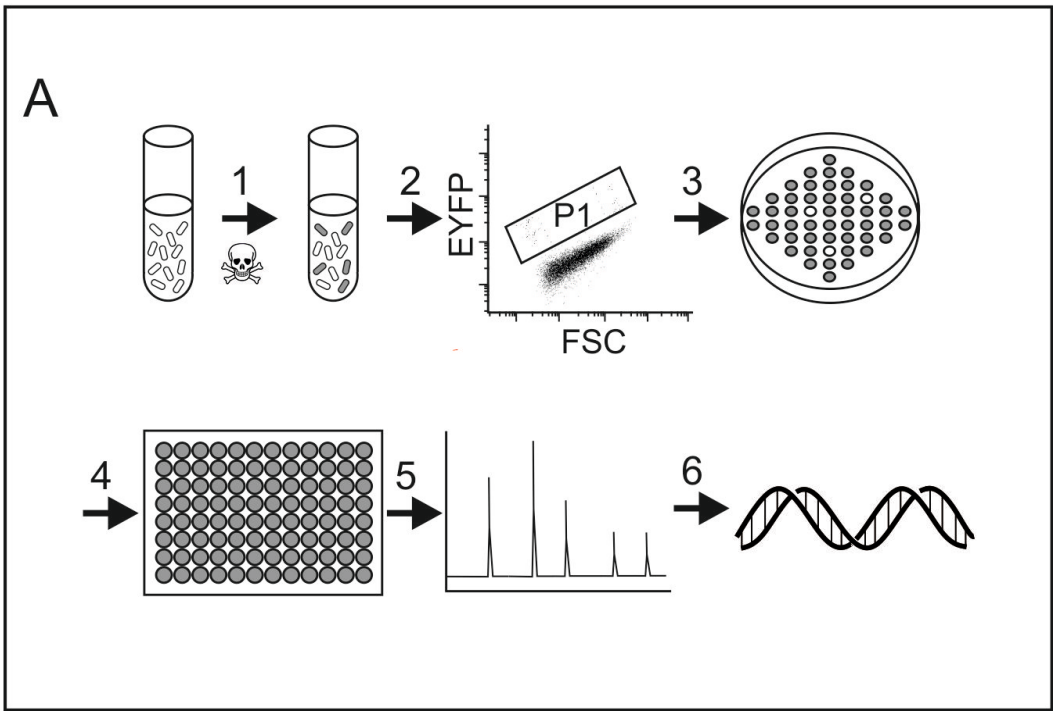

Figure 5. Schematic illustration of flow cytometry and biosensor-based high-throughput screening. (1) Generation of genetic diversity by chemical mutagenesis. (2) Screening of mutant library and isolation of single mutant cells *via* FACS. (3) Sorting of single cells on plates, (4) cultivation in microtiter plates and (5) quantification of external amino acids *via* uHPLC. (6) Genome sequencing for target identification (adapted from Mustafi *et al.*, 2012).

5.2.1. Flow cytometry

In recent years, more and more attention was drawn to the use of flow cytometry as a convenient HT-compatible method allowing the measurement of multiple parameters in a single microbial cell (Tracy *et al.*, 2010; Müller & Nebe-von-Caron, 2010). Parameters which can be assessed by flow cytometry include the cellular scattering properties (indicative for cell size and cellular complexity) as well as every phenotype which can be directly or indirectly linked to a fluorescent output (Müller & Nebe-von-Caron, 2010). For *C. glutamicum* single cell analysis and screening approaches based on flow cytometry have, however, been only used in a few recent studies including the biosensor-based HT screenings performed with pSenLys and the Lrp-sensor (Mustafi *et al.*, 2012; Binder *et al.*, 2012). Recently, Neumeyer *et al.* reported on the use of multiparameter flow cytometry to assess different phenotypic parameters of *C. glutamicum*, such as cell size, cell granularity, DNA content, membrane potential and integrity (Neumeyer *et al.*, 2013). Fluorescent dyes and staining procedures were evaluated regarding their suitability to monitor multiple parameters in *C. glutamicum* populations. Application of these procedures revealed, in fact, phenotypic heterogeneity in terms of viability, membrane potential and growth activity of *C. glutamicum* grown on standard minimal or complex media.

Current efforts aim at the establishment of downstream approaches for the analysis of subpopulations to not only monitor, but, more importantly, understand the molecular basis of the observed phenotypic variation. Müller and coworkers recently described a workflow for combining FACS cell sorting with mass spectrometry based proteomic analysis of subpopulations (Jehmlich *et al.*, 2010; Müller & Hiller, 2012). Current advances in mass

spectrometry and sequencing technologies bring the analysis of small subpopulations or even single cells into reach. Furthermore, a variety of fluorescent dyes and staining protocols is available to assess multiple parameters at single cell resolution. The implementation of metabolite sensing biosensors into this framework will represent a further important step towards a systems level analysis of microbial populations in bioprocesses.

5.2.2. Microscopy and live cell imaging

In contrast to the snapshot analysis provided by flow cytometry, live cell imaging approaches offer the advantage of long term cell observation and analysis during homogenous and well controllable cultivation in microscale environments (Schmid *et al.*, 2010; Szita *et al.*, 2010; Gulati *et al.*, 2009; Locke & Elowitz, 2009). Recently, Grünberger *et al.* reported on the fabrication and implementation of a microfluidic picoliter bioreactor allowing parallel studies of multiple microcolonies growing in a monolayer (Figure 6 A,B) (Grünberger *et al.*, 2012). First studies investigating growth of *C. glutamicum* in these microfluidic devices revealed a 50% higher growth rate of the wild type strain compared to cultivation in shake flasks. Optimal growth conditions, such as continuous medium flow ensuring optimal supply with nutrients and oxygen as well as the removal of secreted by-products, offer an explanation for the observed increase in growth rate of *C. glutamicum* (Dusny *et al.*, 2012; Grünberger *et al.*, 2013).

This experimental setup was used in first live cell imaging studies to monitor L-valine production of *C. glutamicum* Δ*aceE* in real-time (Figure 6C). Therefore, the respective strain was transformed with the Lrp-sensor to study growth and amino acid production at single cell resolution. Live cell imaging of microcolonies (30-40 cells) grown from one single ancestor cell in the abovementioned picoliter bioreactor revealed variations in doubling time, cell size and, most interestingly, single cell fluorescence, suggesting significant cell-to-cell variation with respect to L-valine production (Mustafi *et al.*, 2012). The observed phenotypic heterogeneity within isogenic microcolonies would have hardly been detected in typical shake flask experiments as here L-valine accumulates in the supernatant and thus influences internal L-valine levels. Overall this experimental setup in combination with a genetically-encoded sensor system provided a first glimpse into phenotypic heterogeneity of a *C. glutamicum* strain in terms of growth and metabolite production. Further studies are, however, required to benchmark the use of biosensors for real-time monitoring of metabolite production and to study the influence of sensor expression on the physiology of the particular cell or population.

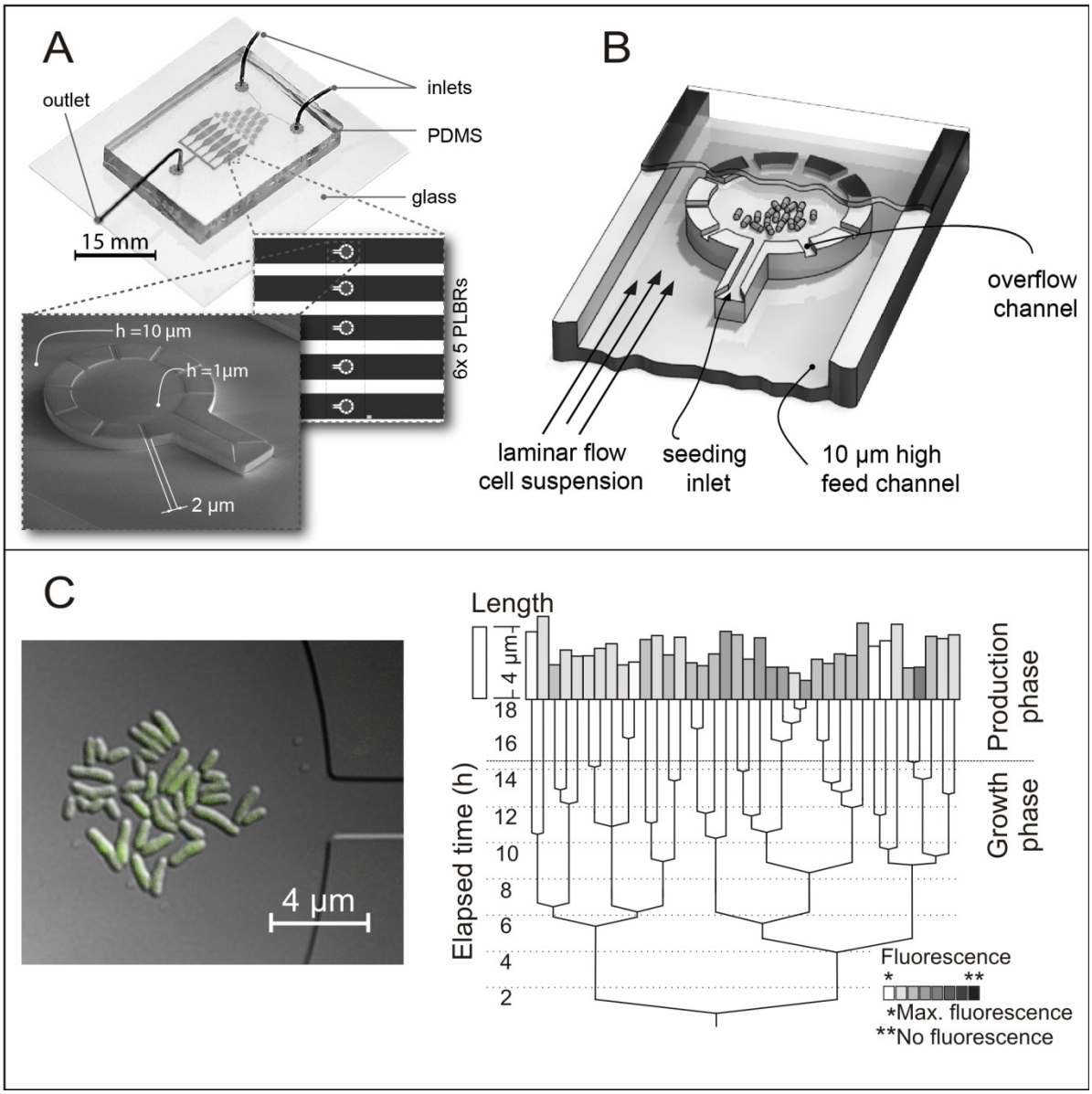

Figure 6. Biosensor-based analysis of production strains in lab-on-a-chip devices. (A) Images showing the fabricated microfluidic chip devices (at the top), zooming into one growth array (in the middle). Scanning electron microscopy image (at the bottom) and **(B)** schematic illustration of a single picoliter bioreactor. **(C)** Microscopic image of an isogenic *C. glutamicum* Δ*aceE* microcolony containing the biosensor and the respective lineage tree, illustrating variation in doubling time, cell size and fluorescence at the single-cell level (adapted from Grünberger *et al.*, 2012 and Mustafi *et al.*, 2012).

6. Future Perspectives and Concluding Remarks

In the last few years the development of biosensors as well as their implementation in HT screenings and single cell analysis, is a rapidly emerging field of research in industrial biotechnology. However, the great potential of biosensors based on regulatory circuits (transcription factors or RNA aptamers) for the detection and quantification of industrial-relevant metabolites has not been exploited so far. First studies reporting on the design of *C. glutamicum* biosensors for the intracellular detection of amino acids already highlighted the impact this novel approach might have on future attempts regarding strain development and bioprocess monitoring. First biosensor-based FACS HT screenings resulted in the isolation of numerous mutant strains producing the respective amino acid of interest. Furthermore, current advances in the development of novel microfluidic devices for live cell imaging allow high resolution insights into phenotypic heterogeneity within clonal populations. However, also several critical issues need to be addressed in future studies: What are the limitations of the system? To which extent impacts the production of fluorescent reporter proteins the physiological state and, thus, the phenotype of the respective cell? Is this approach limited to a few selected success stories or can we believe the promises of synthetic biology that a specific and sensitive sensor system can be developed and adapted for almost every small molecule of interest? Time will tell.

References

Albrecht, M., Takaichi, S., Steiger, S., Wang, Z.Y. & Sandmann, G. (2000) Novel hydroxycarotenoids with improved antioxidative properties produced by gene combination in *Escherichia coli*. *Nature Biotechnology* 18: 843-846.

Amantonico, A., Urban, P.L. & Zenobi, R. (2010) Analytical techniques for single-cell metabolomics: state of the art and trends. *Analytical and Bioanalytical Chemistry* 398: 2493-2504.

An, G.H., Bielich, J., Auerbach, R. & Johnson, E.A. (1991) Isolation and characterization of carotenoid hyperproducing mutants of yeast by flow-cytometry and cell sorting. *Bio-Technology* 9: 70-73.

Andersen, J.B., Sternberg, C., Poulsen, L.K., Bjorn, S.P., Givskov, M. & Molin, S. (1998) New unstable variants of green fluorescent protein for studies of transient gene expression in bacteria. *Applied and Environmental Microbiology* 64: 2240-2246.

Arnold, F.H. & Georgiou, G., (2003) *Directed enzyme evolution: screening and selection methods.* HumanaPress, Totowa, NJ.

Azuma, T., Harrison, G.I. & Demain, A.L. (1992) Isolation of a gramicidin-s hyperproducing strain of *Bacillus brevis* by use of a fluorescence activated cell sorting system. *Applied Microbiology and Biotechnology* 38: 173-178.

Bailey, J.E. (1991) Towards a science of metabolic engineering *Science* 252: 1668-1675.

Becker, J. & Wittmann, C. (2012) Bio-based production of chemicals, materials and fuels - *Corynebacterium glutamicum* as versatile cell factory. *Current Opinion in Biotechnology* 23: 631-640.

Belkin, S. (2003) Microbial whole-cell sensing systems of environmental pollutants. *Current Opinion in Microbiology* 6: 206-212.

Bellmann, A., Vrljic, M., Patek, M., Sahm, H., Krämer, R. & Eggeling, L. (2001) Expression control and specificity of the basic amino acid exporter LysE of *Corynebacterium glutamicum*. *Microbiology-Sgm* 147: 1765-1774.

Bernhardt, P., McCoy, E. & O'Connor, S.E. (2007) Rapid identification of enzyme variants for reengineered alkaloid biosynthesis in periwinkle. *Chemistry & Biology* 14: 888-897.

Bertels, F., Merker, H. & Kost, C. (2012) Design and characterization of auxotrophy-based amino acid biosensors. *Plos One* 7.

Binder, S., Schendzielorz, G., Stäbler, N., Krumbach, K., Hoffmann, K., Bott, M. & Eggeling, L. (2012) A high-throughput approach to identify genomic variants of bacterial metabolite producers at the single-cell level. *Genome Biology* 13: R40.

Bintu, L., Buchler, N.E., Garcia, H.G., Gerland, U., Hwa, T., Kondev, J., Kuhlman, T. & Phillips, R. (2005a) Transcriptional regulation by the numbers: applications. *Current Opinion in Genetics & Development* 15: 125-135.

Bintu, L., Buchler, N.E., Garcia, H.G., Gerland, U., Hwa, T., Kondev, J. & Phillips, R. (2005b) Transcriptional regulation by the numbers: models. *Current Opinion in Genetics & Development* 15: 116-124.

Blombach, B. & Eikmanns, B.J. (2011) Current knowledge on isobutanol production with *Escherichia coli, Bacillus subtilis* and *Corynebacterium glutamicum*. *Bioengineered bugs* 2: 346-350.

Blombach, B., Schreiner, M.E., Holatko, J., Bartek, T., Oldiges, M. & Eikmanns, B.J. (2007) L-valine production with pyruvate dehydrogenase complex-deficient *Corynebacterium glutamicum*. *Applied and Environmental Microbiology* 73: 2079-2084.

Burkholder, P.R. (1951) Determination of vitamin-B12 with a mutant strain of *Escherichia coli*. *Science* 114: 459-460.

Burkovski, A., (2008) *Corynebacteria: genomics and molecular biology*. Caister Academic Press, Norfolk UK.

Burmann, F., Sawant, P. & Bramkamp, M. (2012) Identification of interaction partners of the dynamin-like protein DynA from *Bacillus subtilis*. *Communicative & integrative biology* 5: 362-369.

Chalova, V.I., Kim, W.K., Woodward, C.L. & Ricke, S.C. (2007) Quantification of total and bioavailable lysine in feed protein sources by a whole-cell green fluorescent protein growth-based *Escherichia coli* biosensor. *Applied Microbiology and Biotechnology* 76: 91-99.

Cho, S., Yang, S. & Rhie, H. (2012) The gene encoding the alternative thymidylate synthase ThyX is regulated by sigma factor SigB in *Corynebacterium glutamicum* ATCC 13032. *FEMS Microbiology Letters* 328: 157-165.

Daunert, S., Barrett, G., Feliciano, J.S., Shetty, R.S., Shrestha, S. & Smith-Spencer, W. (2000) Genetically engineered whole-cell sensing systems: Coupling biological recognition with reporter genes. *Chemical Reviews* 100: 2705-2738.

de la Pena Mattozzi, M., Tehara, S.K., Hong, T. & Keasling, J.D. (2006) Mineralization of paraoxon and its use as a sole C and P source by a rationally designed catabolic pathway in *Pseudomonas putida*. *Applied and Environmental Microbiology* 72: 6699-6706.

Dietrich, J.A., McKee, A.E. & Keasling, J.D. (2010) High-throughput metabolic engineering: advances in small-molecule screening and selection. *Annual Review of Biochemistry* 79: 563-590.

Donovan, C., Schwaiger, A., Krämer, R. & Bramkamp, M. (2010) Subcellular localization and characterization of the ParAB system from *Corynebacterium glutamicum*. *Journal of Bacteriology* 192: 3441-3451.

Drepper, T., Eggert, T., Circolone, F., Heck, A., Krauss, U., Guterl, J.-K., Wendorff, M., Losi, A., Gärtner, W. & Jaeger, K.-E. (2007) Reporter proteins for *in vivo* fluorescence without oxygen. *Nature Biotechnology* 25: 443-445.

Drepper, T., Huber, R., Heck, A., Circolone, F., Hillmer, A.-K., Büchs, J. & Jaeger, K.-E. (2010) Flavin mononucleotide-based fluorescent reporter proteins outperform green fluorescent protein-like proteins as quantitative *in vivo* real-time reporters. *Applied and Environmental Microbiology* 76: 5990-5994.

Dusny, C., Fritzsch, F.S.O., Frick, O. & Schmid, A. (2012) Isolated microbial single cells and resulting micropopulations grow faster in controlled environments. *Applied and Environmental Microbiology* 78: 7132-7136.

Eggeling, L. & Bott, M., (2005) *Handbook of Corynebacterium glutamicum*. Academic Press, Inc., Boca Raton, FL: CRC Press.

Eggeling, L. & Sahm, H. (1999) L-Glutamate and L-lysine: traditional products with impetuous developments. *Applied Microbiology and Biotechnology* 52: 146-153.

Elowitz, M.B. (2002) Stochastic gene expression in a single cell. *Science* 297: 1183-1186.

Erickson, A.M., Diaz, I.B.Z., Kwon, Y.M. & Ricke, S.C. (2000) A bioluminescent *Escherichia coli* auxotroph for use in an *in vitro* lysine availability assay. *Journal of Microbiological Methods* 40: 207-212.

Friedberg, E.C., Walker, G.C. & Siede, W., (2005) *DNA repair and mutagenesis*. American Society for Microbiology, Washington, D.C.

Frommer, W.B., Davidson, M.W. & Campbell, R.E. (2009) Genetically encoded biosensors based on engineered fluorescent proteins. *Chemical Society Reviews* 38: 2833.

Frunzke, J., Bramkamp, M., Schweitzer, J.E. & Bott, M. (2008) Population heterogeneity in *Corynebacterium glutamicum* ATCC 13032 caused by prophage CGP3. *Journal of Bacteriology* 190: 5111-5119.

Galvao, T.C., Mencia, M. & de Lorenzo, V. (2007) Emergence of novel functions in transcriptional regulators by regression to stem protein types. *Molecular Microbiology* 65: 907-919.

Ghim, C.-M., Lee, S.K., Takayama, S. & Mitchell, R.J. (2010) The art of reporter proteins in science: past, present and future applications. *Bmb Reports* 43: 451-460.

Giliberti, J., O'Donnell, S., van Etten, W.J. & Janssen, G.R. (2012) A 5 '-terminal phosphate is required for stable ternary complex formation and translation of leaderless mRNA in *Escherichia coli*. *Rna-a Publication of the Rna Society* 18: 508-518.

Grünberger, A., Paczia, N., Probst, C., Schendzielorz, G., Eggeling, L., Noack, S., Wiechert, W. & Kohlheyer, D. (2012) A disposable picolitre bioreactor for cultivation and investigation of industrially relevant bacteria on the single cell level. *Lab on a Chip* 12: 2060.

Grünberger, A., van Ooyen, J., Paczia, N., Rohe, P., Schiendzielorz, G., Eggeling, L., Wiechert, W., Kohlheyer, D. & Noack, S. (2013) Beyond growth rate 0.6:*Corynebacterium glutamicum* cultivated in highly diluted environments. *Biotechnology and Bioengineering* 110: 220-228.

Gulati, S., Rouilly, V., Niu, X., Chappell, J., Kitney, R.I., Edel, J.B., Freemont, P.S. & deMello, A.J. (2009) Opportunities for microfluidic technologies in synthetic biology. *Journal of The Royal Society Interface* 6: S493-S506.

Hakkila, K., Maksimow, M., Karp, M. & Virta, M. (2002) Reporter genes *lucFF, luxCDABE, gfp*, and *dsred* have different characteristics in whole-cell bacterial sensors. *Analytical Biochemistry* 301: 235-242.

Harms, H., Wells, M.C. & van der Meer, J.R. (2006) Whole-cell living biosensors - are they ready for environmental application? *Applied Microbiology and Biotechnology* 70: 273-280.

Heinemann, M. & Zenobi, R. (2011) Single cell metabolomics. *Current Opinion in Biotechnology* 22: 26-31.

Hentschel, E., Will, C., Mustafi, N., Burkovski, A., Rehm, N. & Frunzke, J. (2012) Destabilized eYFP variants for dynamic gene expression studies in *Corynebacterium glutamicum*. *Microbial Biotechnology* 6: 196-201.

Ikeda, M. (2003) Amino acid production processes. *Advances in biochemical engineering/biotechnology* 79: 1-35.

Jehmlich, N., Hübschmann, T., Salazar, M.G., Völker, U., Benndorf, D., Müller, S., von Bergen, M. & Schmidt, F. (2010) Advanced tool for characterization of microbial

cultures by combining cytomics and proteomics. *Applied Microbiology and Biotechnology* 88: 575-584.

Kalisky, T. & Quake, S.R. (2011) Single-cell genomics. *Nature Methods* 8: 311-314.

Keiler, K.C. (2008) Biology of trans-Translation. *Annual Review of Microbiology* 62: 133-151.

Kennerknecht, N., Sahm, H., Yen, M.R., Patek, M., Saier, M.H. & Eggeling, L. (2002) Export of L-isoleucine from *Corynebacterium glutamicum*: a two-gene-encoded member of a new translocator family. *Journal of Bacteriology* 184: 3947-3956.

Kim, M.I., Yu, B.J., Woo, M.-A., Cho, D., Dordick, J.S., Cho, J.H., Choi, B.-O. & Park, H.G. (2010) Multiplexed amino acid array utilizing bioluminescent *Escherichia coli* auxotrophs. *Analytical Chemistry* 82: 4072-4077.

Kinoshita, S., Udaka, S. & Shimono, M. (1957) Studies on the amino acid fermentation: I. Production of L-glutamic acid by various microorganisms. *The Journal of General and Applied Microbiology* 3: 193–205.

Lange, C., Mustafi, N., Frunzke, J., Kennerknecht, N., Wessel, M., Bott, M. & Wendisch, V.F. (2012) Lrp of C*orynebacterium glutamicum* controls expression of the *brnFE* operon encoding the export system for L-methionine and branched-chain amino acids. *Journal of Biotechnology* 158: 231-241.

Leslie, M. (2011) The power of one. *Science* 331: 24-26.

Lidstrom, M.E. & Konopka, M.C. (2010) The role of physiological heterogeneity in microbial population behavior. *Nature Chemical Biology* 6: 705-712.

Livshits, V.A., Zakataeva, N.P., Aleshin, V.V. & Vitushkina, M.V. (2003) Identification and characterization of the new gene *rhtA* involved in threonine and homoserine efflux in *Escherichia coli*. *Research in Microbiology* 154: 123-135.

Locke, J.C.W. & Elowitz, M.B. (2009) Using movies to analyse gene circuit dynamics in single cells. *Nature Reviews Microbiology* 7: 383-392.

Lutz, R. & Bujard, H. (1997) Independent and tight regulation of transcriptional units in *Escherichia coli via* the LacR/O, the TetR/O and AraC/I-1-I-2 regulatory elements. *Nucleic Acids Research* 25: 1203-1210.

Marin, K. & Krämer, R., (2007) Amino acid transport systems in biotechnologically relevant bacteria. In: Amino acid biosynthesis - pathways, regulation and metabolic engineering. Wendisch, V.F. (ed). Microbiol Monographs, Springer-Verlag, pp. 289-325.

Michener, J.K. & Smolke, C.D. (2012) High-throughput enzyme evolution in *Saccharomyces cerevisiae* using a synthetic RNA switch. *Metabolic Engineering* 14: 306-316.

Michener, J.K., Thodey, K., Liang, J.C. & Smolke, C.D. (2012) Applications of genetically-encoded biosensors for the construction and control of biosynthetic pathways. *Metabolic Engineering* 14: 212-222.

Moll, I., Grill, S., Gualerzi, C.O. & Blasi, U. (2002) Leaderless mRNAs in bacteria: surprises in ribosomal recruitment and translational control. *Molecular Microbiology* 43: 239-246.

Müller, S., Harms, H. & Bley, T. (2010) Origin and analysis of microbial population heterogeneity in bioprocesses. *Current Opinion in Biotechnology* 21: 100-113.

Müller, S. & Hiller, K. (2012) From multi-*omics* to basic structures of biological systems. *Current Opinion in Biotechnology*.

Müller, S. & Nebe-von-Caron, G. (2010) Functional single-cell analyses: flow cytometry and cell sorting of microbial populations and communities. *FEMS Microbiology Reviews*.

Mustafi, N., Grünberger, A., Kohlheyer, D., Bott, M. & Frunzke, J. (2012) The development and application of a single-cell biosensor for the detection of L-methionine and branched-chain amino acids. *Metabolic Engineering* 14: 449-457.

Neidhardt, F.C., Ingraham, J.L. & Schaechter, M., (1990) Physiology of the bacterial cell: a molecular approach. In.: Sinauer Associates, Sunderland, MA, pp. 507.

Neumeyer, A., Hübschmann, T., Müller, S. & Frunzke, J. (2013) Monitoring of population dynamics of *Corynebacterium glutamicum* by multiparameter flow cytometry. *Microbial Biotechnology* 6 (2): 157-167.

Ohlendorf, R., Vidavski, R.R., Eldar, A., Moffat, K. & Möglich, A. (2012) From dusk till dawn: one-plasmid systems for light-regulated gene expression. *Journal of Molecular Biology* 416: 534-542.

Ohnishi, J., Mitsuhashi, S., Hayashi, M., Ando, S., Yokoi, H., Ochiai, K. & Ikeda, M. (2002) A novel methodology employing *Corynebacterium glutamicum* genome information to generate a new L-lysine-producing mutant. *Applied Microbiology and Biotechnology* 58: 217-223.

Okumoto, S., Jones, A. & Frommer, W.B., (2012) Quantitative imaging with fluorescent biosensors. In: Annual Review of Plant Biology, Vol 63. Merchant, S.S. (ed). Palo Alto: Annual Reviews, pp. 663-706.

Patek, M., (2005) Regulation of gene expression. In: Handbook of *Corynebacterium glutamicum.* Academic Press, Inc., Boca Raton, FL: CRC Press, pp. 81-98.

Payne, J.W., Bell, G. & Higgins, C.F. (1977) Use of an *Escherichia coli* lys-auxotroph to assay nutritionally available lysine in biological-materials. *Journal of Applied Bacteriology* 42: 165-177.

Pennington, J.M. & Rosenberg, S.M. (2007) Spontaneous DNA breakage in single living *Escherichia coli* cells (vol 39, pg 797, 2007). *Nature Genetics* 39: 1174-1174.

Portnoy, V.A., Bezdan, D. & Zengler, K. (2011) Adaptive laboratory evolution—harnessing the power of biology for metabolic engineering. *Current Opinion in Biotechnology* 22: 590-594.

Rey, D.A., Pühler, A. & Kalinowski, J. (2003) The putative transcriptional repressor McbR, member of the TetR-family, is involved in the regulation of the metabolic network directing the synthesis of sulfur containing amino acids in *Corynebacterium glutamicum*. *Journal of Biotechnology* 103: 51-65.

Rückert, C., Milse, J., Albersmeier, A., Koch, D.J., Pühler, A. & Kalinowski, J. (2008) The dual transcriptional regulator CysR in *Corynebacterium glutamicum* ATCC 13032 controls a subset of genes of the McbR regulon in response to the availability of sulphide acceptor molecules. *BMC Genomics* 9: 483.

Santos, C.N.S. & Stephanopoulos, G. (2007) Melanin-based high-throughput screen for L-tyrosine production in *Escherichia coli*. *Applied and Environmental Microbiology* 74: 1190-1197.

Schmid, A., Kortmann, H., Dittrich, P.S. & Blank, L.M. (2010) Chemical and biological single cell analysis. *Current Opinion in Biotechnology* 21: 12-20.

Shaner, N.C., Steinbach, P.A. & Tsien, R.Y. (2005) A guide to choosing fluorescent proteins. *Nature Methods* 2: 905-909.

Storz, G. & Hengge, R., (2011) *Bacterial stress responses, 2nd edition.* American Society for Microbiology, Washington, D.C.

Strack, R.L., Hein, B., Bhattacharyya, D., Hell, S.W., Keenan, R.J. & Glick, B.S. (2009) A rapidly maturing far-red derivative of DsRed-Express2 for whole-cell labeling *Biochemistry* 48: 9704-9704.

Szita, N., Polizzi, K., Jaccard, N. & Baganz, F. (2010) Microfluidic approaches for systems and synthetic biology. *Current Opinion in Biotechnology* 21: 517-523.

Tabor, J.J., Groban, E.S. & Voigt, C.A. (2009) Performance characteristics for sensors and circuits used to program *E. coli.* In: Systems biology and biotechnology of *Escherichia coli.* New York: Springer, pp. pp. 402–433.

Tang, S.-Y. & Cirino, P.C. (2011) Design and application of a mevalonate-responsive regulatory protein. *Angewandte Chemie-International Edition* 50: 1084-1086.

Teramoto, H., Watanabe, K., Suzuki, N., Inui, M. & Yukawa, H. (2011) High yield secretion of heterologous proteins in *Corynebacterium glutamicum* using its own Tat-type signal sequence. *Applied Microbiology and Biotechnology* 91: 677-687.

Tracy, B.P., Gaida, S.M. & Papoutsakis, E.T. (2010) Flow cytometry for bacteria: enabling metabolic engineering, synthetic biology and the elucidation of complex phenotypes. *Current Opinion in Biotechnology* 21: 85-99.

Trötschel, C., Deutenberg, D., Bathe, B., Burkovski, A. & Krämer, R. (2005) Characterization of methionine export in *Corynebacterium glutamicum*. *Journal of Bacteriology* 187: 3786-3794.

van der Meer, J.R., (2010) *Bacterial sensors: synthetic design and application principles*. Morgan & Claypool, UK.

van der Meer, J.R. & Belkin, S. (2010) Where microbiology meets microengineering: design and applications of reporter bacteria. *Nature Reviews Microbiology* 8: 511-522.

Vasicova, P., Patek, M., Nesvera, J., Sahm, H. & Eikmanns, B. (1999) Analysis of the *Corynebacterium glutamicum dapA* promoter. *Journal of Bacteriology* 181: 6188-6191.

Vrljic, M., Sahm, H. & Eggeling, L. (1996) A new type of transporter with a new type of cellular function: L-lysine export from *Corynebacterium glutamicum*. *Molecular Microbiology* 22: 815-826.

Wall, M.E., Hlavacek, W.S. & Savageau, M.A. (2004) Design of gene circuits: lessons from bacteria. *Nature Reviews Genetics* 5: 34-42.

Wendisch, V.F., (2007) *Amino acid biosynthesis - pathways, regulation and metabolic engineering*. Microbiol Monographs, Springer-Verlag.

Wieschalka, S., Blombach, B., Bott, M. & Eikmanns, B.J. (2012) Bio-based production of organic acids with *Corynebacterium glutamicum*. *Microbial Biotechnology* 6 (2): 87-102.

Willardson, B.M., Wilkins, J.F., Rand, T.A., Schupp, J.M., Hill, K.K., Keim, P. & Jackson, P.J. (1998) Development and testing of a bacterial biosensor for toluene-based environmental contaminants. *Applied and Environmental Microbiology* 64: 1006-1012.

Zhang, F. & Keasling, J. (2011) Biosensors and their applications in microbial metabolic engineering. *Trends in Microbiology* 19: 323-329.

4 Discussion

Nowadays, *C. glutamicum* due to its high capacity for amino acid production represents one of the most important platform organisms in industrial biotechnology. Amino acids are inconspicuous small molecules, thus, screening for their production demands on appropriate selection strategies. In the present work, the sensitivity of the transcriptional regulator Lrp of *C. glutamicum* was exploited for the development of a genetically-encoded single cell biosensor capable of converting amino acid formation into an easily accessible phenotype, *i.e.* fluorescence readout. Lrp activates the expression of the *brnFE* operon encoding the exporter for branched-chain amino acids and L-methionine, in response to increasing cytoplasmic concentrations of L-methionine or the branched-chain amino acids, L-leucine, L-isoleucine and L-valine (Kennerknecht *et al.*, 2002; Trötschel *et al.*, 2005; Lange *et al.*, 2012). The biosensors specificity towards the effector amino acids and its sensitivity in the low to medium mM range allows to distinguish easily between cells with wild type-levels from cells with enhanced cytosolic levels of L-methionine and branched-chain amino acids. These features present the Lrp-biosensor as valuable tool for implementation in novel screening approaches for amino acid producing strains.

4.1. Implementation of the Lrp-biosensor in FACS-based HT screenings

Nowadays, a major drawback in strain development is the typically low-throughput of analytical techniques applied for product detection and quantification, *e.g.* chromatography and mass spectrometry methods. Screening strategies based on flow cytometry allow for high-throughput (HT) single cell analysis of large populations (up to 80.000 cells *per* second) and thus, can notably improve screening efficiency since no individual cultivation step for each clone is required and interesting clones can directly be identified and isolated (Dietrich *et al.*, 2010; Brehm-Stecher & Johnson, 2004). However, this demands on an easily accessible phenotype while the majority of biotechnological interesting metabolites are represented by small, inconspicuous molecules. Genetically-encoded single cell biosensors offer the advantage to transform information about a specific metabolite into a fluorescence readout which interfaces with FACS-(fluorescence-activated cell sorting) based high-throughput (HT) screenings.

In this work, we implemented the Lrp-biosensor in FACS-based screening approaches for the isolation of amino acid producing strains. In first screenings, mutant libraries of chemically

mutagenized *C. glutamicum* wild type cells carrying the Lrp-sensor were screened *via* FACS for cells showing a significantly increased fluorescent signal. In a subsequent screen, amino acid concentrations were determined in the supernatant of positively screened mutants *via* uHPLC to discriminate "false positive" clones, which accumulated exclusively internal high concentrations of the effector amino acids (*e.g.* defects in export). Finally, selected genes of interesting mutants were sequenced to identify novel and unexpected targets for strain development.

The first screening approach using the Lrp-sensor resulted in the isolation of 20% positive clones that produced branched-chain amino acids. Application of a gating strategy based on fluorescence properties of the mutant library revealed a clear pattern: populations exhibiting higher fluorescence showed a comparatively higher number of positive clones excreting the effector amino acids in higher concentration levels. Overall, the top five mutants produced up to 8 mM L-valine, up to 2 mM of L-leucine and up to 1 mM L-isoleucine after 48 h cultivation in CGXII minimal medium. Since biosynthesis of the branched-chain amino acids is closely linked and shares the same enzymes in *C. glutamicum* (Patek, 2007), namely acetohydroxyacid synthase (*ilvBN*), acetohydroxyacid isomeroreductase (*ilvC*), dihydroxyacid dehydratase (*ilvD*), and transaminase B (*ilvE*), the respective genes were sequenced in the top five mutants revealing mutations in *ilvD* (*ilvD*^{G528D}) and *ilvN* (*ilvN*^{S311F}). To analyze the actual impact of these mutations on synthesis of branched-chain amino acids, re-introduction into the wild type chromosome is required. We further analyzed pyruvate dehydrogenase complex (PDHC) activity, which is crucial for the production of L-valine in *C. glutamicum* (Blombach *et al.*, 2007). Two of the top five mutants showed a decreased PDHC activity, however, sequencing of *aceE*, encoding the Ep1 subunit of PDHC, revealed wild type situation in all of the top five mutants. Yet, reduced PDHC activity might be caused by an impaired supply of the cofactors thiamine pyrophosphate, lipoic acid, FAD, CoA, NAD^+ and Mg^{2+} or mutations in genes encoding regulatory proteins (Blombach *et al.*, 2009; Schreiner *et al.*, 2005; Reed, 1974; Yeaman, 1989).

For chemical mutagenesis, we used the alkylating agent MNNG, which has often been used as the mutagen of choice in previous studies, as it is described to offer the highest possible frequency of mutants *per* survivor (Baltz, 1986). However, chemical mutagenesis based on alkylating agents or base analogs induces mainly point mutations with favored single-base substitutions, for example, MNNG induces preferentially GC→AT transitions and, to a minor extent, AT → GC transitions, as shown for several organisms including *C. glutamicum*

(Ohnishi *et al.*, 2008; Wang *et al.*, 1996; Gee *et al.*, 1994). In order to expand the spectrum of mutations, alternatives as transposon-based mutagenesis or physical mutagenesis, *e.g.* UV-rays, X- or γ-rays can be applied. The commonly used UV-light mutagenesis mainly induces pyrimidine diamerization resulting in AT→GC transition. Ionizing radiation based on X- or γ-rays often causes deletions and genomic rearrangements due to occurring breaks of the DNA strand (Parekh *et al.*, 2000). Complete gene inactivation can also be induced using transposon-based mutagenesis. Moreover, random integration of transposable and insertion (IS) elements in the genome can result in altered gene expression. While chemically or UV-based mutagenesis mainly causes amino acid substitutions which can result in altered activity of interesting enzymes for biosynthesis of target metabolites, *e.g.* reduction of feedback resistance, inactivation of entire genes can reveal unknown obstacles in metabolic pathways. Thus, extension of mutant libraries by the abovementioned techniques would be a promising approach to cover a wide range of potential modifications in biosensor-based screenings aiming for the isolation of amino acid producing mutants.

Transposon-mutant libraries of *C. glutamicum* have been successfully screened to identify amino acid transporters in previous studies. However, isolation of the respective mutants relied on time-consuming screening strategies, where growth analysis was performed of every single mutant in presence of dipeptides containing the interesting amino acid (Kennerknecht *et al.*, 2002; Simic *et al.*, 2001). Implementation of the biosensor in a FACS-based screening set up for the identification of novel transport systems would significantly increase throughput of such an approach. Inactivation of the respective export systems by integration of a transposon will cause internal accumulation of the effector amino acid, which can be displayed by enhanced fluorescence emission of the biosensor. For instance, the Lrp-sensor can be used to screen for the second low affinity transport system of L-methionine in *C. glutamicum* which has been postulated in studies in the group of R. Krämer during their work on BrnFE (Trötschel *et al.*, 2005).

Due to the biosensors wide versatility (Figure 4), further interesting applications include *e.g.* adaptive laboratory evolution approaches. Laboratory evolution has proven to be a straight forward approach for strain development as it allows microorganisms to adapt to different environmental conditions or to make them utilize non-native substrates (Portnoy *et al.*, 2011). The implementation of a biosensor reporting on single cell productivity *via* fluorescence emission in such an approach can exert a selective pressure on the cells in *e.g.* FACS-based screenings. Iterative cultivation and screening of the cells should finally yield clones with

increased productivity compared to the ancestor strain. In contrast to rational engineering or random mutagenesis, this approach allows for the occurrence of non-intuitive and spontaneous mutations without the accumulation of undesired mutations with negative impact.

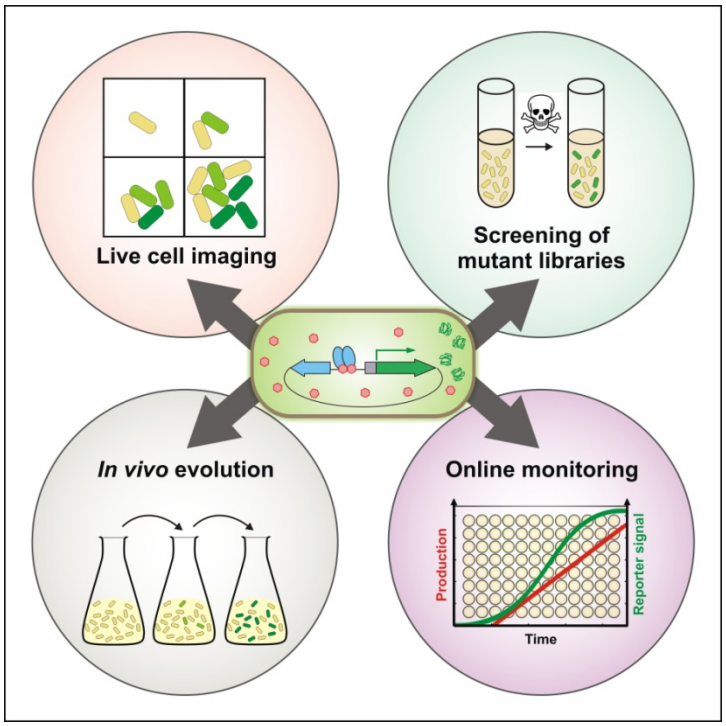

Figure 4. Versatile application of biosensor in live cell imaging studies of metabolite production, screening of mutant libraries, *in vivo* evolution approaches and online monitoring of product formation.

4.2. Towards L-methionine overproduction

The worldwide growing demand for amino acids is forecasted to reach a global market of US$11.6 billion by the year 2015 (Global Industry Analysts, 2012). The major market is represented by the animal feed sector, where the essential amino acids, in particular L-lysine, L-methionine, L-threonine, and L-tryptophan are provided as feed additives. Current research activities focus on the establishment of a biotechnological production process for L-methionine, which in contrast to all other large-scale produced amino acids is still produced on petrochemical basis. Several studies aiming at fermentation-based production of L-methionine indicate some progress at lab-scale, nevertheless, the desired success of a L-methionine overproducing strain was not yet obtained (Kumar & Gomes, 2005).

In this work we applied the Lrp-sensor based FACS HT screening approach to search in particular for *C. glutamicum* mutants accumulating L-methionine. The initial screen starting

from the wild type obviously favored the isolation of branched-chain amino acids producing mutants, since no L-methionine accumulating mutants were obtained. Thus, we used in following screenings *C. glutamicum* strains as parental background, which already harbored genetic modifications assumed to be beneficial for L-methionine production. The manipulations included deletions of *metP* and *metQNI* encoding the importer systems in order to prevent reuptake of excreted L-methionine as well as deletion of *mcbR* coding for the repressor of stringently regulated L-methionine biosynthesis genes (Rey *et al.*, 2003; Trötschel *et al.*, 2008). In addition, media composition for cultivation of the mutants was altered by providing alternative sulfur sources to reduce the high NADPH demand of the cells for reduction of sulfate, normally used as S-source in minimal medium.

On the whole, the screening approach originating from *C. glutamicum* Δ*mcbR* resulted in the best achievements. In total, about 50% positive clones were obtained, which produced at least twice as much L-methionine as the parental strain *C. glutamicum* Δ*mcbR*. Among these the top three mutants produced up to 8 mM L-methionine after 48 h cultivation in minimal medium. Whole genome sequencing of the best producing mutants (six mutants in total) revealed several mutations in genes of terminal L-methionine biosynthesis as well as pathways supplying building blocks, precursors (C_1- and sulfur metabolism), and redox power (pentose phosphate pathway). Additionally, mutations in genes were found coding for the L-methionine export system BrnFE, as well as for the transcriptional regulators involved in sulfonate utilization, SsuR, and sulfate reduction, CysR (Koch *et al.*, 2005; Rückert *et al.*, 2008; Trötschel *et al.*, 2005).

In general, the stringent transcriptional regulation of genes involved in sulfur metabolism makes overproduction of L-methionine difficult in *C. glutamicum*. Hence, identified mutations in two of the three described regulators of sulfur metabolism (SsuR, CysR, McbR) represent an interesting target for future analysis. Transcription of *cysR* and *ssuR* is repressed by the master regulator McbR. In turn, CysR binding to target genes is regulated by the availability of *O*-acetyl-L-serine (OAS) and *O*-acetyl-L-homoserine (OAH), which represent acceptor molecules for sulfide. Thus, the CysR-activated pathway for the reduction of sulfate to sulfide is only initiated, when sulfide can be incorporated *via* OAS and OAH into L-cysteine and homocysteine. Mutations in regulatory domains of CysR might alter binding affinities of this regulator towards its effector molecules or towards the DNA in the promoter of the target genes. Generally, increased expression of the CysR regulon might result in an enhanced availability of reduced sulfide, which finally could be incorporated in L-methionine

biosynthesis (Rückert *et al.*, 2008). In this context, identified mutations in *cysH* encoding an adenosine phosphosulfate reductase, involved in reduction of sulfate to sulfite and in *fpr2* encoding a potential NADP(+)–ferredoxin reductase, described to be involved in reduction of sulfite to sulfide, might contribute to enhanced sulfide formation (Rückert & Kalinowski, 2008). Transcriptional activation of the SsuR regulon is inhibited by sulfate and to a minor extent by adenosine 5′-phosphosulfate, sulfite, and sulfide. Hence, SsuR-dependent sulfonate uptake and utilization is strictly controlled by the concentrations of inorganic sulfur compounds in the cell. Again, mutations in the SsuR regulator and identified mutations in *seuA* and *seuC*, encoding FMNH2-dependent monooxygenases involved in sulfonate ester utilization (Koch *et al.*, 2005; Krömer *et al.*, 2008), could impact supply with sulfide, thus, being beneficial for L-methionine overproduction. No mutations were found in the *mcbR* gene or in identified binding sites of McbR target genes. However, promoter regions of the SsuR and CysR regulon were not analyzed so far.

Interestingly, a mutation in *metH* coding for the vitamin B_{12}-dependent methionine synthase was identified. Methylation of L-homocysteine to yield L-methionine is regarded as a limiting step in *C. glutamicum* (Krömer *et al.*, 2005). In contrast to all other enzymes of the terminal pathway of L-methionine biosynthesis (MetX, MetY, MetB, MetC), no feedback inhibition has been described for MetH as well as for the second methionine synthase MetE (vitamin B_{12}-independent). So far, only transcriptional regulation of *metH* and *metE* by McbR is reported. Thus, mutations in MetH could reduce currently unknown inhibition of this enzyme and enhance methylation rate of L-homocysteine. Systematic investigation of the described mutations in future studies, including transcriptome analysis and reintegration into the parental strain *C. glutamicum* Δ*mcbR*, will show the actual impact of the identified mutations on L-methionine synthesis.

As mentioned before the major bottleneck for efficient overproduction in *C. glutamicum* is represented by the tight repression of L-methionine biosynthesis genes. Therefore, deletion of *mcbR* is considered as prerequisite in the development of a L-methionine production strain. However, detailed metabolome analysis in the *C. glutamicum mcbR* deletion strain revealed no increased production of L-methionine, although all intermediates of the L-methionine pathway showed enhanced concentrations compared to levels in the wild type (Krömer *et al.*, 2005). Overall, deletion of *mcbR* was shown to severely affect growth and biomass yield of the particular strain. This might be caused by the derepressed/induced expression of sulfite reductase (*cysI*) which is a likely candidate for generating reactive oxygen species, thus,

inducing oxidative stress in the cell (Krömer *et al.*, 2008). Further, genetic modification of the *mcbR* deletion mutant are complicated (C. Rückert, personal communication), thus making construction of a *C. glutamicum* Δ*mcbR* based L-methionine production strain difficult. In order to circumvent a *mcbR* knockout mutant, binding sides within the promoter region of particular target genes could be modified or deleted.

Besides the exploitation of *C. glutamicum* for successful overproduction of L-lysine, L-leucine, L-isoleucine, and L-threonine, *E. coli* proved as competitive microbial producer for overproduction of amino acids of the L-aspartate family (Park & Lee, 2010). In the case of L-methionine production, metabolic pathway investigations based on elementary flux mode analysis revealed an even higher theoretical, optimal yield of *E. coli* 0.52 (C-mol) $(C\text{-mol})^{-1}$ compared to *C. glutamicum* 0.49 (C-mol) $(C\text{-mol})^{-1}$ (Krömer *et al.*, 2006). The reasons for the higher potential productivity of *E. coli* are assumed to be linked to NADPH generation and demand. Although *C. glutamicum* and *E. coli* require similar amounts of NADPH *per* mol L-methionine synthesis (8 mol and 8.5 mol, respectively), the generation of methyl-tetrahydrofolate, which provides the C_5-methyl group for methylation of L-homocysteine, demands a twofold reduced NADPH amount in *E. coli*. Furthermore, *E. coli* possesses a membrane-bound transhydrogenase for generation of additional NADPH, which is not present in *C. glutamicum* (Krömer *et al.*, 2008). Taken this into account, future work should include screenings of *E. coli* mutant libraries for isolation of L-methionine producing mutants. This, however, demands the development of a suitable biosensor for this organism, since the Lrp-biosensor was not functional in *E. coli.* For the design of a suchlike biosensor, native regulatory devices of *E. coli* or related Gram-negative species sensitive to L-methionine could be integrated, such as MdeR, a member of the leucine-responsive regulator protein (Lrp) family which was shown to activate expression of genes involved in the degradative metabolism of L-methionine in *Pseudomonas putida* (Inoue *et al.*, 1997). Alternatively, the use of *E. coli* specific promoter sequences and/or ribosome binding sides as well as the adaption of the codon usage could improve transcription and translation efficiency of the Lrp-sensor in *E. coli*, thus, making the biosensor compatible for amino acid detection in this organism.

Taken as a whole, the presented workflow starting from the generation of mutant libraries of strains previously engineered for L-methionine production, implementing biosensor-based FACS HT screening for mutant isolation, and applying whole genome sequencing technologies on interesting mutants, enabled successful isolation of L-methionine producing

mutants and rapid access to genetic modifications within weeks. Certainly, obtained production yields are far away from being competitive to petrochemical-based production. Nevertheless, further HT screenings of *C. glutamicum* and *E. coli* based mutants libraries and subsequent detailed genomic and transcriptome analysis might bring the breakthrough of L-methionine overproducing strains in commercial production processes into reach.

4.3. Online monitoring of amino acid production

Online monitoring techniques in bioprocesses offer the advantage to identify bioprocess problems at the time they occur, thus, providing valuable information for optimization of the production process. The general performance of the Lrp-biosensor for online monitoring of amino acid production in biotechnological production strains was assessed by analysis of gradually engineered *C. glutamicum* L-valine producers based on deletion of the E1p subunit of the PDHC (*aceE*). Blocking the conversion of pyruvate to acetyl-CoA by deletion of the *aceE* gene results in acetate-dependent growth of these strains. Thus, L-valine production can be controlled and decoupled from growth by acetate feed control during biotechnological processes. This facilitates validation of the biosensor, since production of L-valine in batch fermentation starts after several hours when acetate is consumed and thus, the correlation of biosensor output and L-valine production can be assayed. Studies of the L-valine production strains proved the Lrp-biosensor as convenient tool to report on the initiation of L-valine production, to monitor amino acid production in the course of time, and to distinguish between different levels of productivity in high yield and basic production strains. Thus, biosensor-based investigation of the strains paves the way for revealing bottlenecks in current production processes and enable screening of cultivation conditions for optimization of processes in future.

4.4. Biosensor-based live cell imaging

Efficient performance of biotechnological processes demands on highly productive strains which show less cell-to-cell variation in regard to physiological states and metabolite production. Nevertheless, traditional strategies for bioprocess optimization often rely on the measurement and interpretation of average data obscuring cell-to-cell variation and giving no information about development of inefficient subpopulations. Recent studies of Neumeyer *et*

al. using multiparameter flow cytometry revealed phenotypic heterogeneity of *C. glutamicum* populations with respect to membrane integrity (viability), membrane potential, and growth activity (Neumeyer *et al.*, 2013). In this work, we presented first qualitative insights into cell-to-cell heterogeneity in particular during production processes of *C. glutamicum* by application of the amino acid sensing Lrp-sensor.

Population heterogeneity is not exclusively based on biological sources, but can additionally arise in response to environmental gradients. Thus, potential reasons for cell-to-cell variability cannot clearly be identified in highly fluctuating cultivation conditions using lab-scale reactors or shake-flasks. Therefore, we performed investigations of L-valine production strains in microfluidic systems allowing for cultivation at environmental constant and defined conditions. As the Lrp-sensor allows the visualization of cytosolic amino acid concentrations in single cells, we studied in first experiments isogenic microcolonies of low yield L-valine production strain Δ*aceE* (without plasmid-bound overexpression of L-valine biosynthesis genes *ilvBNCE*) in microfluidic systems under conditions supporting L-valine production. Strikingly, these studies revealed cell-to-cell variation of fluorescence emission suggesting significant variability of L-valine production within the microcolony. Based on this first glimpse of cell-to-cell heterogeneity in productivity levels in *C. glutamicum* Δ*aceE*, we analyzed improved L-valine production strains *C. glutamicum* Δ*aceE*/pJC4-ilvBNCE-E2-Crimson, *C. glutamicum* Δ*aceE* Δ*pqo*/pJC4-ilvBNCE-E2-Crimson, *C. glutamicum* Δ*aceE* Δ*pqo* Δ*pgi*/pJC4-ilvBNCE-E2-Crimson, and *C. glutamicum* Δ*aceE* Δ*pqo* Δ*pgi* Δ*pyc*/pJC4-ilvBNCE-E2-Crimson in further studies. Since these strains were step by step engineered towards efficient L-valine overproduction, we planned to investigate to what extend cell-to-cell variation regarding metabolite production depends on different factors, such as precursor availability of pyruvate (*aceE, pqo, pyc*), NADPH supply (*pgi*), and overproduction of L-valine biosynthesis genes (*ilvBNCE*). However, we could not observe a decreasing cell-to-cell variability in the gradually engineered strains, indicating that despite pyruvate and NADPH supply or *ilvBNCE* overexpression other factors cause the observed variations at the single cell level. Factors which might influence L-valine production include *e.g.* cofactor supply of the involved enzymes, carbon source uptake, or general energy level of the individual cells.

Time-lapse microscopy based on long-term observation of isogenic microcolonies with high temporal and spatial resolution gave us deep insights into the growth and productivity of single cells and the ancestry of forming subpopulations. In all analyzed production strains we observed a fraction of non-fluorescing cells in the production phase. This was in agreement

with results obtained by FACS measurements of cells during cultivation in the 1L bioreactor. Single cell tracking revealed besides the presence of dormant cells, neither producing nor growing in course of time, sudden and progressive cell lysis. Additionally cells were tracked, which displayed unhampered growth and did not initiate L-valine production at all. Uncontrolled growth of cells can result in a predominant non-producing population, which depletes all provided nutrient resources for biomass instead of product formation. Obviously, this may result in a tremendously reduced production efficiency of the entire biotechnological processes.

Live cell imaging of cells during cultivation in microfluidic devices which mimicked the short time of transition from growth to production phase in fermentation processes, showed the development of a phenotypic bistability within the microcolonies when conditions supporting L-valine production were triggered by the medium switch. Besides expected initiation of L-valine production, cells showed either unhampered growth and cell division, or a time-delayed switch to L-valine production. Factors influencing the transition from growth to production might be different energetic levels of the cells or a higher capability for uptake of residual carbon sources due to higher abundance of transporter proteins. Energy states or glucose uptake rates could be monitored by application of biosensors reporting on *e.g.* glucose (Veetil *et al.*, 2010; Takanaga *et al.*, 2008), ATP:ADP ratio (Berg *et al.*, 2009) or NADPH levels (Siedler, Bringer, and Bott unpublished) of the cell. However, suchlike sensors are currently not available for *C. glutamicum.* An alternative to assess glucose uptake is represented by the use of fluorescent glucose analogues (Yoshioka *et al.*, 1996).

Overall, these studies proved the Lrp-sensor as powerful tool to access valuable information of single cell productivity and physiology during production processes under physiological and non-invasive conditions. Biosensor-based studies investigating cell-to-cell variation in biotechnological production strains allow us to gain a deeper knowledge of the complex phenotypic structure of microbial populations and thus, represent a new approach for strain analysis and improvement in future. In-depth investigation, however, demands on the establishment of *omics*-based downstream methods to profile subpopulations (Fritzsch *et al.*, 2012; Wang & Bodovitz, 2010; Müller & Hiller, 2013). In this context, Müller and coworkers described recently a promising advance by combination of FACS cell sorting with mass spectrometry based proteomic analysis, so-called *Cytomics,* enabling detailed physiological analysis of subpopulations (Jehmlich *et al.*, 2010).

4.5. Limitations of the sensor system

Studies reported within this work highlight the great potential of single cell biosensors in the emerging field of single cell analysis in industrial biotechnology. However, future work has to address critical issues and limitations of suchlike sensor systems.

The high specificity of the biosensor, which is an important prerequisite in screenings for the desired molecule, represents simultaneously a drawback of the system, since it is limited to specific metabolites and does not allow quantification of several different metabolites in the same cell at the same time. Integration of further reporter constructs can widen the spectrum of detectable metabolites, nevertheless, this reaches its limits when physiology of the interrogated cell is affected by the use of multicolor fluorescent proteins (Heinemann & Zenobi, 2011; Tecon & van der Meer, 2006).

Alternatives for single cell measurement of metabolites are represented by analytical techniques based on *e.g.* mass spectrometry enabling the detection of a wide range of metabolites. Meanwhile, modern mass spectrometers allow for detection in the low attomole range which is the range required for single cell metabolomics, considering the volume of *E. coli* to be approximately 1 fL (Amantonico *et al.*, 2008). Promising approaches aim for sample preparation on a microfluidic chip with subsequent transfer of the single cell content to a mass spectrometer or on arraying of single cells on sample plates for MALDI-MS analysis (Heinemann & Zenobi, 2011; Fritzsch *et al.*, 2012; Amantonico *et al.*, 2010). However, these techniques are still in the early stage of development, a workflow integrating all different units is yet not realized.

Despite the detailed characterization of the biosensors performance features describing the relationship between effector input and reporter output, quantitative analysis providing precise metabolite concentrations are hardly feasible. This would require an elaborated calibration of the sensor system for each strain under study and for each technological application, *e.g.* flow cytometry, microscopy and microplate reader systems. In any case, photobleaching and cellular movement would prevent accurate measurements (Heinemann & Zenobi, 2011; Tecon & van der Meer, 2006).

Another limitation of the system is the use of GFP derivatives as fluorescent reporters. On the one hand, chromophore maturation depends on molecular oxygen and protein folding is very time-consuming, on the other hand, the long half-life of GFP-derived fluorescent proteins (GFP>24 h) hampers dynamic measurements. Alternative options are, for example, the

recently described flavin mononucleotide (FMN)-binding fluorescent proteins (FbFPs), which do not demand on oxygen for chromophore formation (Drepper *et al.*, 2007; Drepper *et al.*, 2010). Meanwhile, GFP variants exhibiting much faster folding kinetics (20 min, superfolder GFP; 11 min, superfast GFP) without loss in fluorescence intensity are available (Pedelacq *et al.*, 2006; Fisher & DeLisa, 2008). Recently, destabilized eYFP-variants with protein half-lives of 22 and 8 min for *C. glutamicum* were reported enabling dynamic studies (Hentschel *et al.*, 2012). Furthermore, RNA aptamers were described that bind molecules resembling the fluorophore of GFP, leading to fluorescence emission upon binding. In contrast to the use of fluorescent proteins, fluorescence is emitted directly after RNA aptamer transcription (Paige *et al.*, 2011).

The production of a particular biosensor within the cell might have a significant influence on cellular physiology. During measurements, cells are exposed to light of different wavelengths and the impact thereof has not been studied so far for *C. glutamicum*. Especially in live cell imaging studies, cells are exposed for many times during long time observation (typically in 15 min intervals), thus, an influence on cellular physiology cannot be excluded. Furthermore, expression of the biosensors reporter gene *eyfp* encoding the yellow fluorescent protein places an additional metabolic burden on cells. This burden might also impact the physiological state and phenotype of cells, making productivity analysis of single cells difficult. An important step to alleviate the burden of *eyfp* expression was done by integration of the previously plasmid-encoded biosensor into the chromosome of *C. glutamicum,* significantly reducing the expression level from ten copies of *eyfp* to one copy per cell. Nevertheless, future studies have to address this problem and will analyze the actual impact of biosensor production on cellular physiology.

The difficulties of single cell measurements have nicely been highlighted by Oren and later also by Bridson and Gould, who applied Heisenberg's uncertainty principle described in the quantum mechanics to single cell analysis in biology (Bridson & Gould, 2000; Oren, 1998). In this context, the individual cell is defined as the quantal unit, which is either subject of the measurement or not. However, the observation or measurement itself influences the result thereof. Since this excludes an appropriate control experiment, the actual impact of the measurement itself on the individual cell will never be completely revealed (Brehm-Stecher & Johnson, 2004). Consequently, some uncertainness will always remain.

5 References

Acar, M., Mettetal, J.T. & van Oudenaarden, A. (2008) Stochastic switching as a survival strategy in fluctuating environments. *Nature Genetics* 40: 471-475.

Adrio, J.L. & Demain, A.L. (2006) Genetic improvement of processes yielding microbial products. *Fems Microbiology Reviews* 30: 187-214.

Ajinomoto Co., I. (2011) Feed-use amino acids buisness. *http://www.ajinomoto.com/en/ir/pdf/Feed-useAA-Oct2011.pdf*.

Ajinomoto Co., I. (2012) Food products business. *http://www.ajinomoto.com/en/ir/pdf/Food-Oct2012.pdf*.

Alper, H. & Stephanopoulos, G. (2004) Metabolic engineering challenges in the post-genomic era. *Chemical Engineering Science* 59: 5009-5017.

Alper, H. & Stephanopoulos, G. (2009) Engineering for biofuels: exploiting innate microbial capacity or importing biosynthetic potential? *Nature Reviews Microbiology* 7: 715-723.

Amantonico, A., Oh, J.Y., Sobek, J., Heinemann, M. & Zenobi, R. (2008) Mass spectrometric method for analyzing metabolites in yeast with single cell sensitivity. *Angewandte Chemie-International Edition* 47: 5382-5385.

Amantonico, A., Urban, P.L. & Zenobi, R. (2010) Analytical techniques for single-cell metabolomics: state of the art and trends. *Analytical and Bioanalytical Chemistry* 398: 2493-2504.

Bailey, J.E. (1991) Towards a science of metabolic engineering *Science* 252: 1668-1675.

Balaban, N.Q., Merrin, J., Chait, R., Kowalik, L. & Leibler, S. (2004) Bacterial persistence as a phenotypic switch. *Science* 305: 1622-1625.

Baltz, R.H., (1986) Mutagenesis in *Streptomyces spp.* In: Manual of industrial microbiology and biotechnology. Demain AL, S.N.e. (ed). Washington: Am Soc Microbiol, pp. 184-190.

Becker, J. & Wittmann, C. (2012) Bio-based production of chemicals, materials and fuels – *Corynebacterium glutamicum* as versatile cell factory. *Current Opinion in Biotechnology* 23: 631-640.

Becker, J., Zelder, O., Häfner, S., Schroeder, H. & Wittmann, C. (2011) From zero to hero-Design-based systems metabolic engineering of *Corynebacterium glutamicum* for L-lysine production. *Metabolic Engineering* 13: 159-168.

Berg, J., Hung, Y.P. & Yellen, G. (2009) A genetically encoded fluorescent reporter of ATP:ADP ratio. *Nature Methods* 6: 161-166.

Blombach, B., Crämer, A., Eikmanns, B.J. & Schreiner, M. (2009) RamB is an activator of the pyruvate dehydrogenase complex subunit E1p gene in *Corynebacterium glutamicum*. *Journal of Molecular Microbiology and Biotechnology* 16: 236-239.

Blombach, B. & Eikmanns, B.J. (2011) Current knowledge on isobutanol production with *Escherichia coli, Bacillus subtilis* and *Corynebacterium glutamicum*. *Bioengineered bugs* 2: 346-350.

Blombach, B., Riester, T., Wieschalka, S., Ziert, C., Youn, J.-W., Wendisch, V.F. & Eikmanns, B.J. (2011) *Corynebacterium glutamicum* tailored for efficient isobutanol production. *Applied and Environmental Microbiology* 77: 3300-3310.

Blombach, B., Schreiner, M.E., Bartek, T., Oldiges, M. & Eikmanns, B.J. (2008) *Corynebacterium glutamicum* tailored for high-yield L-valine production. *Applied Microbiology and Biotechnology* 79: 471-479.

Blombach, B., Schreiner, M.E., Holatko, J., Bartek, T., Oldiges, M. & Eikmanns, B.J. (2007) L-Valine production with pyruvate dehydrogenase complex-deficient *Corynebacterium glutamicum*. *Applied and Environmental Microbiology* 73: 2079-2084.

Brehm-Stecher, B.F. & Johnson, E.A. (2004) Single-cell microbiology: tools, technologies, and applications. *Microbiology and Molecular Biology Reviews* 68: 538-559.

Bridson, E.Y. & Gould, G.W. (2000) Quantal microbiology. *Letters in Applied Microbiology* 30: 95-98.

Burkovski, A. (2008) *Corynebacteria: genomics and molecular biology*. Caister Academic Press, Norfolk UK.

Cai, L., Friedman, N. & Xie, X.S. (2006) Stochastic protein expression in individual cells at the single molecule level. *Nature* 440: 358-362.

Cantoni, G.L. (1953) S-adenosylmethionine - a new intermediate formed enzymatically from L-methionine and adenosinetriphosphate. *Journal of Biological Chemistry* 204: 403-416.

Diaz, M., Herrero, M., Garcia, L.A. & Quiros, C. (2010) Application of flow cytometry to industrial microbial bioprocesses. *Biochemical Engineering Journal* 48: 385-407.

Dietrich, J.A., McKee, A.E. & Keasling, J.D., (2010) High-throughput metabolic engineering: advances in small-molecule screening and selection. In: Annual Review of Biochemistry, Vol 79. Kornberg, R.D., Raetz, C.R.H., Rothman, J.E. & Thorner, J.W. (eds). pp. 563-590.

Drepper, T., Eggert, T., Circolone, F., Heck, A., Krauss, U., Guterl, J.-K., Wendorff, M., Losi, A., Gärtner, W. & Jaeger, K.-E. (2007) Reporter proteins for *in vivo* fluorescence without oxygen. *Nature Biotechnology* 25: 443-445.

Drepper, T., Huber, R., Heck, A., Circolone, F., Hillmer, A.-K., Büchs, J. & Jaeger, K.-E. (2010) Flavin mononucleotide-based fluorescent reporter proteins outperform green fluorescent protein-like proteins as quantitative *in vivo* real-time reporters. *Applied and Environmental Microbiology* 76: 5990-5994.

Dubnau, D. & Losick, R. (2006) Bistability in bacteria. *Molecular Microbiology* 61: 564-572.

Eggeling, L. & Bott, M., (2005) *Handbook of Corynebacterium glutamicum*. Academic Press, Inc., Boca Raton, FL: CRC Press.

Elowitz, M.B. (2002) Stochastic gene expression in a single cell. *Science* 297: 1183-1186.

Enfors, S.O., Jahic, M., Rozkov, A., Xu, B., Hecker, M., Jurgen, B., Kruger, E., Schweder, T., Hamer, G., O'Beirne, D*., et al.* (2001) Physiological responses to mixing in large scale bioreactors. *Journal of Biotechnology* 85: 175-185.

Figge, R.M., (2007) Methionine biosynthesis in *Escherichia coli* and *Corynebacterium glutamicum*. In: Amino acid biosynthesis - pathways, regulation and metabolic engineering. Wendisch, V.F. (ed). Microbiol Monographs, Springer-Verlag, pp. 163-193.

Fisher, A.C. & DeLisa, M.P. (2008) Laboratory evolution of fast-folding green fluorescent protein using secretory pathway quality control. *Plos One* 3.

Fritzsch, F.S.O., Dusny, C., Frick, O. & Schmid, A. (2012) Single-cell analysis in biotechnology, systems biology, and biocatalysis. *Annual Review of Chemical and Biomolecular Engineering* 3: 129-155.

Frommer, W.B., Davidson, M.W. & Campbell, R.E. (2009) Genetically encoded biosensors based on engineered fluorescent proteins. *Chemical Society Reviews* 38: 2833-2841.

Gee, P., Maron, D.M. & Ames, B.N. (1994) Detection and classification of mutagens - a set of base-specific *Salmonella* tester strains. *Proceedings of the National Academy of Sciences of the United States of America* 91: 11606-11610.

Global Industry Analysts, I. (2012) *Amino acids - a global strategic business report*.

Gonzalez-Pastor, J.E., Hobbs, E.C. & Losick, R. (2003) Cannibalism by sporulating bacteria. *Science* 301: 510-513.

Grossmann, K., Herbster, K. & Mack, M. (2000) Rapid cloning of *metK* encoding methionine adenosyltransferase from *Corynebacterium glutamicum* by screening a genomic library on a high density colony-array. *Fems Microbiology Letters* 193: 99-103.

Gulati, S., Rouilly, V., Niu, X., Chappell, J., Kitney, R.I., Edel, J.B., Freemont, P.S. & deMello, A.J. (2009) Opportunities for microfluidic technologies in synthetic biology. *Journal of the Royal Society Interface* 6.

Haijema, B.J., Hahn, J., Haynes, J. & Dubnau, D. (2001) A ComGA-dependent checkpoint limits growth during the escape from competence. *Molecular Microbiology* 40: 52-64.

Harms, H., Wells, M.C. & van der Meer, J.R. (2006) Whole-cell living biosensors - are they ready for environmental application? *Applied Microbiology and Biotechnology* 70: 273-280.

Hasegawa, S., Suda, M., Uematsu, K., Natsuma, Y., Hiraga, K., Jojima, T., Inui, M. & Yukawa, H. (2013) Engineering of *Corynebacterium glutamicum* for high-yield L-valine production under oxygen deprivation conditions. *Applied and Environmental Microbiology* 79: 1250-1257.

Heinemann, M. & Zenobi, R. (2011) Single cell metabolomics. *Current Opinion in Biotechnology* 22: 26-31.

Hentschel, E., Will, C., Mustafi, N., Burkovski, A., Rehm, N. & Frunzke, J. (2012) Destabilized eYFP variants for dynamic gene expression studies in *Corynebacterium glutamicum*. *Microbial Biotechnology* 6: 196-201.

Hewitt, C. & Nienow, A. (2007) The scale-up of microbial batch and fed-batch fermentation processes. *Journal of Biotechnology* 131: 134-135.

Hüser, A.T., Chassagnole, C., Lindley, N.D., Merkamm, M., Guyonvarch, A., Elisakova, V., Patek, M., Kalinowski, J., Brune, I., Puhler, A.*, et al.* (2005) Rational design of a *Corynebacterium glutamicum* pantothenate production strain and its characterization by metabolic flux analysis and genome-wide transcriptional profiling. *Applied and Environmental Microbiology* 71: 3255-3268.

Hwang, B.J., Kim, Y., Kim, H.B., Hwang, H.J., Kim, J.H. & Lee, H.S. (1999) Analysis of *Corynebacterium glutamicum* methionine biosynthetic pathway: isolation and analysis of *metB* encoding cystathionine gamma-synthase. *Molecules and Cells* 9: 300-308.

Hwang, B.J., Yeom, H.J., Kim, Y. & Lee, H.S. (2002) *Corynebacterium glutamicum* utilizes both transsulfuration and direct sulfhydrylation pathways for methionine biosynthesis. *Journal of Bacteriology* 184: 1277-1286.

Ikeda, M. (2006) Towards bacterial strains overproducing L-tryptophan and other aromatics by metabolic engineering. *Applied Microbiology and Biotechnology* 69: 615-626.

Ikeda, M. & Nakagawa, S. (2003) The *Corynebacterium glutamicum* genome: features and impacts on biotechnological processes. *Applied Microbiology and Biotechnology* 62: 99-109.

Ikeda, M., Ohnishi, J., Hayashi, M. & Mitsuhashi, S. (2006) A genome-based approach to create a minimally mutated, *Corynebacterium glutamicm* strain for efficient L-lysine production. *Journal of Industrial Microbiology & Biotechnology* 33: 610-615.

Inoue, H., Inagaki, K., Eriguchi, S.I., Tamura, T., Esaki, N., Soda, K. & Tanaka, H. (1997) Molecular characterization of the *mde* operon involved in L-methionine catabolism of *Pseudomonas putida*. *Journal of Bacteriology* 179: 3956-3962.

Inui, M., Kawaguchi, H., Murakami, S., Vertes, A.A. & Yukawa, H. (2004a) Metabolic engineering of *Corynebacterium glutamicum* for fuel ethanol production under oxygen-deprivation conditions. *Journal of Molecular Microbiology and Biotechnology* 8: 243-254.

Inui, M., Murakami, S., Okino, S., Kawaguchi, H., Vertes, A.A. & Yukawa, H. (2004b) Metabolic analysis of *Corynebacterium glutamicum* during lactate and succinate productions under oxygen deprivation conditions. *Journal of Molecular Microbiology and Biotechnology* 7: 182-196.

Jehmlich, N., Hübschmann, T., Salazar, M.G., Völker, U., Benndorf, D., Müller, S., von Bergen, M. & Schmidt, F. (2010) Advanced tool for characterization of microbial

cultures by combining cytomics and proteomics. *Applied Microbiology and Biotechnology* 88: 575-584.

Jo, S.-J., Maeda, M., Ooi, T. & Taguchi, S. (2006) Production system for biodegradable polyester polyhydroxybutyrate by *Corynebacterium glutamicum*. *Journal of Bioscience and Bioengineering* 102: 233-236.

Jojima, T., Fujii, M., Mori, E., Inui, M. & Yukawa, H. (2010) Engineering of sugar metabolism of *Corynebacterium glutamicum* for production of amino acid L-alanine under oxygen deprivation. *Applied Microbiology and Biotechnology* 87: 159-165.

Kærn, M., Elston, T.C., Blake, W.J. & Collins, J.J. (2005) Stochasticity in gene expression: from theories to phenotypes. *Nature Reviews Genetics* 6: 451-464.

Kalinowski, J., Bathe, B., Bartels, D., Bischoff, N., Bott, M., Burkovski, A., Dusch, N., Eggeling, L., Eikmanns, B.J., Gaigalat, L., *et al.* (2003) The complete *Corynebacterium glutamicum* ATCC 13032 genome sequence and its impact on the production of L-aspartate-derived amino acids and vitamins. *Journal of Biotechnology* 104: 5-25.

Kearns, D.B. (2005) Cell population heterogeneity during growth of *Bacillus subtilis*. *Genes & Development* 19: 3083-3094.

Kennerknecht, N., Sahm, H., Yen, M.R., Patek, M., Saier, M.H. & Eggeling, L. (2002) Export of L-isoleucine from *Corynebacterium glutamicum*: a two-gene-encoded member of a new translocator family. *Journal of Bacteriology* 184: 3947-3956.

Kim, J.W., Kim, H.J., Kim, Y., Lee, M.S. & Lee, H.S. (2001) Properties of the *Corynebacterium glutamicum metC* gene encoding cystathionine beta-lyase. *Molecules and Cells* 11: 220-225.

Kind, S., Kreye, S. & Wittmann, C. (2011) Metabolic engineering of cellular transport for overproduction of the platform chemical 1,5-diaminopentane in *Corynebacterium glutamicum*. *Metabolic Engineering* 13: 617-627.

Kinoshita, S., Udaka, S. & Shimono, M. (1957) Studies on the amino acid fermentation: I. Production of L-glutamic acid by various microorganisms. *The Journal of General and Applied Microbiology* 3: 193–205.

Koch, D.J., Rückert, C., Albersmeier, A., Hüser, A.T., Tauch, A., Pühler, A. & Kalinowski, J. (2005) The transcriptional regulator SsuR activates expression of the *Corynebacterium glutamicum* sulphonate utilization genes in the absence of sulphate. *Molecular Microbiology* 58: 480-494.

Koffas, M., Roberge, C., Lee, K. & Stephanopoulos, G. (1999) Metabolic engineering. *Annual Review of Biomedical Engineering* 1: 535-557.

Korobkova, E., Emonet, T., Vilar, J.M.G., Shimizu, T.S. & Cluzel, P. (2004) From molecular noise to behavioural variability in a single bacterium. *Nature* 428: 574-578.

Krause, F.S., Blombach, B. & Eikmanns, B.J. (2010) Metabolic engineering of *Corynebacterium glutamicum* for 2-ketoisovalerate production. *Applied and Environmental Microbiology* 76: 8053-8061.

Krömer, J.O., Bolten, C.J., Heinzle, E., Schröder, H. & Wittmann, C. (2008) Physiological response of *Corynebacterium glutamicum* to oxidative stress induced by deletion of the transcriptional repressor McbR. *Microbiology* 154: 3917-3930.

Krömer, J.O., Heinzle, E., Schröder, H. & Wittmann, C. (2005) Accumulation of homolanthionine and activation of a novel pathway for isoleucine biosynthesis in *Corynebacterium glutamicum mcbR* deletion strains. *Journal of Bacteriology* 188: 609-618.

Krömer, J.O., Wittmann, C., Schröder, H. & Heinzle, E. (2006) Metabolic pathway analysis for rational design of L-methionine production by *Escherichia coli* and *Corynebacterium glutamicum*. *Metabolic Engineering* 8: 353-369.

Kumar, D. & Gomes, J. (2005) Methionine production by fermentation. *Biotechnology Advances* 23: 41-61.

Kussell, E. & Leibler, S. (2005) Phenotypic diversity, population growth, and information in fluctuating environments. *Science* 309: 2075-2078.

Lai, S., Zhang, Y., Liu, S., Liang, Y., Shang, X., Chai, X. & Wen, T. (2012) Metabolic engineering and flux analysis of *Corynebacterium glutamicum* for L-serine production. *Science China-Life Sciences* 55: 283-290.

Lange, C., Mustafi, N., Frunzke, J., Kennerknecht, N., Wessel, M., Bott, M. & Wendisch, V.F. (2012) Lrp of *Corynebacterium glutamicum* controls expression of the *brnFE* operon encoding the export system for L-methionine and branched-chain amino acids. *Journal of Biotechnology* 158: 231-241.

Lara, A.R., Galindo, E., Ramirez, O.T. & Palomares, L.A. (2006) Living with heterogeneities in bioreactors. *Molecular Biotechnology* 34: 355-381.

Lee, S.Y., Kim, H.U., Park, J.H., Park, J.M. & Kim, T.Y. (2009) Metabolic engineering of microorganisms: general strategies and drug production. *Drug Discovery Today* 14: 78-88.

Lencastre Fernandes, R., Nierychlo, M., Lundin, L., Pedersen, A.E., Puentes Tellez, P.E., Dutta, A., Carlquist, M., Bolic, A., Schäpper, D., Brunetti, A.C.*, et al.* (2011) Experimental methods and modeling techniques for description of cell population heterogeneity. *Biotechnology Advances* 29: 575-599.

Leuchtenberger, W., Huthmacher, K. & Drauz, K. (2005) Biotechnological production of amino acids and derivatives: current status and prospects. *Applied Microbiology and Biotechnology* 69: 1-8.

Li, P.-P., Liu, Y.-J. & Liu, S.-J. (2009) Genetic and biochemical identification of the chorismate mutase from *Corynebacterium glutamicum*. *Microbiology-Sgm* 155: 3382-3391.

Liden, G. (2002) Understanding the bioreactor. *Bioprocess and Biosystems Engineering* 24: 273-279.

Lidstrom, M.E. & Konopka, M.C. (2010) The role of physiological heterogeneity in microbial population behavior. *Nature Chemical Biology* 6: 705-712.

Litsanov, B., Brocker, M. & Bott, M. (2012a) Towards homosuccinate fermentation: metabolic engineering of *Corynebacterium glutamicum* for anaerobic production of succinate from glucose and formate. *Applied and Environmental Microbiology* 78: 3325-3337.

Litsanov, B., Kabus, A., Brocker, M. & Bott, M. (2012b) Efficient aerobic succinate production from glucose in minimal medium with *Corynebacterium glutamicum*. *Microbial Biotechnology* 5: 116-128.

Lu, S.C. (2000) S-Adenosylmethionine. *International Journal of Biochemistry & Cell Biology* 32: 391-395.

Maamar, H., Raj, A. & Dubnau, D. (2007) Noise in gene expression determines cell fate in *Bacillus subtilis*. *Science* 317: 526-529.

Marienhagen, J. & Bott, M. (2013) Metabolic engineering of microorganisms for the synthesis of plant natural products. *Journal of Biotechnology* 163: 166-178.

Matsumoto, K.i., Kitagawa, K., Jo, S.-J., Song, Y. & Taguchi, S. (2011) Production of poly(3-hydroxybutyrate-co-3-hydroxyvalerate) in recombinant *Corynebacterium glutamicum* using propionate as a precursor. *Journal of Biotechnology* 152: 144-146.

Michener, J.K. & Smolke, C.D. (2012) High-throughput enzyme evolution in *Saccharomyces cerevisiae* using a synthetic RNA switch. *Metabolic Engineering* 14: 306-316.

Michener, J.K., Thodey, K., Liang, J.C. & Smolke, C.D. (2012) Applications of genetically-encoded biosensors for the construction and control of biosynthetic pathways. *Metabolic Engineering* 14: 212-222.

Mimitsuka, T., Sawai, H., Hatsu, M. & Yamada, K. (2007) Metabolic engineering of *Corynebacterium glutamicum* for cadaverine fermentation. *Bioscience Biotechnology and Biochemistry* 71: 2130-2135.

Müller, S., Harms, H. & Bley, T. (2010) Origin and analysis of microbial population heterogeneity in bioprocesses. *Current Opinion in Biotechnology* 21: 100-113.

Müller, S. & Hiller, K. (2013) From multi-*omics* to basic structures of biological systems. *Current Opinion in Biotechnology* 24: 1-3.

Müller, S. & Nebe-von-Caron, G. (2010) Functional single-cell analyses: flow cytometry and cell sorting of microbial populations and communities. *Fems Microbiology Reviews* 34: 554-587.

Neidhardt, F.C., Ingraham, J.L. & Schaechter, M., (1990) Physiology of the bacterial cell: a molecular approach. In.: Sinauer Associates, Sunderland, MA, pp. pp. 507.

Neumeyer, A., Hübschmann, T., Müller, S. & Frunzke, J. (2013) Monitoring of population dynamics of *Corynebacterium glutamicum* by multiparameter flow cytometry. *Microbial Biotechnology* 6 (2): 157-67.

Niimi, S., Suzuki, N., Inui, M. & Yukawa, H. (2011) Metabolic engineering of 1,2-propanediol pathways in *Corynebacterium glutamicum*. *Applied Microbiology and Biotechnology* 90: 1721-1729.

Novus International, I. (2010) Methionine global outlook: the next decade. *http://www.novusint.com/portals/0/v2/multimedia/pdf/whitepapers/Methionine_Global_Outlook.pdf*.

Ohnishi, J., Mizoguchi, H., Takeno, S. & Ikeda, M. (2008) Characterization of mutations induced by *N*-methyl-*N'*-nitro-*N*-nitrosoguanidine in an industrial *Corynebacterium glutamicum* strain. *Mutation Research-Genetic Toxicology and Environmental Mutagenesis* 649: 239-244.

Okino, S., Noburyu, R., Suda, M., Jojima, T., Inui, M. & Yukawa, H. (2008a) An efficient succinic acid production process in a metabolically engineered *Corynebacterium glutamicum* strain. *Applied Microbiology and Biotechnology* 81: 459-464.

Okino, S., Suda, M., Fujikura, K., Inui, M. & Yukawa, H. (2008b) Production of D-lactic acid by *Corynebacterium glutamicum* under oxygen deprivation. *Applied Microbiology and Biotechnology* 78: 449-454.

Okumoto, S., Jones, A. & Frommer, W.B. (2012) Quantitative imaging with fluorescent biosensors. *Annual Review of Plant Biology* 63: 663-706.

Oren, D.A. (1998) Heisenberg meets photobiology? *Science* 279: 969-969.

Paige, J.S., Wu, K.Y. & Jaffrey, S.R. (2011) RNA mimics of green fluorescent protein. *Science* 333: 642-646.

Parekh, S., Vinci, V.A. & Strobel, R.J. (2000) Improvement of microbial strains and fermentation processes. *Applied Microbiology and Biotechnology* 54: 287-301.

Park, J.H. & Lee, S.Y. (2010) Metabolic pathways and fermentative production of L-aspartate family amino acids. *Biotechnology Journal* 5: 560-577.

Park, S.D., Lee, J.Y., Kim, Y., Kim, J.H. & Lee, H.S. (1998) Isolation and analysis of *metA*, a methionine biosynthetic gene encoding homoserine acetyltransferase in *Corynebacterium glutamicum*. *Molecules and Cells* 8: 286-294.

Patek, M., (2007) Branched-chain amino acids. In: Amino acid biosynthesis - pathways, regulation and metabolic engineering. Wendisch, V.F. (ed). Microbiol Monographs, Springer-Verlag, pp. 129-162.

Pedelacq, J.D., Cabantous, S., Tran, T., Terwilliger, T.C. & Waldo, G.S. (2006) Engineering and characterization of a superfolder green fluorescent protein. *Nature Biotechnology* 24: 79-88.

Peters-Wendisch, P., Stolz, M., Etterich, H., Kennerknecht, N., Sahm, H. & Eggeling, L. (2005) Metabolic engineering of *Corynebacterium glutamicum* for L-serine production. *Applied and Environmental Microbiology* 71: 7139-7144.

Portnoy, V.A., Bezdan, D. & Zengler, K. (2011) Adaptive laboratory evolution - harnessing the power of biology for metabolic engineering. *Current Opinion in Biotechnology* 22: 590-594.

Reed, L.J. (1974) Multienzyme complexes. *Accounts of Chemical Research* 7: 40-46.

Rey, D.A., Pühler, A. & Kalinowski, J. (2003) The putative transcriptional repressor McbR, member of the TetR-family, is involved in the regulation of the metabolic network directing the synthesis of sulfur containing amino acids in *Corynebacterium glutamicum*. *Journal of Biotechnology* 103: 51-65.

Rossol, I. & Pühler, A. (1992) The *Corynebacterium glutamicum aecD* gene encodes a C-S lyase with α,β-elimination activity that degrades aminoethylcysteine. *Journal of Bacteriology* 174: 2968-2977.

Rückert, C. & Kalinowski, J., (2008) Sulfur metabolism in *Corynebacterium glutamicum*. In: Corynebacteria: genomics and molecular biology. Burkovski, A. (ed). Caister Academic Press, Norfolk UK.

Rückert, C., Milse, J., Albersmeier, A., Koch, D.J., Pühler, A. & Kalinowski, J. (2008) The dual transcriptional regulator CysR in *Corynebacterium glutamicum* ATCC 13032 controls a subset of genes of the McbR regulon in response to the availability of sulphide acceptor molecules. *BMC Genomics* 9: 483.

Rückert, C., Pühler, A. & Kalinowski, J. (2003) Genome-wide analysis of the L-methionine biosynthetic pathway in *Corynebacterium glutamicum* by targeted gene deletion and homologous complementation. *Journal of Biotechnology* 104: 213-228.

Sasaki, M., Jojima, T., Inui, M. & Yukawa, H. (2010) Xylitol production by recombinant *Corynebacterium glutamicum* under oxygen deprivation. *Applied Microbiology and Biotechnology* 86: 1057-1066.

Sawada, K., Zen-in, S., Wada, M. & Yokota, A. (2010) Metabolic changes in a pyruvate kinase gene deletion mutant of *Corynebacterium glutamicum* ATCC 13032. *Metabolic Engineering* 12: 401-407.

Schäfer, A., Tauch, A., Droste, N., Pühler, A. & Kalinowski, J. (1997) The *Corynebacterium glutamicum cglIM* gene encoding a 5-cytosine methyltransferase enzyme confers a specific DNA methylation pattern in an McrBC-deficient *Escherichia coli* strain. *Gene* 203: 95-101.

Schmid, A., Kortmann, H., Dittrich, P.S. & Blank, L.M. (2010) Chemical and biological single cell analysis. *Current Opinion in Biotechnology* 21: 12-20.

Schneider, J. & Wendisch, V.F. (2010) Putrescine production by engineered *Corynebacterium glutamicum*. *Applied Microbiology and Biotechnology* 88: 859-868.

Schreiner, M.E., Fiur, D., Holatkoj, J., Patek, M. & Eikmanns, B.J. (2005) E1 enzyme of the pyruvate dehydrogenase complex in *Corynebactetium glutamicum*: molecular analysis of the gene and phylogenetic aspects. *Journal of Bacteriology* 187: 6005-6018.

Simic, P., Sahm, H. & Eggeling, L. (2001) L-threonine export: use of peptides to identify a new translocator from *Corynebacterium glutamicum*. *Journal of Bacteriology* 183: 5317-5324.

Smith, K.M., Cho, K.-M. & Liao, J.C. (2010) Engineering *Corynebacterium glutamicum* for isobutanol production. *Applied Microbiology and Biotechnology* 87: 1045-1055.

Stäbler, N., Oikawa, T., Bott, M. & Eggeling, L. (2011) *Corynebacterium glutamicum* as a host for synthesis and export of D-amino acids. *Journal of Bacteriology* 193: 1702-1709.

Stephanopoulos, G. (1999) Metabolic fluxes and metabolic engineering. *Metabolic Engineering* 1: 1-11.

Stephanopoulos, G., Alper, H. & Moxley, J. (2004) Exploiting biological complexity for strain improvement through systems biology. *Nature Biotechnology* 22: 1261-1267.

Stephanopoulos, G., Aristodou, A. & Nielsen, J., (1998) *Metabolic engineering: principles and methodologies*. Academic Press, San Diego.

Stephanopoulos, G. & Vallino, J.J. (1991) Network rigidity and metabolic engineering in metabolite overproduction. *Science* 252: 1675-1681.

Swain, P.S., Elowitz, M.B. & Siggia, E.D. (2002) Intrinsic and extrinsic contributions to stochasticity in gene expression. *Proceedings of the National Academy of Sciences of the United States of America* 99: 12795-12800.

Szita, N., Polizzi, K., Jaccard, N. & Baganz, F. (2010) Microfluidic approaches for systems and synthetic biology. *Current Opinion in Biotechnology* 21: 517-523.

Takanaga, H., Chaudhuri, B. & Frommer, W.B. (2008) Glut1 and Glut9 as major contributors to glucose influx in HepG2 cells identified by a high sensitivity intramolecular FRET glucose sensor. *Biochimica Et Biophysica Acta-Biomembranes* 1778: 1091-1099.

Takors, R. (2012) Scale-up of microbial processes:impacts, tools and open questions. *Journal of Biotechnology* 160: 3-9.

Tecon, R. & van der Meer, J.R. (2006) Information from single-cell bacterial biosensors: what is it good for? *Current Opinion in Biotechnology* 17: 4-10.

Tracy, B.P., Gaida, S.M. & Papoutsakis, E.T. (2010) Flow cytometry for bacteria: enabling metabolic engineering, synthetic biology and the elucidation of complex phenotypes. *Current Opinion in Biotechnology* 21: 85-99.

Trötschel, C., Deutenberg, D., Bathe, B., Burkovski, A. & Krämer, R. (2005) Characterization of methionine export in *Corynebacterium glutamicum*. *Journal of Bacteriology* 187: 3786-3794.

Trötschel, C., Follmann, M., Nettekoven, J.A., Mohrbach, T., Forrest, L.R., Burkovski, A., Marin, K. & Krämer, R. (2008) Methionine uptake in *Corynebacterium glutamicum* by MetQNI and by MetPS, a novel methionine and alanine importer of the NSS neurotransmitter transporter family. *Biochemistry* 47: 12698-12709.

van der Meer, J.R. & Belkin, S. (2010) Where microbiology meets microengineering: design and applications of reporter bacteria. *Nature Reviews Microbiology* 8: 511-522.

Veening, J.-W., Smits, W.K. & Kuipers, O.P. (2008) Bistability, epigenetics, and bet-hedging in bacteria. *Annual Review of Microbiology* 62: 193-210.

Veetil, J.V., Jin, S. & Ye, K. (2010) A glucose sensor protein for continuous glucose monitoring. *Biosensors & Bioelectronics* 26: 1650-1655.

Vertès, A.A., Inui, M. & Yukawa, H. (2012) Postgenomic approaches to using *Corynebacteria* as biocatalysts. *Annual Review of Microbiology* 66: 521-550.

Vinuselvi, P., Park, S., Kim, M., Park, J.M., Kim, T. & Lee, S.K. (2011) Microfluidic technologies for synthetic biology. *International Journal of Molecular Sciences* 12: 3576-3593.

Wang, D. & Bodovitz, S. (2010) Single cell analysis: the new frontier in *'omics'*. *Trends in Biotechnology* 28: 281-290.

Wang, X., Kitamura, K. & Yamamoto, K. (1996) Mutagenic specificity of *N*-methyl-*N'*-nitro-*N*-nitrosoguanidine in the *tonB* gene on the chromosome of *Escherichia coli recA*$^{+}$ and *recA*$^{-}$ cells. *Biochemical and Biophysical Research Communications* 227: 334-339.

Wendisch, V.F., (2007) *Amino acid biosynthesis - pathways, regulation and metabolic engineering*. Microbiol Monographs, Springer-Verlag.

Wieschalka, S., Blombach, B. & Eikmanns, B.J. (2012) Engineering *Corynebacterium glutamicum* for the production of pyruvate. *Applied Microbiology and Biotechnology* 94: 449-459.

Win, M.N. & Smolke, C.D. (2007) A modular and extensible RNA-based gene-regulatory platform for engineering cellular function *Proceedings of the National Academy of Sciences of the United States of America* 104: 14283-14288.

Yadav, V.G., De Mey, M., Lim, C.G., Ajikumar, P.K. & Stephanopoulos, G. (2012) The future of metabolic engineering and synthetic biology: towards a systematic practice. *Metabolic Engineering* 14: 233-241.

Yeaman, S.J. (1989) The 2-oxo acid dehydrogenase complexes - recent advances. *Biochemical Journal* 257: 625-632.

Yoshioka, K., Takahashi, H., Homma, T., Saito, M., Oh, K.B., Nemoto, Y. & Matsuoka, H. (1996) A novel fluorescent derivative of glucose applicable to the assessment of glucose uptake activity of *Escherichia coli*. *Biochimica Et Biophysica Acta-General Subjects* 1289: 5-9.

Yukawa, H., Omumasaba, C.A., Nonaka, H., Kos, P., Okai, N., Suzuki, N., Suda, M., Tsuge, Y., Watanabe, J., Ikeda, Y.*, et al.* (2007) Comparative analysis of the *Corynebacterium glutamicum* group and complete genome sequence of strain R. *Microbiology-Sgm* 153: 1042-1058.

Zhang, F. & Keasling, J. (2011) Biosensors and their applications in microbial metabolic engineering. *Trends in Microbiology* 19: 323-329.

Zhao, Z., Ding, J.-Y., Li, T., Zhou, N.-Y. & Liu, S.-J. (2011) The *ncgl1108* (*PheP*$_{Cg}$) gene encodes a new L-Phe transporter in *Corynebacterium glutamicum*. *Applied Microbiology and Biotechnology* 90: 2005-2013.

6 Appendix

6.1. Supplemental information (SI) - The development and application of a single-cell biosensor for the detection of L-methionine and branched-chain amino acids

Experimental procedures

Microfluidic chip fabrication

The microfluidic chip was fabricated using replica molding (Xia and Whitesides, 1998). In brief, a two-layer mold was fabricated under cleanroom conditions at the Helmholtz Nanoelectronic Facility (HNF)Jülich. Two layers of SU-8 photoresist, 1.2 µm thick and 8 µm thick respectively, were spin-coated onto the wafer and structured by lithography techniques. Using soft-lithographic methods, a disposable transparent poly(dimethylsiloxane) (PDMS) (Sylgard 184 Silicone Elastomer, Dow Corning Corp., Midland, MI, USA) microfluidic chip was fabricated. Liquid PDMS was poured over the mold and thermally cured. Uncured PDMS monomer residue was removed by washing the PDMS slab in pentane, acetone. This was followed by drying overnight (Lee et al., 2003). Prior to bonding, the chip was thoroughly rinsed with isopropanol to ensure sterile culture conditions. After drying with nitrogen, the PDMS surface was activated by oxygen plasma and permanently bonded to a 170 µm thick glass slide. Each disposable culture chip contains several cultivation chambers in parallel. The height of the growth regions is only 1.2 µm high, ensuring that cells grow in one focal plane.

Live cell imaging in microfluidic devices

The inlet and outlet of the microfluidic chip were connected to silicon tubing (Tygon S-54-HL, inner diameter = 0.25 mm, outer diameter =0.76 mm) and 1 ml sterile glass syringes (ILS Innovative Labor SystemeGmbH, Germany). Media supply and flow control was realized with a high precision syringe pump (neMESYS, Cetoni, Germany; Syringes, ILS). The chip was flushed with media prior to seeding of the bacteria. The device was placed on a fully motorized inverted microscope (Nikon Eclipse Ti) suitable for time-lapse live cell imaging. Briefly, the setup was further equipped with a focus assistant (Nikon PFS) compensating for thermal drift during long-term microscopy, Apo TIRF 100x Oil DIC N objective, objective heater (ALA OBJ-Heater, Ala Scientific Instruments, USA), NIKON DS-Vi1 color camera, ANDOR LUCA R DL604 camera, Xenon fluorescence light source for fluorescence excitation and standard filters for the proper excitation of the chromophoreeYFP (excitation: 490 nm-510 nm; emission: 520 nm-550 nm) and detection of its emission. DIC microscopy

images as well as fluorescence images were captured and analyzed using the Nikon NIS Elements AR software package.

Growth of microcolonies

*C. glutamicum*Δ*aceE* was grown overnight in CGXII minimal medium containing 4% glucose (w/v) and 1.5% (w/v) potassium acetate. The overnight culture was used to inoculate a preculture that was grown for 4 hours (exponential phase), before being loaded into the microfluidic chip. Cultivation was done in sterile medium. Prior to cell seeding, the system was warmed to 30°C usinga heated microscope objective and immersion oil film. Single cells were seeded into the chip device by flushing the cell suspension (OD_{600}~4) through the channels with 300 nl/min. Once single cells were trapped, CGXII medium with 4% glucose (w/v)and 1.5% (w/v) potassium acetate was infused using a syringe pump with a flow rate of ~25 nl/per minute per cultivation chamber. During time-lapse microscopy, colony growth was followed for approximately five generations. To initiate the L-valine production phase, the medium was switched to medium containing only 4% glucose (w/v) (Figure 3B).

Images were acquired at 15 minute intervals. Image analysis and data acquisition for the lineage tree was performed as follows: Division intervals were determined for every division event; for the final analysis of the microcolony (after 18 hours, see Figure 3B), the length of the bacteria was measured manually (± 0.1µm) and fluorescence emission was quantified through mean intensity of every defined region of interest (ROIs), which encompasses the cell area. The cell area was manually assigned through the cell shape of the DIC figure of each cell. The fluorescence was pseudo-colored and categorized into seven classes, with white representing the maximum emitted fluorescence and black no fluorescence.

Supporting Tables

Table S1: Positive clones obtained from FACS screening. Production of branched-chain amino acids after 48 hour cultivation in CGXII medium with 4% glucose, 1.5% acetate and 0.1% yeast extract. For top five mutants see Table 3.

Strains[a]	L-valine (mM)	L-leucine (mM)	L-isoleucine (mM)
Screening of mutants directly after mutagenesis (Gate S1-P1)			
1 (top5: Mutant1)	8.7	1.3	0.9
2 (top5: Mutant 2)	5.1	1.0	1.3
3	5.1	0.7	n.d.
4 (top5: Mutant 5)	4.6	1.2	1.2
5	3.8	0.5	n.d.
6	3.1	n.d.	n.d.
7	3.0	n.d.	n.d.
8	0.8	n.d.	n.d.
9	0.7	n.d.	n.d.
10	0.5	n.d.	n.d.
11	0.4	n.d.	n.d.
Screening of mutants with high fluorescence emission after iterative screen (Gate S2-P1)			
12	3.4	n.d.	n.d.
13 (top5: Mutant 3)	4.8	1.0	1.0
14	3.0	n.d.	n.d.
15	2.9	n.d.	n.d.
16	2.7	n.d.	n.d.
17	2.7	n.d.	n.d.
18	2.7	n.d.	n.d.
19	2.7	n.d.	n.d.
20	2.5	n.d.	n.d.
21	2.4	n.d.	n.d.

22	2.3	n.d.	n.d.
23	2.2	n.d.	n.d.
24	1.8	n.d.	n.d.
25	1.8	n.d.	n.d.
26	1.3	n.d.	n.d.
27	0.8	n.d.	n.d.
28	0.6	n.d.	n.d.
Screening of mutants with middle fluorescence emission after iterative screen (S2-P2)			
29 (top5: Mutant 4)	4.6	n.d.	2.1
30	4.0	n.d.	n.d.
31	2.5	n.d.	n.d.
32	1.7	n.d.	n.d.
33	1.4	n.d.	n.d.
34	1.3	n.d.	n.d.
35	0.6	n.d.	n.d.
36	0.2	n.d.	n.d.
37	0.1	n.d.	n.d.
Screening of mutants with low fluorescence emission after iterative screen (S2-P3)			
38	2.1	n.d.	n.d.
39	1.4	n.d.	n.d.

a) Mutant clones obtained from high-throughput screening are ordered by FACS gate shown in Figure 4. For screening approach S1, cells were sorted 6 hours after mutagenesis in gate S1-P1; for approach S2, cells were sorted after iterative screen from three gates differing in fluorescence signal (S2-P1: high, S2-P2: medium, S2-P3: low).

Supporting Figures

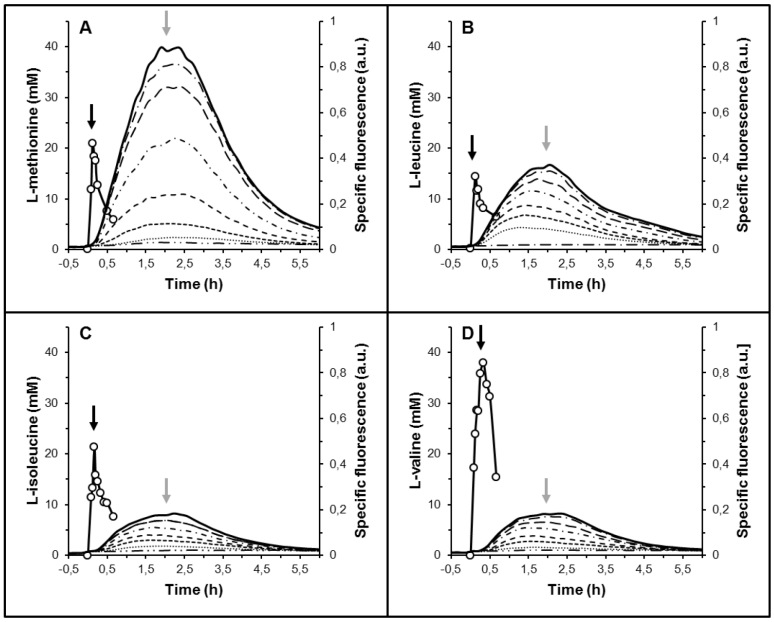

Fig. S1: Intracellular amino acid concentration (○) of *C. glutamicum* sensor cells after incubation with 3 mM of Ala-Met (A), Ala-Leu (B), Ala-Ile (C), and Ala-Val (D) dipeptideand the resulting specific fluorescence (—) of the cells. For the adjustment of the internal amino acid concentration, different ratios of dipeptide mixtures were added: 3 mM Ala-X(—), 2.7 mM Ala-X + 0.3 mM Ala-Ala (–·–), 2.1 mM Ala-X + 0.9 mM Ala-Ala (– –), 1.5 mM Ala-X + 1.5 mM Ala-Ala (-·-), 0.9 mM Ala-X + 2.1 mM Ala-Ala (--), 0.6 mM Ala-X + 2.4 mM Ala-Ala (--),0.3 mM Ala-X + 2.7 mM Ala-Ala (····), and 0.03 mM Ala-X + 2.97 mM Ala-Ala (-···-). For the determination of the intracellular amino acid concentration, samples were taken at the time of the highest internal concentration (black arrow) and set into relation with the maximal eYFP emission of the cells (grey arrow).

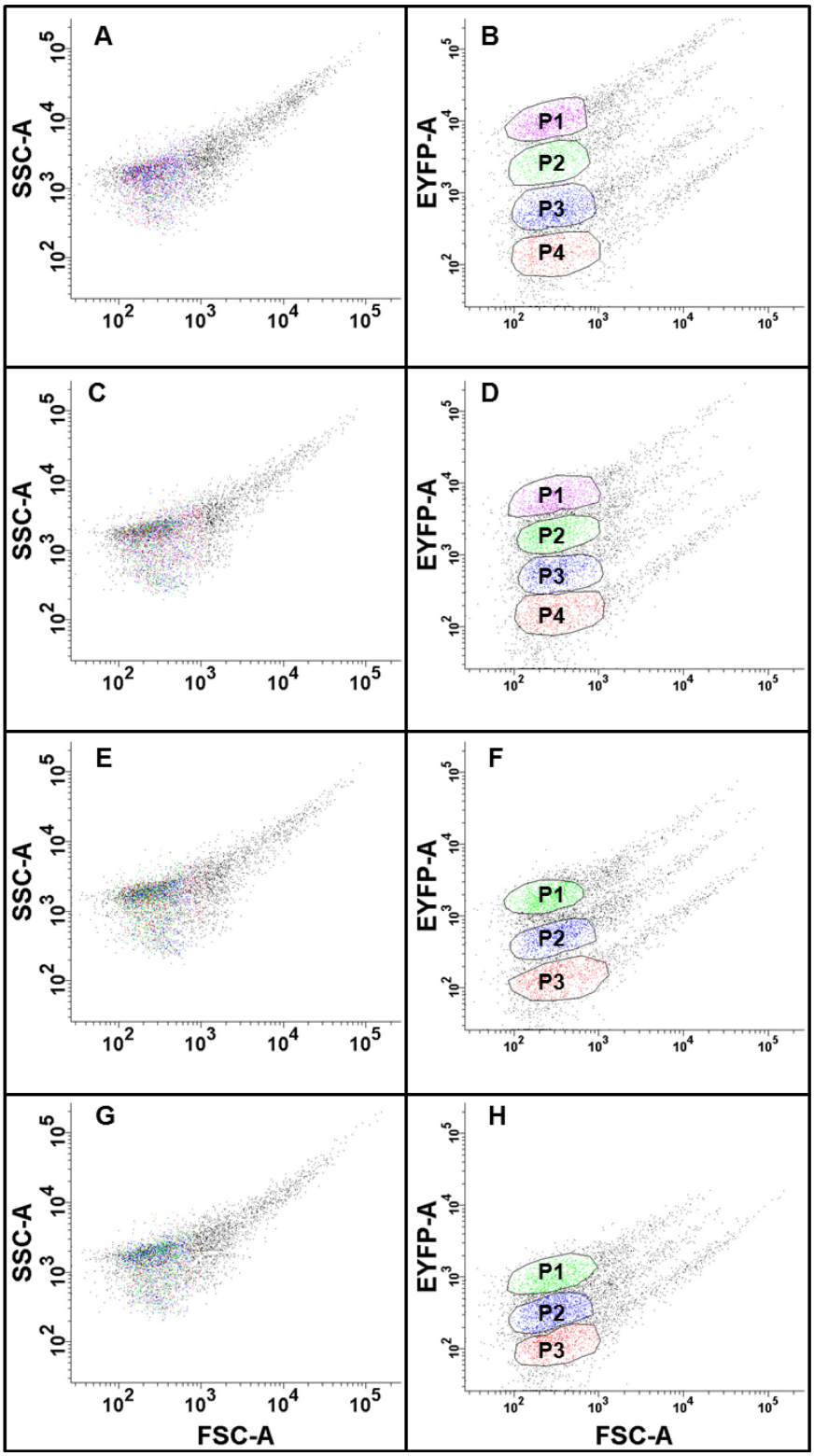

Fig. S2:Gating strategy used for discriminating the populations shown in Figure 2 B-E. Dot plots in the left column display the FCS and SSC signals of *C. glutamicum* cells with different internal effector concentrations (see Figure 2).Dot plots of the right column display the FCS signal versus the eYFP signal of the same populations. (A) and (B) L-methionine, (C) and (D) L-leucine, (E) and (F) L-isoleucine, and (G) and (H) L-valine.

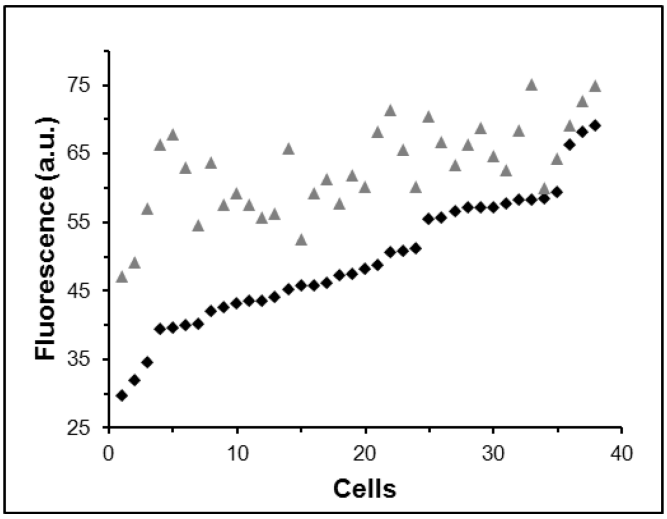

Fig. S3: Fluorescence signal of individual *C. glutamicumΔaceE* cells at the time of fluorescence measurement shown in Fig. 3B (♦). The flow was stopped for two hours and the fluorescence emission of each cell was quantified again (▲).

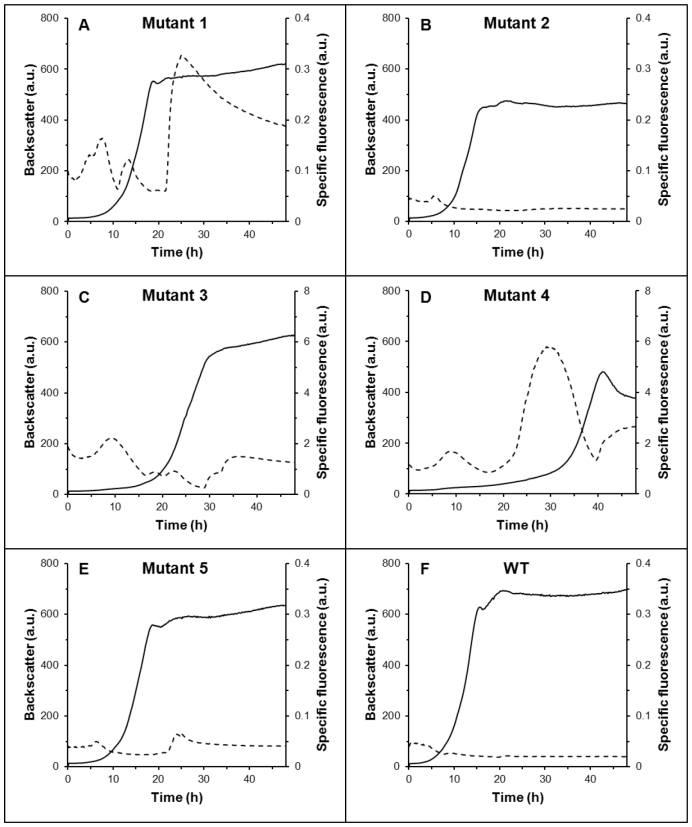

Fig. S4: Growth (—) and specific fluorescence (--) of *C. glutamicum* wild type (F) and *C. glutamicum* mutants 1-5 (A-E) excreting 8.7 mM (mutant 1), 5.1 mM (mutant 2), 4.8 mM (mutant 3), and 4.6 mM L-valine (mutant 4 and 5) and low amounts of L-leucine and L-isoleucine (see Table 3). Cells were cultivated for 48 hours in CGXII minimal medium with the supplement of 4% glucose, 1.5% acetate, and 0.1% yeast extract. Data represent average values of two independent cultivations.

Online Movies

Video S1:A time-lapse movie of the growth phase (1-15 hours) of the *C. glutamicum* **Δ***aceE* microcolony, with 15 minutes between frames (see Figure 3B).

Supporting References

Lee, J.N., Park, C., Whitesides, G.M. (2003) Solvent compatibility of poly(dimethylsiloxane)-based microfluidic devices. *Anal. Chem.***75**: 6544-6554.

Xia, Y.N., Whitesides, G.M. (1998) Soft lithography. *Angewandte Chemie-International Edition***37**: 551-575.

6.2. Supplemental information (SI) - L-methionine producing mutants of *Corynebacterium glutamicum* isolated by biosensor-based high throughput screening

Table 1: Overview of mutations which were identified in genes coding for (putative) transcriptional regulators. Shown are mutations resulting in amino acid exchange (indicated by x), those that are silent and those leading to a stop codon.

Gene ID	Gene name and annotation	CgN373 mutant no. 16	CgN373 mutant no. 33	CgN373 mutant no. 75	Δ*mcbR* mutant no. 58	Δ*mcbR* mutant no. 62	Δ*mcbR* mutant no. 63
cg0012	*ssuR*, sulfonate utilization transcriptional regulator SsuR	x					x
cg0019	Putative transcriptional regulator, LysR-family		x	x			silent
cg0039	Putative transcriptional regulator		2 x	x		x	
cg0090	*citB*, two-component response regulator CitB			x, silent			
cg0146	*atlR*, transcriptional regulator for arabitol metabolism						x
cg0150	Putative transcriptional regulatory protein, Fic/Doc family		x			x	
cg0156	*cysR*, transcriptional regulator involved in sulfonate utilization, CysR	x					
cg0330	*cgtR1*, putative two component response regulator		x				
cg0343	Putative transcriptional regulator, MarR-family	x		x			
cg0725	Putative transcriptional regulator, MarR-family		x				
cg0897	*pdxR*, pyridoxine biosynthesis transcriptional regulator, aminotransferase	x		x		x, silent	
cg1084	*cgtR10*, putative two component response regulator			x			
cg1143	Putative transcriptional regulator, GntR-family	x					
cg1324	*rosR*, regulator of oxidative stress response			stop			
cg1410	*rbsR*, transcriptional repressor of ribose transport	x					
cg1648	Putative transcriptional regulator, RpiR-family			x			stop
cg2103	Transcriptional regulator, DtxR-family			x			
cg2115	*sugR*, DeoR-type transcriptional regulator of *ptsG*, *ptsS* and *cg2118-fruK-ptsF*	x					x
cg2140	*recX*, regulatory protein involved in DNA repair, RecX family			x			
cg2320	Putative transcriptional regulator, ArsR-family		x				
cg2516	Putative transcriptional regulator, HrcA-family						x
cg2544	Putative transcriptional regulator, GntR-family						x
cg2627	*pcaO*, transcriptional regulator of 4-hydroxybenzoate, protocatechuate, p-cresol pathway			x	x		x
cg2641	Putative transcriptional regulator, LuxR-family			x	silent		x
cg2648	Putative transcriptional regulator, ArsR-family	x	x	x			
cg2783	*gntR1*, gluconate-responsive repressors of genes involved in gluconate catabolism and the pentose phosphate pathway			x			
cg2910	Putative transcriptional regulator, LacI-family	x					
cg2965	Putative transcriptional regulator, Arac-family		2 x				
cg3061	*cgtR6*, putative two component response regulator		x				
cg3202	Transcriptional regulator, GntR-family	x			x	x	
cg3239	Putative transcriptional regulator, LysR-family				x		
cg3261	Putative transcriptional regulator, GntR-family				x		

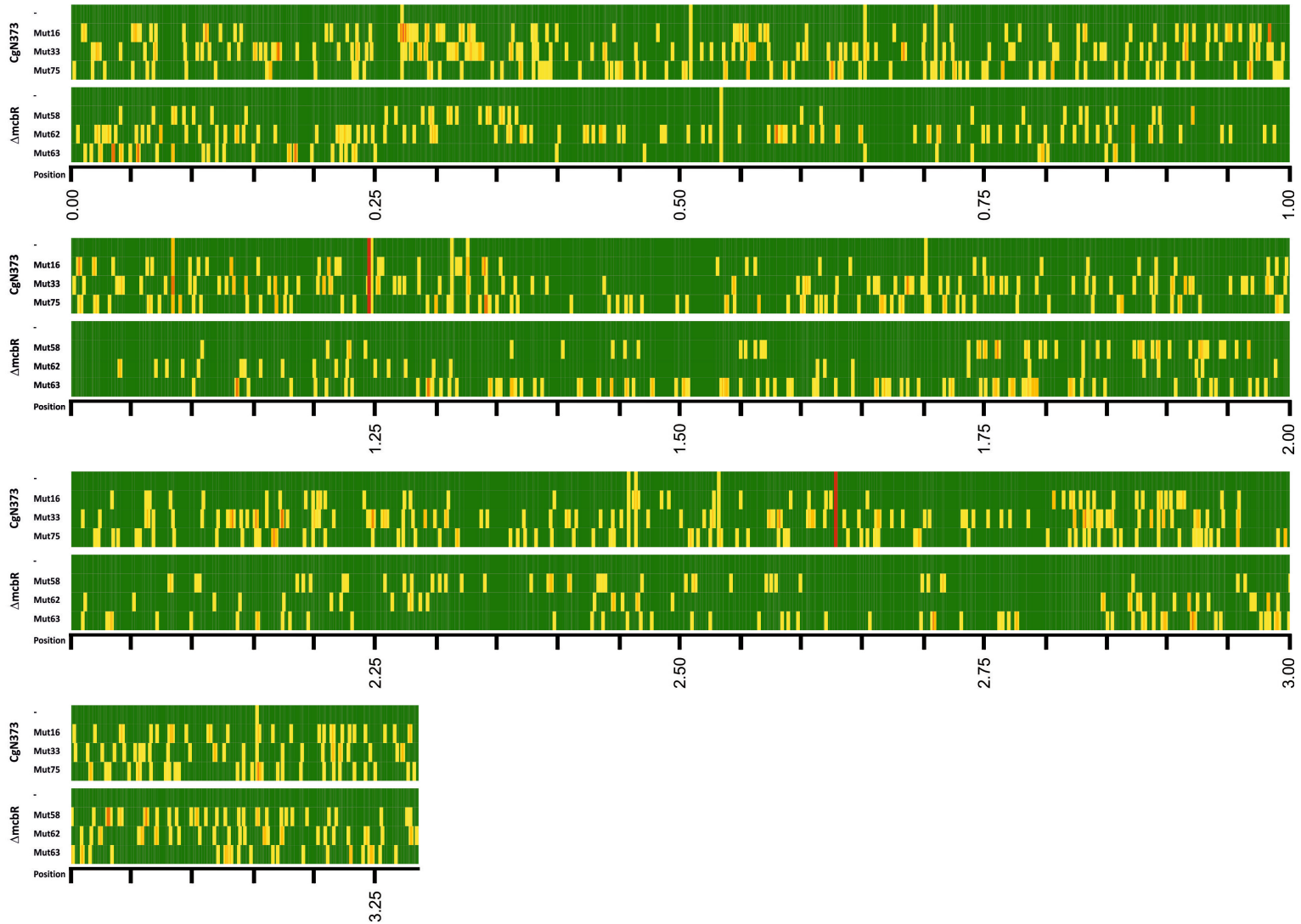

Figure S1: Localization of SNPs in the genome of CgN373, CgN373 mutant no. 16, CgN373 mutant no. 33, CgN373 mutant no. 75, *C. glutamicum* Δ*mcbR*, *C. glutamicum* Δ*mcbR* mutant no. 58, *C. glutamicum* Δ*mcbR* mutant no. 62 and *C. glutamicum* Δ*mcbR* mutant no. 63. Mutations were counted in a window (segment) of 3000 bp with a 1000 bp stepping. Segments in the respective mutants carrying one mutation are indicated in yellow, two mutations in orange, three mutations in dark orange, four mutations in red and no mutation in green.

JOURNAL OF BACTERIOLOGY, Dec. 2011, p. 6864–6873 Vol. 193, No. 24
0021-9193/11/$12.00 doi:10.1128/JB.05465-11

Deletion of the Aconitase Gene in *Corynebacterium glutamicum* Causes Strong Selection Pressure for Secondary Mutations Inactivating Citrate Synthase▽†

Meike Baumgart, Nurije Mustafi, Andreas Krug, and Michael Bott*

Institut für Bio- und Geowissenschaften, IBG-1: Biotechnologie, Forschungszentrum Jülich, D-52425 Jülich, Germany

Received 5 June 2011/Accepted 3 October 2011

The aconitase gene *acn* of *Corynebacterium glutamicum* is regulated by four transcriptional regulators, indicating that the synthesis of this enzyme is carefully controlled. To understand the causes for this elaborate regulation, the properties of the Δ*acn*-1 deletion mutant were analyzed in detail. The mutant was glutamate auxotrophic in glucose minimal medium, showed a strong growth defect, and secreted large amounts of acetate. None of these phenotypes could be complemented by plasmid-encoded aconitase, suggesting the presence of a secondary mutation. In fact, a point mutation within the *gltA* gene encoding citrate synthase was identified that caused the instability of the protein and an almost complete lack of its enzymatic activity. Subsequently, 27 further, independent Δ*acn* clones were isolated, and 15 of them were found to contain distinct mutations in *gltA*, causing the loss of citrate synthase activity. A similar result was observed for mutants lacking the isocitrate dehydrogenase gene *icd*. In this case, 8 of 24 Δ*icd* clones contained additional mutations in *gltA*. Indirect evidence was obtained that elevated intracellular citrate concentrations could be the cause of this selection pressure. Accordingly, the careful control of aconitase synthesis might have evolved due to the necessity to avoid inhibitory cytoplasmic citrate levels on the one hand and to prevent the excessive synthesis of an oxygen-sensitive protein requiring both iron and sulfur on the other hand.

For most organisms, the tricarboxylic acid (TCA) cycle, also known as the Krebs cycle, is a key metabolic pathway. In its catabolic function, acetyl-coenzyme A (CoA), a product of the degradation of sugars, fatty acids, amino acids, and other carbon sources, is oxidized to CO_2, thereby generating reducing equivalents (NADH and reduced quinones) for respiration and ATP by substrate-level phosphorylation. In its anabolic function, the TCA cycle produces 2-oxoglutarate and oxaloacetate as precursors of the glutamate family and the aspartate family of amino acids, respectively, in addition to other important intermediates, such as succinyl-CoA. Moreover, in many bacteria, NADPH is produced for biosynthetic purposes by the isocitrate dehydrogenase reaction.

The TCA cycle has been studied quite intensively in *Corynebacterium glutamicum*. This Gram-positive soil bacterium is used for large-scale industrial amino acid production, with the major products being the flavor enhancer L-glutamate (as monosodium salt) and the feed additive L-lysine, both of which are derived from intermediates of the TCA cycle. Many enzymes have been characterized, for example, citrate synthase (13), aconitase (4), isocitrate dehydrogenase (12), the 2-oxoglutarate dehydrogenase complex (25, 43, 59), fumarase (19), succinate dehydrogenase (34), malate-menaquinone oxidoreductase, and malate dehydrogenase (18, 40, 41). In addition, a complex regulatory network for the control of TCA cycle activity has been elucidated (for a review, see reference 7) that includes a variety of transcriptional regulators and a novel mechanism for the control of 2-oxoglutarate dehydrogenase activity involving the inhibitor protein OdhI, which acts as a phosphorylation-dependent molecular switch (43).

The relevance of individual TCA cycle enzymes in *C. glutamicum* has been explored with the help of mutants in which the corresponding genes were disrupted or deleted, such as strains lacking citrate synthase (13, 47), isocitrate dehydrogenase (12), 2-oxoglutarate dehydrogenase (25), malate-quinone oxidoreductase (41), and malate dehydrogenase (40, 41). In the case of citrate synthase, which catalyzes the first, irreversible step of the TCA cycle, this approach revealed the presence of alternative enzymes which can at least partially take over the function of the deleted protein. Initially it was shown that an inactivation of *gltA* (cg0949) leads to citrate or glutamate auxotrophy, suggesting that *gltA* codes for the only citrate synthase in *C. glutamicum* (13). Later, two methylcitrate synthases were identified, PrpC1 (cg0798) and PrpC2 (cg0762), which also can catalyze the formation of citrate from oxaloacetate and acetyl-CoA (47). Their activity usually is not sufficient to substitute for the one of GltA, but enhanced *prp* gene expression due to the inactivation of the repressor PrpR allows for the partial complementation of a Δ*gltA* mutant (47).

In the present work, we have analyzed the properties of aconitase deletion mutants. According to the genome sequence, *C. glutamicum* contains only a single aconitase gene, named *acn* (cg1737). No other enzyme that can metabolize citrate, such as citrate lyase or ATP-citrate lyase, currently is known in this species. Aconitase of *C. glutamicum* recently has been characterized biochemically and was found to have properties similar to those of aconitases from other sources (4). It contains a 4Fe-4S cluster and is highly oxygen sensitive. The

* Corresponding author. Mailing address: Institut für Bio- und Geowissenschaften, IBG-1: Biotechnologie, Forschungszentrum Jülich, D-52425 Jülich, Germany. Phone: 49 2461 613294. Fax: 49 2461 612710. E-mail: m.bott@fz-juelich.de.

† Supplemental material for this article may be found at http://jb.asm.org/.

▽ Published ahead of print on 7 October 2011.

TABLE 1. Strains and plasmids used in this study

Strain or plasmid	Relevant characteristic(s)	Source or reference
E. coli		
DH5α	F$^-$ ϕ80d*lac*Δ(*lacZ*)M15 Δ(*lacZYA-argF*)*U169 endA1 recA1 hsdR17* (r_K^- m_K^+) *deoR thi-1 phoA supE44* λ$^-$ *gyrA96 relA1*; used for cloning procedures	23
C. glutamicum		
ATCC 13032	Biotin-auxotrophic wild type	30
ATCC 13032 Δ*acn*-1, Δ*acn*-2, . . . , Δ*acn*-30 (inclusive)	Independently isolated clones with an in-frame deletion of the aconitase gene *acn*	This work
ATCC 13032 Δ*icd*-1, Δ*icd*-2, . . . , Δ*icd*-39 (inclusive)	Independently isolated clones with an in-frame deletion of the isocitrate dehydrogenase gene *icd*	This work
Plasmids		
pK19*mobsacB*	Kan^r; vector for allelic exchange in *C. glutamicum*; pK18 *ori*$V_{E.\ coli}$ *sacB*, *lacZ*α	51
pK19*mobsacB*-Δ*acn*	Kan^r; pK19*mobsacB* derivative containing a PCR product covering the up- and downstream regions of the *acn* gene	This work
pK19*mobsacB*-Δ*icd*	Kan^r; pK19*mobsacB* derivative containing a PCR product covering the up- and downstream regions of the *icd* gene	This work
pEKEx2	Kan^r; *C. glutamicum*/*E. coli* shuttle vector for regulated gene expression; P_{tac}, *lacI*^{q}, pBL1 *ori*$V_{C.\ glutamicum}$, pUC18 *ori*$V_{E.\ coli}$	11
pEKEx2-acn	Kan^r; pEKEx2 derivative containing the *acn* gene of *C. glutamicum* under the control of the *tac* promoter	This work
pAN6	Kan^r; *C. glutamicum*/*E. coli* shuttle vector for regulated gene expression, derivative of pEKEx2	16
pAN6-acn	Kan^r; pAN6 derivative containing the *acn* gene of *C. glutamicum* under the control of the *tac* promoter; expression without Strep tag	This work
pAN6-acn-gltA	Kan^r; pAN6 derivative containing the *acn* and the *gltA* gene of *C. glutamicum* under the control of the *tac* promoter	This work
pAN6-icd	Kan^r; pAN6 derivative containing the *icd* gene of *C. glutamicum* under the control of the *tac* promoter	This work
pAN6-icd-gltA	Kan^r; pAN6 derivative containing the *icd* and the *gltA* gene of *C. glutamicum* under the control of the *tac* promoter	This work
pAN6-citH	Kan^r; pAN6 derivative containing the *citH* gene of *C. glutamicum* under the control of the *tac* promoter	This work

expression of the *acn* gene is extensively regulated by at least four different transcriptional regulators, AcnR, RipA, RamA, and GlxR. Whereas the physiological role of *acn* repression by AcnR is not yet clear, repression by RipA is part of iron homeostasis and serves to reduce the iron demand under iron limitation (15, 33, 65). The activation of *acn* transcription by RamA serves to allow the increased carbon flux through the TCA cycle during growth on acetate (14). GlxR is a global regulator that directly influences the expression of about 14% of the annotated genes of *C. glutamicum* (31). It binds to the *acn* promoter and presumably represses its transcription in the presence of cyclic AMP (cAMP) (22).

In eukaryotes and some prokaryotes, aconitase also has a regulatory function by binding to certain mRNAs and inhibiting or increasing their translation (1, 3, 5, 24, 54–56). This function is exhibited only when the Fe-S cluster is absent (5, 64). In *Bacillus subtilis*, for example, aconitase is required for the late sporulation phase (52). The *Escherichia coli* enzymes AcnA and AcnB have been shown to positively autoregulate their synthesis under oxidative stress by stabilizing their own mRNA (54). In addition, both proteins were found to be involved in the control of superoxide dismutase (56). Whether *C. glutamicum* aconitase also exhibits a regulatory function by binding to certain mRNAs is not known yet.

In this work, a detailed analysis of aconitase deletion mutants of *C. glutamicum* was performed with the aim of understanding the reasons for the elaborate transcriptional regulation of the *acn* gene and to test for a possible regulatory function of aconitase. In the course of our studies, it became evident that the deletion of the *acn* gene causes a strong selection pressure for secondary mutations within the *gltA* gene, which might be caused by a growth-inhibitory level of cytoplasmic citrate.

MATERIALS AND METHODS

Bacterial strains, plasmids, and growth media. The bacterial strains and plasmids used in this study are listed in Table 1. The *C. glutamicum* type strain ATCC 13032 was used as the wild type. The Δ*acn* and Δ*icd* mutants are derivatives of the wild type containing an in-frame deletion of either the aconitase gene *acn* or the isocitrate dehydrogenase gene *icd*. For growth experiments, 20 ml of brain heart infusion broth (BHI; Difco Laboratories, Detroit, MI) supplemented with 4% (wt/vol) glucose (final concentration of 4.2% [wt/vol] glucose) was inoculated with a colony from a fresh BHI agar plate and incubated overnight at 30°C and 120 rpm. Cells of this preculture were washed once in phosphate-buffered saline (PBS; 137 mM NaCl, 2.7 mM KCl, 4.3 mM Na_2HPO_4, 1.4 mM KH_2PO_4, pH 7.3) and used to inoculate the main culture to an optical density at 600 nm (OD_{600}) of about 1. Main cultures were incubated at 30°C and 120 rpm in 500-ml baffled Erlenmeyer flasks containing 50 ml CGXII minimal medium (29) supplemented with 3,4-dihydroxybenzoate (30 mg liter^{-1}) as an iron chelator and glucose, L-glutamate, L-glutamine, or sodium citrate as a carbon source at the concentrations specified throughout the text. For high-performance liquid chromatography (HPLC) analyses, citrate determination, DNA microarrays, and two-dimension (2D) gel analysis, a second preculture was included using the same medium as that for the main culture. For plasmid-harboring strains, the medium was supplemented with 25 μg ml^{-1} kanamycin. For the induction of the expression of the target genes cloned into the expression plasmid pEKEx2 or pAN6, isopropyl β-D-1-thiogalactopyranoside (IPTG) was

used at the concentrations indicated. For cloning purposes, *Escherichia coli* DH5α was used and cultivated at 37°C in lysogeny broth (LB) (50).

Recombinant DNA work. The enzymes for recombinant DNA work were obtained from New England BioLabs (NEB; Frankfurt, Germany) or Fermentas (St. Leon-Rot, Germany). The oligonucleotides used in this study were obtained from Operon (Cologne, Germany) and are listed in Table S1 in the supplemental material. Routine methods, such as PCR, DNA restriction, and ligation, were performed using standard protocols (50). Chromosomal DNA of *C. glutamicum* was prepared as described previously (13). *E. coli* plasmids were isolated using the QIAprep spin miniprep kit (Qiagen, Hilden, Germany). *E. coli* was transformed using the RbCl method (23). *C. glutamicum* was transformed by electroporation (60). DNA sequencing was performed by AGOWA (Berlin, Germany).

The in-frame *acn* and *icd* deletion mutants of *C. glutamicum* were constructed via a two-step homologous recombination protocol as described previously (42). The up- and downstream regions (~500 bp) of the genes were amplified using the oligonucleotide pairs acn-A-fw-EcoRI/acn-B-rev, acn-C-fw/acn-D-BamHI, icd-A-fw-EcoRI/icd-B-rev, and icd-C-fw/icd-D-BamHI, respectively. The resulting PCR products served as templates for overlap extension PCR using the oligonucleotide pairs acn-A-fw-EcoRI/acn-D-BamHI and icd-A-fw-EcoRI/icd-D-BamHI. The resulting DNA fragments were digested with EcoRI and BamHI and cloned into pK19*mobsacB*. The plasmids were checked by sequencing to exclude errors. The transfer of the resulting plasmids pK19*mobsacB*-Δ*acn* and pK19*mobsacB*-Δ*icd* into *C. glutamicum* and screening for the first and second recombination event were performed as described previously (42). Kanamycin-sensitive and saccharose-resistant clones were tested by colony PCR analysis with the oligonucleotide pairs acn-upstream/acn-D-BamHI and icd-upstream/icd-D-BamHI for the deletion of *acn* and *icd*, respectively.

For the construction of plasmid pEKEx2-acn, the *acn* coding region of the *C. glutamicum* wild type was amplified with an artificial ribosome binding site using the oligonucleotide pair acn-RBS-BamHI-fw/acn-BamHI-rv and cloned into the BamHI site of pEKEx2. The plasmid was sequenced to exclude errors. For complementation experiments, the plasmids pAN6-acn and pAN6-acn-gltA were constructed as follows. The *acn* coding region was amplified using the primer pair acn-NdeI-fw/acn-NheI-STOP-rv and cloned into pAN6 via the NdeI and NheI sites. The plasmid was sequenced to exclude errors. The *gltA* coding region was amplified using the primer pair gltA-RBS-NheI-fw/gltA-NheI-rv, which introduces a ribosome binding site (GAGATA) 5 bp upstream of the start codon of *gltA*. The product was cloned into the NheI site of pAN6-acn. The sequence and the orientation of *gltA* in pAN6-acn-gltA were checked by sequencing. The plasmids pAN6-icd and pAN6-icd-gltA were constructed analogously. The *icd* coding region was amplified using the primer pair icd-NheI-fw/icd and cloned into pAN6 via the NdeI and NheI sites. The cloning of the *gltA* gene was performed as described above.

Determination of specific activities of aconitase and citrate synthase. Aconitase activity was measured in cell extracts as described previously (33). For citrate synthase activity measurements, the Δ*acn* strains were grown for 16 h in 50 ml BHI medium supplemented with 4% (wt/vol) glucose, harvested, washed once in 50 mM Tris-HCl buffer (pH 7.5), and resuspended in a buffer (the volume was equal to the OD of the culture multiplied by 0.2 ml) containing 50 mM Tris-HCl, pH 7.5, and 200 mM potassium glutamate. One ml of the cell suspension was mixed with 250 mg zirconia/silica beads (0.1-mm diameter; Biospec, Bartlesville, OK) in a 2-ml Eppendorf tube, and the cells were mechanically disrupted by three 30-s shakings in a Silamat S5 (Ivoclar Vivadent, Ellwangen, Germany). For the determination of citrate synthase activity in Δ*icd* mutants, 1 ml of the cell suspension was mixed with 400 mg zirconia/silica beads in a 2-ml screw-cap tube, and the cells were mechanically disrupted by 3 min of shaking in a SpeedMill P12 homogenizer (Analytik Jena AG, Jena, Germany). Cell debris and unbroken cells were separated by two 15-min centrifugations at 16,000 × *g* at 4°C. Between the two centrifugation steps the supernatant was transferred to a new tube. The resulting cell extract was kept on ice until it was used for the assay, which was based on the reaction of coenzyme A with 5,5′-dithiobis(2-nitrobenzoic acid). The absorbance of the resulting yellow 2-nitro-5-thiobenzoate dianion was measured spectrophotometrically at 412 nm as described previously (47). Protein concentrations were determined using the bicinchoninic acid (BCA) protein assay kit (Pierce, Bonn, Germany) with bovine serum albumin as the standard.

Determination of glucose and organic acids. Glucose and organic acid concentrations in supernatants were determined by ion-exchange chromatography using an Agilent 1100 LC system (Agilent Technologies, Waldbronn, Germany) equipped with a cation exchange column (organic acid Refil column; 300 by 8 mm; CS-Chromatography GmbH, Langerwehe, Germany). Substances were eluted with 100 mM H_2SO_4 for 42 min at 40°C using a flow rate of 0.4 ml min^{-1}. Eluted organic acids and glucose were detected by a diode array detector at a wavelength of 215 nm or by a refraction index detector, respectively. The substances were quantified by comparing the signal areas with calibration curves based on external standards. Citrate concentrations also were determined enzymatically using a citrate assay kit (Megazyme, Bray, Ireland) according to the manufacturer's instructions.

Western blot analysis. For the detection of citrate synthase, aconitase, or isocitrate dehydrogenase in cell extracts of *C. glutamicum* strains, Western blot analysis was performed. Cell extract corresponding to 10 μg protein was separated on sodium dodecyl sulfate (SDS)-polyacrylamide gels (10% separating gel) and then electroblotted onto a nitrocellulose membrane (Hybond-C extra; GE Healthcare, Munich, Germany) using a Transblot semidry transfer cell (Bio-Rad, München, Germany) and buffer containing 25 mM Tris, 192 mM glycine, and 20% methanol (58). The blocking of nonspecific binding was performed with 5% (wt/vol) skim-milk powder in PBST buffer (137 mM NaCl, 2.7 mM KCl, 4.3 mM Na_2HPO_4, 1.4 mM KH_2PO_4, 500 μl l^{-1} Tween 20). Polyclonal rabbit antibodies were prepared against purified citrate synthase, aconitase, and isocitrate dehydrogenase of *C. glutamicum* by BioGenes (Berlin, Germany). The primary antibodies were used in a 1:10,000 dilution. The secondary antibody was a goat anti-rabbit immunoglobulin G alkaline phosphatase conjugate (Bio-Rad) and used at a 1:10,000 dilution. Detection was performed in alkaline phosphatase buffer (100 mM Tris-HCl, pH 9.5, 100 mM NaCl, 10 mM $MgCl_2$) containing 0.3 g $liter^{-1}$ nitroblue tetrazolium chloride and 0.2 g $liter^{-1}$ 5-bromo-4-chloro-3-indolylphosphate.

Sequencing of the *gltA* coding region in selected clones of *C. glutamicum*. To sequence the *gltA* gene of selected *C. glutamicum* strains, the *gltA* coding region, including the promoters, was amplified by colony PCR using the primers gltA-fw and gltA-rv. The PCR product was purified and sequenced using the primers gltA-seq-f and gltA-seq-b, which anneal roughly in the middle of the *gltA* gene facing in opposite directions.

RESULTS

Phenotypic properties of an aconitase deletion mutant. To study the role of aconitase in *Corynebacterium glutamicum*, *acn* (cg1737) in-frame deletion mutants were constructed and verified by colony PCR as described in Materials and Methods. Four independent clones were isolated (Δ*acn*-1 to Δ*acn*-4 clones), and the Δ*acn*-1 clone was chosen for further characterization. As expected, the mutant was not able to grow in CGXII glucose minimal medium without the supplementation of L-glutamate or L-glutamine. As shown in Fig. S1 in the supplemental material, the final optical density (OD_{600}) depended on the glutamate or glutamine concentration. The maximal optical densities achieved were ~5 for 5 mM L-glutamine, ~10 for 20 mM L-glutamine, ~17 for 40 mM L-glutamine, and ~30 for 100 mM L-glutamine or L-glutamate. The growth rates were about 0.15 h^{-1} for 5, 20, and 40 mM L-glutamine and about 0.18 h^{-1} for 100 mM L-glutamine or L-glutamate. Under the given conditions, the *C. glutamicum* wild type showed a growth rate of about 0.35 h^{-1} and a final OD_{600} of about 60 to 70.

The deletion of the *acn* gene also was confirmed by measuring the specific activity of aconitase in cell extracts. Whereas the wild type showed a specific activity of 0.20 ± 0.05 U mg^{-1}, which corresponds to previously published values (33), only background activity (<0.01 U mg^{-1}) was found for the Δ*acn*-1 strain. Aconitase activity could be restored (2.44 ± 0.37 U mg^{-1}) by introducing a plasmid encoding aconitase (pEKEx2-acn) into *C. glutamicum* Δ*acn*-1 and the induction of expression with 1 mM IPTG. Surprisingly, neither the growth defect nor the glutamate auxotrophy could be complemented.

Organic acid formation in the wild type and Δ*acn* mutant. Transcriptome and proteome analyses of the Δ*acn*-1 mutant in the exponential growth phase at an OD_{600} of about 5 revealed strongly increased mRNA and protein levels for enzymes involved in acetate metabolism, in particular for isocitrate lyase

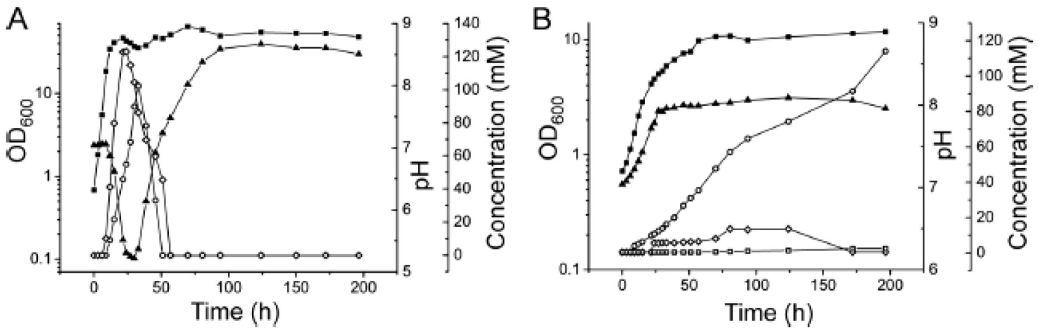

FIG. 1. Growth, pH profile, and organic acid production of the *C. glutamicum* wild type (A) and the Δ*acn*-1 mutant (B). Cells were cultivated in CGXII medium with 4% (wt/vol) glucose and 100 mM L-glutamate. At the indicated time points, 1-ml samples were taken and used for the determination of the optical density (OD_{600}). Subsequently, the samples were centrifuged and the supernatant was used for pH and HPLC analysis. ■, OD_{600}; ▲, pH; ○, acetate; ◇, lactate; □, citrate. Representative results from three independent experiments are shown. In the supernatant of the wild-type culture, citrate could not be detected by HPLC, therefore the corresponding curve was omitted.

and malate synthase (see sections SD and SE in the supplemental material). As these enzymes are known to be induced in the presence of acetate (48, 49), the excretion of organic acids and the pH profile of the mutant and the wild type were measured during cultivation in CGXII minimal medium containing 222 mM glucose and 100 mM L-glutamate. In the exponential growth phase, the pH of the wild-type cultures dropped significantly to about 5.2 due to the accumulation of lactate (up to 120 mM) and acetate (up to 100 mM) in the medium (Fig. 1A). When the cells reached the stationary growth phase, lactate and acetate were consumed again, causing a rise of the pH, which finally stabilized at about 8.0. The accumulation of lactate is a consequence of oxygen limitation and is typical for the cultivation conditions used. In contrast, the strong acetate formation is not observed in CGXII medium containing only glucose as a carbon source. Perhaps the flux into the TCA cycle is partially controlled by the availability of glutamate and becomes reduced when high concentrations of glutamate are present, leading to increased acetate secretion. Both lactate and acetate formation started when the wild-type cultures had reached an OD_{600} of about 18. The profiles of the Δ*acn*-1 strain were very different from that of the wild type (Fig. 1B). Besides the lower growth rate and the lower final OD, the pH never dropped but started to increase right from the beginning of the cultivation and stabilized at around pH 8.0. Lactate formation was strongly reduced and reached concentrations of only 15 mM. In contrast, acetate was excreted immediately after the start of the cultivation and reached final concentrations of up to 120 mM. The acetate was not consumed again. Minor concentrations of citrate (at most 2 mM) were detected in the supernatant of stationary-phase cultures of the Δ*acn*-1 mutant, whereas citrate was not detectable by HPLC in the supernatant of the wild-type cultures. When an enzymatic assay was used, citrate concentrations at a maximum of 0.5 mM were detected in the wild-type culture supernatants (data not shown).

The observation that the Δ*acn*-1 mutant formed acetate right from the beginning of the cultivation explains the strongly increased mRNA levels of the isocitrate lyase (*aceA*) and malate synthase (*aceB*) genes compared to those of the wild type (see Table S4 in the supplemental material). The transcription of *aceA* and *aceB* is known to be strongly activated in the presence of acetate by the transcriptional regulator RamA (10). The RNA used for the DNA microarray experiments was isolated from cells at an OD_{600} of about 5, at which point the wild type had not yet started forming acetate.

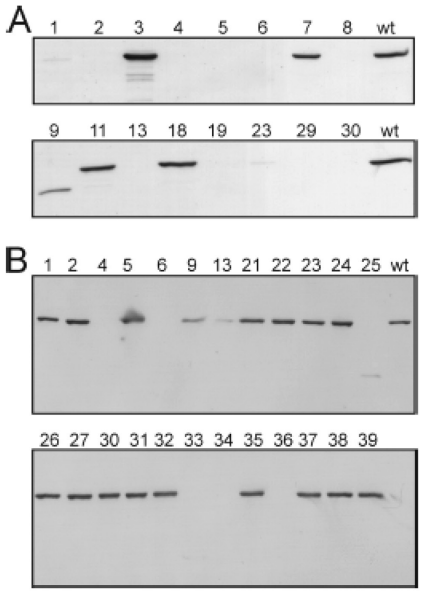

FIG. 2. Western blot analysis of selected Δ*acn* and Δ*icd* clones with citrate synthase-specific antibodies. (A) Western blot with citrate synthase-specific antibodies of the Δ*acn* clones carrying a mutation in the chromosomal *gltA* gene. (B) Western blot analysis of all Δ*icd* clones analyzed in this work. Cells were cultivated in BHI medium supplemented with 4% (wt/vol) glucose for 16 h, harvested, and washed once with PBS buffer. The cells were disrupted, and cell extract corresponding to 10 μg protein (A) or 8 μg protein (B) was used for SDS-PAGE. The proteins then were blotted onto a nitrocellulose membrane. The membranes were probed with polyclonal citrate synthase-specific rabbit antibodies and an anti-rabbit alkaline phosphatase-conjugated secondary antibody. The numbers above the lanes are those given to the individual Δ*acn* or Δ*icd* clones tested. wt, *C. glutamicum* wild type.

TABLE 2. Overview of the Δ*acn* clones analyzed in this study

Wild type or Δ*acn* mutant no.	Change in:		Presence of citrate synthase:	
	gltA[a]	GltA[b]	Protein[c]	Activity[d]
Wild type			+	+
1	C1196→T	Pro399→Leu	−	−
2	C385→T	Gln129→STOP	−	−
3	C723→A	Asn24→Lys	+	−
4	IS*Cg1d* (cg2600) insertion before G160, Gly54		−	−
5	Insertion of A at A899	Frameshift	−	−
6	IS*Cg13b* (cg1782) insertion 50 bp upstream of start codon		−	−
7	C1255→T	Pro419→Ser	+	−
8	IS*Cg5* (cg0824 or cg2915) insertion before A124, Met42		−	−
9	C1017-A1223 missing	69 amino acids missing	+ (smaller)[e]	−
10			+	+
11	C188→T	Ser63→Leu	+	−
12			+	+
13	G1127-T1172 doubled	Frameshift	−	−
14			+	+
15			+	+
16			+	+
18	A947→T	His316→Leu	+	−
19	C493→T	Gln165→STOP	−	−
20			+	+
21			+	+
22			+	+
23	IS*Cg1a* (cg1213) insertion in the −10 region of promoter P1		(+)[f]	−
24a			+	+
24b			+	+
27			+	+
28			+	+
29	+C after C538	Frameshift	−	−
30	T941 missing	Frameshift	−	−

[a] Mutation on the DNA level.
[b] Consequences on the protein level.
[c] Plus and minus indicate that the protein was detectable or undetectable, respectively, by Western blotting.
[d] A plus indicates activity of >0.5 U (mg protein)$^{-1}$; a minus indicates background activity of <0.03 U (mg protein)$^{-1}$. Measurements were performed in triplicate with cell extract from one culture of each mutant.
[e] Due to the partial deletion of 207 bp, the resulting protein is 69 amino acids smaller than the native protein (41.0 kDa and 48.9 kDa, respectively).
[f] Due to the insertion of the IS element into the promoter of *gltA*, the strain shows an intermediate phenotype with a significantly reduced amount of citrate synthase protein present in the cell [indicated by (+)].

Activity and content of citrate synthase in selected *C. glutamicum* strains. In view of the fact that the citrate synthase reaction is irreversible under physiological conditions and no other citrate-converting enzymes besides aconitase are known in *C. glutamicum*, higher concentrations of citrate had been expected in the Δ*acn*-1 mutant. The oxaloacetate required for citrate synthesis can be formed by phosphoenolpyruvate (PEP) carboxylase, pyruvate carboxylase, or from glutamate via the TCA cycle. One explanation for the low citrate accumulation could be low citrate synthase activity. To test this hypothesis, both the enzymatic activity and the protein level of citrate synthase were determined. With 0.016 U mg^{-1}, citrate synthase activity of cell extracts of the *C. glutamicum* Δ*acn*-1 and Δ*acn*-3 strains was about 50 times decreased compared to that of the wild type (0.756 U mg^{-1}). The residual activity of the Δ*acn*-1 strain is similar to that measured in a *gltA* insertion mutant (13). To probe whether citrate synthase is present (but inactive) in or absent from *C. glutamicum* Δ*acn*, a Western blot analysis with citrate synthase-specific antibodies was performed. It revealed close to wild-type levels of citrate synthase in the Δ*acn*-3 strain but an almost complete absence of citrate synthase protein from the Δ*acn*-1 strain (Fig. 2A).

Identification of secondary mutations in Δ*acn* strains causing the loss of citrate synthase activity. The results described above suggested the presence of mutations in the citrate synthase genes of the aconitase deletion strains. Therefore, the *gltA* coding region in Δ*acn*-1 and Δ*acn*-3 strains was sequenced. In the Δ*acn*-1 strain, a mutation causing a Pro399→Leu exchange that presumably leads to the misfolding and subsequent degradation of the mutated protein was detected. The *gltA* gene of the Δ*acn*-3 strain contained a mutation leading to an Asn241→Lys exchange, which probably caused an inactivation of citrate synthase. With the knowledge of these secondary mutations in *gltA*, another approach was used to complement the glutamate auxotrophy of the Δ*acn*-1 strain with an expression plasmid containing not only *acn* but also *gltA* (pAN6-acn-gltA). In this case, both the glutamate auxotrophy and the growth defect could be abolished (see Fig. S2 in the supplemental material).

To test whether the absence of aconitase always causes suppressor mutations within the *gltA* gene, new Δ*acn* clones were isolated and analyzed by the sequencing of the *gltA* gene, citrate synthase activity assays, and Western blot analysis with citrate synthase-specific antibodies. Table 2 shows an overview of the results. Of the 28 Δ*acn* clones in total, 16 contained an

TABLE 3. Overview of the Δ*icd* clones analyzed in this study

Wild type or Δ*icd* mutant no.	Change in:		Presence[f] of citrate synthase:	
	gltA[a]	GltA[b]	Protein[c]	Activity[d]
Wild type			+	+
1			+	+
2			+	+
4	IS*Cg1d* (cg2600) insertion before G160, Gly54		−	−
5			+	+
6	IS*Cg1a* (cg1213) insertion before G160, Gly54		−	−
9	IS*Cg1* between P1 and P2, 292 bp upstream of the translational start		(+)	(+)[e]
13	IS*Cg1b* (cg2725) between P1 and P2, 146 bp upstream of the translational start		(±)	(±)[e]
21			+	+
22			+	+
23			+	+
24			+	+
25	C966 missing	Frameshift	(+) (smaller)[g]	−
26			+	+
27			+	+
30			+	+
31			+	+
32			+	+
34	+A after A972	Frameshift	−	−
35			+	+
36	A552-C564 missing		−	−
37			+	+
38			+	+
39			+	+
Δicd_old	G161→T	Gly54→Val	+	−

[a] Mutation on the DNA level.
[b] Consequences on the protein level.
[c] Plus and minus indicate that the protein was detectable or undetectable, respectively, by Western blotting.
[d] A plus indicates activity of >0.25 U (mg protein)$^{-1}$; a minus indicates background activity of <0.03 U (mg protein)$^{-1}$. Measurements were performed in triplicate with cell extract from one culture of each mutant.
[e] Δ*icd*-9 strain, 0.18 U (mg protein)$^{-1}$; Δ*icd*-3 strain, 0.04 (mg protein)$^{-1}$.
[f] Symbols indicate amounts of protein in the following order: + > (+) > (±) > −.
[g] Due to a frameshift caused by the absence of C966, the resulting protein is 115 amino acids smaller than the native protein (35.6 kDa and 48.9 kDa, respectively).

altered *gltA* gene, and remarkably all 16 *gltA* mutations were different. The following mutations were observed: five single amino acid exchanges, four insertion sequence (IS) element insertions, three frameshifts, two nonsense mutations, one 200-bp deletion, and one partial duplication. Whenever a mutation was observed in the *gltA* coding region, there was no citrate synthase activity measurable in the cell extract of the respective clone (Table 2). Figure 2A shows the Western blot analysis of the Δ*acn* clones with a mutated *gltA* gene. The majority of the clones (no. 1, 2, 4, 5, 6, 8, 13, 19, 23, 29, and 30) lacked detectable citrate synthase protein. The clones 3, 7, 11, and 18 contained citrate synthase protein in amounts close to the wild-type level, and clone 9 contains a shortened version of citrate synthase caused by the partial deletion.

Analysis of Δ*icd* strains. During the studies of the Δ*acn* strains, a Δ*icd* strain was tested and showed no citrate synthase activity. The sequencing of the *gltA* gene of this strain revealed a Gly54→Val exchange (Table 3, Δ*icd*_old). The deletion of *icd* therefore seemed to have an effect similar to that of the *acn* deletion. To further test this hypothesis, 23 additional Δ*icd* clones were isolated and analyzed by the sequencing of the *gltA* gene, citrate synthase activity assays, and Western blot analysis with citrate synthase-specific antibodies (Fig. 2B and Table 3). The Western blot also was probed with isocitrate dehydrogenase-specific antibodies to confirm the absence of this enzyme. Eight of 24 Δ*icd* clones contained a mutated *gltA* gene. Interestingly, two of the eight clones carried an IS element between the two promoters of *gltA*, which in the case of the Δ*icd*-9 strain was located further upstream of the transcriptional start site than in the case of the Δ*icd*-13 mutant. The Δ*icd*-13 clone showed a strong decrease of citrate synthase activity and protein content, whereas the Δ*icd*-9 clone showed an intermediate phenotype.

Complementation studies were performed with the Δ*icd*-2 (active citrate synthase) and Δ*icd*-4 (inactive citrate synthase) strains using the plasmids pAN6, pAN6-icd, and pAN6-icd-gltA. The glutamate auxotrophy of the Δ*icd*-2 strain containing an intact *gltA* gene could be complemented with pAN6-icd, whereas for the complementation of the Δ*icd*-4 mutant with a mutated *gltA* gene the plasmid encoding both isocitrate dehydrogenase and citrate synthase was necessary (data not shown). The results suggest that the selection pressure for citrate synthase inactivation is less strong in Δ*icd* mutants than in Δ*acn* mutants, which might be related to the possibility that Δ*icd* mutants metabolize isocitrate via the glyoxylate shunt.

Evidence for growth inhibition by cytoplasmic citrate accumulation. The results reported above show that the deletion of the aconitase gene or the isocitrate dehydrogenase gene in *C. glutamicum* triggered a selection pressure for secondary mutations in the citrate synthase gene, causing the loss of citrate synthase activity. A possible reason for this phenomenon could be a growth-inhibitory effect of elevated intracellular citrate levels. By gas chromatography-mass spectrometry (GC-MS) analysis, it was shown qualitatively that the Δ*acn*-1 strain in fact

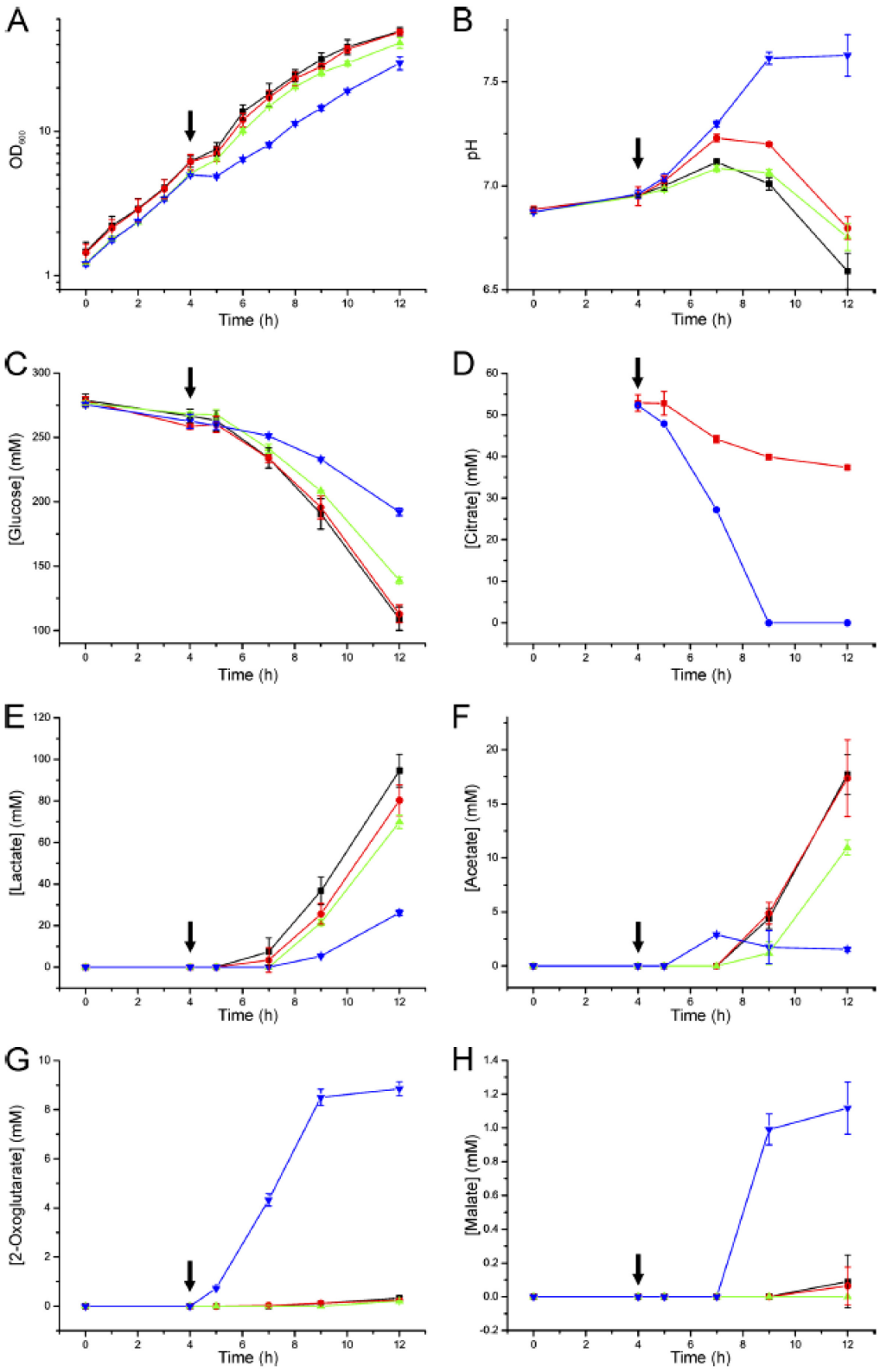
A
OD600
Time (h)
B
pH
Time (h)
C
[Glucose] (mM)
Time (h)
D
[Citrate] (mM)
Time (h)
E
[Lactate] (mM)
Time (h)
F
[Acetate] (mM)
Time (h)
G
[2-Oxoglutarate] (mM)
Time (h)
H
[Malate] (mM)
Time (h)

contained significantly more citrate within the cells than the wild type cultivated under the same conditions (data not shown). To get some evidence for the growth-inhibitory effect of citrate, an experiment was performed in which *C. glutamicum* faces a sudden import of citrate into the cell. Citrate utilization and its regulation have been studied recently in *C. glutamicum* (8, 44). This species possesses two citrate uptake systems, CitH and TctABC. Citrate transport by CitH is dependent on Ca^{2+} or Sr^{2+}, whereas TctCBA requires Mg^{2+} or Ca^{2+}. The transcription of *citH* and *tctCBA* is activated by a two-component regulatory system composed of the sensor kinase CitA and the response regulator CitB when citrate is present in the medium. Cells adapted to citrate consumed it in parallel with glucose.

To analyze the response to a sudden high intracellular citrate concentration, the *C. glutamicum* wild type was transformed with the expression plasmid pAN6-citH, which carries the *citH* gene under the control of the *tac* promoter. The experimental setup is presented in Fig. S4 in the supplemental material. Two parallel cultures of the wild type carrying pAN6-citH and of the wild type carrying the control plasmid pAN6 were grown in CGXII glucose medium with 1 mM IPTG. After 4 h, 50 mM sodium citrate and 5 mM $CaCl_2$ were added to one set, whereas no addition was made to the second set of cultures. Samples were taken during cultivation and analyzed for OD_{600}, pH, substrate consumption, and organic acid production (Fig. 3). Before the addition of citrate, all strains showed the same growth rate. After the addition of citrate, a weak transient growth defect was observed for the control strain carrying pAN6 and for the cultures that were not supplemented with citrate. This was due to the multiple samplings at this time point and was not observed in experiments where only a single sample was taken (data not shown). Strikingly, citrate addition to the strain overexpressing *citH* caused a complete growth stop, which lasted for about 1 h. Thereafter the culture resumed growth and reached a similar growth rate and the same final OD_{600} as the control cultures. Regarding the pH profile, glucose consumption, lactate formation, and acetate formation, the cultures with and without citrate of the strain carrying pAN6 and the cultures without citrate of the strain carrying pAN6-citH behaved similarly (Fig. 3). In contrast, the cultures with citrate of the strain carrying pAN-citH showed very different behavior. The pH significantly increased after citrate addition and remained in the alkaline region. Glucose consumption was significantly retarded, whereas citrate was rapidly consumed. In the control strain carrying pAN6, measurable citrate utilization started after a lag phase of about 1 h, which presumably was required for the activation of *citH* and *tctCBA* expression by the CitAB two-component system. Lactate and acetate formation of the citrate-containing cultures of the strain with pAN6-citH was much lower than that of the other cultures, presumably due to the reduced glucose consumption. Instead, immediately after citrate addition this strain started to excrete 2-oxoglutarate (up to 10 mM) and, later, small concentrations (1.5 mM) of malate. The formation of 2-oxoglutarate indicates a metabolic bottleneck at the 2-oxoglutarate dehydrogenase complex.

To get clues to the mechanism of citrate toxicity, the transcriptomes of the wild type carrying pAN6-citH 20 min after citrate addition and those before citrate addition were compared (see Table S7 in the supplemental material). In total, 864 genes showed a more than 2-fold altered mRNA ratio. A similar comparison was done for the control strain carrying pAN6, and in this case 218 genes had an mRNA level altered 2-fold (see Table S8 in the supplemental material). Despite these many changes, it was not possible to get obvious hints on the mechanisms of citrate toxicity. However, the fact that a sudden rapid uptake of citrate leads to a complete, transient growth stop supports the assumption that high intracellular citrate concentrations are harmful to *C. glutamicum* cells.

DISCUSSION

The results described in this work show that the deletion of the aconitase gene or of the isocitrate dehydrogenase gene in *C. glutamicum* causes selection pressure to lose citrate synthase activity (Tables 2 and 3). In four of the Δ*acn* and four of the Δ*icd* mutants, *gltA* (or its promoter region) was disrupted by the transposition of IS elements. The genome of *C. glutamicum* ATCC 13032 contains 24 IS elements (27), and so far only two of them have been analyzed further, IS*Cg1* (62) and IS*Cg2* (46). Our results show that IS*Cg1*, IS*Cg5*, and IS*Cg13* are induced in *C. glutamicum* under citrate stress conditions.

The strong selection pressure in Δ*acn* and Δ*icd* mutants for secondary mutations in the *gltA* gene was assumed to be due to a toxic effect of citrate accumulation in the cells. In the food industry, sodium citrate is used as an antibacterial agent (36), confirming that this metabolite can inhibit growth when present at unphysiologically high concentrations. *C. glutamicum* presumably possesses no alternative enzymes or pathways for citrate catabolism (6) except for aconitase and the TCA cycle. The mechanism(s) of the assumed toxic effect of elevated citrate concentrations still is not clear, but it seems to be important for *C. glutamicum* to keep the intracellular citrate level below a certain threshold. This also can explain why the expression of aconitase and citrate synthase (61) is extensively controlled at the transcriptional level by three or four different regulators and perhaps also by additional, still unknown mechanisms.

FIG. 3. Influence of citrate addition on growth, pH profile, substrate consumption, and product formation of the *C. glutamicum* wild type carrying either pAN6-citH (green and blue symbols) or the control plasmid pAN6 (black and red symbols). After the first preculture in BHI medium during the day, a second preculture was performed in CGXII minimal medium with 4% (wt/vol) glucose, 25 μg/ml kanamycin, and 100 μM IPTG overnight. The main culture was performed in CGXII minimal medium with 4% (wt/vol) glucose, 25 μg/ml kanamycin, and 1 mM IPTG. After 4 h of cultivation (OD_{600} ~5), two of the cultures (indicated by the blue and red symbols) were supplemented with 50 mM trisodium citrate and 5 mM $CaCl_2$ (black arrows), whereas the two other cultures did not receive a supplement (green and black symbols). Samples were taken at the indicated time points and analyzed for OD_{600} (A), pH of the supernatant (B), glucose consumption (C), citrate consumption (D), lactate formation (E), acetate formation (F), 2-oxoglutarate formation (G), and malate formation (H). The data shown are average values and standard deviations from three independent cultivations.

Studies on the phenotype of aconitase or isocitrate deletion mutants have been performed with a number of different organisms. In the Gram-positive soil bacterium *Bacillus subtilis*, the mutation of *citB* coding for an aconitase leads to glutamate auxotrophy and to an early sporulation defect (9). Aconitase deletion strains accumulated up to 2 mM citrate in the culture supernatant. The supplementation of the growth medium with a high excess of Mn or Fe ions could partially complement the sporulation defect, indicating that it partially results from a restricted availability of these cations due to their chelation by citrate. A triple mutant lacking *citB*, *citA*, and *citZ* (the latter two genes code for citrate synthases) had a 100-fold higher sporulation frequency than the *citB* single mutant and did not accumulate citrate. Comparable results were observed for Δ*icd* mutants of *B. subtilis* (26, 38).

The Gram-negative bacterium *E. coli* possesses two genes coding for aconitases (*acnA* and *acnB*). An *acnA* single deletion mutant did not show a growth defect, probably because the aconitase activity was taken over by AcnB (21). The growth of an *acnB* single mutant was impaired but not abolished in glucose minimal medium (20). An *acnAB* mutant did not grow in glutamate-supplemented glucose minimal medium under aerobic conditions until it became rapidly overgrown by mutants that also lacked citrate synthase activity (20). In 1976 it was reported that *E. coli* strains lacking both *icd* and *gltA* grew faster than *icd* single mutants (35). For an isocitrate dehydrogenase deletion mutant of *E. coli* BL21(DE3), it could be shown that this strain accumulates large amounts of citrate and isocitrate intracellularly (up to 11.8 and 0.5 mM, respectively) as well as in the medium (up to 3.5 and 0.4 mM, respectively) (2).

Another organism which was subject to aconitase deletion studies is *Streptomyces coelicolor* (63). As in *C. glutamicum* and *B. subtilis*, *S. coelicolor* has just one aconitase gene (*acoA*), and its deletion leads to glutamate auxotrophy in glucose minimal medium and to defects in growth, antibiotic biosynthesis, and aerial hypha formation (63). The mutant secreted citrate (up to 14 mM), acetate (up to 11 mM), and pyruvate (up to 0.45 mM), causing an acidification of the growth medium to a pH of about 3.5. The growth defect of the *acoA* single mutant could be partially suppressed by an additional mutation of the *citA* gene coding for citrate synthase. For the nitrogen-fixing bacterium *Sinorhizobium meliloti* 1021, it was shown that the deletion of citrate synthase can restore the growth of an aconitase deletion mutant (32). For Δ*icd* mutants of this bacterium, it was observed that there appeared to be spontaneous mutations in the gene coding for citrate synthase (39). For the human pathogen *Staphylococcus aureus*, an aconitase deletion mutant has been described (53), but its growth properties in glucose-based minimal medium have not been described. In *Bradyrhizobium japonicum*, the deletion of *acnA* did not lead to a clear glutamate auxotrophy, but growth was severely inhibited and could not be restored by the supplementation of the medium with glutamate (57). As only a single aconitase gene was found in the *B. japonicum* genome sequence (28), the *acnA* disruptant may possess some residual aconitase activity.

The effect of aconitase and isocitrate dehydrogenase deletions on citrate synthase is not restricted to prokaryotes, as a similar phenomenon also was found in yeast. It was shown that Δ*icd* and Δ*aco1* mutants of *Saccharomyces cerevisiae* share several growth phenotypes, for example, poor growth on glycerol, an inability to grow with acetate as the sole carbon source, or a propensity to generate petite segregants, which can be complemented or at least moderated by the codisruption of *cit1* coding for mitochondrial citrate synthase (17, 37, 45).

From this literature survey, it is obvious that several microorganisms lacking aconitase or isocitrate dehydrogenase showed a less severe growth phenotype when citrate synthase activity was absent simultaneously. This study is the first one, however, in which secondary mutations in the citrate synthase gene caused by the deletion of *acn* or *icd* were analyzed in detail and in a set of more than 50 independent mutants. Our results demonstrate that it is impossible to characterize a definitive Δ*acn* mutant, because different clones can vary significantly.

An important result was the finding that the inactivation of citrate synthase is not the only solution to cope with the stress caused by the absence of aconitase or isocitrate dehydrogenase, as 12 Δ*acn* and 16 Δ*icd* mutants were found to have intact citrate synthases.

Further studies, including genome sequence analysis, are required to understand how these mutants handle the stress situation.

ACKNOWLEDGMENTS

This work was supported by the Bundesministerium für Bildung und Forschung (BMBF) and by Evonik Degussa GmbH, as well as by a grant from the Division Health and Nutrition, within the cluster project "SysMAP," to M.B.

We thank Abigail Koch-Koerfges for the development of the HPLC analysis method.

REFERENCES

1. **Alén, C., and A. L. Sonenshein.** 1999. *Bacillus subtilis* aconitase is an RNA-binding protein. Proc. Natl. Acad. Sci. U. S. A. **96:**10412–10417.
2. **Aoshima, M., M. Ishii, A. Yamagishi, T. Oshima, and Y. Igarashi.** 2003. Metabolic characteristics of an isocitrate dehydrogenase defective derivative of *Escherichia coli* BL21(DE3). Biotechnol. Bioeng. **84:**732–737.
3. **Banerjee, S., A. K. Nandyala, P. Raviprasad, N. Ahmed, and S. E. Hasnain.** 2007. Iron-dependent RNA-binding activity of *Mycobacterium tuberculosis* aconitase. J. Bacteriol. **189:**4046–4052.
4. **Baumgart, M., and M. Bott.** 2011. Biochemical characterisation of aconitase from *Corynebacterium glutamicum* J. Biotechnol. **154:**163–170.
5. **Beinert, H., M. C. Kennedy, and C. D. Stout.** 1996. Aconitase as iron-sulfur protein, enzyme, and iron-regulatory protein. Chem. Rev. **96:**2335–2373.
6. **Bott, M.** 1997. Anaerobic citrate metabolism and its regulation in enterobacteria. Arch. Microbiol. **167:**78–88.
7. **Bott, M.** 2007. Offering surprises: TCA cycle regulation in *Corynebacterium glutamicum*. Trends Microbiol. **15:**417–425.
8. **Brocker, M., S. Schaffer, C. Mack, and M. Bott.** 2009. Citrate utilization by *Corynebacterium glutamicum* is controlled by the CitAB two-component system through positive regulation of the citrate transport genes *citH* and *tctCBA*. J. Bacteriol. **191:**3869–3880.
9. **Craig, J. E., M. J. Ford, D. C. Blaydon, and A. L. Sonenshein.** 1997. A null mutation in the *Bacillus subtilis* aconitase gene causes a block in SpoOA-phosphate-dependent gene expression. J. Bacteriol. **179:**7351–7359.
10. **Cramer, A., R. Gerstmeir, S. Schaffer, M. Bott, and B. J. Eikmanns.** 2006. Identification of RamA, a novel LuxR-type transcriptional regulator of genes involved in acetate metabolism of *Corynebacterium glutamicum*. J. Bacteriol. **188:**2554–2567.
11. **Eikmanns, B. J., E. Kleinertz, W. Liebl, and H. Sahm.** 1991. A family of *Corynebacterium glutamicum*/*Escherichia coli* shuttle vectors for cloning, controlled gene expression, and promoter probing. Gene **102:**93–98.
12. **Eikmanns, B. J., D. Rittmann, and H. Sahm.** 1995. Cloning, sequence analysis, expression, and inactivation of the *Corynebacterium glutamicum icd* gene encoding isocitrate dehydrogenase and biochemical characterization of the enzyme. J. Bacteriol. **177:**774–783.
13. **Eikmanns, B. J., N. Thum-Schmitz, L. Eggeling, K. U. Lüdtke, and H. Sahm.** 1994. Nucleotide sequence, expression and transcriptional analysis of the *Corynebacterium glutamicum gltA* gene encoding citrate synthase. Microbiology **140:**1817–1828.
14. **Emer, D., A. Krug, B. J. Eikmanns, and M. Bott.** 2009. Complex expression control of the *Corynebacterium glutamicum* aconitase gene: identification of RamA as a third transcriptional regulator besides AcnR and RipA. J. Biotechnol. **140:**92–98.

15. **Frunzke, J., and M. Bott.** 2008. Regulation of iron homeostasis in *Corynebacterium glutamicum*, p. 241–266. *In* A. Burkovski (ed.), Corynebacteria: genomics and molecular biology. Caister Academic Press, Norfolk, United Kingdom.
16. **Frunzke, J., V. Engels, S. Hasenbein, C. Gätgens, and M. Bott.** 2008. Coordinated regulation of gluconate catabolism and glucose uptake in *Corynebacterium glutamicum* by two functionally equivalent transcriptional regulators, GntR1 and GntR2. Mol. Microbiol. **67:**305–322.
17. **Gadde, D. M., and M. T. McCammon.** 1997. Mutations in the *idh2* gene encoding the catalytic subunit of the yeast NAD^+-dependent isocitrate dehydrogenase can be suppressed by mutations in the *cit1* gene encoding citrate synthase and other genes of oxidative metabolism. Arch. Biochem. Biophys. **344:**139–149.
18. **Genda, T., T. Nakamatsu, and I. Ozaki.** 2003. Purification and characterization of malate dehydrogenase from *Corynebacterium glutamicum*. J. Biosci. Bioeng. **95:**562–566.
19. **Genda, T., S. Watabe, and H. Ozaki.** 2006. Purification and characterization of fumarase from *Corynebacterium glutamicum*. Biosci. Biotechnol. Biochem. **70:**1102–1109.
20. **Gruer, M. J., A. J. Bradbury, and J. R. Guest.** 1997. Construction and properties of aconitase mutants of *Escherichia coli*. Microbiology **143:**1837–1846.
21. **Gruer, M. J., and J. R. Guest.** 1994. Two genetically distinct and differentially regulated aconitases (AcnA and AcnB) in *Escherichia coli*. Microbiology **140:**2531–2541.
22. **Han, S. O., M. Inui, and H. Yukawa.** 2008. Effect of carbon source availability and growth phase on expression of *Corynebacterium glutamicum* genes involved in the tricarboxylic acid cycle and glyoxylate bypass. Microbiology **154:**3073–3083.
23. **Hanahan, D.** 1983. Studies on transformation of *Escherichia coli* with plasmids. J. Mol. Biol. **166:**557–580.
24. **Hentze, M. W., and L. C. Kuhn.** 1996. Molecular control of vertebrate iron metabolism: mRNA-based regulatory circuits operated by iron, nitric oxide, and oxidative stress. Proc. Natl. Acad. Sci. U. S. A. **93:**8175–8182.
25. **Hoffelder, M., K. Raasch, J. van Ooyen, and L. Eggeling.** 2010. The E2 domain of OdhA of *Corynebacterium glutamicum* has succinyltransferase activity dependent on lipoyl residues of the acetyltransferase AceF. J. Bacteriol. **192:**5203–5211.
26. **Jin, S. F., P. A. Levin, K. Matsuno, A. D. Grossman, and A. L. Sonenshein.** 1997. Deletion of the *Bacillus subtilis* isocitrate dehydrogenase gene causes a block at stage I of sporulation. J. Bacteriol. **179:**4725–4732.
27. **Kalinowski, J., et al.** 2003. The complete *Corynebacterium glutamicum* ATCC 13032 genome sequence and its impact on the production of L-aspartate-derived amino acids and vitamins. J. Biotechnol. **104:**5–25.
28. **Kaneko, T., et al.** 2002. Complete genomic sequence of nitrogen-fixing symbiotic bacterium *Bradyrhizobium japonicum* USDA110. DNA Res. **9:**189–197.
29. **Keilhauer, C., L. Eggeling, and H. Sahm.** 1993. Isoleucine synthesis in *Corynebacterium glutamicum*: molecular analysis of the *ilvB-ilvN-ilvC* operon. J. Bacteriol. **175:**5595–5603.
30. **Kinoshita, S., S. Udaka, and M. Shimono.** 1957. Studies on amino acid fermentation. Part I. Production of L-glutamic acid by various microorganisms. J. Gen. Appl. Microbiol. **3:**193–205.
31. **Kohl, T. A., and A. Tauch.** 2009. The GlxR regulon of the amino acid producer *Corynebacterium glutamicum*: detection of the corynebacterial core regulon and integration into the transcriptional regulatory network model. J. Biotechnol. **143:**239–246.
32. **Koziol, U., et al.** 2009. Deletion of citrate synthase restores growth of *Sinorhizobium meliloti* 1021 aconitase mutants. J. Bacteriol. **191:**7581–7586.
33. **Krug, A., V. F. Wendisch, and M. Bott.** 2005. Identification of AcnR, a TetR-type repressor of the aconitase gene *acn* in *Corynebacterium glutamicum*. J. Biol. Chem. **280:**585–595.
34. **Kurokawa, T., and J. Sakamoto.** 2005. Purification and characterization of succinate:menaquinone oxidoreductase from *Corynebacterium glutamicum*. Arch. Microbiol. **183:**317–324.
35. **Lakshmi, T. M., and R. B. Helling.** 1976. Selection for citrate synthase deficiency in *icd* mutants of *Escherichia coli*. J. Bacteriol. **127:**76–83.
36. **Lee, Y. L., T. Cesario, J. Owens, E. Shanbrom, and L. D. Thrupp.** 2002. Antibacterial activity of citrate and acetate. Nutrition **18:**665–666.
37. **Lin, A. P., K. W. Hakala, S. T. Weintraub, and L. McAlister-Henn.** 2008. Suppression of metabolic defects of yeast isocitrate dehydrogenase and aconitase mutants by loss of citrate synthase. Arch. Biochem. Biophys. **474:**205–212.
38. **Matsuno, K., et al.** 1999. Metabolic imbalance and sporulation in an isocitrate dehydrogenase mutant of *Bacillus subtilis*. J. Bacteriol. **181:**3382–3391.
39. **McDermott, T. R., and M. L. Kahn.** 1992. Cloning and mutagenesis of the *Rhizobium meliloti* isocitrate dehydrogenase gene. J. Bacteriol. **174:**4790–4797.
40. **Molenaar, D., M. E. van der Rest, A. Drysch, and R. Yücel.** 2000. Functions of the membrane-associated and cytoplasmic malate dehydrogenases in the citric acid cycle of *Corynebacterium glutamicum*. J. Bacteriol. **182:**6884–6891.
41. **Molenaar, D., M. E. van der Rest, and S. Petrovic.** 1998. Biochemical and genetic characterization of the membrane-associated malate dehydrogenase (acceptor) from *Corynebacterium glutamicum*. Eur. J. Biochem. **254:**395–403.
42. **Niebisch, A., and M. Bott.** 2001. Molecular analysis of the cytochrome bc_1-aa_3 branch of the *Corynebacterium glutamicum* respiratory chain containing an unusual diheme cytochrome c_1. Arch. Microbiol. **175:**282–294.
43. **Niebisch, A., A. Kabus, C. Schultz, B. Weil, and M. Bott.** 2006. Corynebacterial protein kinase G controls 2-oxoglutarate dehydrogenase activity via the phosphorylation status of the OdhI protein. J. Biol. Chem. **281:**12300–12307.
44. **Polen, T., D. Schluesener, A. Poetsch, M. Bott, and V. F. Wendisch.** 2007. Characterization of citrate utilization in *Corynebacterium glutamicum* by transcriptome and proteome analysis. FEMS Microbiol. Lett. **273:**109–119.
45. **Przybyla-Zawislak, B., D. M. Gadde, K. Ducharme, and M. T. McCammon.** 1999. Genetic and biochemical interactions involving tricarboxylic acid cycle (TCA) function using a collection of mutants defective in all TCA cycle genes. Genetics **152:**153–166.
46. **Quast, K., B. Bathe, A. Pühler, and J. Kalinowski.** 1999. The *Corynebacterium glutamicum* insertion sequence IS*Cg2* prefers conserved target sequences located adjacent to genes involved in aspartate and glutamate metabolism. Mol. Gen. Genet. **262:**568–578.
47. **Radmacher, E., and L. Eggeling.** 2007. The three tricarboxylate synthase activities of *Corynebacterium glutamicum* and increase of L-lysine synthesis. Appl. Microbiol. Biotechnol. **76:**587–595.
48. **Reinscheid, D. J., B. J. Eikmanns, and H. Sahm.** 1994. Characterization of the isocitrate lyase gene from *Corynebacterium glutamicum* and biochemical analysis of the enzyme. J. Bacteriol. **176:**3474–3483.
49. **Reinscheid, D. J., B. J. Eikmanns, and H. Sahm.** 1994. Malate synthase from *Corynebacterium glutamicum*: sequence analysis of the gene and biochemical characterization of the enzyme. Microbiology **140:**3099–3108.
50. **Sambrook, J., E. F. Fritsch, and T. Maniatis.** 1989. Molecular cloning, a laboratory manual, 2nd ed. Cold Spring Harbor Laboratory Press, Cold Spring Harbor, NY.
51. **Schäfer, A., A. Tauch, W. Jäger, J. Kalinowski, G. Thierbach, and A. Pühler.** 1994. Small mobilizable multipurpose cloning vectors derived from the *Escherichia coli* plasmids pK18 and pK19–selection of defined deletions in the chromosome of *Corynebacterium glutamicum*. Gene **145:**69–73.
52. **Serio, A. W., M. B. Pechter, and A. L. Sonenshein.** 2006. *Bacillus subtilis* aconitase is required for efficient late-sporulation gene expression. J. Bacteriol. **188:**6396–6405.
53. **Somerville, G. A., et al.** 2002. *Staphylococcus aureus* aconitase inactivation unexpectedly inhibits post-exponential-phase growth and enhances stationary-phase survival. Infect. Immun. **70:**6373–6382.
54. **Tang, Y., and J. R. Guest.** 1999. Direct evidence for mRNA binding and post-transcriptional regulation by *Escherichia coli* aconitases. Microbiology **145:**3069–3079.
55. **Tang, Y., J. R. Guest, P. J. Artymiuk, R. C. Read, and J. Green.** 2004. Post-transcriptional regulation of bacterial motility by aconitase proteins. Mol. Microbiol. **51:**1817–1826.
56. **Tang, Y., M. A. Quail, P. J. Artymiuk, J. R. Guest, and J. Green.** 2002. *Escherichia coli* aconitases and oxidative stress: post-transcriptional regulation of *sodA* expression. Microbiology **148:**1027–1037.
57. **Thöny-Meyer, L., and P. Künzler.** 1996. The *Bradyrhizobium japonicum* aconitase gene (*acnA*) is important for free-living growth but not for an effective root nodule symbiosis. J. Bacteriol. **178:**6166–6172.
58. **Towbin, H., T. Staehelin, and J. Gordon.** 1979. Electrophoretic transfer of proteins from polyacrylamide gels to nitrocellulose sheets–procedure and some applications. Proc. Natl. Acad. Sci. U. S. A. **76:**4350–4354.
59. **Usuda, Y., et al.** 1996. Molecular cloning of the *Corynebacterium glutamicum* ("*Brevibacterium lactofermentum*" AJ12036) *odhA* gene encoding a novel type of 2-oxoglutarate dehydrogenase. Microbiology **142:**3347–3354.
60. **van der Rest, M. E., C. Lange, and D. Molenaar.** 1999. A heat shock following electroporation induces highly efficient transformation of *Corynebacterium glutamicum* with xenogeneic plasmid DNA. Appl. Microbiol. Biotechnol. **52:**541–545.
61. **van Ooyen, J., et al.** 2011. Citrate synthase in *Corynebacterium glutamicum* is encoded by two *gltA* transcripts which are controlled by RamA, RamB, and GlxR. J. Biotechnol. **154:**140–148.
62. **Vertès, A. A., M. Inui, M. Kobayashi, Y. Kurusu, and H. Yukawa.** 1994. Isolation and characterization of IS31831, a transposable element from *Corynebacterium glutamicum*. Mol. Microbiol. **11:**739–746.
63. **Viollier, P. H., et al.** 2001. Roles of aconitase in growth, metabolism, and morphological differentiation of *Streptomyces coelicolor*. J. Bacteriol. **183:**3193–3203.
64. **Walden, W. E., et al.** 2006. Structure of dual function iron regulatory protein 1 complexed with ferritin IRE-RNA. Science **314:**1903–1908.
65. **Wennerhold, J., A. Krug, and M. Bott.** 2005. The AraC-type regulator RipA represses aconitase and other iron proteins from *Corynebacterium* under iron limitation and is itself repressed by DtxR. J. Biol. Chem. **280:**40500–40508.

Curriculum vitae

Nurije Mustafi

Date of birth:	11.09.1985
Place of birth:	Tetovo, Macedonia
Nationality:	German

Education:

08/1992-07/1996	Primary School, Remscheid
08/1996-06/2005	Getrud-Bäumer-Gymnasium, Remscheid
10/2005-12/2008	Studies of Biology at the Heinrich-Heine Universität Düsseldorf
01/2009-12/2009	Diploma thesis in the group of Prof. Dr. Michael Bott at the Institute of Biotechnology 1, Research Centre Jülich. Ttile: "Posttranslationale Proteinmodifizierung in *Corynebacterium glutamicum*."
01/2010-03/2013	Experimental PhD thesis in the group of Dr. J. Frunzke at the Institute of Bio- and Geosciences, Biotechnology (IBG-1), Research Centre Jülich.

Danksagung

Ein ganz besonderer Dank gilt Frau Dr. Julia Frunzke für die Überlassung des interessanten Themas, ihr stetiges Interesse am Fortgang dieser Arbeit, die zahlreichen inspirierenden Diskussionen und die hervorragende Betreuung in den letzten drei Jahren.

Herrn Prof. Karl-Erich Jaeger danke ich für die freundliche Übernahme des Zweitgutachtens.

Bei Herrn Prof. Michael Bott bedanke ich mich für die freundliche Unterstützung und das stete Interesse am Fortschritt dieser Arbeit.

Dem Bundesministerium für Bildung und Forschung danke ich für die finanzielle Unterstützung dieser Arbeit im Rahmen des Flex-Fit Projekts. Allen Projektmitgliedern möchte ich für die freundliche und kreative Zusammenarbeit danken.

Für die angenehme Atmosphäre im Labor und im Büro bedanke ich mich bei allen jetzigen und ehemaligen Mitgliedern der Arbeitsgruppe, Conni, Antonia, Eva, Arun, Andrea, Kim, Meike, Jasintha, Regina und Kerstin. Zudem danke ich Conni für die tatkräftige Unterstützung bei den Fermentationsversuchen. Regina danke ich herzlich für die Unterstützung bei den letzten Experimenten sowie für die kritische Durchsicht dieser Arbeit.

Allen Mitarbeitern des IBG-1 danke ich für die gute Arbeitsatmosphäre und für die stete Hilfsbereitschaft. Ein ganz besonderer Dank gilt hierbei Alexander Grünberger für die tolle Kooperation in den letzten Jahren. Georg, Michael, Simon und Jan danke ich für die tausend wertvollen Tipps zur Bedienung der HPLC und der Fermenter.

Boris und Xenia danke ich für die tollen Gespräche und Diskussionen, die so manche Autofahrt, Mittagspause und Wartezeit interessant gemacht haben.

Aus ganzem Herzen danke ich meinen lieben Eltern und meiner Schwester für ihre Unterstützung. *Faliminder!*

Erklärung

Ich versichere an Eides Statt, dass die Dissertation von mir selbständig und ohne unzulässige fremde Hilfe unter Beachtung der „Grundsätze zur Sicherung guter wissenschaftlicher Praxis an der Heinrich-Heine-Universität Düsseldorf“ erstellt worden ist. Die Dissertation wurde in der vorgelegten oder in ähnlicher Form noch bei keiner anderen Institution eingereicht. Ich habe bisher keine erfolglosen Promotionsversuche unternommen.

_____

Düsseldorf, den 12.03.2013